THE ROLE OF OSTEOPROTEGERIN AND RECEPTOR ACTIVATOR OF NUCLEAR FACTOR κB IN OSTEOTROPIC PROSTATE AND BREAST CANCERS

by

Sioned Owen

Cardiff University

2014

Doctor of Philosophy

Declaration

This work has not previously been accepted in substance for any degree and is not concurrently submitted in candidature for any degree.

Signed …… Date……

STATEMENT 1
This thesis is being submitted in partial fulfilment of the requirements for the degree of PhD.

Signed …… Date ……

STATEMENT 2
This thesis is the result of my own independent work/investigation, except where otherwise stated. Other sources are acknowledged by explicit references.

Signed …… Date ……

STATEMENT 3
I hereby give consent for my thesis, if accepted, to be available for photocopying and for interlibrary loan, and for the title and summary to be made available to outside organisations.

Signed …… Date ……

For Mum,

Thank you for believing in me.

You showed me the way and I dedicate this to you and your memory.

“Success is not final, failure is not fatal: it is the courage to continue that counts.”

Winston Churchill

Acknowledgments

First and foremost, I would like to thank my supervisors, Professors W.G. Jiang and M.D. Mason, and Cancer Research Wales for providing me with this opportunity to contribute to the field of cancer research.

I would also like to thank all staff and students, past and present, from MARG and CUPUCI for making these last three years so enjoyable as well as worthwhile. A special thank you goes to Dr. Andrew Sanders for his unwavering and invaluable support and advice throughout this study while a “humongous” thank you goes to Dr. Jane Lane and Miss Fiona Ruge for their camaraderie and humour in the lab.

Finally, a special thank you to all my family and to Debbie, Jessica, Natalie and Sian for their help, encouragement and wine supply.

Publications and Presentations

Full papers

Owen S, Ye L, Sanders AJ, Mason MD, Jiang WG. Expression profile of receptor activator of nuclear κB (RANK), RANK ligand (RANKL) and osteoprotegerin (OPG) in breast cancer. Anti Cancer Research 2013 Jan 33:199-206.

Frewer NC, Ye L, Sun PH, **Owen S**, Ji K, Frewer KA, Hargest R, Jiang WG. Potential implication of IL-24 in lymphangiogenesis of human breast cancer. International Journal of Molecular Medicine 2013: May 5:1097-1104.

Frewer KA, Sanders AJ, **Owen S**, Frewer NC, Hargest R, Jiang WG. A role for WISP-2 in colorectal cancer cell invasion and motility. Cancer Genomics Proteomics 2013 July-Aug 10(4):187-196.

Owen S, Sanders AJ, Sobkowicz A, Ye L, Mason MD, Jiang WG. Implications of OPG and RANK in prostate cancer cell homing to the bone. In preparation.

Poster Presentations

Owen S, Ye L, Sanders AJ, Mason MD, Jiang WG. Expression profile of Receptor Activator of Nuclear κB in clinical breast cancer. 7th Chinese Clinical Oncology Annual Congress and 13th Cross-Strait Cancer Symposium, September 8th 2012, Beijing.

Owen S, Sanders AJ, Ye L, Mason MD, Jiang WG. Osteomodulin expression profile in breast cancer cohort.European Cancer Congress, September 28th 2013 Amsterdam. Diagnostics/ Biomarkers, Abstract Number 958.

Oral Presentation

Owen S, Ye L, Sanders AJ, Mason MD, Jiang WG. Bone turnover molecules expression profiles in Breast Cancer. 7th Chinese Clinical Oncology Annual Congress and 13th Cross-Strait Cancer Symposium, September 9th 2012, Beijing

Abbreviations

ABS – Antibiotics

ADAMs – Adamalysin-related membrane proteases

ADAMTS – A disintegrin-like and metalloproteinase with thrombospondin motifs

APO1 – Apoptosis antigen 1

APS – Ammonium persulfate

AR – Androgen receptor

ATCC – American Type Culture Collection

Bcl-x_L - B-cell lymphoma-extra large

BME – Bone matrix extract

BMPs – Bone morphogenetic protein

BMUs – Basic multicellular units

BPH – Benign prostate hyperplasia

Bps – Base pairs

BSA – Bovine serum albumin

BSP – Bone sialoprotein

BSS – Balanced saline solution

CASR – Calcium-sensing receptor

CATK - Cathepsin K

CB1 – Cannabinoid receptor type 1

Cbfa 1 – Core binding factor α1

CBL – Casitas B-lineage Lymphoma

Cdc42 – Cell division control protein 42

cDNA – Complementary deoxyribonucleic acid

CSFs – Colony stimulating factors

CSF-1R – Colony stimulating factor 1 receptor

CTx – Carboxy-terminal collagen crosslinks

CXCR4 – C-X-C chemokine receptor type 4

DAB – Diaminobenzidine

DEPC –Diethyl pyrocarbonate

DHT – Dihydrotestosterone

DKK-1 – Dickkopf-1

DMEM – Dulbecco’s modified eagles medium

DMSO – Dimethyl sulphoxide

DR – Death receptor

DRE – Digital rectal examination

DNA – Deoxyribonucleic acid

ECIS – Electric cell-substrate impedance sensing

ECM – Extracellular matrix

EDTA – Ethylenediaminetetraacetic acid

EGF – Epidermal growth factor

EGFR – Epidermal growth factor receptor

EMT – Epithelial-mesenchymal transition

ER – Oestrogen receptor

ERG – ETS related gene

ET-1 - Endothelin-1

ETS – Erythroblast transformation specific

ETV1 – ETS translocation variant 1

ETV4 – ETS translocation variant 4

F-12K – Kaighn’s modification of Ham’s F-12 medium

FAK – Focal adhesion kinase

FCS – Foetal calf serum

FGF – Fibroblast growth factor

FOXA1 – Forkhead box A1

FRP – Frizzled-related protein family

Fz – Frizzled

GAB1 – GRB2-associated binding protein 1

GAPDH – Glyceraldehyde 3-phosphate dehydrogenase

G-CSF – Granulocyte-colony stimulating factor

GM-CSF – Granulocyte macrophage colony stimulating factor

Grb2 – Growth factor receptor-bound protein 2

GTP – Guanosine triphosphate

HEPES – Hydroxyethyl piperazineethane sulphonic acid

HER2 – Human epidermal growth factor receptor 2

HGF – Hepatocyte growth factor

HSC – Haemotopoietic stem cells

Ibsp – Integrin-binding sialoprotein

IFN – Interferon

IGF-1 – Insulin-like growth factor -1

IGF1R – Insulin-like growth factor -1 receptor

IGFBP-3 – IGF-binding protein 3

IL – Interleukin

JNK – c-Jun N terminal kinase

LB – Liquid broth

LOH – Loss of heterozygosity

LRP – Lipoprotein-related protein

M-CSF – Macrophage colony stimulating factor

MET – Mesenchymal-epithelial transition

MITF – Microphthalmia-associated transcription factor

MMPs – Matrix metalloproteinases

MPA – Medroxyprogesterone acetate

mRNA – Messenger ribonucleic acid

Myc – Myelocytomatosis

NFATC1 – nuclear factor of activated T cells 1

NF-κB – Nuclear factor kappa light chain enhancer of activated B cells

NK3 – Neurokinin-3 receptor

NKX3.1 – NK3 homeobox 1

nRANKL – Neutralising RANKL

NPI – Nottingham prognostic index

NTX – N-telopeptide

ODF – Osteoclast differentiation factor

ON - Osteonectin

OPG - Osteoprotegerin

OPN – Osteopontin

Osx – Osterix

PCA3 – Prostate cancer antigen 3

PCR – Polymerase chain reaction

PDGF – Platelet-derived growth factor

PDGFR – PDGF- receptor

PI3K – Phosphoinositol triphosphate kinase

PIN – Prostatic intraepithelial neoplasia

PKB – Protein kinase B

PLCy – Phosphoinositide phospholipase C gamma

PSA – Prostate specific antigen

PTEN – Phosphotase and tensin homologue

PTH – Parathyroid hormone

PTHrP – Parathyroid hormone related protein

PVDF – Polyvinylidene difluoride

qPCR – Quantitative polymerase chain reaction

RAG1 – Recombinase activating gene

RANK – Receptor activator of nuclear factor κB

RANKL – Receptor activator of nuclear factor κB Ligand

Rac – Ras-related C3 botulinum toxin substrate

Ras – Rat sarcoma gene

Ras-GAP – Ras GTPase activating protein

Rho – Ras homologue gene

rhOPG – Recombinant human OPG

RT-PCR – Reverse transcription polymerase chain reaction

RT – Reverse transcription

RTK – Receptor tyrosine kinase

Runx2 – Runt-related transcription factor 2

SCID – Severe combined immunodeficiency

SDF-1 – Stromal-derived factor-1

SDS-PAGE – Sodium dodecyl sulphate polyacrylamide gel electrophoresis

sFRP – Secreted frizzled-related protein

SH – Src homology

SOS – Son of Sevenless

SOC – Super optimal broth with catabolite repression

SRE – Skeletal related events

Stat3 – Signal Transducer and activator of transcription 3

TACE – TNF-α converting enzyme like protease

TBE – Tris-Boric acid EDTA

TBS – Tris buffered saline

TEMED - tetramethylethylenediamine

TGF-β – Transforming growth factor - β

TIMPs – Tissue inhibitors of metalloproteinases

TMPRSS2 – Transmembrane protease, serine 2

TNF – Tumour necrosis factor

TNFR – Tumour necrosis factor receptor

TNFRSF – Tumour necrosis factor receptor superfamily

TNM – Tumour node metastasis

tPA – Tissue plasminogen activator

TRAF – TNFR-associated factors

TRAIL – TNF – related apoptosis-inducing ligand

TRANCE - Tumour necrosis factor-related activation-induced cytokine

TRAP – Tartrate-resistant acid phosphate

TRUS – Transrectal ultrasound-guided biopsy

uPA – Urokinase-type plasminogen activator

VCAM-1 – Vascular cell adhesion protein 1

VEGF – Vascular endothelial growth factor

VEGFR1 – Vascular endothelial growth factor receptor 1

WIF -1 – Wnt inhibitory factor

Summary

Osteoprotegerin (OPG), Receptor Activator of Nuclear Factor κB (RANK) and RANK ligand (RANKL), are members of the tumour necrosis factor receptor superfamily (TNFRSF), signal transducers which have pleiotropic actions. Each family member has unique structural attributes shown to couple them directly to specific signalling pathways involved in cell proliferation, differentiation and survival. Previous studies have clinically correlated OPG, RANK and RANKL expression, at both transcript and protein levels, with increasing cancer tumour burden, metastatic bone involvement and androgen status, however the mechanisms by which these molecules exert their effects remain elusive. This study aimed to establish what influence targeting OPG, RANK and RANKL expression may have on osteotrophic prostate and breast cancer cells *in vitro* and to subsequently explore the effect(s) Hepatocyte Growth Factor (HGF) and Bone Matrix Extract (BME) might also exert on cancer cell behaviour following manipulation of these molecules.

The current study utilised 2 prostate cancer cell lines with varying androgen status, metastatic potential and bone metastasis phenotypes. Initial screening showed that the more aggressive osteolytic PC-3 cells expressed OPG, whilst weakly metastatic mixed-osseous LNCaP cells had very low expression. Whilst RANK was present in both cell lines, RANKL expression was only detected in the LNCaP cells. Reduction of OPG expression in the PC-3 cells resulted in increased cell invasion *in vitro*, which was further enhanced when treated with BME. No other cellular traits were affected by targeting OPG directly, however, cell migration was enhanced when the manipulated cells were exposed to the representative bone microenvironment. In contrast the addition of a recombinant form of OPG to LNCaP cells resulted in decreased cell invasion, a trend which was reversed when combined with BME. Combination of OPG and BME treatment reduced the migratory response of LNCaP cells, whilst combination of OPG and HGF were pro-migratory. The targeting of RANK in PC-3 cells affected cell proliferation and matrix adhesion *in vitro* though the addition of HGF or BME appeared to have no further direct influence on these manipulated cells. Targeting of the RANKL expression with a neutralising monoclonal antibody had little effect on cancer cell behaviour; however combined exposure with HGF or BME resulted in similar behaviour patterns seen under the OPG treatments.

In our breast cancer cohort, RANK and RANKL expression were correlated with bone metastases and survival rates. Though OPG did not appear to be associated with grading, data also implied a role in overall survival. In the aggressive osteolytic MDA-MB-231 breast cancer cells, reduced OPG expression resulted in increased motility and invasion, traits which were little affected upon exposure to HGF or BME. In contrast the targeting of RANK expression in MDA-MB-231 cells resulted in reductions in all the cancer cell behaviours studied, but again these appeared unaffected under the influence of HGF or BME.

The complexity of the bone environment underpins the vast number of soluble factors, signalling pathways and transcription regulators which can influence osteotrophic cancer cells. As indicated by the licensing of Denosumab, one therapeutic approach is not suitable for all osteotrophic cancers. Therefore further elucidation into the intricacies of these interactions is needed.

List of Figures:

List of Tables:

Contents

Chapter 1

General Introduction

1.1 Prostate

The prostate gland, found exclusively in mammals, is a partly glandular partly muscular organ, the size and shape of a walnut, which completely surrounds the prostatic portion of the urethra. It is located within the lower pelvis deep to the superior fascia of the urogenital diaphragm, inferior to the urinary bladder and anterior to the rectum.

1.1.1 Formation and morphogenesis

Prostate formation is a feature of embryogenesis which occurs through epithelial budding from the urogenital sinus. The prostate gland originates from the intermediate region, known as the pelvic part. The maturation time of the prostate gland, the lengthening and branching of prostatic ducts, differs greatly within the population, largely occurring in response to testosterone metabolites, including dihydrotestosterone (DHT), secreted from the developing testes during puberty (Vis and Schroder 2009a).

DHT is the primary intracellular, intraprostatic androgen which plays an essential role in prostate development and growth due to its high binding affinity for the androgen receptor (AR) and its capability of stabilising the ligand-androgen receptor complex (Vis and Schroder 2009b). DHT exhibits differing functions dependent on the individual's developmental stage. *In utero*, DHT is vital for normal differentiation of external male genitalia and the prostate whilst during puberty DHT is responsible for facial hair, acne and prostate growth (Marks 2004, Imperato-McGinley 2002).

1.1.2 Structure

The prostate gland is enclosed within a fibrous capsule. It consists of several glandular and non-glandular regions formed by the urethra and the ejaculatory ducts that extend through the gland (Martini and Nath 2009). The capsule consists of prostatic stromal smooth muscle which gradually extends into fibrous tissue that terminates with loose connective and adipose tissue. Extensive bands of smooth muscle course throughout the prostate to form a meshwork that supports the glandular tissue. Prostate anatomy was first defined by McNeal as three distinct morphological regions: the peripheral zone; transition zone and the central zone (Figure 1.1) (McNeal 1969, 1988b). Each zone has different pathological tendencies; benign hyperplasia (BPH) develops in the transition zone whilst prostate cancer tends to originate in the peripheral zone (Table 1.1) (McNeal 1988a).

1.1.3 Function

Contraction of the prostatic smooth muscle results in expulsion of the contents of the gland, and provides part of the propulsive force needed to ejaculate semen. Discharge from the prostate makes up approximately 40% of the volume of the semen (Martini and Nath 2009). The thin, milky prostatic secretion assists spermatic motility by acting as a liquefying agent. Its alkalinity also protects the sperm during their passage through the acidic environment of the female vagina. The prostate also secretes several enzymes including acid phosphatase, which is often measured clinically to assess prostate function and possibly highlight the presence of cancer (Ludwig and Weidner 2000, Zielie *et al* 2004).

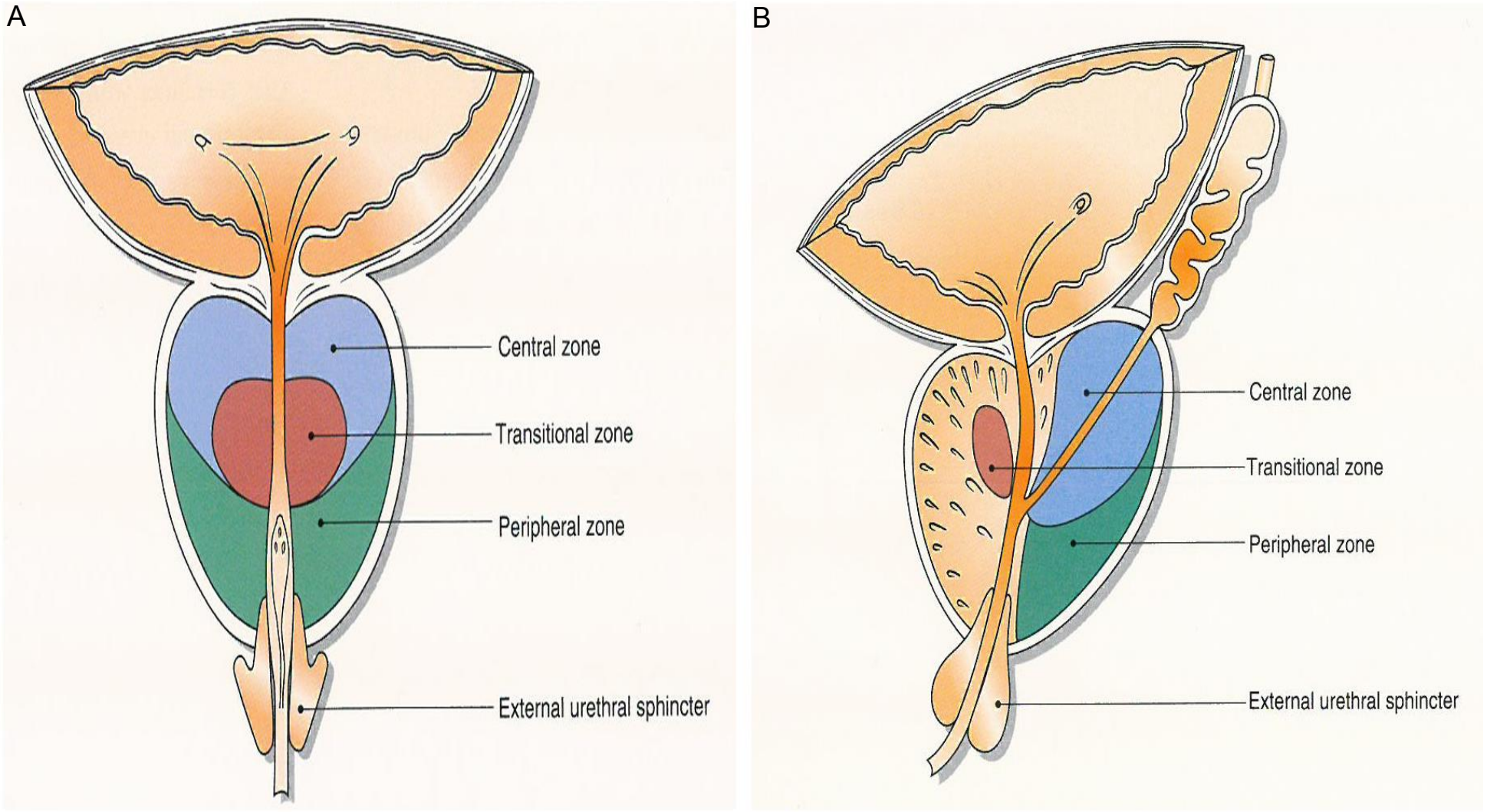

Figure 1.1 - Prostate Anatomy

Prostate has three distinct morphological zones shown in the frontal (A) and sagittal (B) planes, highlighting the three distinct regions identified by McNeal (Figure adapted from Kirby 2003)

Table 1.1 - Anatomical mass of the individual zones in the prostate, their location and the incidence of prostate related conditions that originate in each zone (adapted from Crawford 2009)

Zone	Mass (%)	Location	% of cancer case origins
Transition	5-10	Surrounds the urethra proximal and entry of the ejaculatory ducts	BPH and ~ 10-15% cancer cases
Central	20-25	Below the proximal urethral segment. The ejaculatory duct passes through the central zone before entering the urethra	~ 15-20%
Peripheral	70-75	A double row of duct buds that laterally surrounds the central zone and occupies the apical region of the prostate	~ 70%

1.1.4 Natural History and Pathophysiology

The majority of prostate cancers remain clinically silent or are slow-progressing malignancies not associated with, or attributed as, cause of death. However, it is not yet possible to predict which of these histological cancers will progress to aggressive clinical disease requiring intervention and therapy. Autopsy data suggests that the prevalence of prostate cancer could be as high as 90% in men aged 70-90 (Guileyardo *et al* 1980, Yatani *et al* 1988, Sakr *et al* 1993). Retrospective data analysis from patient studies also found that highly or moderately differentiated tumours at time of diagnosis yielded an 87% 10 year disease-specific survival rate, whilst poorly differentiated tumours were associated with only a 34% survival rate (Chodak *et al* 1994, Johansson *et al* 2004).

Early prostate tumourigenesis appears to be associated with a dysplasia starting with proliferative inflammatory atrophy, which progresses to prostatic intraepithelial neoplasia (PIN), which in turn may lead to some cases of carcinoma. The majority of all prostate cancer cases are adenocarcinomas and very few have neuroendocrine morphology (Dunn and Kazer 2011). Most cases are multifocal, multicentric lesions of varying grades presenting in different zones of the prostate (Crawford 2009).

1.1.4.1 Benign Prostatic Hyperplasia

Benign Prostatic Hyperplasia (BPH) is a non-malignant overgrowth of the epithelium and fibromuscular tissue in the transition zone and periurethral area of the prostate (Kirby 2003, Crawford 2009). The development of BPH includes three pathologic stages: nodule formation, nodule enlargement and diffuse expansion of the transition zone and periurethral tissue (Bostwick *et al* 2004). In younger men (<70 years) diffuse expansion and nodule formation predominates. However, in older

men the presence of epithelial proliferation and expansive growth of existing nodules occurs, possibly due to aberrant stimulation by androgens and other hormones (Berry *et al* 1984, Bostwick *et al* 2004). Histologically, BPH includes expansion of the basal layer, stromal hyperplasia, including fibrosis, and associated inflammation ((McNeal 1978, McNeal 1988a) (Figure 1.2).

1.1.4.2 Prostatic Intraepithelial Neoplasia

Prostatic Intraepithelial Neoplasia (PIN) is characterised by the multi-layering of luminal epithelial cells and a disappearing basal epithelial cell layer (Figure 1.3) (Kirby 2003). PIN is often referred to as the precancerous end of a continuum of cellular proliferations within the epithelial lining of prostatic ducts, ductules and acini, whilst cytologic changes mimic cancer by nuclear and nucleolar enlargement (Bostwick 2000, Bostwick *et al* 2000). PIN, by retaining a fragmented basal layer, can coexist with cancer (Bostwick *et al* 2004). Evidence suggests PIN are androgen dependent lesions which show heterogeneity and have a multifocal appearance, although obtaining tissue for study is difficult (Bostwick and Cheng 2012). In normal prostate epithelium, luminal secretory cells are more sensitive to the absence of androgen than basal cells, indicating that PIN shares this androgen sensitivity. A marked decrease in high-grade PIN has been reported after androgen-deprivation therapy compared with untreated lesions, also supporting this theory (Bostwick and Cheng 2012). The continuum that culminates in high-grade PIN and early invasive cancer is characterised by progressive basal cell layer disruption, abnormalities in secretory differentiation markers, increased cell proliferation, increased nuclear and nucleolar alterations, increased genetic instability and variation in DNA content (Bostwick and Brawer 1987).

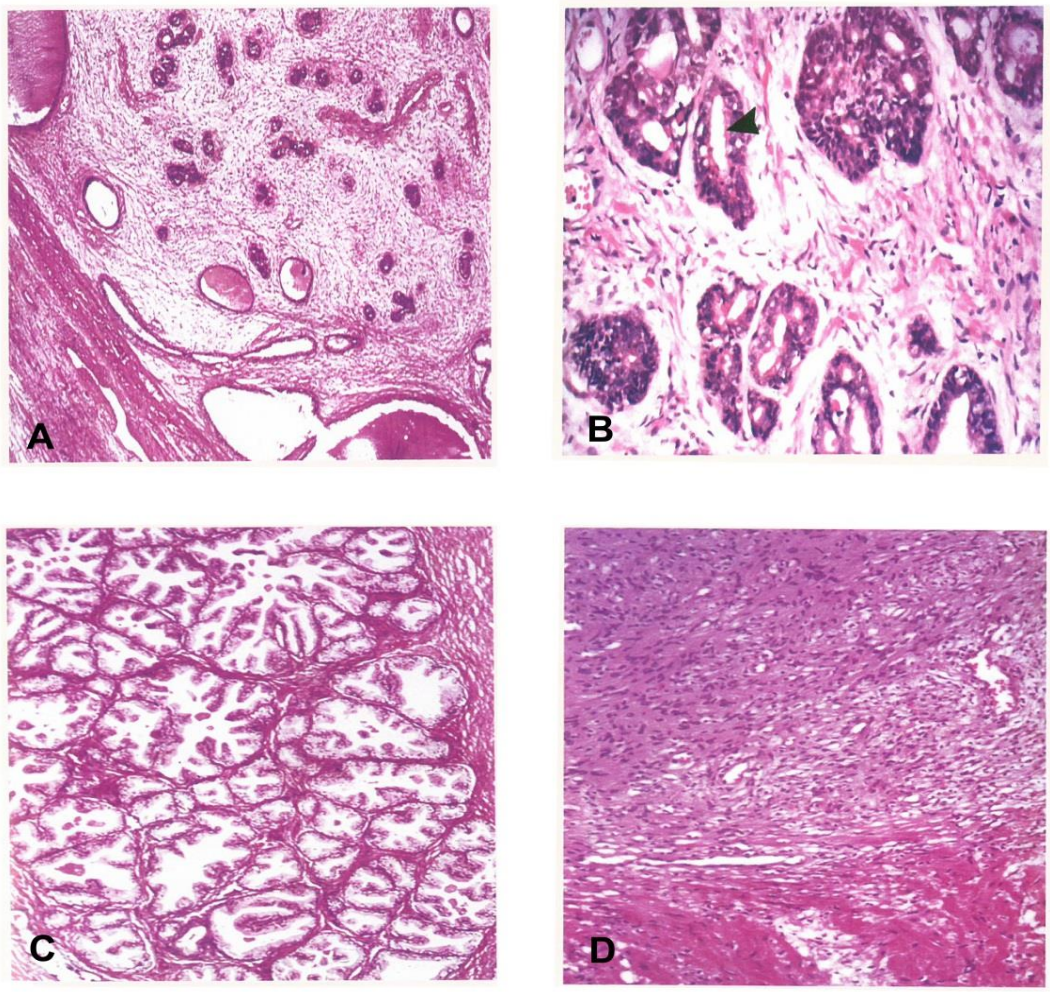

Figure 1.2 – Benign Prostate Hyperplasia (BPH) Histology

Histologically BPH is generally characterised by proliferation of stromal and epithelial components resulting in nodule formation. (A) Histological evidence of hyperplastic nodules of epithelium and stroma. (B) BPH basal cell hyperplasia showing stratified layers of compressed tall columnar cells. Double cell layers of LP34 positive and PSA positive luminal cells confirm benign nature of specimen (as shown by arrow head). (C) Histological example of epithelial hyperplastic nodules (D) Histological example of stromal overgrowth in hyperplastic nodules, generally periurethral, often situated beneath the urethral epithelium (adapted from Kirby 2003)

Studies have reported that PIN tends to occur predominantly in the peripheral zone of the prostate, or simultaneously in the transitional and peripheral zones, where most cancers arise (Epstein *et al* 1990, Quinn *et al* 1990). Appearance of high grade PIN lesions generally precedes the appearance of carcinoma by at least 10 years, however PIN lesions do not produce high levels of prostate specific antigen (PSA), they are only detectable by biopsy (Bostwick and Cheng 2012). Several studies have made associations between PIN and prostate cancer on epidemiologic, clinical, genetic and molecular levels (Nagle *et al* 1991, Bostwick *et al* 1993, Montironi *et al* 1993). Cancerous prostates were shown to have significantly increased (82%) evidence of PIN compared to spontaneous cancerous prostates without any previous evidence of PIN lesions (43%) (McNeal and Bostwick 1986, McNeal *et al* 1986, Bostwick and Brawer 1987).

1.2 Prostate cancer

Amongst men in Western society, prostate cancer is a highly prevalent non-cutaneous disease. Within the UK, it accounts for 25% of newly diagnosed male cancer cases per year (2010 – 41,700 diagnosed in UK) and it was fatal in 10,721 cases (Cancer Research UK CancerStats, 2012). The European age-standard incidence rate of prostate cancer is significantly higher in Wales (114.0/100,000 male population), than in any other constituent part of the UK. Increasing incidence in developing parts of the world underwrites concerns for future healthcare systems and increasing financial burdens associated with cancer management and treatment, thus driving the need for a better understanding about this disease, its risk factors and its progression.

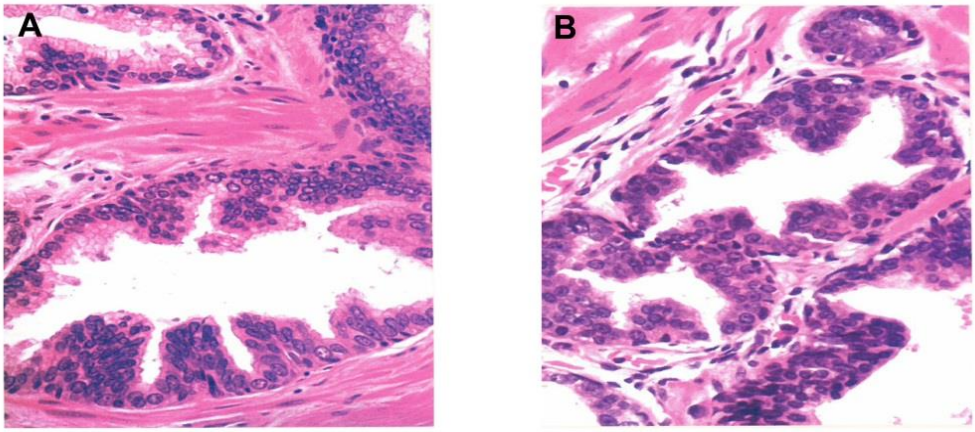

Figure 1.3 – Prostatic Intraepithelial neoplasia (PIN) Histology

PIN may be a precursor for most prostate cancer cases; (A) Low grade PIN showing stratified epithelium and the nuclei are larger than those of the normal acini. (B) High grade PIN shows stratified epithelium, cells that have lost their polarity and nuclei are larger and contain nucleoli. The outer layer of basal cells can still be seen (adapted from Kirby 2003)

1.2.1 Epidemiology and risk factors

There remains a need to identify risk factors and the multiple genetic changes which are involved in the development of prostate cancer, with particular emphasis on recognising those patients who will develop highly aggressive forms of the disease. Data suggests that more men will die with indolent prostate cancer than those who will die as a result of prostate cancer (Crawford 2009). However, as life expectancy increases, incidence of prostate cancer will continue to be a major health concern worldwide.

1.2.1.1 Age

Prostate cancer incidence and mortality is strongly correlated with increasing age. In the UK, between 2008 and 2010, 75% of prostate cancer cases were diagnosed in men over 65 years, whilst the under 50's accounted for just 1% (Figure 1.4).

1.2.1.2 Ethnicity

The highest age adjusted incidence rate of prostate cancer is found within the African American community (272/100,000), almost twice as prevalent as in Caucasians, whilst the lowest age-adjusted incidence rate is found within Asian and Pacific Islanders communities (93.8/100,000). However these statistics do not always reflect the influence of migration. Evidence has shown when Japanese men relocated to the United States, or other western countries, their prostate cancer incidence statistics started to resemble those of the local (Caucasian) population (Dunn 1975, Locke and King 1980). This can be further compounded by the age at time of relocation and the length of time spent in this environment which also correlated with increased risk (Shimizu *et al* 1991).

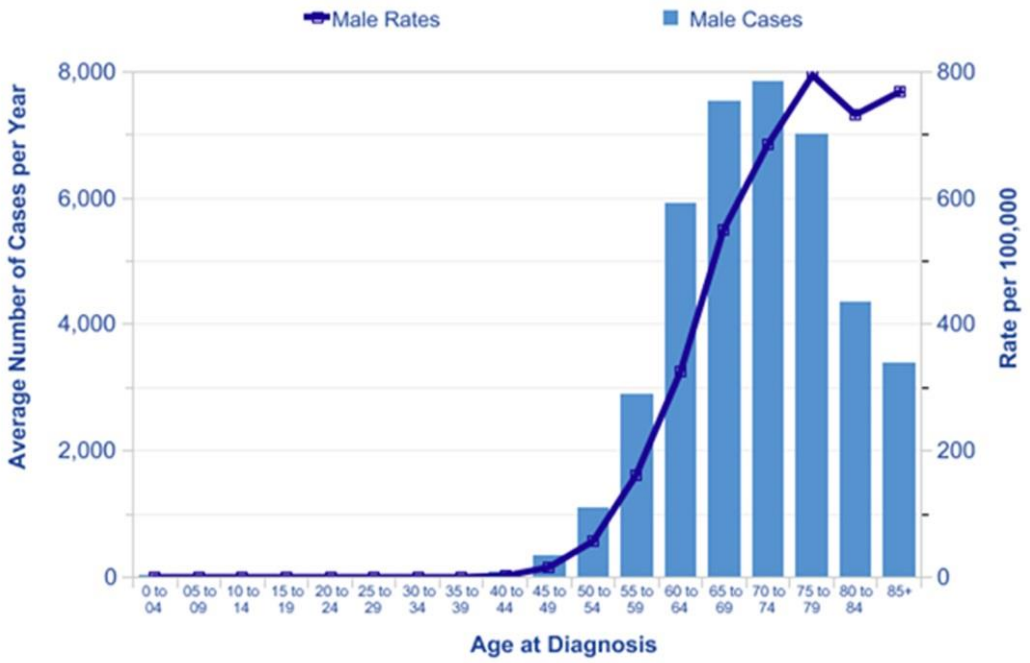

Figure 1.4 - Age related incidence of prostate cancer

Graph showing the average number of new prostate cancer cases per year and the age specific incidence within UK men between 2008 and 2010 (Cancer Research UK CancerStats, 2012)

1.2.1.3 Family history

Familial susceptibility was first associated with prostate cancer in the 1950's, however it was not until the early 1990's that the concept of hereditary prostate cancer was established and susceptible loci identified (Steinberg *et al* 1990, Carter *et al* 1992a). Two familial susceptibility loci have been mapped to the X chromosome, region 1q (Smith *et al*, 1996, Xu *et al* 1998). Through linkage analysis, subsequent research has highlighted several other susceptible chromosomal loci, though there are many contradicting studies in the literature (Table 1.2).

Hereditary factors account for approximately 10% of diagnosed prostate cancer cases and are generally associated with early disease onset (Carter *et al* 1992a, Carter *et al* 1993). The risk of prostate cancer increases approximately two-fold for men with a first degree relative with prostate cancer, showing a stronger familial component than colon and breast cancer (Carter *et al* 1993, Bostwick *et al* 2004). This risk is further increased if relatives were diagnosed before the age of 60 years or if more than one first degree relative has been diagnosed (Gronberg *et al* 1999, Bratt *et al* 1999, Cotter *et al* 2002). Several epidemiological studies have indicated that the risk of developing prostate cancer is stronger in brothers than it is in sons, suggesting environmental factors may also have a strong role (Narod *et al* 1995, Lesko *et al* 1996, Cerhan *et al* 1999, Bratt 2002, Bratt *et al* 2002). Also based on these observations a strong X-linked recessive inheritance has been suggested to affect some families.

Several studies report an increased incidence of prostate cancer linked to men who have a first degree female relative with breast cancer (Thiessen 1974, Rodriguez *et al* 1998), though this remains contentious.

Table 1.2 – List of the main loci linked to prostate cancer (info from OMIM, Bratt 2002 and Brown *et al* 2004)

Loci	Association	Chromosomal location	Reference(s) in favour	Reference(s) against
HPC1	Increased copy number in advanced prostate cancer specimens, not strongly linked with sporadic disease	1q24 – 25	Smith *et al* 1996, Cher *et al* 1996,	Ahman *et al* 2000, Latil *et al* 1997
PCaP (HPC8)	Pre-disposition to develop prostate cancer	1q42.2-43	Berthon *et al* 1998, Cancel-Tassin *et al* 2001b	Berry *et al* 2000a, Bergthorsson *et al* 2000
CAPB	Early onset of prostate cancer	1p36	Gibbs *et al* 1999	Berry *et al* 2000a, Suarez *et al* 2000
HPCX	Recessive inheritance	Xq27-28	Xu *et al* 1998, Farnham *et al* 2005	Bergothorsson *et al* 2000, Hsieh *et al* 2001
HPC3 (HPC20)	Later onset of disease	20q13	Berry *et al* 2000b, Zheng *et al* 2001, Bock *et al* 2001	Cancel-Tessin *et al* 2001a
MSR1	Susceptibility to developing prostate cancer in both European and African-American men	8p23-p22	Latil and Lidereau 1998, Xu *et al* 2001, Xu *et al* 2002, Maier *et al* 2005	Wang *et al* 2003, Maier *et al* 2006

1.2.1.4 Diet

Dietary components have also been proposed to have a role in prostate cancer incidence (Nelson 2003). Dietary differences among racial groups, socio- economic classes and geographic locations may contribute for some differences seen in prostate cancer epidemiology and biologic behaviour (Whittemore *et al* 1995, Crawford 2009). Gaziano and Heenekens (1995) found a positive association between prostate cancer risk and fat intake, especially polyunsaturated fat. Other studies have identified that obese men may be more susceptible to developing prostate cancer. Japanese men consume a relatively low-fat diet, however as the fat content of the Japanese diet has increased towards Western levels, the incidence of prostate cancer has also increased (Marks *et al* 2004). Early detection efforts and detection bias may account for some of this, though it is unlikely to account for all.

Many vitamins have also been associated with prostate cancer risk (Bostwick *et al* 2004). Vitamin D deficiency has been implicated in prostate cancer development, as the hormonal form, 1-25-dihydroxyvitamin D, exhibited anti-proliferative and anti-differentiative effects on prostate cancer cells as well as inhibiting cancer cell invasiveness (Bostwick *et al* 2004). Whilst a prospective study into the active form of Vitamin D, 1,25-dihydroxycholecalciferol, found an association between low serum levels and an increased risk of prostate cancer in elderly men, however, this did not translate to lower age groups (Corder *et al* 1993). The retinoids, including vitamin A, have also been shown to help regulate epithelial cell differentiation and proliferation, and therefore may also have a positive association with prostate cancer risk (Bostwick *et al* 2004, Tang and Gudas 2011).

Many other studies have been conducted to examine the influence of dairy intake, red meat consumption and prostate cancer incidence (Rodriguez *et al* 2006, Park *et al* 2007b). Initially believed to be associated with the fat content of dairy products, a

more recent hypothesis is that the increased dietary calcium levels may suppress production of 1-25-dihydroxyvitamin D thereby increasing the risk of prostate cancer (Chan and Giovannucci 2001, Rodriguez *et al* 2003, Giovannucci 1998).

This field however remains controversial and several studies have been conducted to analyse the prophylactic effects of vitamin supplements. As an antioxidant, Vitamin E (α-tocopherol) has been shown to inhibit prostate cancer cell growth through apoptosis (Fleshner *et al* 1999). In a large, controlled clinical trial in Finland a daily intake of Vitamin E was shown to decrease the risk of prostate cancer by 32% (Heinonen *et al* 1998, Knekt *et al* 1988).

1.2.2 Grading and staging system

At time of diagnosis, prostate carcinomas are scored, based on histological patterns using the Gleason grading system, first described in 1966 (Figure 1.5) (Gleason 1966). Morphologically heterogeneous, prostate cancer behaves in accordance with the average morphology; therefore the two dominant grades are identified and combined to arrive at the reported total Gleason score (Table 1.3). As most lesions are multifocal, the most prominent histological pattern is assigned grade 1-5, whilst the other grade is assigned to the second most common pattern (Table 1.4) (Humphrey 1994).

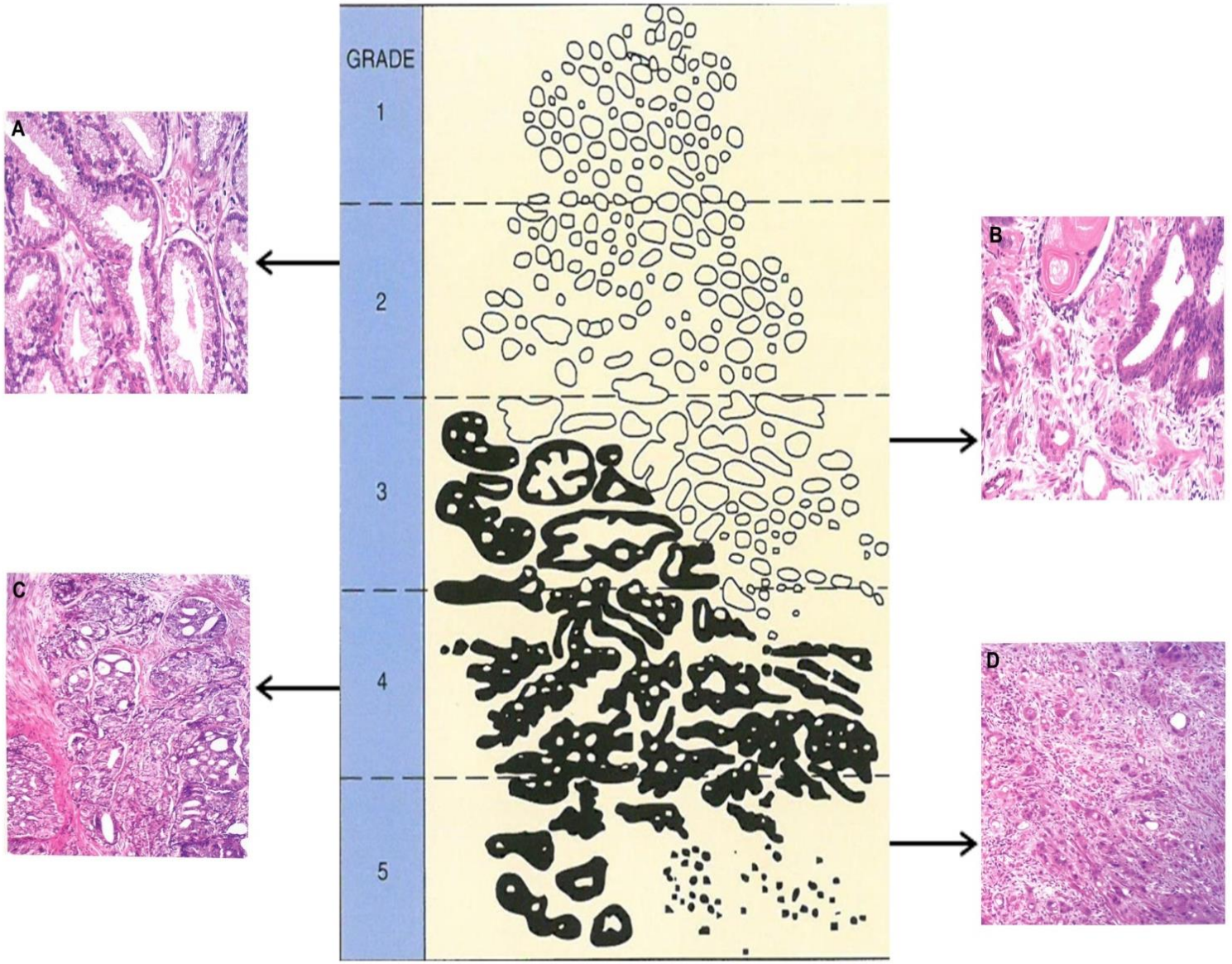

Figure 1.5 – Prostate Cancer Staging

Visual of the Gleason grading system devised between 1960 - 1975. Patterns were arranged into five grades with numbers corresponding to increasing malignancy determined by mortality data.

Histology specimen of Gleason grade 2 (A), Histology of Gleason grade 3 specimen (B), Histology of Gleason grade 4 specimen(C) Histology of Gleason grade 5 (D)

(Adapted from Kirby 2003)

Table 1.3 – Total differentiation scores of prostate cancer (adapted from Che and Grignon 2002)

Total Grade classification	Differentiation
5-7	Intermediate grade, moderately differentiated
8-10	High grade, poorly differentiated

Table 1.4 – Descriptions of the histology observed for each grade of the Gleason scoring system (adapted from Che and Grignon 2002)

Gleason Grade	Description
1	Acini which are consistent in size and well defined nodules
2	Closely packed acini, less consistent in size
3	An irregular mass of malignant acini typically small and angular which have started to infiltrate benign acini
4	Malignant acini have fused to form irregular masses
5	Sheets of anaplastic malignant cells with little evidence of gland formation

1.2.3 Screening and detection

In most cases prostate cancer is slow growing and therefore may not result in clinical symptoms during a patient's lifetime. However, tumours are frequently detected due to routine testing which can result in unnecessary clinical intervention causing adverse effects on the patient (Berry *et al* 1984, Holman *et al* 1999, Lilja *et al* 2008). When aggressive prostate cancer does progress it results in a burden to the patient's health which translates into increased morbidity and mortality. Therefore great effort continues to develop effective detection markers, schemes and accurate prognostics which might be able to distinguish between indolent and aggressive prostate diseases (Abate-Shen and Shen 2000, Berrruti *et al* 2005).

Currently the Prostate-Specific Antigen (PSA) test and the Digital Rectal Examination (DRE) are used as primary screening tools whilst Transrectal Ultrasound-guided biopsy (TRUS) is performed to confirm diagnosis.

1.2.3.1 Guidelines for screening and early detection

Efforts continue to educate men regarding the benefits and limitations of early detection and treatment of prostate cancer to enable them to make informed decisions about testing (Heidenreich *et al* 2011b). Within the UK and other parts of the developed world, experts disagree on the usefulness of the PSA test (Detchokol and Frauman 2011). Alongside this, the economic burden and adverse effects of overtreatment mean that there is no widespread screening programme for prostate cancer. However, the American Cancer Society recommends PSA tests and DRE for men over 50 years old who have at least a 10-year life expectancy (Ulmert *et al* 2008).

A recent study in the USA (Prostate, Lung, Colorectal and Ovary trial (PLCO)) found that there was no correlation between annual PSA and DRE assessments and a decline in mortality rates compared to those who had standard treatment with some monitoring (Andriole *et al* 2005, Andriole 2009, Andriole *et al* 2009). A similar large randomised study conducted in Europe (European Randomised Study of screening for Prostate Cancer (ERSPC)) initially supported the findings of the PLCO study. However more recent retrospective analysis from the ERSPC has shown that the relative risk of prostate cancer metastases and prostate cancer specific mortality was significantly lower in the screening arm than in the control group (Djavan 2011).

For men in high risk groups, the American Urological Association recommends PSA testing should begin as early as 45 years, especially amongst African-American men with a first degree relatives diagnosed with prostate cancer before the age of 65 years (Dunn and Kazer 2011).

1.2.3.2 Prostate-Specific Antigen (PSA) test

Elevated serum PSA levels have been associated with prostate cancer and therefore PSA is used as the standard screening tool for disease detection (Dimakakos *et al* 2014). However, BPH, inflammation, TRUS, biopsy and transurethral prostatectomy also increase serum PSA levels, and thus its role as a specific marker for detecting prostate cancer remains under intense scrutiny (Stamey *et al* 1987, Hernandez and Thomson 2004, Ablin and Piana 2014). In men displaying elevated serum levels of PSA, 30-50% of cases were associated with BPH whilst only 25% of cases were prostate cancer related (Andriole Jr 2012, Schroder 2009). Further evidence has also demonstrated that serum PSA levels can be affected by several drugs including 5α-reductase inhibitors such as finasteride (Thompson *et al* 2006). PSA serum levels detected within the range of

2.6-4.0ng/ml are associated with tumours that are generally significantly smaller and organ confined, compared with tumours detected when PSA serum levels are greater than 4.0ng/ml (Krumholtz *et al* 2002). However serum levels of PSA do not correlate to tissue PSA expression levels at any stage of prostate cancer (Qiu *et al* 1990). Whilst there is a lack of evidence, it is hypothesised that elevated serum PSA levels may be due to the loss of architecture in the normal prostate, which is integral to confining it to the prostate gland (Lilja *et al* 2008). Based on this theory it is serum PSA levels which are used to direct which management strategy is recommended for patients. For those who have a serum PSA level of less than 10ng/ml and low grade tumours active surveillance is recommended. However in patients with serum PSA levels of 10-20ng/ml and a life expectancy of 10 years radical prostecomy is indicated (Heidenreich *et al* 2011).

To improve the utility of the PSA test, increased specificity and sensitivity for prostate cancer parameters such as PSA velocity or PSA density have been proposed and explored. Carter and colleagues found that a PSA velocity increase of 0.75ng/ml/annum was significantly associated with clinical prostate cancer (Carter *et al* 1992b). More recent data highlights that these approaches have limited additional diagnostic use to the stand-alone PSA test as definitive diagnosis of prostate cancer still required needle biopsy of the prostate (O'Brien *et al* 2009, Vickers *et al* 2009, Lilja *et al* 2008).

1.2.3.3 Other tumour markers

Clinicians, pharmaceutical companies and research laboratories around the world continue to strive to identify new, specific and sensitive markers for prostate cancer. The best markers would have the potential to distinguish between BPH, PIN, indolent and malignant cancer with high sensitivity and specificity (Chodak 2006).

Potential tests should use a selection of positive and negative markers whilst also being easy to use, inexpensive, non-invasive and quick to analyse (Chodak 2006). Varambally *et al* (2005) showed that, in prostate cancer tissue samples, the equivalence between RNA transcript levels and protein products ranged between 48% and 62%. This has resulted in more focused efforts to identify protein biomarkers involved in prostate cancer development.

Prostate cancer antigen 3 (PCA3), is one of the most promising candidates to emerge. PCA3 RNA has been measured in urine sediment after prostatic massage (Deras *et al* 2008). Testing this biomarker as a prostate cancer marker currently continues to be experimental and data looks promising at a population level, however, using this test for isolating those patients more susceptible to aggressive disease remains questionable (Heidenreich *et al* 2011).

Similarly, TMPRSS2:ERG gene fusion is frequently present in 50% of prostate cancer cases but is not detected in normal prostate tissue or BPH (Cerveira *et al* 2006, Park *et al* 2010, van Leenders *et al* 2011). Non-invasive detection of this gene fusion has been achieved using real-time PCR on urinary sediment, with 93% specificity, for prostate cancer (Dimakakos *et al* 2014). This is a potential diagnostic candidate for the future, as it can also be used in combination with other markers (Hessels *et al* 2007, Salami *et al* 2013).

1.2.3.4 Metastatic disease detection

Autopsy data has shown that 90% of the metastatic prostate cancer cases metastasised to the bone, whilst the other 10% of detected metastases sites were in organs such as the lungs and liver (Bubendorf *et al* 2000). Hess *et al* (2006) concluded from their study, for 86% of patients, bone metastases were the only detected metastatic site. This, combined with a study which demonstrated an

inverse relationship between spine and lung metastases, indicates the possibility of two independent metastatic patterns (Thobe *et al* 2011). Despite a variety of studies there remains no way of predicting the sub-group of prostate cancer patients which are at high risk of developing metastatic disease (Briganti *et al* 2014).

Based on current clinical data from the European Association of Urology and European Society of Medical Oncology the combination of an increased PSA (≥15-20ng/ml) and a high biopsy Gleason score (>7) enhances the possibility and presence of bone metastases (P<0001) and dictates a bone scan and an MRI or CT for the possibility of soft tissue metastases (Crawford *et al* 2013). Primarily, diagnosis of bone metastases relies on radioactive bisphosphonates such as technetium-99m methylene-diphosphonate and conventional x-ray, though more modern approaches such as positron emission tomography-computed tomography (PET-CT) are providing more specific and sensitive screening, but are also associated with greater financial costs (Tombal and Lecouvet 2012).

Nuclear scintigraphy has the ability to reveal bone metastases significantly earlier than that of conventional x-ray. For a reliable method of detecting and monitoring bone metastases nuclear medicine is used, however, upon detection of metastatic bone disease; treatment options remain limited (Storey and Torti 2007).

1.2.4 Management

Treatment of localised prostate cancer disease has made major advances in the last decade. If the cancer is detected at an early stage prior to it metastasising it can often be treated successfully by surgery or local irradiation, potentially curing the patient (Chambers *et al* 2002). Yet despite recent advances in bone targeted therapies, half of metastatic prostate cancer patients will die from the disease within 30-35 months as treatment plans still do not ultimately prevent the formation of new

bone lesions, further morbidity and disease progression (Buijs and van der Pluijm 2009, Suva *et al* 2011).

Patients who do not initially present with metastases at the time of primary diagnosis may already have metastases, though they may not be clinically apparent, which can further complicate therapy (Buijs and van der Pluijm 2009). Data has shown that in castration-resistant prostate cancer patients with no identifiable metastases at time of diagnosis, 33% developed bone metastases within 2 years (Smith *et al* 2005).

1.2.4.1 Treatment of localised disease

The approach taken to treat localised prostate cancer disease varies greatly based on the harm-balance benefits to the patient. Advances are constantly being made in this area, attempting to minimise adverse effects on the patient both during therapy and with potential long term complications. The current main stays of prostate cancer treatment include surgery or localised irradiation (Table 1.5).

1.2.4.2 Treatment of advanced disease

Prostate cancer can be considered a chronic disease if treatments have slowed disease progression. However if the disease has metastasised currently further therapeutic interventions are rarely curative. Until recently the main-stay of metastatic prostate cancer treatments have focused on targeting the tumour cells by using androgen ablation or cytotoxic therapies. However, as understanding of the disease and the bone microenvironment has evolved newer, more selective targeted therapies have emerged. Despite this, treatments so far have only had modest effects on patient survival (Ye *et al* 2007).

Table 1.5 – List of main management options of localised prostate cancer (Adapted from prostatecanceruk.org)

	Treatment	Approach
Monitoring	Active surveillance Watchful waiting	Long term monitoring of slow growing prostate cancers which may never progress or cause symptoms
Surgery	Radical prostatectomy	Operation to remove the prostate gland. Suitable for patients where cancer is contained within the gland but otherwise healthy
	Cyrosurgery	Using freeze thawing to kill cancer cells in the prostate.
Therapies	Permanent seed brachytherapy	Implant of a radioactive seed into the prostate gland. Can be used in combination with external beam radiotherapy and hormone therapy
	Hormone therapy	Helps control prostate cancer by stopping the hormone testosterone from reaching the prostate cancer cells. Not curative but helps to manage symptoms Can be used in combination with brachytherapy or radiotherapy
	Temporary brachytherapy	Insertion of a high dose rate radiation for very short periods of time
	External beam radiotherapy	Uses high energy x-ray beams to treat prostate cancer. Can be used in combination with permanent or temporary seed brachytherapy or after surgery
	High intensity focused ultrasound	Uses high frequency ultrasound waves. Newer therapy, long term effects remain unknown

Transition to metastatic disease includes local invasion into the seminal vesicles, followed primarily by the development of bone metastasis. The disturbance to normal bone turnover associated with bone metastases leads to debilitating skeletal-related events (SREs) including intractable pain, pathological fracture, spinal cord and nerve compression and hypercalcaemia (Coleman 2006).

During all stages of prostate cancer, patients may suffer from generalised bone loss or localised decreases in bone integrity, as lower bone mineral density has been reported in hormone therapy naïve patients with early stage prostate cancer (Saad *et al* 2004). The risk with the current first line treatments for advanced disease is that most are associated with accelerated bone loss, a process which can contribute to SREs particularly to increased risk of fractures (Ye *et al* 2007).

Androgen deprivation therapy, the most common intervention for prostate cancer treatment, is achieved by surgical ablation (orchiectomy) and/or pharmacological inhibition of gonadotrophin signalling *e.g.* luteinising-releasing or gonadotropin-releasing hormone agonist. There has been strong evidence to support the idea that androgen deficiency can increase osteoclast-mediated bone resorption and affect the bone microenvironment, which may ultimately increase the risk of bone metastasis (Ye *et al* 2007). Initially, 75-80% of metastatic prostate cancer cases respond to androgen ablation therapy, which can help to alleviate bone pain, however this is only a palliative measure because the metastatic prostate cancer will eventually lethally progress, with hormone resistance (Ye *et al* 2007).

Recent advances in hormone therapy have led to the approval of Abiraterone and Triptorelin, from NICE, for the treatment of advanced prostate cancer which had stopped responding to other hormone therapies. Both therapies, by blocking the synthesis of testosterone, result in decreases in serum PSA levels and reductions in tumour size (Attard *et al*., 2008, Reid *et al* 2010, Ploussard and Mongiat-Atrus

2013). Abiraterone has also been approved for use in combination with the chemotherapy agent prednisolone.

After the development of hormone resistant prostate cancer, the systemic line of therapy is chemotherapy. A combination of docetaxel and prednisolone is now the standard of care for hormone resistant prostate cancer patients (Berthold *et al* 2005, Berthold *et al* 2008). Other ongoing clinical trials combining other chemotherapy agents such as calcitriol in combination with docetaxel are also underway (Beer *et al* 2007, Scher *et al* 2011). Though the signs are encouraging, survival benefits remain modest and more effective alternatives continue to be sought (Ye *et al* 2007).

For the majority of patients, external beam radiotherapy or radiopharmaceuticals provide palliation for localised metastatic bone pain (Storey and Torti 2007). Radiation therapy can temporarily control bone pain in 50-90% of treated patients and may prevent bone lesion progression, although repetitive treatments can result in cumulative toxicities. Strontium-89 is the prototypic example of a wide field bone targeted radioisotope, functioning as a calcium analogue, preferentially taken up at sites of bone formation (Porter *et al* 1993). As it subsequently decays over time, radioactive β particles are emitted throughout the tumour-bone microenvironment (Coleman 2001b, Storey and Torti 2007). Samarium-153 has also been shown to be preferentially taken up at sites of bone formation; emitting both β and γ particles whilst also having significant effects on bone pain and analgesic consumption (Coleman 2001b).

The most successful strategy for targeting bone metastasis or preventing bone loss induced by other therapies targeting prostate cancer is the use of bisphosphonates, such as zoledronate, which are generally well tolerated in long term use and can be co-administered with chemotherapy agents (Saad *et al* 2004, Taichman *et al* 2007).

Bisphosphonates, as analogues of pyrophosphates, target the bone remodelling process directly by inhibiting osteoclast maturation and function (Taichman *et al* 2007). Much debate still remains on the optimum time to administer bisphosphonates to prostate cancer patients (Coleman 2001c, Storey and Torti 2007).

1.2.4.3 Therapies in trial

The unique pattern of metastases associated with prostate cancer, has resulted in rapid identification and exploration of potential therapeutic targets which might be capable of disrupting interactions between prostate cancer cells and the bone (Storey and Torti 2007). New approaches being explored include targeting specific pathways using synthetic peptides or immunotherapy (Table 1.6). Unfortunately, despite the advances in prostate cancer therapy and the continued identification of potential new targets, prostate cancer still remains one of the major leading causes of death for men in developed countries. Therefore a better understanding of the aetiology of prostate cancer and the co-operation between the bone niche and prostate cancer cells may help to drive future therapeutics.

Table 1.6 – List of main targets being investigated to treat prostate cancer (adapted from Taichman *et al* 2007 and Deng *et al* 2014)

Cell type		Target	Sample agent	References
Prostate cancer cell		Aberrant growth factor receptor activation	EGFR: gefitinib; PDGFR: imatinib; IGF1R:A12; IL-6: CNT0328	Craft *et al*1999, Bajaj *et al* 2007, Wu *et al* 2006, Wallner *et al* 2006
		Bcl-2	AT101	Wang *et al* 2006
		Microtubules	Ixabepilone halichondrin	Tan 2006, Calabro and Stenberg 2007, Berthold *et al* 2005
		DNA replication	Satraplatin	Oh *et al* 2007
		Histone deacetylase	Vorinostat	Marrocco *et al* 2007
		Proteasome	Bortezomib	Ikezoe *et al* 2004
		mTOR	Rapamycin analogs	Majumder and Sellers 2005
		Clusterin	OGX-011	Miyake *et al* 2006
		Proliferative agents	Calcitriol, DN-101	Beer *et al* 2007
Bone	**Bone Formation**	Endothelin-1 receptor	Atrasentan, Zibotentan	Carducci *et al* 2007, Nelson *et al* 2012
	Bone resorption	Pyrophosphate	Zoledronic acid, Clondrate	Prakash and Gautam 2013, Rodrigues *et al* 2011, Dearnaley *et al* 2009
		RANKL	Denosumab, OPG-Fc, RANK-Fc	Fizazi *et al* 2011, Smith *et al* 2012, Virk *et al* 2011, Miller *et al* 2008, Whang *et al* 2005
		SRC	Daatinib, Saracatinib, Bosutinib	Yu *et al* 2009, Rabbani *et al* 2010,
Endothelial cell		VEGF	Bevacizumab. VEGF-TRAP	Ryan *et al* 2006, Baka *et al* 2006, Roberts *et al* 2013
		VEGFR	Sunitinib, vatalanib, sorafenib	Flaherty 2007, Pantuck *et al* 2007
		$A_v\beta_{3/5}$ integrin	Cilengitide	Eskens *et al* 2003
		Permeability	Dimethylxanthenone	Seshadri *et al* 2007

1.3 Biology of prostate cancer

The development of prostate cancer, and progression to an androgen independent (hormone refractory) disease, is a complex process that involves many alterations in multi-step signalling pathways. Molecular components of these pathways include cell signalling, cell cycle, cell survival/apoptotic molecules and angiogenic factors which can be affected by activation of oncogenes or loss-of-function of tumour suppressor genes. Better understanding of molecular traits and somatic alterations, which promote neoplastic prostate growth and drive formation to incurable prostate cancer, have the potential to result in more specific and sensitive screening tests and targeted therapies.

1.3.1 Androgens, transcription factors and receptor sensitivity

Androgens and AR signalling are vital for all prostate cellular functions and architectural maintenance. Androgens, usually in the form of DHT bind to receptors in the cytoplasm causing the receptor-ligand complex to translocate to the nucleus, these engage with androgen responsive elements in promoter regions of target genes, which directly or indirectly stimulate proliferation and inhibit apoptosis (Heemers and Tindall 2007). Transcription factor Forkhead box A1 (FOXA1) is a co-activator for AR, facilitating AR accessibility to chromatin, and regulates expression of AR target genes (Lorente and De Bono 2014). Androgen ablation therapy coupled with AR antagonists is the standard therapy for disseminated prostate cancer; however, despite initially proving effective, recurrent hormone refractory prostate cancer, with disrupted AR signalling, is often detected (Balk and Knudsen 2008). Evidence suggests that the mechanisms of androgen independence can either involve or bypass the AR, with potential for both mechanisms to co-exist in prostate cancer (Linja *et al* 2001, Tomlins *et al* 2006b). These different outcomes

can be achieved by AR amplification, AR hypersensitivity or through AR mutations (Feldman and Feldman 2001).

Testosterone, DHT and AR signalling have also been shown to play active roles in prostate tumour growth and early stage cancer progression, though not autonomously, and thus remain a major area of research focus (Heemers and Tindall 2007, Balk and Knudsen 2008).

Epidemiologic studies suggest that AR polymorphisms may contribute to the clinical behaviour of prostate cancer. Studies indicate that individuals with fewer than 18 CAG repeats in exon 1 of the AR gene show a two-fold increased risk of developing advanced-stage prostate cancer compared to those with greater than 26 CAG repeats (Giovannucci *et al* 1997, Standford *et al* 1997). A point mutation in codon 877, in the hormone binding site, of AR has been shown to alter receptor specificity allowing for activation by several steroid hormones (De La Taille *et al* 2001).

Immunohistochemistry staining has revealed heterogeneous AR distribution, becoming more variable with higher grade tumours (De La Taille *et al* 2001). Approximately 30% of tumours which become androgen independent have amplified AR gene expression and upregulated AR expression, a response almost exclusively seen in recurrent hormone refractory disease (Feldman and Feldman 2001). AR sensitivity has also been linked to prostate cancer progression, involving increased stability and enhanced nuclear localisation of AR in recurrent cells *in vivo*. This was coupled with hypersensitivity to DHT for growth stimulatory effects compared to androgen dependent cells (~4 times lower) (Feldman and Feldman 2001).

Several proteins can activate AR directly or indirectly which alter the expression and activity of these regulatory proteins also contributing to the androgen-independent state associated with lethal prostate cancer progression. Epidermal growth factor

(EGF), insulin-like growth factor-1 (IGF-1) and keratinocyte growth factor have all been shown to stimulate transcription of reporter genes driven by AR-responsive elements in the absence of androgen, whilst Protein kinase A and HER2/neu have also been shown to induce the expression of AR-responsive genes such as PSA, independent of androgen (Feldman and Feldman 2001).

1.3.2 Oncogenes

1.3.2.1 Receptor tyrosine kinases (EGFR and HER2/neu)

Acting as a mitogen for normal prostate epithelial cells, EGFR is also highly expressed in prostate cancer cells (Peehl *et al* 1989, Fowler *et al* 1988). Activation of EGFR signalling is linked to increased cell proliferation, malignant transformation and progression (Mansour *et al* 1994, Magi-Galluzzi *et al* 1997, Gioeli *et al* 1999). Increased EGFR expression also correlates with disease relapse and progression to the androgen-independent state (Di Lorenzo *et al* 2002).

HER2/*neu* is a transmembrane glycoprotein containing a tyrosine kinase domain structurally related to the EGFR superfamily, with overexpression linked to breast and ovarian cancer progression (Di Lorenzo *et al* 2004). Results implicating HER2 in prostate cancer have been contradictory (Scher 2000). Increased expression of HER2, associated with *HER2* gene amplification, has been found in some prostate tumours, though less frequently in localised prostate cancer (Mellon *et al* 1992, Kuhn *et al* 1993, Ross *et al* 1997, Kallakury *et al* 1998, Mark *et al* 1999). Several studies have also linked increased HER2 overexpression with disease progression, including a switch from androgen dependence to androgen independence (Signoretti *et al* 2000, Osman *et al* 2001, Di Lorenzo *et al* 2004). Jorda *et al* (2002) found that HER2 over expression was present in as many as 60% of patients with hormone refractory prostate cancer correlating with decreased survival, whilst Di

Lorenzo *et al* (2004) also showed a potential link between relapsed patients and HER2 expression levels.

1.3.2.2 MYC

The *MYC* oncogene is a transcription factor that has pleiotropic effects on cell growth and differentiation and amplification or overexpression of c-MYC is found in many human cancers including prostate cancer (Shen and Shen 2010). The chromosomal region 8q24, encompasses the *MYC* gene, a locus which is often found amplified in prostate cancer, with amplification significantly higher in metastatic disease compared to primary disease correlating with disease progression, increasing Gleason score and poor prognosis (Fleming *et al* 1986, Buttyan *et al* 1987, Gburek *et al* 1997, Nupponen *et al* 1998, Sato *et al* 1999). Recent evidence, of upregulation of nuclear *MYC* protein in PIN and prostate cancer, suggests that *MYC* upregulation may also be involved in prostate cancer initiation though this remains controversial (Jenkins *et al* 1997, Gurel *et al* 2008, Schrecengost and Knudson 2013).

1.3.2.3 TMPRSS2:ERG Fusion

Several studies have identified chromosomal rearrangements which activate the Erythroblast transformation specific (ETS) transcription factors of which ERG, ETV1 and ETV4 have been implicated in prostate cancer (Shen and Shen 2010). Approximately 50% of primary and metastatic prostate cancers contain a variation of this fusion which correlates with high tumour grade and poor prognosis (Mosquera *et al* 2007, Mosquera *et al* 2008, Demichelis *et al* 2007). The most common of these rearrangement fusions is the *TMPRSS2-ERG* fusion gene.

Fusions between the 5' untranslated region of TMPRSS2 and 3' exon of ERG, which occurs through unbalanced interchromosomal translocation, results in the N-terminal expression of truncated ERG protein with the androgen responsive promoter of *TMPRSS2* (Shen and Shen 2010). Though initially hypothesised to be involved in prostate cancer initiation due to evidence that *TMPRSS2-ERG* gene fusions first appear in late PIN lesions, subsequent *in vitro* and clinical data suggest that ETS fusions in prostate cancer may be involved in invasion and metastatic spread (Tomlins *et al* 2006a, Clark *et al* 2008, Mosquera *et al* 2008, Albadine *et al* 2009).

1.3.3 Tumour suppressor genes

1.3.3.1 p53

Somatic mutations in p53 have been identified in a diverse range of cancers, typically resulting in reduced cell-cycle control and increased genetic instability (De La Taille 2001). The prevalence of detected *p53* mutations in prostate cancer varies between different studies, it is clear that mutations are rare events in localised prostate cancer (25-30% of cases), however, become more frequent in advanced, metastatic and hormone refractory tumours (Navone *et al* 1993, Bookstein *et al* 1993, Viskorpi *et al* 1992, Barbieri *et al* 2013). For example, p*53* mutations were found in as many as 75% of prostate cancer associated bone metastases, identifying that this subgroup of patients having a worse prognosis (Navone *et al* 1999, Bauer *et al* 1995).

1.3.3.2 Phosphatase and Tensin Homologue

The Phosphatase and Tensin Homologue (PTEN) gene located on chromosome 10q23 is one of the most commonly mutated tumour suppressor genes in cancer (Barbieri *et al* 2013). In prostate cancer the region containing PTEN is a frequent target of mutations and deletion in both primary and metastatic disease. Approximately 70% of primary prostate cancers have PTEN mutations or alterations resulting in loss of function correlating with high tumour grade. Whilst allelic deletion of PTEN is a frequent occurrence seen in metastatic disease (Li *et al* 1997, Vliestra *et al* 1998, Whang *et al* 1998, Tomlins *et al* 2006b, Attard *et al* 2009, Choucair *et al* 2012). In addition to prostate cancer, mouse models have demonstrated that PTEN loss also alters AR signalling and cellular response to therapy and therefore may be a key determinant in the formation of androgen independent advanced disease (Schrecengost and Knudson 2013).

1.3.3.3 NKX3.1

NKX3.1 transcription factor is a member of the NK subfamily of homeobox genes, which has been instrumental in prostatic bud formation. Whilst the *nkx3.1* gene has been shown to be androgen regulated, *in vivo* studies suggest alternative mechanisms of expression exist during prostate development (Bhatia-Gaur *et al* 1999, Schrecengost and Knudson 2013). Down regulation of the *nkx3.1* gene, located on chromosome 8p12-22, is one of the most frequent chromosomal aberrations in prostate cancer and is believed to be critical in prostate cancer initiation (Bova *et al* 1993, Macoska *et al* 1995, Abate-Shen *et al* 2008). Frequency of LOH at region 8p21.2 has been detected in up to 50% of primary prostate cancers and 80% of metastatic cancers correlating with increased tumour grade. However, evidence suggests the remnant *nkx3.1* allele remains unaffected

(Emmert-Buck *et al* 1995, Vocke *et al* 1996, Swalwell *et al* 2002, Bethel *et al* 2006, Schrecengost and Knudson 2013). This possibly highlights that reduction rather than loss of NKX3.1 expression is involved in cancer progression (Shen and Shen 2010).

These factors in isolation all have their merit, but when combined with other altered pathways their lethality becomes apparent. For example loss of both p53 and PTEN increases tumour progression rate, whilst over expression of HER2 confers poor prognosis in those patients who also have low PTEN expression (Martin *et al* 2011, Ahmad *et al* 2011).

1.4 Metastasis

Metastases are responsible for 90% of human cancer deaths due to the resultant impairment of multiple vital organs (Hanahan and Weinberg 2000, Weigelt *et al* 2005). In spite of the significant advances in cancer diagnosis, surgical techniques and therapies, most metastases still remain resistant to conventional therapies and patient prognosis remains little improved from decades ago (Fidler 2003b, Sporn 1997). The main clinical obstacle to treating cancer metastases is the biological heterogeneity between the primary cancer and its metastases, which is further hindered by the evidence of co-existence of sub-groups of cell types within a tumour (Fidler 2003a, Talmadge and Fidler 2010). A better understanding into the pathogenesis of metastases at systemic, cellular and molecular levels and the many genetic and biochemical determinants that drive this process must be identified (Mehlen and Puisieux 2006). This approach may further promote the development of more targeted metastatic therapies which focus on the potential metastatic site(s) as well as the tumour cells themselves.

1.4.1 Theories

In 1889 Stephen Paget, an English surgeon, published an article in *The Lancet* describing the susceptibility of various types of cancer to form metastases in specific organ patterns from autopsy studies (Paget 1889). In fatal breast cancer cases, Paget observed that high incidence of metastases were occurring in the livers, ovaries and specific bones, however not in the spleen (Paget 1889). Paget proposed that these non-random patterns were due to the dependence and affinity the cancer cell (seed) may have on the secondary organ site (soil). This contradicted the prevailing Virchow theory that metastasis was the result of tumour cell arrest and emboli formation in the vasculature (Virchow R 1858). In the 1920's Paget's theory was challenged by James Ewing (Ewing J, 1928), who suggested that circulatory patterns and mechanical factors between a primary tumour and specific secondary organs were sufficient to account for organ-specific metastasis. However, more recent research suggests that these theories are not mutually exclusive and that there is validity for each of the proposed theories in the metastatic spread of cancer (Fidler and Kripke 1977, Hart and Fidler 1980).

1.4.2 Metastatic Cascade

Successful metastasis to distant organs requires a series of co-ordinated, complex interrelated processes, all of which must be successfully completed for establishment of a secondary tumour at a distant site from the disseminating primary cancer (Figure 1.6).

In principle, the core metastatic events are the same for all tumours, including the development of a vascular network (angiogenesis) and invasive potential, evasion of the immune response and ability to respond and colonise organ specific environments (Fidler *et al* 1978, Price *et al* 1988). This predisposition arises from

specific molecular signals and interactions extensively supported by disseminated tumour cells' autocrine effects, host responses and organ microenvironments (Talmadge and Fidler 2010). Initially, local invasion at the primary site together with angiogenesis must occur for the tumour to survive. During this process, sub-populations of malignant cells down-regulate their cell-cell contacts and cell-matrix adhesive characteristics, become motile and acquire the ability to breakdown the extra-cellular matrix (ECM) by the production of various proteolytic enzymes such as matrix metalloproteinases (MMPs), tissue serine proteinases and adamalysin-related membrane proteases (ADAMs). Once the malignant cell(s) has reached the interstitium it enters the vascular and lymph circulation through intravasation and undergoes distal migration (Bogenrieder and Herlyn 2003).

For site-specific establishment of metastases following migration and survival in the circulation, malignant cells arrest and attach to the endothelial lining. Extravasation, by breaching the endothelial barriers at secondary sites, allows the cancer cells to transmigrate into the new interstitium. Colonisation of this environment occurs allowing subsequent cancer cell proliferation, or dormancy, which will ultimately result in secondary tumour formation when the environment is favourable.

The metastatic process is highly inefficient with only 0.001-0.02% of cancer cells experimentally introduced into the circulation forming metastatic foci (Fidler 1970). Metastatic tumour cells also have the potential to undergo a period of dormancy, which may already have occurred in subgroups of patients presenting with primary disease, which can result in cancer recurrence after years or possibly decades of remission, even after primary cancer removal. Tarin *et al* (1984) and Kasimir-Bauer (2009), have demonstrated that, though there may be detectable tumour cells in patient circulation or bone marrow, which have potential prognostic implications, not all of these cells, if any, may result in metastatic foci, due to a number of factors including host response or tumour cell dormancy (Talmadge and Fidler 2010).

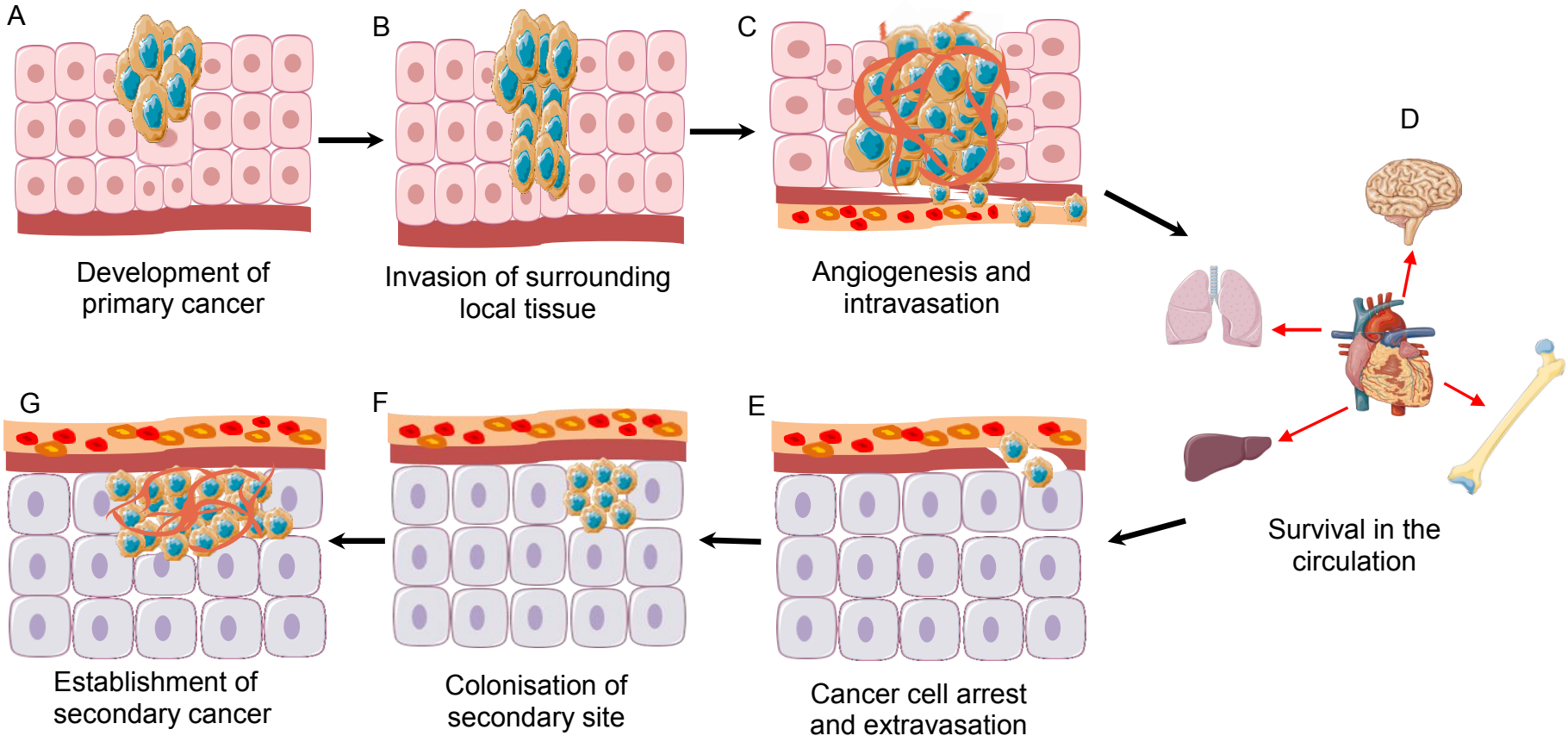

Figure 1.6 – Metastatic cascade
Representation of the processes that occur in the metastatic cascade, initially the primary tumour develops and invades local tissue supporting itself with blood vessel growth (A and B). Tumour cells invade the vasculature and enter the circulation (C and D), after which they settle and invade into a secondary site (E). Tumour cells colonise the new environment and adapt to the different stimuli to present as metastases (F and G). Adapted from Fidler 2003 and Talmadge and Fidler 2010

1.4.3 Factors implicated in the metastatic cascade

Extensive research effort continues to elucidate the factors which are involved in the successful formation of metastasis associated with all types of cancers and to develop targeted therapies which will block malignant cell growth without impairing healthy cells. The discovery of a variety of growth factors, chemo-attractants, signalling pathways and genes have made some major advances in our understanding of the metastatic cascade in recent years.

1.4.3.1 Cell proliferation and Survival

Tumour cells can inhibit intrinsic apoptotic pathways by upregulating apoptotic suppressors such as Bcl2, Bcl-X_L and simultaneously decreasing mitochondrial membrane disruption and cytochrome c release, or by down regulation of critical apoptotic inducers such as the caspases, in particular caspase-2, -3, -7 and -9 (Swanton *et al* 1999, Coffey *et al* 2001, Fiandalo and Kyprianou 2012). In lung cancer several caspase 9 polymorphisms have been identified which resulted in impaired caspase 9 activity and ultimately blocking apoptosis induction, however the role caspases play in prostate cancer still remains under investigation (Park *et al* 2006). Chemotherapy and radiotherapy can re-initiate this intrinsic apoptotic therapy by damaging mitochondria resulting in the release of apoptogenic factors including cytochrome c release (Johnstone *et al* 2002).

The extrinsic apoptotic pathway is a pathway which remains under intense investigation for novel anti-cancer therapies. This pathway is triggered by the activation of death receptors belonging to the Tumour Necrosis Factor (TNF) superfamily, which include Fas/APO1, TNFR and TRAIL (Jin and El-Deiry 2005). TRAIL mRNA expression, unlike most other family members, is not tightly regulated and has been constitutively detected in a range of tissues. It has been shown to

induce apoptosis through interaction with DR4 and DR5 receptors, which can be inhibited by DcR1, DcR2 and Osteoprotegerin (OPG) (Wiley *et al* 1995, Wu 2009). Most cancer cells are resistant to TRAIL induced apoptosis and evidence suggests if death receptor-mediated apoptosis is impaired, TRAIL may promote cancer cell proliferation and survival, but how this is achieved is yet to be fully elucidated (Ehrhardt *et al* 2003 , Baader *et al* 2005).

Of great relevance to prostate cancer and disease progression is the role AR can also play in modulating cell proliferation and apoptosis via several mechanisms. One of the most important contributors to the anti-apoptotic effects exerted by AR is p21, which has been proven to protect against p53 mediated apoptosis as androgens enhance the transcription of p21 (Wen *et al* 2014).

1.4.3.2 Lymph/angiogenesis

Tumour angiogenesis, whether it is an early pathological event or in response to hypoxia and nutrient deprivation, involves a complex interplay between pro- and anti angiogenic factors which influence tumour cells, endothelial cells and surrounding stroma (Mukherji *et al* 2013). Therefore targeting one aspect of this remodelling process may initially produce a response; however it does not guarantee that it will not promote another angiogenic response via a different pathway (Weis and Cheresh 2011). Several key factors have been identified in prostate cancer progression and metastasis, including vascular endothelial growth factor (VEGF), fibroblast growth factor (FGF) and hepatocyte growth factor (HGF) (Strohmeyer *et al* 2000, Doll *et al* 2001, Humphrey *et al* 1995). HGF can have direct effects on endothelial cell proliferation, migration and tubule formation whilst also inducing the expression of other pro-angiogenic factors such as VEGF, thus contributing to cancer progression (Ferrer *et al* 1997, Wojta *et al* 1999, Jiang *et al* 2005b).

1.4.3.3 Adhesion/De-adhesion to the ECM

An integral part of the metastatic cascade is the changing adhesive capabilities of cancer cells that dictate their interactions with the ECM and each other. The majority of cell-adhesion molecules which have been identified fall into one of three categories; integrins, immunoglobulin superfamily or the cadherins, all of which have been implicated in cancer metastases (Bogenrieder and Herlyn 2003).

Cell-matrix binding is largely mediated by integrins, a family of 24 heterodimeric binding proteins comprising α- and β-chain subunits which combine and ligate several ECM proteins (Hynes 2002). The integrin family have shown aberrant expression on a variety of tumour cells which contributes to their ability to mediate physical interactions with the ECM and regulate signalling pathways. Both of these are fundamental to cancer cell adhesion as well as pro-survival, proliferative, angiogenesis and control the actin cytoskeleton and cell movement essential for establishment of a secondary tumour at another site (Hynes *et al* 2002, Goel *et al* 2008).

Some of the integrin subunits implicated in prostate cancer progression are listed in Table 1.7. Integrin β_1 associates with many α subunits, some of which are up-regulated in prostate cancer, predominately as $\alpha_2\beta_1$ or $\alpha_6\beta_1$ (Fornaro *et al* 2001, Alam *et al* 2007). Goel *et al* (2005) has shown expression of β_{1A} integrin variant is upregulated and necessary for cancer cells to be able to grow in an anchorage-independent manner, suggesting that this integrin may be important in prostate cancer progression.

Some of the integrins best characterised for their role in prostate cancer progression have also been linked with the bone environment, and therefore may contribute to the osteotrophic nature of the disease progression, by aiding the settling of disseminating cancer cells. Zheng *et al* (1999) demonstrated that integrin $\alpha_v\beta_3$ was

up-regulated in prostate cancer cells compared to the normal prostate epithelium. The $\alpha_v\beta_3$ integrin has also been shown to interact with several bone derived factors including osteopontin (OPN), bone sialprotein (BSP), fibronectin and vitronectin and therefore influencing osteotrophic phenotypes in several cancer types, including breast and prostate (Sun *et al* 2007, McCabe *et al* 2007, Zhao *et al* 2007). Several other studies have shown that breast cancer cells expressing $\alpha_v\beta_3$ are associated with higher rates of bone metastasis, tumour associated osteolysis and bone colonization, potentially through the co-operation with MMP-2 and -9 promoting invasion (Sloan *et al* 2006, Karadag *et al* 2004, Rolli *et al* 2003, Gupta *et al* 2012).

For any cancer to progress, tumour cells must intravasate and metastasise, which can be achieved by loss of cell polarity and cell-cell binding and a switch from an epithelial to a mesenchymal phenotype, a process referred to as epithelial to mesenchymal transition (EMT) (Micalizzi *et al* 2010). The cadherin-catenin complex is essential for both morphogenesis and subsequent structural and functional organisation of epithelia. Disruption of either of the interactive components produces significant alterations in cellular behaviour (Lynch *et al* 2010). This can occur within the tumour by down regulation of molecular binding complexes, such as the E-cadherin/β-catenin complex, which are associated with an epithelial phenotype, resulting in tumour cells assuming a mesenchymal phenotype associated with increased N-cadherin expression (Cadherin switching), giving them the ability to intravasate through the basement membrane and migrate to distant sites (Micalizzi *et al* 2010).

The locus coding E-cadherin (16q22.1) is considered to be a tumour-suppressor gene; loss of function enables cell detachment and induces an invasive phenotype and occasionally, mutations of the E-cadherin gene can lead to the absence of or expression of a non-functional protein. E-cadherin is the prototypic type I cadherin

Table 1.7 – Integrins implicated in prostate cancer (adapted from Goel *et al* 2008)

	Deregulation	**References**
α Subunit		
α_2	Downregulated in 70% of low grade (II and III) cancers. Upregulated in metastases	Bonkhoff *et al* 1993, Nagle *et al* 1994
α_3, α_4, α_5	Downregulated in adenocarcinoma	Nagle *et al* 1994
α_6	Polarised distribution in BPH, less polarised with increasing grade. Upregulated in metastases	Bonkhoff *et al* 1993, Knox *et al* 1994, Nagle *et al* 1995, Davis *et al* 2001
α_7	Downregulated and mutated in adenocarcinoma and recurrent adenocarcinoma	Ren *et al* 2007
β Subunit		
β_1	Upregulated in adenocarcinoma; redistrubtion with progression	Knox *et al* 1994, Murant *et al* 1997,
β_{1C}	Expressed at mRNA and protein levels in normal prostate epithelium but downregulated in adenocarcinoma regardless of Gleason score (II to V)	Fornaro *et al* 1996, Fornaro *et al* 1998, Fornaro *et al* 1999, Perlino *et al* 2000
β_3	Absent in normal prostate cancer cells. Expressed in adenocarcinoma and metastatic lesions,	Zheng *et al* 1999
β_4	Downregulated in adenocarcinoma regardless of Gleason score (II to V)	Nagle *et al* 1995, Allen *et al* 1998, Davis *et al* 2001
β_6	Absent in normal prostate cells. Upregulated in adenocarcinoma and metastases	Goel *et al* 2008

which mediates homophilic interactions by forming adhesive bonds between one or several immunoglobulin domains in the extracellular region, connecting to actin microfilaments, to stabilise the complex, indirectly via α- and β-catenin in the cytoplasm (Kemler 1993). The integrity of the cadherin-catenin complex and its anchorage to the actin cytoskeleton are required for E-cadherin-mediated intercellular adhesion. Loss of E-cadherin expression seems heavily involved in EMT as it has emerged as the caretaker of the epithelial phenotype (Thiery 2002). *In vitro* experiments have shown there is a direct correlation between the lack of E-cadherin production and the loss of the epithelial phenotype. Down regulation of E-cadherin during cancer progression occurs by epigenetic mechanisms, including transcriptional repression and promoter hypermethylation (Graff *et al* 1995). E-cadherin production is maintained in most differentiated tumours, including prostate and breast, but there does appear to be an inverse correlation between E-cadherin expression and increasing tumour grade, presence of bone metastases and poor patient survival (Umbas *et al* 1994). An archival study of primary prostate tissue and prostatic bone metastases from the same patients also showed decreased expression of E-cadherin messenger RNA in metastases in nine of the total cases (Bryden *et al* 1999).

β-catenin has dual functions in prostatic and other tissues. As well as its role in the cadherin-catenin complexes, β-catenin also regulates signal transduction by binding to DNA and activating gene transcription factors such as Tcf and Lef in the nucleus, which may function as co-activators of AR (Semba *et al* 2001). Less than 4% of primary prostate tumours have β-catenin mutations, however aberrant β-catenin expression seems to affect the function of cadherin-catenin complexes (Voeller *et al* 1998). In a study of paired primary or bone metastases, 13 out of the 14 primary tumours had high β-catenin expression, whereas 12 of the 14 metastases showed down regulation of β-catenin mRNA levels compared with their primary tumours

(Bryden *et al* 1999). Whilst Umbas *et al* (1992) and Bryden *et al* (2002b) showed reduced or absent β-catenin to be associated with high grade prostate tumours and prostatic bone metastasis.

1.4.3.4 Degradation of the ECM

Cancer invasion requires the degradation of the ECM. The ECM is comprised of basement membrane and connective tissue. In cancer this degradation of the ECM is achieved by families of protetases including MMPs and serine proteases such as urokinase-type plasminogen activator (uPA) (Overall and Lopez-Otin 2002).

MMPs are zinc binding pro-enzymes of which 24 different members have been identified to date. MMP activity is regulated by tissue inhibitor of metalloproteinases (TIMPs), an imbalance in the MMP:TIMP ratio due to either TIMP downregulation or increased MMP production by tumour cells can induce an invasive phenotype (Lokeshwar *et al* 1993). This mechanism is vital for endothelial barrier degradation for cancer cell escape from the primary site or to colonise and establish at a different site *e.g.* in the bone (Chambers *et al* 2002). MMPs require proteolytic cleavage, for example in prostate cancer MMP-2 and MMP-13, activated by membrane-type 1 MMP, once activated can activate MMP-9 (Morgia *et al* 2005). Both MMP9 and MMP2 levels and the ratios of MMP-2/9:TIMP-1 have been shown to be increased in primary prostate cancer tissues compared to normal prostate epithelium and were associated with higher Gleason score and poorer patient survival (Wood *et al* 1997, Lichtinghahen *et al* 2002, Trudel *et al* 2003).

The degradation of the ECM is also facilitated through the action of uPA converting plasminogen to plasmin, as well as having the ability to activate other latent proteinases including MMPs, of which MMP-2 and -9 have been linked to prostate cancer and the development of metastases (Jin *et al* 2011, Hart *et al* 2002).

1.4.3.5 Cell Migration

Cell migration, initiated by extracellular stimuli, is co-ordinated by several inter-dependent steps involving the cytoskeleton and ECM. Cell motility and migration in prostate and other cancers are linked integrally to Ras and other GTP-binding proteins *e.g.* Rho and Rac which are important for cytoskeletal assembly, intracellular signalling and physical movement of cell membranes and whole cells (Clarke *et al* 2009).

The Ras family, comprising h-ras, k-ras, n-ras, r-ras and m-ras, are transmembrane glycosylated proteins that regulate downstream cellular activities including cell proliferation, nuclear transcription, apoptosis and invasion (Hu *et al* 2003, Adjei 2001). Ras acts as a membrane transducer, allowing extracellular signals (*e.g.* EGF, FGF, IGF) to bind to receptor tyrosine kinases which in turn activate the sub-family GTPases, which have major influence on cell signalling. Rho GTPases are similar to Ras in their structure and synthesis; their activation lies downstream of Ras and they are therefore Ras dependent (Clarke *et al* 2009). The Rho GTPase family, comprised of Rho A, B, C, E and G, Rac1, Rac2, cdc42-H5 and TC10, are all proteins involved in cell motility acting through actin dynamics, guiding morphological changes, including cell growth and movement (Giniger 2002, Clarke *et al* 2009). Cell movement may occur through the extension of filopodia bound to the cortical actin network and a fixed extracellular ligand, resulting in net movement of the whole cell.

The predominant theory is that the Ras-Rho axis is activated in prostate cancer metastasis and this underpins the acquisition of cell motility that is fundamental for successful metastasis. Therefore therapeutic strategies have been developed to prevent Rho synthesis or activity resulting in reduced cell motility, with a corresponding reduction in invasion across endothelial barriers. Montague *et al*

(2004), using bisphosphonates to inhibit the mevalonate pathway (RhoA) in prostate cancer, showed that cell motility and transmigration of prostate cancer cells across human bone marrow endothelial barriers and human bone marrow stroma were inhibited in the presence of zoledronic acid. A further study examined the effects of inhibiting the farnesyl and geranyl-geranyl prenylation pathways and showed that migration and motility of prostate cancer cells were reduced dramatically by inhibition of Ras prenylation and therefore also inhibition of Rho activation (Clarke *et al* 2009).

1.4.3.6 Homing/ Colonisation

In solid tumours, malignant cells increasingly enter the circulation as the tumour load grows. Once cells intravasate and survive in the circulation they have the potential to, at their preferred metastatic site(s), extravasate through the local vascular endothelial lining and gain access to underlying stroma (Jin *et al* 2011). However, what drives these processes and dictates where they will occur remains poorly understood. Though in recent years the theory of cancer cells creating a pre-metastatic niche, in which cells can prepare sites for metastases, has evolved (Weilbaecher *et al* 2011). The tendency for prostate cancer to predominantly metastasise to the bone, and the increasing incidence associated with other cancers, drives the need for better understanding of how bone metastases develop.

The complex bone environment is a pre-metastatic niche which is capable of being affected by endocrine signals from tumour cells and the circulation thus aiding homing and colonisation. For example systemic factors, like parathyroid hormone related protein (PTHrP), are produced by a variety of tumours promoting bone resorption and enhancing the production of local bone factors including chemokines (Weilbaecher *et al* 2011). Breast cancer cells have been shown to increase bone

resorption by producing herpanase (Kelly *et al* 2005), whilst prostate cancer cells have been shown to upregulate OPN from both tumour cells and fibroblasts, and MMPs from osteoclasts, promoting bone marrow cell recruitment and tumour formation (Pazolli *et al* 2009, Lynch *et al* 2005). Kaplan *et al* (2006) showed that in melanoma and lung cancer models VEGFR1 positive bone marrow derived haematopoietic stem cells homed to sites of future metastases, forming cellular clusters, producing inflammatory cytokines and up-regulating fibronectin production, preceding tumour cell arrival (Hiratsuka *et al* 2002).

Despite the introduction and accessibility of PSA testing, approximately 22% of newly diagnosed prostate cancers have metastatic components (Wolff *et al* 1998). Morgan *et al* (2009) showed that, in prostate cancer patients who had undergone a radical prostatectomy, up to 72% had detectable disseminated tumour cells in their bone marrow, demonstrating the metastatic potential of the skeleton. Metastatic prostate cancer cells have been shown to directly compete for occupancy in the haematopoietic stem cell niche during localisation to the bone, subsequently driving them into progenitor pools (Shiozawa *et al* 2011).

Both osteoblasts and bone marrow endothelial cells express CXC chemokine stromal-derived factor-1 (SDF-1), which has been shown to promote prostate cancer cell migration and upregulate MMP-9 and $\alpha_v\beta_3$ in prostate cancer cells (Sun *et al* 2005, Sun *et al* 2007, Chinni *et al* 2006). Integrin $\alpha_v\beta_3$ interacts with OPN, fibronectin and vitronectin and its expression has been associated with higher rates of bone metastases and tumour induced osteolysis (Clezardin 2009, Schneider *et al* 2011). Tumour cell expression of β1 integrin family members, including $\alpha_5\beta_1$, $\alpha_2\beta_1$ and $\alpha_4\beta_1$, which are receptors for fibronectin, collagen I and VCAM-1 have been implicated in interactions between tumour cells and bone marrow stroma (Korah *et al* 2004, Hall *et al* 2008, Hall *et al* 2006, Michigami *et al* 2000).

Once cells have undergone colonisation of the secondary environment, this does not always result in immediate tumour formation, dormancy can also occur. Prostate cancer cells have been shown to bind to osteoblast annexin II receptors, which are well known dormancy inducers, and were found to reduce cell cycle progression of prostate cancer cells, thus implicating osteoblasts as facilitators for tumour dormancy in bone (Shiozawa *et al* 2010).

1.5 Biology of bone

Bone is a specialised dynamic tissue which provides structural support and protective functions whilst also regulating calcium levels and providing a reservoir of hematopoietic cells. There are three distinct cell types within bone which account for 90% of all cells in the adult skeleton (Sommerfeldt and Rubin 2001), all of which play a pivotal role in bone homeostasis, remodelling and pathophysiology (Coleman 2001a). The skeleton, comprising this dynamic tissue, receives 5-10% of cardiac output, which supplies cells of the marrow, tissue and periosteum with the required nutrients through an elaborate structure of vasculature canals, ensuring that no cell lies more than 300µm from a blood vessel even within the densest parts of the cortical bone tissue.

1.5.1 Bone structure

All bones throughout the human body are classified by their shape, which includes short, long and flat bones and consist of a central reservoir of fatty or hematopoietic marrow which provides a constant source of stem cells. These bones are composed of two types of osseous tissues, cortical and trabecular, in differing concentrations to facilitate their versatile functional demands (Buckwalter *et al* 1996a). Cortical

bone, due to its structural role in the skeleton, is mainly found in the shafts of long bones whilst, in contrast, trabecular bone, with its loosely organised structure and porous matrix, is generally located in the interior of metabolically active bone ends which undergo greater remodelling than cortical bone.

Long bones are divided into three sections:-

The diaphysis refers to the long, narrow shaft of the bones mainly composed of cortical bone, made from overlapping osteons (cylindrical units), with a central canal of nerves and blood vessels surrounded by densely packed collagen fibrils in concentric lamellae providing a protective outer layer. This dense organisation provides maximum strength and load bearing capacity (Rauner *et al* 2012).

Epiphysis are located above the growth plates at the ends of long bones and are characterised by the orderly proliferation and maturation of cells which provide bone elongation, throughout childhood and puberty, until the skeleton has reached maturity, generally in the mid-twenties (Buckwalter *et al* 1996a). During this constant proliferation, cartilage is continuously replaced with bone matrix, after which the epiphysis becomes completely ossified.

The area called the metaphysis is located between the diaphysis and the epiphysis and encapsulates the growth plates at the ends of long, flat and vertebral bones where multidirectional force may be applied. The metaphysis contains a meshwork of trabecular bone surrounded by hematopoietic cells, fatty marrow and blood vessels, providing a large metabolically active surface area, encased in a thin shell of cortical bone (Clarke 2008).

The periosteum is a fibrous connective tissue which surrounds the outer cortical surface of bone, though not at the sites of joints (Clarke 2008). The periosteum consists of two layers: a dense fibrous outer layer which has high collagen content, and an inner layer, also known as the osteogenic layer, which has a looser cellular

structure (Buckwalter *et al* 1996a). During bone elongation, remodelling and repair, the cells of the osteogenic layer secrete the organic matrix aiding enlargement of the bone diameter (Buckwalter *et al* 1996b).

1.5.2 Bone matrix

Bone matrix is a composite material consisting of organic and inorganic mineral components some of which are derived exogenously and may help to regulate matrix mineralisation (Clarke 2008). Approximately 90% of bone matrix is organic and resembles the matrix of dense fibrous tissue. The majority of organic matrix proteins are collagenous, predominantly composed of type I collagen along with small amounts of types III, V and XII. Type I collagen is distinguished from other collagens by its unique amino-acid content and the relatively large diameter of its fibrils which gives bone its form and provides great strength, durability and stability which remains essentially unchanged, even after death (Buckwalter *et al* 1996b).

The remaining 10% of the bone matrix, the inorganic matrix, serves as a reservoir for 99% of the body's calcium, 85% of the phosphorous and between 40-60% of the sodium and magnesium (Sommerfeldt and Rubin 2001). Tight regulation of these ions, to and from the extracellular fluid, is vital for normal physiological conditions as they influence processes such as nerve conduction and muscle contraction. It also consists of non-collagenous glycoproteins, bone-specific proteoglycans and growth factors which can influence matrix organisation, bone mineralisation and the differentiation and function of bone cells. Examples of these proteins which help to initiate calcification include osteocalcin, osteonectin (ON), BSP, bone phosphoproteins and small proteoglycans. Growth factors which have been identified as present in the bone matrix include transforming growth factor β (TGFβ) family, insulin like growth factor (IGF-) -1 and -2, bone morphogenic proteins

(BMPs), platelet derived growth factors (PDGF), interleukins (IL-) -1 and -6 and colony stimulating factors (CSFs).

1.5.3 Bone marrow

The bone marrow, found within axial and long bones, consists of hematopoietic tissue and adipose cells surrounded by vascular tissue interspersed within trabecular bone (Travlos 2006). Normal bone marrow has a defined architecture within the bone which allows it to play an inter-dependent role in cell differentiation (Compston 2002). Bone marrow angiogenesis and osteogenesis, in developing and mature bones, have been shown to be closely linked both under normal physiology and pathophysiology (Compston 2002).

1.5.4 Bone cells

Due to the diverse range of processes in bone remodelling and mineral homeostasis, bone cells assume specialised forms distinguishable by morphology, function and characteristic location. There are three integral types of bone cells, osteoblasts, osteoclasts and osteocytes, which originate from two distinct stem cell lines under the influence of a variety of osteotropic hormones and cytokines (Nakamura 2007). The mesenchymal stem cell line, which has the potential to become osteoblasts, bone lining cells or osteocytes, consists of undifferentiated cells which reside in bone canals, the endosteum, periosteum and marrow. The hematopoietic stem cell line consists of circulating marrow monocytes which can become osteoclasts.

1.5.4.1 Osteoblasts

Osteoblasts are responsible for creating and maintaining skeletal architecture by producing extracellular matrix proteins and regulating matrix mineralisation, initially during bone formation and later during bone remodelling. The life span of a human osteoblast is 8 weeks in which it can lay down between 0.5-1.5μm of osteoid per day (Sommerfeldt and Rubin 2001). Osteoblasts are highly anchorage dependent and rely on extensive cell-matrix and cell-cell contacts, via a variety of transmembrane proteins and specific receptors, to maintain cellular function and responsiveness to metabolic and mechanical stimuli. Osteoblasts also regulate osteoclast differentiation and resorption activity by the secretion of cytokines or by direct cell-cell contact (Buckwalter *et al* 1996b).

1.5.4.1.1 Morphology and physiology

Osteoblasts develop from irregular shaped cells containing a single nucleus, few organelles and minimal cytoplasm (pre-osteoblasts) into a rounded polyhedral form with an osteoid seam separating them from the mineralised matrix (immature osteoblasts) (Clarke 2008). Mature active osteoblasts secrete bone matrix and are cuboidal cells, with large Golgi apparatus and abundant rough endoplasmic reticulum, with regions of the plasma membrane specialised for the trafficking and secretion of vesicles which facilitate the deposition of new bone matrix (Anderson 2003). Cytoplasmic components of the osteoblasts extend through the osteoid matrix to come into direct contact with osteocytes within the mineralised matrix, thus providing co-ordinated activity from both cell types. Tight junctions also form between all active osteoblasts allowing communications to occur between each other (Shin *et al* 2000).

1.5.4.1.2 Osteoblast differentiation and maturation

Osteoblasts and osteocytes are of pluripotent mesenchymal stem cell origin (Caplan 1991, Owen 1988, Pittenger *et al* 1999), which prior to committing to become osteoblasts, can also differentiate into other mesenchymal cells including fibroblasts, chondrocytes, myoblasts and bone marrow stromal cells depending on the activated signalling transcription pathways (Friedenstein *et al* 1987, Yamaguchi *et al* 2000). Three distinct osteoblast development stages have been identified: osteoblast proliferation, osteoblast maturation and lastly matrix synthesis and mineralisation which allow progressive development of the osteoblast phenotype, from an immature proliferating mesenchymal cell to a mature active bone matrix secreting osteoblast, characterised by a definitive sequential expression of tissue-specific genes (Buckwalter *et al* 1996b).

Runx-2, a *runt*-related gene, plays a crucial role in the early commitment of mesenchymal cells to osteoblast differentiation. This has been demonstrated in *Runx-2* deficient mice models which completely lacked bone formation, because of the absence of osteoblasts (Komori 2010, Otto *et al* 1997). *Runx-2* induces the expression of major bone matrix protein genes or activates their promoters including Ibsp/BSP, Fn1/Fibronectin and TNFRSF11b/OPG, which are involved in the production of bone matrix proteins such as type I collagen, OPN, BSP and osteocalcin (Ducy *et al* 1997, Lee *et al* 2000, Thirunavukkarasu *et al* 2000). This, accompanied by Sp7 and canonical Wnt signalling, leads to an increase in immature non-functioning osteoblasts by blocking differentiation of mesenchymal cells into chrondrocytes (Hill *et al* 2005, Hu *et al* 2005). *Runx-2* expression is not essential to maintain bone matrix protein gene expression as demonstrated by it being down-regulated in the late stage of osteoblast maturation, and in mature active osteoblasts (Komori 2010).

Several other specific transcription factors, including Osterix (Osx) and core binding factor α1 (Cbfa 1) are critical mediators in the commitment of mesenchymal cells into the osteoblast cell lineage and osteoblast differentiation, though both are not sufficient alone to support the maturation of osteoblasts (Banerjee *et al* 1997, Ducy *et al* 1997, Komori *et al* 1997, Hoshi *et al* 1999, Lee *et al* 1999, Otto *et al* 1997).

The precursors that undergo proliferation and differentiate into immature osteoblasts are elliptical cells that are capable of proliferation but unable to deposit bone matrix. The accumulation of matrix proteins contributes, in part, to the cessation of cell proliferation. For osteoblasts to start matrix synthesis and mineralisation, BMP-2 and BMP-5 play a significant role in increasing alkaline phosphatase activity, osteocalcin synthesis and parathyroid hormone (PTH) responsiveness (Yamaguchi *et al* 1991, Takuwa *et al* 1991). Immediately after growth arrest, a developmental sequence involving the selective expression of specific genes which characterise the differentiated osteoblast phenotype occurs (alkaline phosphatase, osteocalcin) and therefore initiates the process of bone formation (Stein *et al* 1993).

To proliferate and differentiate into mature active osteoblasts the release of a variety of osteotropic hormones and growth factors are also required (PTH, Vitamin D, Prostaglandin-E_2 and IL-11) (Rauner *et al* 2012). During bone matrix secretion and mineralisation mature osteoblasts synthesise and secrete type I collagen, which is oriented along lines of stress, and then deposit bone matrix and various non-collagen proteins including osteocalcin, OPN and BSP. Once this process is complete mature osteoblasts can follow one of three pathways:-

1) They can remain on the bone surface, decrease their synthesising activity and assume a flatter bone-lining cell form and regulate the flux of mineral ions but retain the ability to re-differentiate into secreting

osteoblasts upon exposure to various stimuli, including hormones and mechanical forces

2) They can become embedded within the matrix and become osteocytes
3) They can undergo an apoptotic process by an unknown mechanism.

In adults, at the end of the synthesis and mineralisation of the bone matrix, cellular levels of alkaline phosphatase mRNA decline (Lian and Stein 1995) and approximately 70% of mature osteoblasts undergo apoptosis, whilst the remainder can differentiate into lining cells or osteocytes (Franz-Odendaal *et al* 2006, Lynch *et al* 1995, Clarke 2008).

1.5.4.2 Osteoclasts

Osteoclasts, since their discovery in 1873 have shaped the progression in bone biology, highlighting the complex intercellular environment we know it to be today (Martin 2013). Osteoclasts are highly active, short lived cells with the ability to resorb bone at specific sites called Howship's lacunae (Edwards and Mundy 2011, Clarke 2008). Systemic hormones, *e.g.* PTH and local cytokines stimulate osteoblasts to release mediators which can activate osteoclasts and stimulate osteoclast differentiation.

1.5.4.2.1 Morphology and physiology

Osteoclasts are particularly specialised for their bone resorption role and are characterised as highly migratory, multinucleated, polarised cells with pockets of lysosomal enzymes (Sommerfeldt and Rubin 2001). They show distinctive complex folding of the cytoplasmic membrane (ruffled border) which comes into contact with the site of bone matrix resorption. Typically osteoclasts have between 3-20 nuclei

which, when the cells are active, fill much of the cytoplasm to supply the great amount of energy required to resorb bone, as well as large numbers of mitochondria and lysosomes (Martin 2013).

1.5.4.2.2 Differentiation and maturation

Much of what we understand about osteoclast differentiation and maturation comes from mouse models and pathophysiological conditions such as osteopetrosis and osteoporosis. Unlike other bone cells, osteoclasts originate from a hematopoietic stem-cell precursor within the mononuclear monocyte-macrophage family, found circulating in the marrow and blood stream, under the influence of hormones, growth factors and chemo-attractant factors such as inflammation, red blood cells and platelets (Boyce 2013). When stimulated, mononuclear osteoclast precursors proliferate and fuse to form large multinucleated osteoclasts referred to as polykaryons (Boyle *et al* 2003).

For hematopoietic stem cells to be committed to myeloid precursors activation of PU.1 and MITF transcription factors must occur, however to further commit to the osteoclast lineage, the stimulation of CSF-1R activates other intracellular proteins, including c-Fos and p50/p52, resulting in alterations to cellular structures (Edwards and Mundy 2011, Boyle *et al* 2003). A feature of the mature pre-osteoclast is the up-regulation of the Receptor Activator of Nuclear factor κB (RANK) receptor, which under the influence of haematopoietic factors, M-CSF and RANK Ligand (RANKL), allows osteoclasts to form polykaryons, attach to the bone and begin bone lysis (Boyle *et al* 2003, Edward and Mundy 2011).

Efficient osteoclast activity at the bone surface requires the interaction with the bone surface (Edwards and Mundy 2011). There is strong evidence to suggest that sphingolipid phosphate receptors are one of the major chemo-attractant factors

which attract osteoclast precursors to bone remodelling sites, whilst both M-CSF and RANKL are produced by osteoblasts and bone marrow stromal cells, therefore ensuring that osteoclast differentiation and fusion into polykaryons occurs near active bone remodelling sites (Boyce 2013).

Initially, upon contact with the bone surface, osteoclasts form tight junctions using integrin complexes ($\alpha_v\beta_3$) and RANK, which stimulates Src and results in the formation of the ruffled membrane as secretory vesicles fuse with the membrane (Teitelbaum 2011). During bone reabsorption osteoclasts characteristically create depressions, referred to as Howship lacunae, by secreting a range of ions and enzymes which de-mineralise bone and degrade the matrix. During bone reabsorption osteoclasts have the capacity to phagocytose and degrade some matrix fragments in cytoplasmic vacuoles.

Evidence suggests that most osteoclasts undergo apoptosis during the reversal stage of bone remodelling, which under normal physiology is mediated by oestrogen and TGFβ, which increases Fas-ligand expression inhibiting gene expression essential for mature osteoclast activity (Nakamura *et al* 2007, Boyce 2013).

1.5.4.3 Osteocytes

More than 90% of bone cells in the mature human skeleton are osteocytes, metabolically quiescent mono-nucleated osteoblasts embedded in the bone matrix; they communicate with other bone cells through cell processes and function as strain and stress sensors (Lozupone *et al* 1996). Long, branching cytoplasmic projections from their ellipsoidal or lens-shaped bodies protrude through canaliculi, extend throughout the mineralised bone matrix and come into contact with cytoplasmic processes from other cells (Sommerfeldt and Rubin 2001).

This large, complex network of cells covering the internal and external surfaces of the bone are extremely sensitive to stresses on the bone, and control the movement of ions in and out of the mineralised matrix (Buckwalter *et al* 1996b). This arrangement is critical in allowing the cell-mediated exchange of minerals to take place between the fluid in the bone and the blood. Interconnections between osteocytes, osteoblasts and bone-lining cells also allow this cell network to sense deformation of bone, and therein co-ordinate the formation and resorption of bone.

1.5.5 Bone remodelling

Bone forms in early life mainly through endochondral ossification, in which the initial bone pattern outlined in mineralised cartilage is replaced by mineralised bone and is thereafter maintained throughout life by a tightly regulated remodelling process (Weitzmann 2013). The physiological bone remodelling process is homeostatic, in which the rate of osteoclastic bone resorption is matched by the rate of osteoblastic bone formation, ultimately resulting in bone repair without gain or loss of bone mass (Weitzmann 2013). Annually the remodelling process has the capacity to replace approximately 20% of adult bone tissue, with each cycle lasting up to 8 months, though research has shown this process becomes less effective with age (Murthy *et al* 2009, Weitzmann 2013). The bone remodelling cycle is continuous, occurring in small pockets of cells called basic multicellular units (BMUs) (Proff and Romer 2009). A BMU refers to the collection of functional cells involved in the bone remodelling process in which osteoblasts and osteoclasts are pivotal (Kular *et al* 2012). In 1965, Epker and Frost demonstrated that the interactions between osteoblasts and osteoclasts are essential components of bone remodelling whilst also playing an integral role in its regulation, however it was not until the late 1990's

that more in-depth understanding of how this was achieved emerged (Epker and Frost 1965).

Bone remodelling is a prolonged, tightly regulated process influenced by factors such as injury and age, as well as local and systemic biological stimuli, including blood calcium levels, hormones, cytokines and growth factors induced by bone micro-damage or mechanical loading (Aubin 2001, Murthy *et al* 2009). The bone remodelling cycle consists of five distinct, highly regulated and sequential phases: activation, resorption, reversal, formation and quiescence (Murthy *et al* 2009) (Figure 1.7).

The process is initialised by bone-lining cells, which lie directly against the bone matrix and have an elongated form with extended cytoplasms which penetrate the bone matrix to come into contact with cytoplasmic extensions of osteocytes (Clarke 2008). These connections create an extensive network of intercellular communication, which help to direct sites of remodelling, though there is some evidence to imply that remodelling sites may also develop in a random manner. Osteocytes, when exposed to PTH, result in bone lining cells contracting and secreting enzymes that remove the thin osteoid layer that covers the mineralised matrix, thus appearing to be the first steps in attracting and permitting osteoclasts to attach to the bone surface and begin resorption.

During the activation phase, osteoclastic precursors are recruited to the remodelling site from circulating blood and bone marrow and differentiate into fused polykaryons under the influence of RANKL from the quiescent osteoblasts (Clarke 2008). Structural changes within the osteoclasts result in the formation of a tight junction between the bone surface RGD (arginine, glycine and asparagine)-containing peptides in the bone matrix and the osteoclast basal membrane ($\alpha_v\beta_3$ integrin receptors), resulting in the ruffled border patterns associated with mature

osteoclasts (Boyle *et al* 2003, Clarke 2008). The sealed compartment becomes an acidified milieu as hydrogen and chloride ions are trafficked through the ruffled borders by proton pumps and chloride channels, uniting in the compartment space to form HCl, lowering the pH to 4, the optimal pH for protease cathepsin K (CATK), ultimately resulting in the de-mineralisation of bone (Clarke 2008, Boyce 2013, Martin TJ 2013). Lysosomal vesicles also secrete osteolytic enzymes, including tartrate-resistant acid phosphatase (TRAP), which degrade the bone matrix resulting in the formation of Howship's lacunae in trabecular bone or Haversian canals in cortical bone (Clarke 2008, Boyle *et al* 2003). During the enzymatic degradation, bone products including solubilised calcium and phosphorous ions, are released into the blood stream or reabsorbed by the osteoclasts to be phagocytosed (Murthy *et al* 2009). This stage in the remodelling process is strictly related to the interaction of osteoclasts with bone matrix proteins, including OPN and BSP which would have been secreted by osteoblasts during the previous cycle of bone formation.

During the reversal stage, osteoclasts detach from the bone surface, undergo apoptosis, are replaced by osteoblast precursors which are attracted to the resorption site, and start to proliferate and differentiate. However the signals which influence and control this process still remain elusive.

.

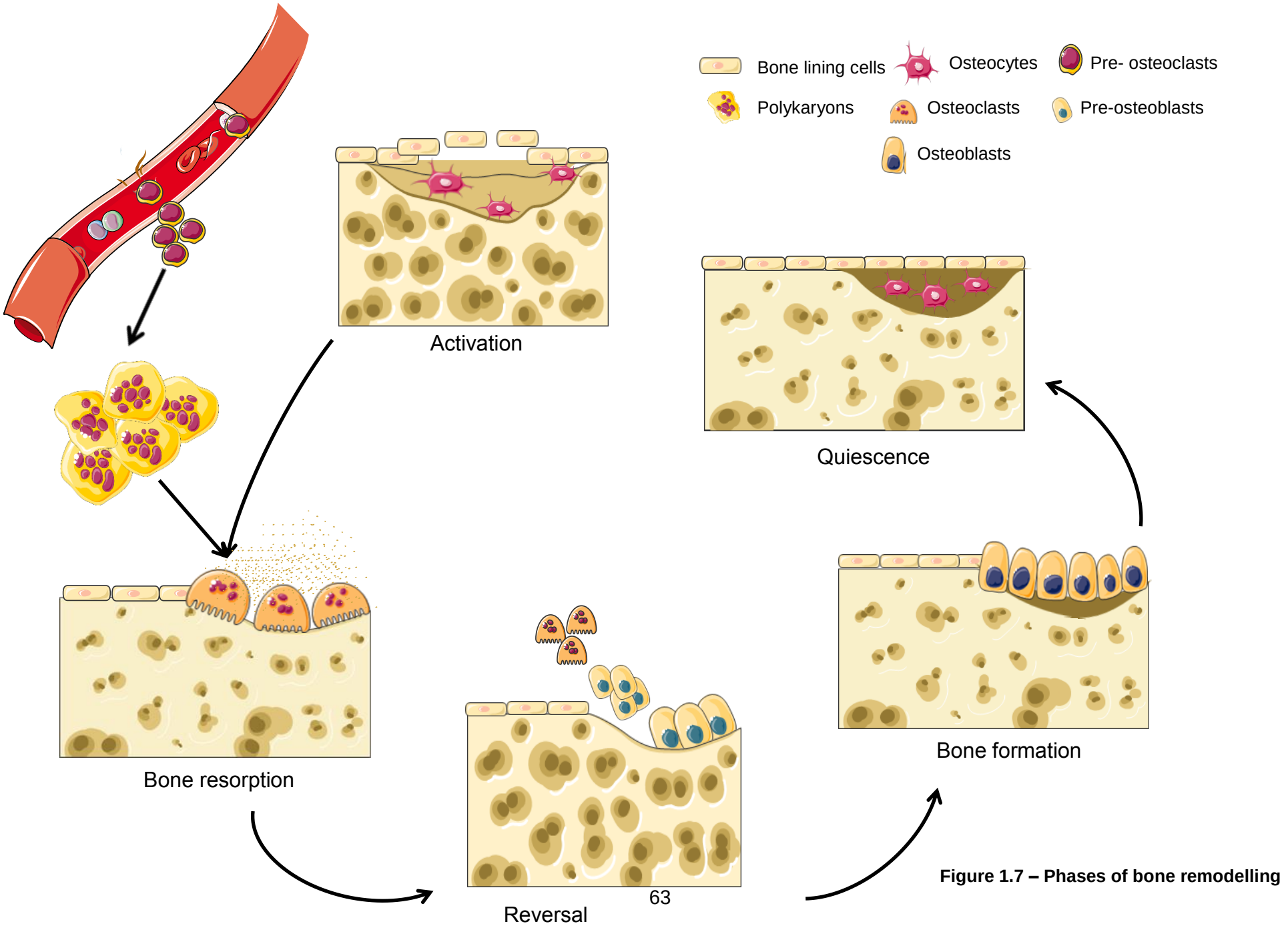

Figure 1.7 – Phases of bone remodelling

During the formation phase, mature osteoblasts synthesise and release osteoid and new collagenous organic matrix. Osteoblasts regulate the mineralisation process by releasing membrane bound vesicles containing concentrated calcium and phosphorous precipitated from the blood stream, released during the absorption phase (Anderson 2003). At the end of this phase the majority of osteoblasts also undergo apoptosis. The remaining osteoblasts become buried in the new matrix and, during the quiescence phase, trans-differentiate into osteocytes and bone lining cells forming an extensive canalicular network (Clarke 2008). It is these cells which regulate the flux of ions and minerals and retain the ability to re-differentiate into osteoblasts upon exposure to PTH or mechanical forces, which in turn can re-induce the bone remodelling cycle (Clarke 2008).

1.5.5.1 Factors influencing bone remodelling

Through intensive research into bone resorption related pathophysiologies, a variety of both paracrine and endocrine factors have been identified which regulate bone remodelling. However, much of this process and the factors involved also remain poorly understood especially those that influence osteoblasts. Several *in vivo* studies have also demonstrated that bone formation can occur without the presence of osteoclasts and bone resorption can occur in the absence of osteoblasts, which suggests that these cells can function independently of each other (Butt and Coral 1998, Kong *et al* 1999, Sims and Gooi 2008).

The RANKL: OPG ratio is a major determinant of bone mass (Hofbauer and Schoppet 2004, Boyce and Xing 2008). Osteoblasts incorporate both pro- and anti-resorptive signals, from hormonal and mechanical changes, balancing and controlling the bone remodelling response through alteration in the expression of the cytokine receptor RANKL and its inhibitor OPG (Yasuda *et al* 1998, Lacey *et al*

1998, Simonet *et al* 1997, Tsuda *et al* 1997). RANKL binds to its receptor RANK on the surface of osteoclast precursors and induces a number of intracellular pathways. These include the NF-κB and Jun N-terminal kinase signalling pathways, which drive differentiation into an osteoclast phenotype, activating bone resorption and osteoclast survival through regulation of many genes involved in osteoclastogenesis, including TRAP, CATK and calcitonin (Boyle *et al* 2003). OPG as the secreted decoy receptor for RANKL from osteoblast cells binds to RANKL preventing its association with RANK and thus inhibiting osteoclast differentiation and promoting osteoclast apoptosis. *In vivo* evidence suggests that PTH and 1,25 $(OH)_2D_3$ increase RANKL mRNA expression and decrease OPG mRNA expression thus increasing bone resorption, whilst bone protective factors such as oestradiol and testosterone tend to increase the expression of OPG relative to RANKL (Table 1.8) (Lee and Lorenzo 1999, Rogers and Eastell 2005, Buxton *et al* 2004, Horwood *et al* 1998).

Whilst the RANKL/OPG/RANK signalling is dominant in the regulation of bone remodelling other signalling molecules have been identified which act directly on osteoclasts, magnifying or diminishing the effect of RANKL. Other factors which have been shown to influence osteoclast formation, activation and resorption include IL-6, macrophage colony stimulating factor (M-CSF), PTH, 1,25-dihydoxvitamin D and calcitonin. The survival of the mature osteoclasts has also been shown to be regulated by RANKL and IL-1, due to the ability of these cytokines to induce NF-κB signalling.

Table 1.8 – Factors which regulate bone remodelling

Factor		Effect/Mechanism of action	Reference(s)
Hormones	PTH, 1,25 $(OH)_2D_3$	Promotes osteoclast differentiation	Lee and Lorenzo 1999
	PTHrP	Induces osteoblast differentiation	Iwanura *et al* 1996
	Calcitonin	Inhibits osteoclast activity	Tian *et al* 2007
	Oestradiol, Androgens	Induces apoptosis in osteoclasts, promotes osteoblast proliferation and differentiation	Majeska *et al* 1994, Hofbauer and Khosla 1999
Local Factors	IGFs	Promotes osteoblast differentiation and prevents osteoblast apoptosis	Gazzerro and Canalis 2006
	BMPs, PDGF-BB	Promotes osteoblast differentiation	Gazzerro and Canalis 2006, Caplan and Correa 2011, Autzen *et al* 1998
	FGF (-1 and -2)	Promotes osteoblast proliferation and differentiation	Dunstan *et al* 1999
	Prostaglandins	Either promotes osteoclast apoptosis (PGD) or osteoclast differentiation (PGE_2)	Durand *et al* 2008, Yue *et al* 2014, Liu *et al* 2005
Cytokines	RANKL	Promotes osteoclast proliferation, differentiation and osteoclastogenesis	Boyce 2013
	OPG	Inhibits osteoclast differentiation, promotes osteoblasts through inhibition of RANKL	Khosla 2001
	TGFβ	Promotes osteoblast proliferation	Dallas *et al* 2002
	IFNγ/IFNβ	Inhibits osteoclast differentiation	Hayashida *et al* 2014, Kim *et al* 2012
	ILs	Promotes osteoclast differentiation (IL-3), promotes osteocytes (IL-6)	Bakker *et al* 2014, Hong *et al* 2013

1.6 Bone metastasis

The variability of metastatic patterns in cancer is undoubtedly influenced by the molecular and cellular characteristics of both the tumour cells and the tissues to which they metastasise (Coleman 2001b). The skeleton is a common site of metastasis for a number of solid tumours but particularly for breast, prostate and lung cancer patients, which may be reflected in the high incidence and relatively long clinical course of these tumours due to improved first line therapies. Patient studies suggest that bone metastasis can occur in 65-80% of metastatic breast and prostate cases. Other bone metastasis incidence is increasing because bone marrow has been shown to act as a reservoir for dormant tumour cells, which resist chemotherapeutic treatment and re-emerge later with metastatic potential in the bone, or other organs (Berg *et al* 2007, Weilbaecher *et al* 2011). Half of patients with metastatic prostate cancer will die of the disease within 30-35 months, whilst subsequent autopsy series have suggested that the majority of these metastatic prostate cancer patients (~85%) died with evidence of bone metastases (Carlin and Andriole 2000, Bubendorf *et al* 2000).

Bone metastases most commonly affect the axial skeleton, a distribution pattern which suggests that physiological properties of bone circulation within the bone marrow cavity, including capillary structure and the sluggish blood flow, assist in the establishment of metastases (Coleman 2000). The spine, pelvis and ribs are the earliest detection sites for bone metastases, whilst the skull, femur, humerus, scapula and sternum are commonly involved at later stages (Koutsiliers 1995). However, Leonard Weiss (1992), in a series of autopsy studies documented that there were larger numbers of bone metastases than would solely be based on blood-flow patterns for both breast and prostate cancer. More recent research has highlighted that tumour invasion into the bone is associated with osteoclast and osteoblast recruitment, resulting in the liberation of growth factors from the bone

matrix which provides a feedback to enhancing tumour cell survival and growth (Weilbaecher *et al* 2011). The bone microenvironment is a complicated place of recruitment and modulation of many other cell types, including platelets, immune cells and nerve cells which have the ability to induce angiogenesis. Once established in the bone microenvironment cancer cells, and the other cell types, participate in complex interplays which result in perturbations of bone metabolism and increased tumour growth which facilitate tumour progression (Figure 1.8).

Clinically, bone metastases cause considerable patient morbidity resulting in poor quality of life. Current treatment options remain palliative, managing symptoms such as debilitating pain, impaired mobility, hypercalcaemia, pathological fracture and spinal cord or nerve compression, with little impact on long term survival (Costa and Major 2009, Lee *et al* 2011). Hypercalcaemia is probably the most common metabolic complication of malignant disease which, if left, becomes severe and causes a number of additional symptoms including dysfunction of the gastrointestinal tract, kidneys and central nervous system. This problem is more prevalent in cancers with increased osteoclastic bone resorption, either multi-focally as in the case of metastatic breast cancer, or as a generalised process, stimulated by PTHrP or other systemic tumour products. Current therapies include bisphosphonates or neutralising receptor activator of NF-kB ligand (RANKL) antibodies, both of which target osteoclastogenesis (Weilbaecher *et al* 2011). However, 30-50% of these patients with such treatment plans will still develop new bone metastasis, skeletal complications and disease progression (Roodman 2004).

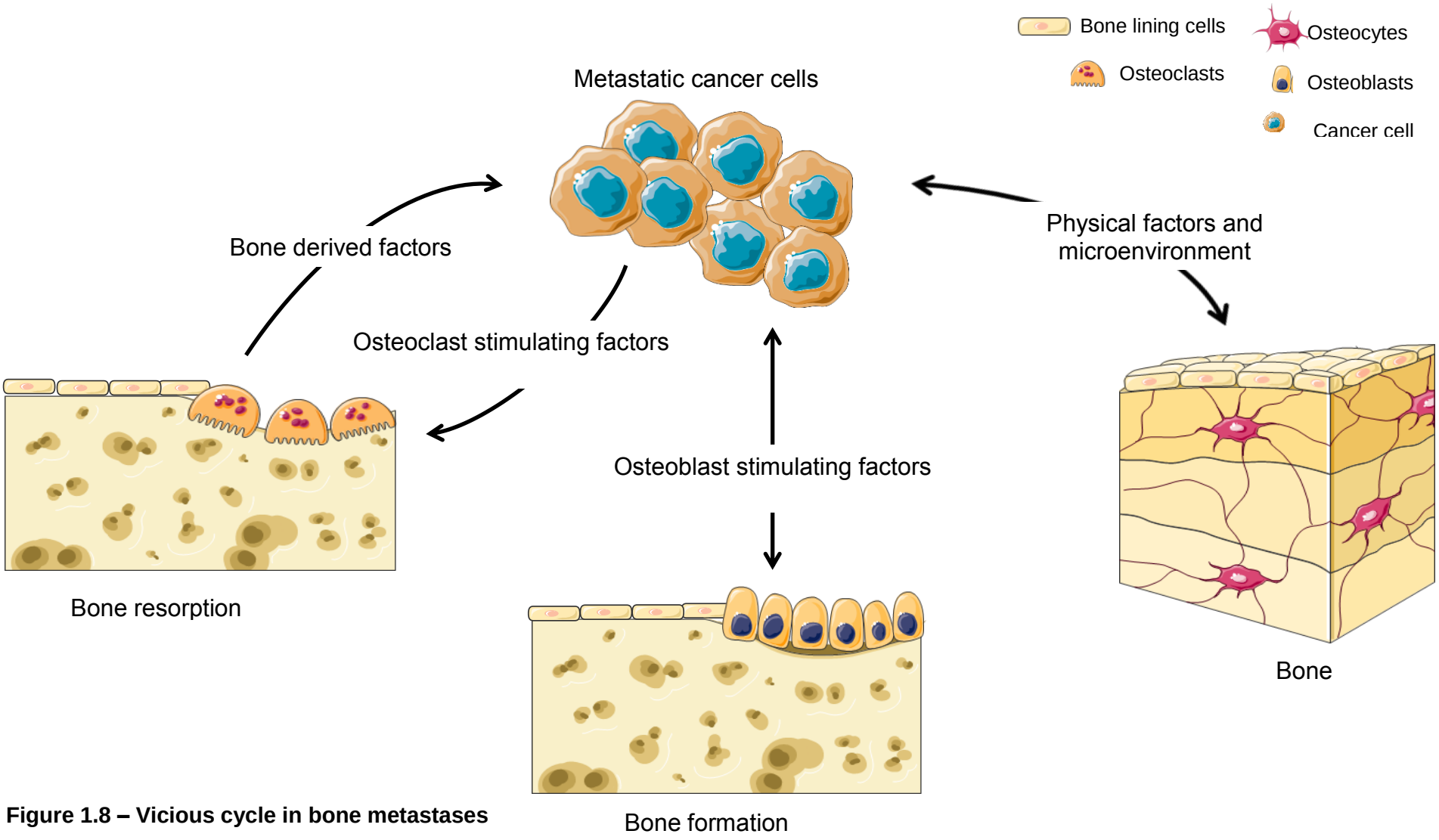

Figure 1.8 – Vicious cycle in bone metastases

1.6.1 Types of bone metastasis

With strong evidence that approximately half of the most common primary solid tumours will eventually metastasise to the bone an understanding of how the different phenotypes arise is needed (Koutsillieris 1995). Bone metastases are typically classified according to their radiographic lesion appearance, generally one of two distinct phenotypes (Figure 1.9). The two distinct bone metastatic phenotypes are a reflection of either dysregulated bone destruction (osteolytic) or bone formation (osteoblastic). In truth this classification is probably overly simplistic, and two extremes of a spectrum, perhaps a better reflection would be that patients exhibit both processes, which are accelerated, in the affected bones (Guise *et al* 2006).

1.6.1.1 Osteolytic metastasis

Cancers commonly associated with profound osteolysis include breast, lung and renal which result in the destruction of bone, by increased numbers of osteoclasts, causing intractable pain and fractures (Roodman 2001). This increase in osteoclasts is as a result of factors secreted by the tumour cells themselves which drive the differentiation of osteoclasts and promote osteoclast survival. This can be done as a consequence of tumour-induced activation of bone-matrix resorption due to tumour cells expressing RANKL, or through the up regulation of RANKL expression in surrounding areas. The exacerbation of bone reabsorption, can induce the vicious cycle, resulting in the release of other factors which can promote tumour cell growth and progression of bone metastases. This, to some degree, has been replicated in *in vivo* models where vitamin D deficiency, oestrogen or androgen deprivation or administration of G-CSF, GM-CSF and PTH can increase osteoclast numbers and

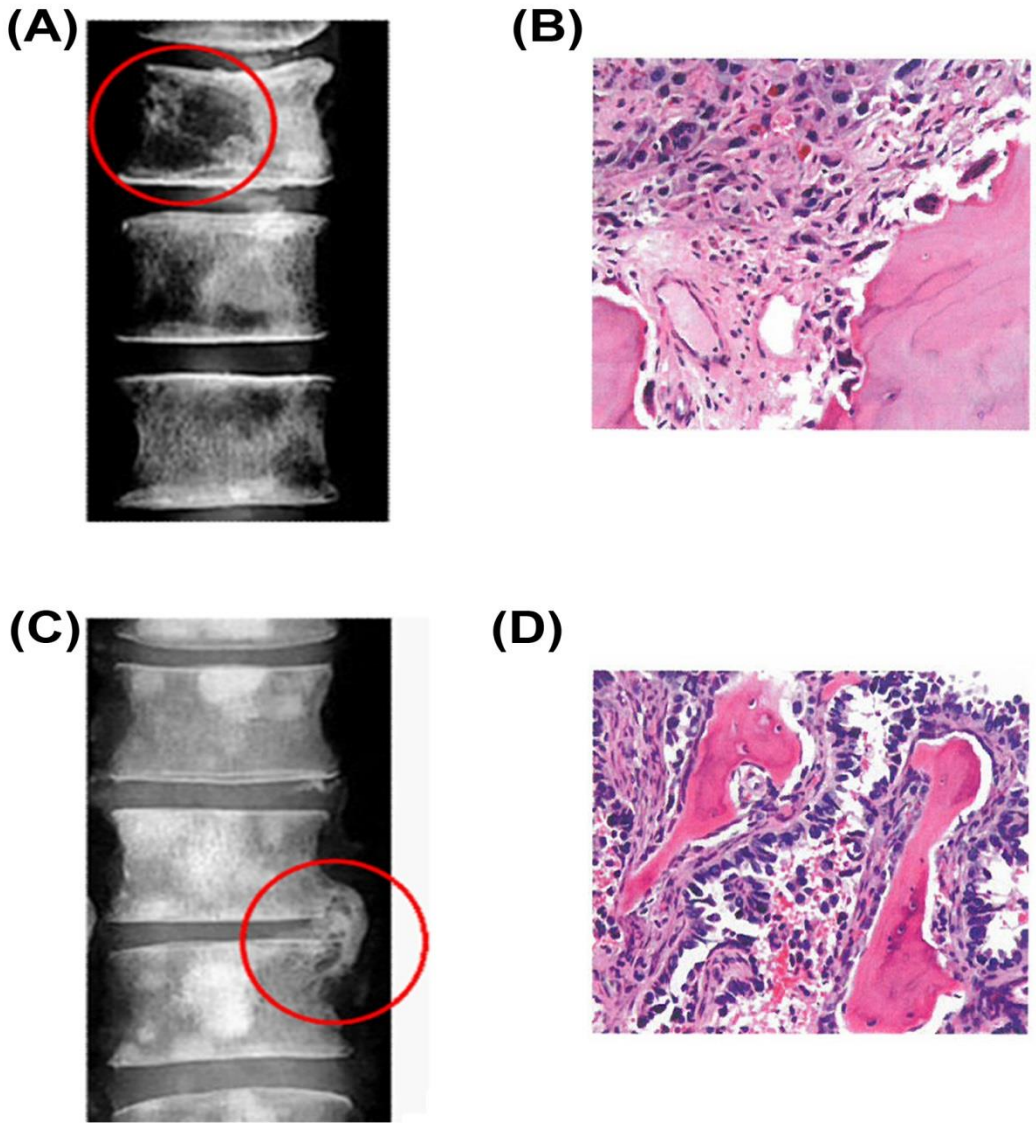

Figure 1.9 – Bone metastasis phenotype

(A) X-ray image of an osteolytic bone metastasis often associated with breast and renal cancer
(B) Osteolytic bone metastasis from renal cancer invading the bone marrow.
(C) X-ray image of an osteoblastic bone metastasis often associated with prostate cancer
(D) Osteoblastic bone metastasis, showing thickened trabeculae with large numbers of osteoblasts surrounding the cancer cells

(Adapted from www.clinicaloptions.com/Urology/ and Chirgwin and Roodman et al 2014)

thus develop and increase osteolytic tumour burden (Scneider *et al* 2005, Ooi *et al* 2010, Hirbe *et al* 2007, Park *et al* 2007a).

1.6.1.2 Osteoblastic metastasis

This type of bone metastases is most commonly associated with prostate cancer. The osteoblastic nature of bone metastases results in the formation of bone, with an immature and woven structure, which is of poor quality, (Clarke *et al* 1991). Reports have shown that in prostate cancer the osteoblastic phenotype accounted for 85% of bone lesions, whilst a mix of lesions was reported in 12% of cases with only 4% of bone lesions being osteolytic (Charhon *et al* 1983, Roudier *et al* 2004).

Clinical and experimental evidence indicates that bone resorption still occurs and is also increased in osteoblastic metastases. The concentration of bone resorption markers, including N-telopeptide (NTX) and C-telopeptide type I collagen (CTx), are elevated in prostate cancer patients with osteoblastic disease and is a strong predictor of morbidity and mortality (Coleman *et al* 2005). New bone formation in osteoblastic metastases is always produced via an osteoblast-dependent mechanism, however osteolysis is also present, produced by osteoclast mediated and tumour cell mediated bone resorption, thus generating a feedback cycle and driving tumour progression in the bone (Galasko 1975).

1.6.2 Prostate cancer osteotropism and osteomimicry

Skeletal metastases in prostate cancer patients are frequently the only sites of disease progression, after long lasting remission achieved by androgen depletion therapies (Kousiliers *et al* 1995). Prostate cancer metastases to the bone follow the natural progression of the disease, typically targeting the lumbar spine, vertebrae

and pelvis. Disseminating prostate cancer cells have been shown to circulate through the blood stream and ultimately colonise the long bones and become metastatic lesions, localised to the red marrow within the metaphysis (Thobe *et al* 2011). There are many factors which are believed to facilitate this high incidence of bone metastases including anatomical, physical, physiological and molecular interactions between tumour cells, bone cells and the bone microenvironment (Saad *et al* 2006, Chirgwin and Guise 2007).

Tumour cells have been demonstrated to preferentially adhere to the bone marrow endothelium, immobilising in capillary beds, using the same physiological mechanism as haemotopoietic stem cells (HSC) homing to the bone (Saad *et al* 2006, Lehr and Pienta 1998, Brenner *et al* 2004, Kang *et al* 2003). Metastatic prostate cancer cells directly compete for the occupancy of the HSC niche during localisation to the bone marrow, which may be accelerated in prostate cancer because of the Baston's plexus of veins and the sluggish nature of blood flow through the bone marrow sinusoids, which may aid bone colonisation. Upon entry into the bone, Goltzman *et al* (1992) reported that prostate cancer cells could preferentially adhere to bone marrow stromal cells. Others have demonstrated that prostate cancer bone colonisation is facilitated by a number of tethering proteins which are expressed in the sinusoid epithelium including VCAM-1, which when combined with the decreased blood flow rates allowed prostate cancer cells to adhere to the epithelium (Scott *et al* 2001, Jacobsen *et al* 1996). This process has also been reported to be mediated by $\alpha_2\beta_1$ integrin, which aids the attachment of prostate cancer cells to extracellular matrix proteins (BSP and type I collagen) possibly in concert with CXCR4 (Hall *et al* 2006, Clezardin and Teti 2007).

Evidence also suggests that growth factors from the bone matrix and prostate cancer cells, when in close proximity, bi-directionally interact as chemo-attractants. Several investigations have reported that type I collagen peptides, components of

bone marrow fibroblast conditioned media, TGF-β, IGF- I and II and ON all act as bone-derived chemo-attractants for prostate cancer cells *in vitro*. This has been supported by evidence that human prostate cancer tissues contain mitogens for osteoblasts and mesenchymal cells (Koutsiliers *et al* 1987, Jacobs and Lawson 1980). Metastatic prostate cancer cells have also been shown to secrete a variety of other factors which also affect osteoblast differentiation and proliferation and thus bone formation facilitating tumour cell growth (Table 1.9).

Prostate cancer cells express the calcium-sensing receptor (CASR) and respond to ionised calcium resulting in inhibition of apoptosis and stimulation of proliferation. The importance of this receptor in prostate cancer progression was demonstrated by short hairpin RNA knockdown of this receptor, reduced expression of CASR reduced tumour localisation to the bone (Liao *et al* 2006). Ionised calcium also leads to an increased PTHRP secretion by tumour cells and hence induces further resorption and calcium release.

uPA is synthesised as a single chain precursor which is converted, by a serine protease, to a two chain entity, linked with a disulphide bridge. Some evidence suggests that high molecular weight uPA can produce a dose-dependent mitogenic effect in osteoblasts (Rabbini *et al* 1992). There is some evidence to suggest that the amino-terminal fragment of the uPA may also have a pro-tumourigenic effect possibly by contributing to the activation of latent growth factors such as TGFβ or IGF-1, which can also independently stimulate osteoblast activity (Koutsilieris *et al* 1993). In a clinical setting, metastatic prostate cancer patients' also present with elevated ET-1 plasma levels (Nelson *et al* 1995).

Table 1.9 - Secreted Prostate Factors which influence osteoblasts (adapted from Logothetis and Lin 2005)

Factor	Target	Effect on osteoblasts	Reference(s)
BMP-2	Osteoblasts	Increases differentiation, osteoblast mitogen	Harris *et al* 1994, Autzen *et al* 1998
TGF-β	Osteoblasts	Increases proliferation	Marquardt *et al* 1987,Shariat *et al* 2001
IGF-1	Osteoblasts	Increased proliferation and differentiation, osteoblast mitogen	Chan *et al* 1998
IGFBP-3	IGF-1	Inhibits proliferation	Li *et al* 2003
PDGF	Osteoblasts	Increased proliferation	Funa *et al* 1991, Fudge *et al* 1994
FGF	Osteoblasts	Increased proliferation and differentiation	Matuo *et al* 1987
VEGF	Osteoblasts, Endothelial cells	Increased proliferation	Ferrer *et al* 1997/ Dai *et al* 2004
WNT	Osteoblasts	Increased proliferation and differentiation	Chen *et al* 2004
ET-1	Osteoblasts	Increased proliferation and differentiation, osteoblast mitogen	Nelson *et al* 1995
PSA	IGFBP-3 and PTHRP	Increased proliferation, osteoblast mitogen	Cramer *et al* 1996, Iwamura *et al* 1996, Cohen *et al* 1992
uPA	IGFBP-3	Increased proliferation, osteoblast mitogen	Rabbani *et al* 1990, Koutsilliers 1993
MDA-BF-1	Osteoblasts	Increased proliferation and differentiation	Vakar-Lopez *et al* 2004

Though the predominant phenotype of bone metastases associated with prostate cancer is osteoblastic, studies have shown that osteolytic factors can also play a role in disease progression. Lynch *et al* (2005) showed that MMP-7 cleavage of RANKL, in prostate cancer, can promote osteoclastic activity. Lu *et al* (2009) also showed that in prostate cancer, osteoclastogenesis could also be indirectly stimulated by MMP-1 and A Disintegrin-like and Metalloproteinase with Thrombospondin Motifs 1 (ADAMTS1) proteolytically cleaving EGF-like ligands to decrease osteoblast-derived OPG.

Other factors which affect prostate cancer progression in the bone include Dickkopf-1 (DKK-1), sclerostin and Wnt-signalling. Upregulation of DKK-1 and sclerostin have been shown to favour osteoclastogenesis and thus inhibit the progression of bone metastases (Yavropoulou *et al* 20102, Diarra *et al* 2007). However, evidence suggests that DKK-1 levels decrease in patients with bone metastases, and is associated with an increase in Wnt promoting osteoblasts and inhibiting osteoclast differentiation, therefore leading to an osteoblastic phenotype (Sottnik *et al* 2012, Tu *et al* 2012).

A prevailing theory about prostate cancer associated bone metastases is that proposed by Koeneman *et al* (1999) in which disseminated prostate cancer cells acquire a 'bone-like phenotype' (osteomimetic) to exploit the bone metastatic niche facilitating both bone localisation and cancer cell proliferation. Koeneman *et al* (1999) showed that prostate cancer cells in culture and *in vivo* can acquire characteristics associated with osteoclastic development and metastasis, relying on expression of osteoblastic genes including *RUNX2* (Blyth *et al* 2005, Clezardin and Teti 2007, Pratap *et al* 2005, Galindo *et al* 2005).

Despite these findings, much of the interplay which occurs between cancer cells, bone cells and the bone environment still needs to be elucidated.

1.7 RANK/ RANKL/OPG proteins and their signalling pathway

The discovery of the OPG/RANK/RANKL system revolutionised our understanding of the molecular mechanisms responsible for the regulation of bone turnover. The interactions between tumour cells, tumour-derived factors and the bone microenvironment are crucial for the initiation and promotion of skeletal malignancies. A better understanding of the processes involved in this complex system is essential for the development of more targeted therapies and specific biomarkers for diagnostic and prognostic uses.

1.7.1 Tumour Necrosis Factor Receptor Superfamily

The tumour necrosis factor receptor superfamily (TNFRSF) is highly conserved and found in all mammals (Croft *et al* 2012). The TNFRSF are comprised of 18 genes encoding 19 type II transmembrane proteins with unique structural attributes that couple them directly to signalling cascades resulting in varied and pleiotropic actions involving cell proliferation, differentiation and survival (Bodmer *et al* 2002, Locksley *et al* 2001). The normal and pathophysiological function of each TNFRSF depends on the 3-fold symmetry that defines their essential signalling stoichiometry and structure (Locksley *et al* 2001). Due to this, the TNFRSF continues to be a major focus for targeted therapies against a wide range of human conditions including atherosclerosis, autoimmune disorders and cancer (Locksley *et al* 2001).

The TNFRSF type II transmembrane proteins contain several cysteine-rich domains; and exist both as membrane-embedded and soluble factors after extracellular cleavage (Idriss and Naismith 2000, Croft *et al* 2012). For most family members, both of these active forms are self-assembling, non-covalent homo-trimers, whose individual chains fold as compact β sandwiches and interact at hydrophobic interfaces (Fesik, 2000, Tansey and Szymkowski 2009). The 25-30%

amino acid similarity between this family of ligands is largely confined within the internal aromatic residues responsible for trimer assembly. There appears to be little sequence similarity elsewhere which could account for the receptor selectivity (Locksley *et al* 2001).

1.7.2 Osteoprotegerin

Osteoprotegerin (OPG), also named osteoclastogenesis inhibitory factor (OCIF), was discovered simultaneously by Simonet *et al* 1997 and Tsuda *et al* in 1997, and has since been characterised as a novel protein integral to the regulation of bone turnover. As a decoy receptor for RANKL, OPG was found to be the paracrine regulator of osteoclast formation produced by osteoblasts constitutively to moderate osteoclast formation from RANKL stimulation (Martin TJ 2013). *In vivo* experiments showed that transgenic mice expressing this secreted protein exhibited a general increase in bone density, associated with a lack of osteoclasts (Boyle *et al* 2003). OPG is classed as a member of the TNFRSF however, unlike other family members, lacks the transmembrane proteins that can elicit signal transduction in a variety of cells resulting in a lack of apparent cell-associated signals (Baud'huin *et al* 2013).

TNFRSF11B is a highly conserved gene, originally isolated in rats, which has been shown to have 94% homology to the human gene. OPG mRNA has been detected in a variety of tissues including vascular tissues, bone, prostate, testis, kidney, liver, lung and heart, however, most extensive work and knowledge is available regarding its role in bone biology (Lacey *et al* 1998). Synthesised by osteoblasts, stromal cells, vascular smooth muscle cells, B lymphocytes and articular chondrocytes, OPG is characterised as a soluble glycoprotein that can exist as both a 60kDa monomer and a 120kDa disulphide-linked dimer.

1.7.2.1 Structure

The human OPG gene, *TNFRSF11B*, is located on chromosome 8q23-24 and contains 5 different exons spread over 29kb. When transcribed, OPG cDNA encodes a 401 amino acid polypeptide chain, which after cleavage of the 21 amino acid signal peptide, at position 22, results in a mature form of 380 amino acids (Figure 1.10 A) (Simonet *et al* 1997).

OPG has features of a secreted glycoprotein including a hydrophobic leader peptide and 4 potential sites of N-linked glycosylation. The N-terminus structure has a strong similarity to all other members of the TNFR superfamily, most notably to TNFR-2 and CD40. However, unlike the transmembrane members of the TNFRSF, OPG is unique because it contains no hydrophobic transmembrane-spanning sequence which is required for intracellular signalling. The N-terminus, contains 4 canonical cysteine rich N-terminal domains involved in the formation of 'tethered loops', conferring ligand binding, which are required for biological activity, including the inhibition of osteoclastogenesis (residues 22-194) (Figure 1.10 B) (Smith *et al* 1994).

At the C-terminus, OPG contains 2 death domain homologous regions (D5 and D6) which mediate cytotoxic signals when they form a chimeric protein with Fas. This is a pattern which shows no known homologies to any other recognisable protein motifs (Yamaguchi *et al* 1998). Domain 7 possesses a heparin-binding site important for the interaction of OPG with proteoglycans. The presence of Cys-400 within domain 7 has been shown to be central to OPG dimer formation (Yamaguchi *et al* 1998).

Initially OPG is synthesised as a 60kDa monomer within the cell which is converted to a secreted disulphide-linked homodimer glycoprotein, approximately 120kDa. It is the dimeric form of this protein which has the highest hypocalcaemic bio-acitivity.

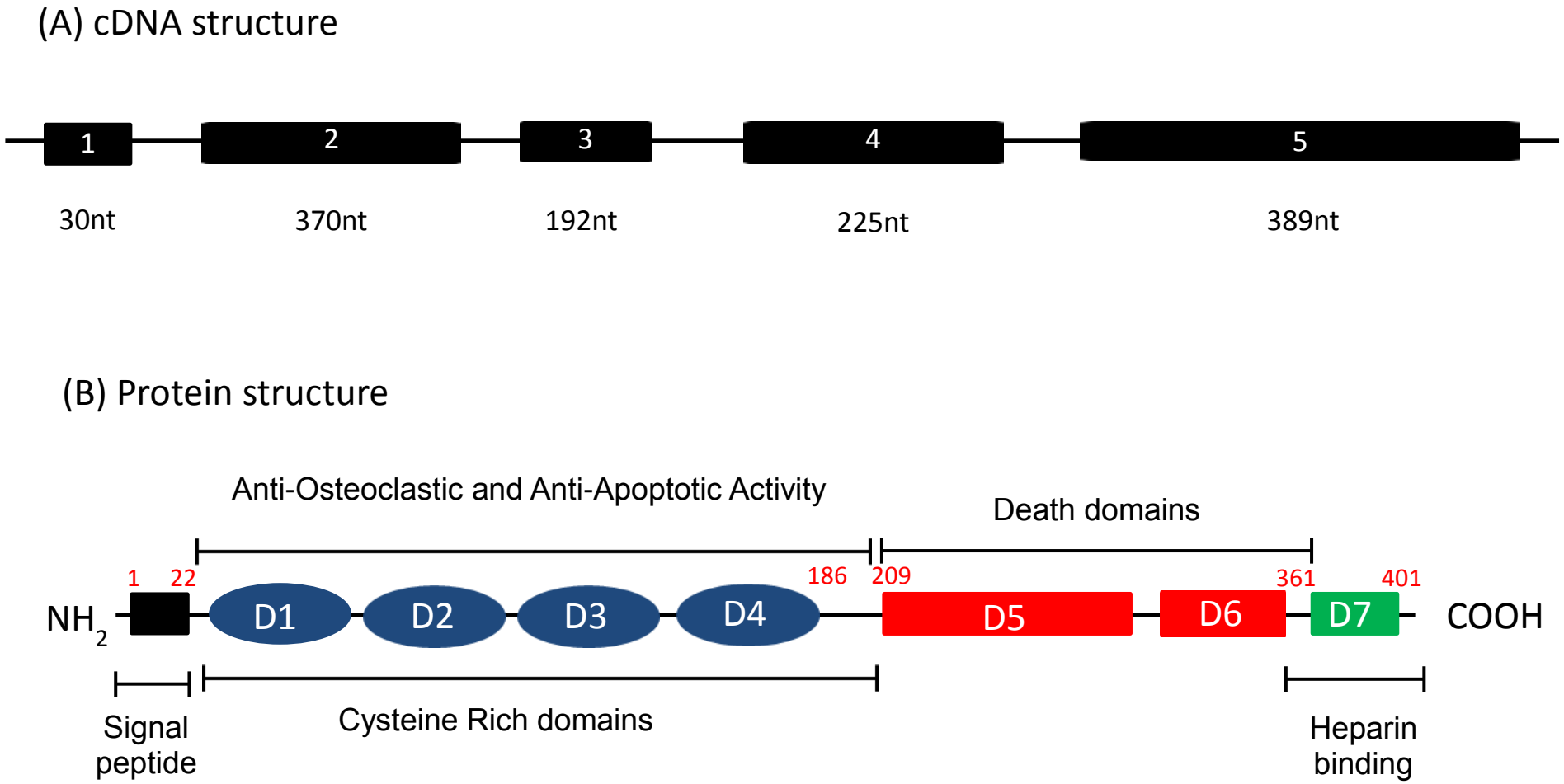

Figure 1.10 – OPG structures

Schematics of DNA and protein structures for OPG

1.7.2.2 Role in bone turnover

Since the identification of OPG in 1997 its role in the regulation of bone turnover through inhibition of RANKL has been best characterised. Binding of RANKL to RANK on pre-osteoclasts and osteoclasts is essential for their maturation and degradation of the bone matrix. OPG represents an endogenous receptor antagonist, produced by osteoblasts, that neutralises the biologic effects of all three forms of RANKL. OPG binding as a homodimer to the homotrimeric RANKL prevents it binding to RANK and subsequent osteoclast activation. *In vitro s*tudies have confirmed the requirement for OPG dimerization in this process, with the monomeric form having reduced RANKL-binding affinity (Schneeweis *et al* 2005).

OPG has been shown, in the skeleton, to systemically inhibit RANKL independent of local bone turnover rates or access to remodelling surfaces. OPG has also been demonstrated to rapidly reduce osteoclast numbers whilst having no direct effect on osteoblasts (Kostenuik 2005).

1.7.2.3 Role in cell survival

In addition to its role in regulating bone turnover, OPG can stimulate cell survival by acting as a receptor for TNF-related apoptosis-inducing ligand (TRAIL) (Emery *et al* 1998). TRAIL is a member of the tumour necrosis factor superfamily produced by immune cells within the tumour microenvironment, such as monocytes, in response to IFN-α and IFN-β. Activation of DR4/DR5 by TRAIL triggers the death signalling cascade common to the TNF family, however OPG is capable of blocking this, and therefore cancer cells which produce OPG have the ability to evade this form of apoptosis (Holen *et al* 2002, Neville-Webbe *et al* 2004, Shipman and Croucher 2003).

1.7.2.4 Role in immunity

OPG expression in a variety of tissues, including those of the vascular and immune system, suggests other roles, both physiologically and pathophysiologically, may exist for OPG. In dendritic cells, TNFα, RANKL, IL-1β and ligation of CD40 have all been demonstrated to up regulate OPG expression (Schoppet *et al* 2007, Yun *et al* 1998).

OPG expression has been shown, both *in vitro* and *in vivo*, to increase with dendritic cell maturity, in human lymphoid tissue possibly involving the NF-κB pathway (Schoppet *et al* 2007). It is believed that OPG may act to down regulate the immune response by decreasing dendritic cell survival through inhibition of RANK-RANKL interactions similar to its role in bone turnover (Reid and Holen 2009). This has been supported by an *in vivo* autoimmunity model, IL-2 deficient mice treated with OPG, prevented T-cell mediated inflammation through a reduction in dendritic cell survival (Ashcroft *et al* 2003).

1.7.2.5 Role in the vascular system

Evidence has emerged of the possible effects OPG exerts on vasculature cells and tissues including the heart, arteries and veins (Collins-Osdoby 2004). Both smooth muscle cells and the endothelium have been shown to produce OPG (Schoppet *et al* 2002, Malyankar *et al* 2000). Several epidemiological studies have shown that increased OPG levels were detected in patients who had died from stroke or cardiovascular event (Browner *et al* 2001, Jono *et al* 2002 and Schoppet *et al* 2003, Kiechl *et al* 2004). Studies have also demonstrated that OPG may act in a paracrine manner on endothelial cells promoting their survival, though the mechanism by which this is achieved remains under debate (McGonigle *et al* 2009, Cross *et al* 2006b, Pritzker *et al* 2004).

1.7.2.6 Role in tumourigenesis

The role OPG may play in tumourigenesis has largely focused on those cancer types which preferentially metastasise to the bone and how it affects tumour cell survival (Zauli *et al* 2009). *In vitro* expression studies have demonstrated that both poorly differentiated hormone independent breast and prostate cancer cell lines produce sufficient OPG to protect themselves against TRAIL-induced apoptosis (Thomas *et al* 1999, Holen *et al* 2002, Holen *et al* 2005). Pettersen *et al* (2005) also reported similar observations in the colorectal cell lines. Whilst subsequent data has suggested that bone marrow stromal cells, which also produce OPG, produce sufficient levels of OPG to protect tumour cells from TRAIL-induced apoptosis (Neville-Webbe *et al* 2004, Nyambo *et al* 2004). Paradoxically, multiple myeloma cells, which do not produce OPG, result in a decrease in OPG production from bone stromal cells, but the bone stromal cells still produce sufficient levels of OPG to prevent myeloma cell apoptosis (Croucher *et al* 2001, Shipman and Croucher 2003, Giuliani *et al* 2001, Pearse *et al* 2001). This suggests there is a fine balance between the beneficial effects of OPG in cancer induced SREs and detrimental inhibition of TRAIL induced apoptosis (Reid and Holen 2009).

One recent study provided a molecular link between prostate cancer cell lines and their metastatic potential. Constitutive OPG mRNA levels were found to be threefold to fourfold higher in prostate cancer cells compared to healthy prostate tissue (Brown *et al* 2001a). These findings are similar to those obtained in osteosarcoma cells, which like prostate cancer forms osteoblastic tumours in bone.

A potential role of OPG in tumour growth angiogenesis is also emerging. Cross *et al* (2006a) demonstrated that, *in vitro*, as well as promoting endothelial cell survival, OPG promotes endothelial cell tubule formation. OPG was also observed to protect endothelial cells from apoptotic cell death under trophic withdrawal though this did

not occur through inhibition of TRAIL, suggesting other unidentified inhibitory mechanisms may also be induced by OPG (Cross *et al* 2006). Secchiero *et al* (2008) also suggested a potential pro-angiogenic role, in which p53 deficient endothelial cells exhibited increased OPG levels.

The majority of *in vivo* models indicate that the presence of OPG can decrease bone lysis associated with cancer-induced SREs, indirectly resulting in a reduction in tumour growth possibly due to space limitations and inhibition in the release of bone-derived growth factors (Reid and Holen 2009). However, the impact on the tumour cells themselves is less well defined, with results not reproducible in subcutaneous xenograft models (Morony *et al* 2001, Zhang *et al* 2001). There is also some evidence to suggest that OPG may play differing roles depending on the source and the cancer type. Fisher *et al* (2006) demonstrated, in a MCF-7 breast cancer model, that OPG overexpression resulted in increased cell proliferation in both the bone and soft tissue. However this was not replicated in a prostate model in which little effect was seen in soft tissue growth, but the tumour burden in the bone and osteolysis were decreased (Corey *et al* 2005).

1.7.2.7 Clinical evidence for role in tumourigenesis

Clinical studies have assessed OPG both in serum and using immunohistochemistry across various cancer types. Lipton *et al* (2002) and Valero *et al* (2006) reported that elevated OPG serum levels were detected in colorectal, pancreatic and squamous cell head and neck cancer. There also appears to be an association with increased OPG serum levels and the presence of bone metastases in breast, lung and prostate cancer (Mountzios *et al* 2007, Brown *et al* 2001b).

In prostate cancer, immunohistochemical staining has shown increased OPG expression in metastatic prostate cancer sections, both osseous and non-osseous,

compared with normal and primary carcinoma tissue (Brown *et al* 2001a). Whilst increased OPG levels correlate with tumour burden, AR-status, metastatic bone disease and relapse following androgen ablation therapy (Brown *et al* 2001a, Jung *et al* 2004, Eaton *et al* 2004, Chen *et al* 2006). These findings suggest OPG could be a suitable candidate for a prognostic biomarker in prostate cancer. Similar patterns of immunohistochemical staining have also been reported in breast cancer. Oestrogen receptor (ER) positive samples were positive for OPG staining, whilst little staining was noted in the ER negative samples (Van Poznak *et al* 2006).

Clinical data also strongly supports a potential role for OPG in tumour angiogenesis. Strong immunohistochemical staining was seen in endothelial cells of malignant tissue across a variety of cancers, including breast and colorectal (Reid and Holen 2009). In the breast cancer study, this endothelial staining was shown to correlate with tumour grade and inversely correlate with ER status (Cross *et al* 2006a, Cross *et al* 2006b). These findings suggest that increased angiogenesis may be an additional mechanism by which OPG can affect tumour progression.

1.7.2.8 Signalling

In vitro and *in vivo* studies have suggested that *TNFRSF11B* gene expression is regulated by the Wnt/β-catenin signalling pathway in osteoblasts (Glass *et al* 2005). Known as a canonical pathway; it promotes osteoblast commitment, proliferation and differentiation and enhances osteoblast and osteocyte survival (Bonewald and Johnson 2008). The Wnt/β-catenin pathway is activated by Wnt binding with a co-receptor complex involving low-density lipoprotein-related protein (LRP5 and LRP6) and one of the frizzled family members (Fz). The complex Wnt/LRP/Fz leads to the release of non-phosphorylated β-catenin into the cytoplasm from where it translocates to the nucleus to modulate gene transcription.

The involvement of the canonical Wnt pathway in bone cells has been revealed in various studies showing that loss-of-function mutations in LRP5 (Gong *et al* 2001) resulted in decreased bone mass, whereas gain of function mutations increased bone mass in humans and mice (Boyden *et al* 2002,). OPG expression is enhanced in osteoblasts derived from mice with loss-of-function mutations in *LRP5*, whereas it is reduced in osteoblasts from gain-of-function mutations, suggesting that the Wnt signalling pathway regulates osteoclasts by increasing the OPG:RANKL ratio (Kubota *et al* 2009).

Wnt signalling is tightly regulated by secreted antagonists, such as the secreted frizzled-related protein family (sFRP) and Wnt inhibitory factor (WIF-1) which antagonise the interaction of Wnt with its receptor Fz (Aberle *et al* 1997).

1.7.3 RANKL

RANKL, also known as OPG-ligand (OPGL), osteoclast differentiation factor (ODF) or TNF-related activation-induced cytokine (TRANCE), is a type II transmembrane protein (317 amino acid) containing a small N-terminal intracellular domain, a transmembrane region and an extracellular C-terminal consisting of a stalk and a receptor binding regions that forms trimers, typical of the TNFRSF.

1.7.3.1 Structure

Anderson *et al* (1997) mapped the RANKL gene, *TNFSF11*, to chromosome 13q14 whilst the protein was discovered and isolated independently by 3 groups (Anderson *et al* 1997, Wong *et al* 1997 and Yasuda *et al* 1998b).

RANKL can exist in three forms, membrane bound, soluble ectodomain form generated by post-translation modification by TNF-α converting enzyme-like protease or soluble secreted form, which is predominately seen in activated T-lymphocytes or cancer cells generated through proteolytic cleavage of the extracellular stalk by MMP14 and ADAM10 (Burgess *et al* 1999, Lacey *et al* 2012). RANKL gene expression is mainly expressed in lymph nodes and bone marrow stromal cells. In the skeleton, RANKL is expressed in the primitive mesenchymal cells, hypertrophying chondrocytes and in areas of primary ossification and re-modelling.

1.7.3.2 Role in bone remodelling

RANKL is an essential factor in the recruitment, differentiation, activation and survival of osteoclasts through binding to its specific receptor RANK, which is present on the surface of osteoclast precursors driving them towards mature osteoclasts and inhibition of apoptosis of mature osteoclasts. RANKL is essential and sufficient for all other steps of the osteoclast life cycle (Dougall *et al* 2014).

Exogenous administration of RANKL to normal mice increased the number and activity of osteoclasts, causing rapid bone loss and promoting the development of severe osteoporosis and lethal hypercalcaemia. Lacey *et al* (1998) also demonstrated that *in vitro* RANKL can directly activate isolated mature osteoclasts. The effects of RANKL are blocked *in vitro* and *in vivo* by the soluble inhibitor OPG, suggesting that these remain integral regulators of osteoclast development. Luan *et al* (2012) revealed that OPG exerts its decoy receptor function by directly blocking the accessibility of interacting residues on RANKL, including arg223, tyr241 and lys257, vital for RANK recognition.

RANKL expression is regulated by various osteotropic cytokines, peptides and steroid hormones that are known modulators of bone resorption and determinants of bone mass. Wong *et al* (1999) demonstrated that RANKL activates the serine/theorine kinase PKB through a signalling complex involving SRC and TRAF6. Upon RANK receptor engagement, SRC and TRAF6 interacted with each other. TRAF6 enhances the kinase activity of SRC, leading to tyrosine phosphorylation of downstream signalling molecules such as CBL. A deficiency in SRC or addition of SRC family kinase inhibitors blocked RANKL mediated PKB activation in osteoclasts.

Ikeda *et al* (2004) generated transgenic mice expressing dominant-negative c-Jun, specifically in the osteoclast lineage, and found that they developed severe osteopetrosis due to impaired osteoclastogenesis. This was also mimicked *in vitro* by the blockade of c-Jun signalling which markedly inhibited soluble RANKL-induced osteoclast differentiation. Overexpression of nuclear factor of activated T cells 1 (NFATC1) promoted differentiation of osteoclast precursor cells into TRAP-positive multinucleated osteoclast-like cells, even in the absence of RANKL. The osteoclastogenic properties of NFATC1 were abrogated by over-expression of dominant-negative c-Jun leading Ikeda *et al* (2004) to conclude that c-Jun signalling, in co-operation with NFAT, is crucial for RANKL-regulated osteoclast differentiation.

Takayanagi *et al* (2002) demonstrated that RANKL induces the IFN-β gene in osteoclast progenitor cells. Interestingly, IFN-β inhibits the differentiation of osteoclasts by interfering with the RANKL-induced expression of c-Fos, an essential transcription factor for the formation of osteoclasts. This therefore highlights the potential for an auto-regulatory mechanism in which RANKL induces its own inhibitor.

1.7.3.3 Role in immunity

RANKL has been described as a T-cell-derived cytokine (TRANCE) and appears to be an important regulator for T-cell-dendritic cell interactions in the immune system. RANKL augmented the ability of dendritic cells to stimulate naïve T-cell proliferation in a mixed lymphocyte reaction and increase the survival of RANK+ T cells generated with IL-4 and TGF-β (Anderson *et al* 1997). RANKL also up-regulated *Bcl-x_L* expression, and thus promoted dendritic cell survival through an inhibition of apoptosis (Chino *et al* 2009).

Kong *et al* (1999) reported that systemic activation of T-cells could directly trigger osteoclastogenesis and bone loss through RANKL *in vivo.* This was supported by a T-cell dependent model of rat adjuvant arthritis characterised by severe joint inflammation and bone and cartilage destruction. Blocking of RANKL with OPG treatment at the onset of disease prevented bone loss and cartilage destruction but not inflammation. These results show that both a systemic and local T-cell activation can lead to RANKL production and subsequent bone loss, providing a potential role for T-cells as regulators in bone physiology. RANKL produced by bone and immune cells (osteoblastic cells, activated T-cells) through the modulation of the differentiation, activation and survival of bone and immune cells (osteoclasts, dendritic cells), indicates that RANKL may represent a crucial paracrine link between bone metabolism and the immune system.

Wong *et al* (1997) reported that a soluble form of RANKL, consisting of the extracellular domain, can activate JNK in T-cells but not in B-cells or bone marrow derived dendritic cells. They suggested that this isoform may also play a specific role in the regulation of T-cell function though further elucidation into how this occurs is needed.

1.7.3.4 Role in tumourigenesis

Bone destruction, caused by aberrant production and activation of osteoclasts, is a prominent feature of multiple myeloma. It has been demonstrated that myeloma cells stimulate osteoclastogenesis by triggering a co-ordinated increase in RANKL and a decrease in its decoy receptor OPG (Pearse *et al* 2001). In co-culture, myeloma cell lines stimulated expression of RANKL and inhibited expression of OPG by stromal cells. This data identified that RANKL and OPG are key cytokines, in which their dysregulation promotes bone destruction and supports myeloma growth. In an *in vivo* mouse model of melanoma metastasis, neutralisation of RANKL by OPG resulted in complete protection from paralysis and a marked reduction in tumour burden in bones but not in other organs (Croucher *et al* 2001).

RANKL mRNA expression was also found to be high in tumour xenografts established using the PC-3 prostate cancer cell line, which has the capacity to induce osteolytic metastases, and low in xenografts of the LNCaP prostate cancer cell line, which lacks this capacity and grows as a mixed osteoblastic-osteolytic tumour (Corey *et al* 2002).

RANKL and RANK have been shown to be involved in mammary gland development and therefore the roles they play in breast cancer are best characterised. Gonzalez-Suarez *et al* (2010) showed that RANK and RANKL are expressed within normal, premalignant and neoplastic mammary epithelium. Using complementary gain-of-function and loss-of-function approaches, a direct contribution of this pathway has been linked to breast tumourigenesis. Accelerated pre-neoplasias and increased mammary tumour formation were observed in MMTV-RANK transgenic mice after treatment with carcinogen inducing hormone, progesterone. Reciprocally, selective pharmacologic inhibition of RANKL attenuated mammary tumour development not only in hormone- and carcinogen treated

MMTV-RANK and wild type mice but also in the MMTV-new transgenic spontaneous tumour model (Gonzalez-Suarez *et al* 2007). The reduction in tumourigenesis after RANKL inhibition was preceded by a reduction in pre-neoplasias as well as rapid and sustained reductions in hormone- and carcinogen-induced mammary epithelial proliferation and cyclin D1 levels. Gonzalez-Suarez *et al* (2010) concluded that RANKL inhibition is acting directly on hormone-induced mammary epithelium, at early stages in tumourigenesis and the permissive contribution of progesterone to increased mammary cancer incidence is due to RANKL-dependent proliferative changes in the mammary epithelium.

Jones *et al* (2006) demonstrated that the cytokine RANKL, in a local environment, can trigger a pro-migratory response in RANK expressing human epithelial cancer cells and melanoma cells. Most RANKL-producing T-cells expressed FOXP3, a transcription factor produced by regulatory T-cells. Tan *et al* (2011) examined whether RANKL, RANK and IKK-α were involved in mammary/breast cancer metastasis. RANK signalling in mammary carcinoma cells which overexpress the proto-oncogene Erbb2 (Neu), which is frequently amplified in human breast cancers, was important in pulmonary metastasis. Metastatic spread of Erbb2-transformed cancer cells also required $CD4^{+}CD25^{+}$ T cells, whose major pro-metastatic function was RANKL induced, especially when located next to smooth muscle actin-positive stromal cells in mouse and human breast cancers. The dependence of pulmonary metastasis on T-cells was replaceable by exogenous RANKL, which also stimulated pulmonary metastasis of RANK-positive human breast cancer cells. Tan *et al* (2011) concluded that these results were consistent with the adverse impact of tumour-infiltrating CD4+ or FOXP3+ T cells on human breast cancer prognosis and suggested that the targeting of RANKL-RANK can be used in conjunction with the therapeutic elimination of primary breast tumours to prevent recurrent metastatic disease.

1.7.4 RANK

Anderson *et al* (1997) identified dendritic cell cDNA which encoded a protein with homology to an extracellular domain of the TNFRSF. This 616 amino acid protein was subsequently named RANK.

1.7.4.1 Structure

The RANK gene, *TNFRSF11A*, is located on chromosome 18q21.33, in some human cell lines encoding a type I homotrimeric transmembrane protein, containing 4 extracellular cysteine-rich pseudo-repeats as seen in the rest of the TNFRSF. Northern blot analysis indicated that the 4.5-kb human RANK mRNA is expressed ubiquitously but particularly apparent on mature osteoclasts, dendritic cells and some cancer cells, including breast and prostate cancers. Anderson *et al* (1997) also detected additional transcripts that were derived from the use of alternative polyadenylation signals in the RANK gene.

1.7.4.2 Role in bone remodelling

Nakagawa *et al* (1998) identified RANK as an osteoclast differentiation factor on osteoclast progenitor cells, essential for osteoclast differentiation which mediated osteoclastogenesis. Much work has gone into elucidating the role RANK and RANKL interaction plays in osteoporosis and the genetic condition Pagets disease. Dougall *et al* (1999) generated RANK -/- mice and found that they had profound osteopetrosis resulting from a block in myeloid osteoclast differentiation. However, RANK was not required for myeloid commitment to macrophage, granulocyte or dendritic cell pathways. RANK -/- mice also exhibited splenic B-cell deficiency and peripheral lymph nodes, except for mucosal associated lymphoid tissues. This

demonstrated that RANK is critical for lymph node organogenesis and osteoclast differentiation.

Li *et al* (2000) generated RANK-null mice to determine the molecular genetic interactions between OPG, RANKL and RANK during bone resorption and the remodelling processes. RANK -/- mice lacked osteoclasts and had a profound defect in bone resorption and remodelling as well as in the development of the cartilaginous growth plates of endochondral bone. The osteopetrosis observed in these mice could be reversed by transplantation of bone marrow from mice nullizygous for the recombinase activating gene (RAG1), indicating that RANK -/- mice have an intrinsic defect in osteoclast function. Calciotropic hormones and pro-resorptive cytokines are capable of inducing bone resorption, in both RANK -/- mice and humans without inducing hypercalcaemia, although TNF-α treatment lead to the rare appearance of osteoclast-like cells near the site of injection (Li *et al* 2000). Osteoclastogenesis could be initiated in RANK -/- mice by transfer of the RANK cDNA back into hematopoietic precursors, suggesting a means to critically evaluate RANK structural features required for bone resorption. Together this data has indicated that RANK is the intrinsic cell surface determinant that mediates RANKL driven effects on bone resorption and remodelling as well as the physiological effects of calciotropic hormones and pro-resorptive cytokines (Li *et al* 2000).

Functional expression and biologic effects of RANK have mainly been characterised in osteoclasts and dendritic cells. After stimulation by RANKL, the activated RANK interacts with TNFR-associated factors (TRAF) 1-6, of which TRAF 6 appears to be essential for signal transduction (Wei *et al* 2013, Yen *et al* 2012). RANK signal transduction then diverges into three separate pathways that regulate distinct aspects of osteoclast functions:

- Protein kinase c-Jun N terminal kinase (JNK) pathway, which modulates c-fos and c-jun, which are expressed sequentially by late stage osteoclastic precursor cells.

- Nuclear factor (NF)-κB pathway, which regulates osteoclastogenesis and proteasome formation.

- Serine/threonine kinase Akt/PKB, which inhibits apoptosis, modulates cytoskeleton reorganisation and may cross-talk to the NF-κB pathway.

1.7.4.3 Role in tumourigenesis

Schramek *et al* (2010) demonstrated that *in vivo* administration of medroxyprogesterone acetate (MPA), used in women for hormone replacement therapy and contraceptives, triggers massive induction of the key osteoclast differentiation factors including RANKL in mammary gland epithelial cells. Genetic inactivation of RANK in mammary gland epithelial cells prevented MPA-induced epithelial proliferation, impaired expansion of CD49f(hi) stem cell-enriched population, and sensitised these cells to DNA damage-induced cell death. Deletion of RANK from the mammary epithelium also resulted in a markedly decreased incidence and delayed onset of MPA-driven mammary cancer. Schramek *et al* (2010) concluded that the RANKL/RANK system controls the incidence and onset of progestin-driven breast cancer.

The establishment and progression of tumour cell growth in bone is a complex and dynamic process that depends on biological characteristics of the tumour cells, the properties of the bone and bone marrow microenvironment, and a network of growth factors, cytokines and chemokines and their antagonists as well as receptors, adhesion molecules and MMPs. With the identification and characterisation of the RANKL/RANK/OPG cytokine system, several studies have implicated RANKL,

RANK and OPG as an essential cytokine system that regulates tumour-bone interactions, though further understanding on how these pathways converge is needed.

1.8 Hepatocyte Growth Factor and its receptor cMET

Hepatocyte growth factor (HGF), also known as scatter factor, was discovered 30 years ago (Nakamura *et al* 1984, Michalopoulos *et al et al* 1984, Russell *et al* 1984). In 1985, Stoker and Perryman discovered a factor which had the ability to scatter tightly packed colonies of epithelial cells; subsequent partial amino acid sequencing has revealed this factor to have over 90% homology to human HGF. HGF has been under intense investigation for potential roles it may play in cancer initiation and progression as it elicits diverse cellular responses in a range of cell types and tissues (Jiang *et al* 1999).

1.8.1 HGF

The human HGF encoding gene is located on chromosome 7q11.1-21 and is composed of 18 exons and 17 introns spanning approximately 70Kb (Weidner *et al* 1991, Fukuyama *et al* 1991, Seki *et al* 1991). Cloning and sequencing of HGF has revealed it to be a single 728 amino acid chain polypeptide, including a 29 amino acid signal sequence and a 25 amino acid pro-peptide sequence (Nakamura 1989).

HGF is synthesised and secreted in a single pro-form which is converted to a mature heterodimeric protein, by extracellular cleavage through enzymatic hydrolysis of the Arg-Val bond within the pro-sequence by a serine protease including hepatocyte growth factor converting enzyme, thrombin, uPA and tissue plasminogen activator (tPA) (Naldini *et al* 1995, Mizuno *et al* 1994, Shimomura *et al*

1993, Mars *et al* 1993). The mature HGF protein consists of a 69kDa α-chain and a 34kDa β-chain.

HGF is a unique growth factor because it has 4 kringle domains each located on the α-subunit. Artificially induced HGF deletions in the N-terminal hairpin structure, or any of the kringle domains, though particularly the first or second kringle domain, results in the loss of biological function possibly due to a lack of protein-protein binding (Matasumoto *et al* 1991, Lerch *et al* 1980, van Zonneveld *et al* 1986).

HGF has since been established as a mitogen that regulates cell growth and death, a motogen that stimulates cell motility, a morphogen that modulates cell morphology and tissue/organ regeneration and a pro-angiogenic and lymphangiogenic factor (Gherardi and Stoker 1990). Osteoblasts have been shown to secrete HGF (Grano *et al* 1996), a process which has been shown to act as a cooperative secretion to stimulate the survival of haematopoietic progenitors (Taichman *et al* 2001). HGF is believed to be a coupling factor between osteoblasts and osteoclasts. HGF is known to play a role in osteoclast formation. HGF receptor, c-MET is expressed by the CD14+ monocyte fraction of human peripheral blood mononuclear cells (PBMC). Adamopoulos *et al* (2006) demonstrated that HGF was able to support monocyte-osteoblast differentiation in the presence of RANKL. Osteoclast formation is stimulated by HGF in the presence of osteoblastic cells but the mechanism(s) behind this remain elusive.

HGF is a heparin binding glycoprotein which initiates intracellular signalling through its receptor, cMET, encoded by the c-Met proto-oncogene (Bottaro *et al* 1991). HGF signals through the tyrosine kinase receptors and phosphorylates common transducers and effectors such as Src, Grb2 and PI3-kinase.

1.8.2 c-MET

The HGF receptor, c-MET, was first identified as an activated oncogene which has been mapped to chromosome 7 at q21-31 and encodes a 1408 amino acid glycoprotein (Park *et al* 1987). c-MET is considered a member of the tyrosine kinase (RTK) family of cell surface molecules, a family which shares common structural organisation: an N-terminal extracellular ligand binding domain, a single transmembrane α-helix and a cytosolic C-terminal domain with intrinsic tyrosine kinase activity. The receptor, encoded by the *c-MET* proto-oncogene, is a two chain protein composed of a 50k-Da α-chain disulphide linked to a 145kDa β chain (Naldini *et al* 1991, Bottaro *et al* 1991). The α chain is exposed at the cell surface whilst the β chain spans the cell membrane and possesses an intracellular tyrosine kinase domain (Giordano *et al* 1993,Park *et al* 1987).

HGF binds to and induces tyrosine phosphorylation of the mature c-MET receptor β chain. Such events are thought to promote binding of intracellular signalling proteins containing *src* homology (SH) regions such as phospholipase Cγ (PLCγ), Ras-GAP, phosphatidylinositol 3-kinase (PI-3K), pp60c-src and the GRB-2-Sos complex to the activated receptor (Ponzetto *et al* 1994, Jiang *et al* 1999, Ponzetto *et al* 1993). Several studies have shown that the two closely spaced tyrosines in the cytoplasmic domain of c-MET (Y1349 and Y1356) are essential for scattering and is the principal determinant of which SH-2 containing protein will bind to the phosphotyrosine (Koch *et al* 1991, Pawson and Gish 1992) . Y14 and Y15 recruit several SH-2 domain containing proteins including adaptor proteins such as Grb2, Shc, Gab1 and Cb1 and effector proteins such as PI-3K, Src, PLCγ, Shp2 as well as transcription factor signal transducer and activator of transcription 3 (Stat3) (Okano *et al* 1993).

Each SH-2 containing protein may activate a different subset of signalling phosphopeptides thus eliciting different responses within the cell. For example,

Gab1 which amplifies the c-MET response, stimulates branching in morphogenesis *in vitro* by activating Shp2 and PLCγ in a sustained manner. Whilst CB1 the other docking protein is involved in signal transduction as well as acting as a E3 ubiquitin ligase that down regulates c-MET. EMT is promoted in a CB1 variant that lacks the part of the ring finger domain required for CB1 ubiquitin ligase activity and by a mutant which lacks the c-MET binding site (Fan *et al* 2001).

1.8.3 The role of HGF and cMET in cancer

Since its discovery, HGF has been strongly implicated in the regulation of tumour cell behaviour, although the degree of response varies between tumour types. The independent discoveries of HGF as a mitogenic agent and a motogenic stimulus, as well as a morphogenic regulator, demonstrate that it is a factor which can elicit different responses in target cells, although these activities are not mutually exclusive. HGF and c-MET have been found to be overexpressed at both mRNA and protein levels in virtually all human solid tumours as well as in haematopoietic-derived malignancies (Jiang *et al* 2005b).

HGF was initially regarded as a protein product from host stromal cells in the context of cancer. However the discovery that epithelial cancer cells showed aberrant HGF transcript and protein expression indicates that the sources and roles of HGF in cancer progression may be from multiple sources rather than from a purely stromal origin. Though additionally, stromal cells in tumour tissues over express the HGF transcript and HGF protein (Boccaccio *et al* 1998). Transcriptional activation of HGF in epithelial cancer cells is thought to be via the c-src and Stat3 pathways. Together with over-expression of c-MET on cancer cells, this creates a mechanism for bi-stimulation of cancer cells: paracrine stimulation (HGF generated by stromal cells) and autocrine stimulation (HGF generated by cancer cells

themselves). In general, paracrine stimulation is probably the stronger of the two, as some tumour cell types are known to be completely free from expressing HGF.

In a variety of cancers, including prostate and pancreatic, HGF has been shown to increase cancer cell proliferation and motility (Humphrey *et al* 1995, Hasegawa *et al* 1995, Pisters *et al* 1995). In breast cancer, HGF has been shown to increase cell motility and cell invasiveness, through increased expression and secretion of proteolytic enzymes from cancer cells including MMP2, MMP7, MMP9 and uPA, and cell-matrix adhesion (Giordano *et al* 1993, Jiang *et al* 1996, Davies *et al* 2001).

1.9 Aims

The current study aimed to assess the importance of the endogenously produced OPG/RANK/RANKL family of proteins in prostate and breast cancer in differing osteotrophic phenotypes and their potential for involvement in dissemination to and colonisation of bone. In addition, the study aimed to explore the therapeutic implications of targeting members of this family in relation to these cancer types. Specific aims were:

1) To generate OPG knockdown models in osteotropic osteolytic PC-3 prostate and MDA-MB-231 breast cancer cell types and explore the impact suppression of OPG has in these lines.
2) To explore the impact of alterations in OPG and RANKL levels through addition of recombinant protein or neutralising antibodies in the mixed osseous LNCaP prostate cell line.
3) To assess the impact of extracellular environmental stimuli (HGF and isolated bone proteins) on these model systems *in vitro* and the potential for these molecules in mediating the signal transduction induced by these growth factors or isolated bone proteins.

4) To assess members of this family in more complex clinical and *in vivo* settings.

Chapter 2

General Materials and Methods

2.1 Cell lines

Six prostate and three breast cancer cell lines were used in this study. Full details of cell origins and characteristics are outlined in Table 2.1. PC-3, MDA-MB-231 and MCF-7 were purchased from the European Collection of Animal Cell Culture (ECACC, Salisbury, UK). All other cells were purchased from the American Type Culture Collection (ATCC, Rockville, Maryland, USA).

2.2 Breast cancer tissue collection

All research involving human tissues was conducted under the ethical approval of the local ethics committee (Bro Taf Local Research Ethics Committee (Panel B) for the Bro Taf Health Board, Cardiff, UK issued 10/12/2001, reference 01/4303). All data was analysed anonymously and informed verbal consent given. As the tissues were collected before the introduction of the Human Tissue Act, UK 2004, no written consent was necessary and documentary measures not required. Primary breast cancer tissue and matching non-neoplastic mammary tissue were collected from the same mastectomy specimens' immediately after surgery and stored at -80^{o}C until use. All the specimens were verified and graded by a consultant pathologist. Medical notes and histology reports were used for the collation of clinical and pathological data at point of surgical intervention and during the postoperative follow-up (Median – 120 months). All tissues were randomly labelled and details of histology, tumour grade, Nottingham prognostic index (NPI) and clinical outcomes were only made known during experimental data analysis.

Table 2.1(A): Prostate Cancer Cell lines

	Cell line	Species	Morphology	Origin	Sources and features
Prostate cancer	PZHPV-7	*Homo sapiens*	Epithelial	Caucasian male aged 70	Derived from prostate epithelial cells cultured from normal tissue within the prostate peripheral zone. Transformed using HPV18 DNA
	CAHPV-10	*Homo sapiens*	Epithelial	Caucasian male aged 63	Derived from prostate adenocarcinoma of Gleason grade 4/4. Cells transformed with HPV18 DNA Non-tumourigenic
	PC-3	*Homo sapiens*	Epithelial	Caucasian male aged 62	Derived from a metastatic bone site of a grade IV prostate adenocarcinoma. Tumourigenic Bone metastasis phenotype - Osteolytic
	DU-145	*Homo sapiens*	Epithelial	Caucasian male aged 69	Derived from brain metastasis of a prostate cancer patient. Not androgen sensitive, only weakly positive for acid phosphatase. Cells do not express PSA
	LNCaP FGC clone	*Homo sapiens*	Epithelial	Caucasian male aged 50	Prostate carcinoma derived from left supraclavicular lymph node Tumourigenic Androgen sensitive and androgen receptor positive Bone metastasis phenotype - Mixed osteolytic and osteoblastic
	MDA PCa 2b	*Homo sapiens*	Epithelial	African American male aged 63	Prostate androgen independent adenocarcinoma Expresses PSA and androgen receptor Bone metastasis phenotype - Osteoblastic

Table 2.1(B): Breast Cancer Cell lines

	Cell line	Species	Morphology	Origin	Sources and features
Breast cancer	ZR-75-1	*Homo sapiens*	Epithelial	Caucasian female aged 63	Derived from ductal breast carcinoma. Oestrogen receptor expressed, mucin expressed
	MCF-7	*Homo sapiens*	Epithelial	Caucasian female aged 69	Derived from pleural effusion of breast cancer. Oestrogen receptor and androgen receptor positive, also expresses IGFP, BP-2, BP-4, BP-5
	MDA MB 231	*Homo sapiens*	Epithelial	Caucasian female aged 51	Derived from metastatic site pleural effusion of breast adenocarcinoma Tumourigenic Express WNT7B oncogene, EGFR and TNF-α receptor Bone metastasis phenotype – Osteolytic

2.3 Primers

Three different categories of primers were used in this study, all of which were designed using the Beacon Design programme (Biosoft International, Palo Alto, California, USA) and synthesised by Sigma Aldrich (Poole, Dorset, UK). This software incorporates features including an automated search for reaction conditions and possible homology amplification of other genes. The conventional reverse transcription polymerase chain reaction (RT-PCR) and quantitative PCR (qPCR) forward and reverse primers used in this study are detailed in Table 2.2. The paired forward and reverse primers for each gene reside in one of two adjacent exons, whilst the amplified genome sequence includes at least one intron boundary.

2.4 Antibodies

Full details of the primary and secondary antibodies used in this study are provided in Table 2.3

Table 2.2: Primers for conventional RT-PCR and qPCR

Gene	Primer name	Primer Sequence (5'-3')	Optimal annealing temperature ºC)	Product size (bps)
OPG	OPGF8	GAACCCCAGAGCGAAATACA	55	509
	OPGR8	CGGTAAGCTTTCCATCAAGC		
	OPGF1	GTTCTGCTTGAAACATAGGAG	55	115
	OPGZR1	ACTGAACCTGACCGTACACGTCT CATTTGAGAAGAACC		
RANK	RANKF9	CAGAGCACAGTGGGTTCAGA	55	462
	RANKR9	GATGATGTCGCCCTTGAAGT		
	RANKF2	TCTGATGCCTTTTCCTCCAC	55	119
	RANKZR2	ACTGAACCTGACCGTACATGGCA GAGAAGAACTGCAAA		
RANKL	RANKLF9	GACTCCATGAAAATGCAGAT	55	500
	RANKLR9	TCCTTTCATCAGGGTATGAG		
	RANKLF1	AAGGAGCTGTGCAAAAGGAA	55	74
	RANKLZR1	ACTGAACCTGACCGTACAATCCA CCATCGCTTTCTCTG		
GAPDH	GAPDHF10	AGCTTGTCATCAATGGAAAT	55	593
	GAPDHR10	CTTCACCACCTTCTTGATGT		
	GAPDHF	CTGAGTACGTCGTGGAGTC	55	93
	GAPDHZR	ACTGAACCTGACCGTACACAGAG ATGATGATGACCCTTTTG		
PDPL	PDPLF	GAATCATCGTTGTGGTTATG	55	
	PDPLZR	ACTGAACCTGACCGTACACTTTC ATTTGCCTATCACAT		

ACTGAACCTGACCGTACA represents the Z sequence

Table 2.3: Antibodies

Primary antibodies				
Name	**Species**	**Molecular Weight (kDa)**	**Supplier**	**Product Code**
Anti-OPG Antigen affinity purified polyclonal IgG	Goat	60	R&D Systems	BAF805
Anti-RANK polyclonal antibody	Rabbit	90	Santa Cruz Biotechnology, Inc	sc-9072
Anti-GAPDH polyclonal antibody	Mouse	37	Santa Cruz Biotechnology Inc	sc-32233
Secondary antibodies				
Name	**Species**		**Supplier**	**Product Code**
Anti-mouse IgG peroxidase conjugate	Rabbit		Sigma-Aldrich	A-9044
Anti-rabbit IgG peroxidase conjugate	Goat		Sigma-Aldrich	A-9169
Anti-goat IgG peroxidase conjugate	Rabbit		Sigma-Aldrich	A-5420

2.5 General reagents and solutions

The following solutions were used throughout this study. All products were sourced from Sigma Aldrich (Poole, Dorset, UK), unless otherwise stated.

2.5.1 Solutions for use in DNA cloning

Ampicillin

A stock solution of 100mg/ml was prepared by dissolving the ampicillin sodium salt (Melford Laboratories Ltd, Suffolk, UK) in sterile BSS and stored at 4ºC until use.

Liquid Broth (LB)

Ten grams of tryptone (Duchefa Biochemie, Haarlem, Netherlands), 10g of NaCl and 5g of yeast extract (Duchefa Biochemie, Haarlem, Netherlands) were dissolved in 1L of distilled water. The pH of the solution was then adjusted to 7.0, autoclaved and stored at room temperature until needed. Selective antibiotics were later added as required.

LB agar

LB agar was prepared by dissolving 10g of tryptone, 5g of yeast extract, 15g of agar and 10g of NaCl in 1L of distilled water before the pH was adjusted to 7.0 and the solution autoclaved. For use, the solution was melted in a microwave, left to cool before ampicillin (100µg/ml) was added, and the solution poured into single vented 10cm^2 petri dishes (Bibby Sterilin Ltd, Staffs, UK). These were left to cool and set before being inverted and stored at 4ºC until use.

2.5.2 Solutions for use in molecular biology

Diethyl pyrocarbonate (DEPC) water

Prior to being autoclaved, 4.75ml of distilled water was supplemented with 250ml of DEPC.

Loading buffer (used for DNA electrophoresis)

Twenty five milligrams of bromophenol blue and 4g of sucrose (Fisons Scientific Equipment, Loughborough, UK) were dissolved in 10ml of distilled water and stored at 4ºC until needed.

Tris-Boric Acid EDTA (TBE) (5x)

A five times stock solution containing 1.1M of TRIS, 900mM of borate, 25mM of EDTA at pH8.3, was made by dissolving 540g of Tris-HCl (Melford Laboratories Ltd, Suffolk, UK), 275g of boric acid (Melford Laboratories Ltd, Suffolk, UK) and 46.5g of EDTA in 10L of distilled water. The pH was adjusted to 8.3 using NaOH, and then stored at room temperature until further use. For preparing agarose gels and DNA electrophoresis the TBE was diluted to 1x concentrate using distilled water.

2.5.3 Solutions for protein use

Amido black stain

To stain protein after electrophoresis 2.5g of amido black was dissolved in 50ml of acetic acid and 125ml of ethanol, after which 325µl of distilled water was added and the solution well mixed.

Amido black destain

One hundred millilitres of acetic acid and 250ml ethanol were added to 650ml distilled water.

10% Ammonium Persulfate (APS)

One gram of APS was dissolved in 10ml of distilled water, separated into 2.5ml aliquots and stored at 4ºC until required.

Coomassie blue stain

One hundred grams of Coomassie blue was dissolved in 100ml of acetic acid and 250ml of ethanol, which was then added to 650ml of distilled water.

Coomassie blue destain

Five hundred millilitres of methanol was mixed with 100ml of acetic acid and then made up to a final volume of 1L using distilled water.

Lysis Buffer

This was made by dissolving 50mM TRIS base (0.61g), 5mM EGTA (0.19g), 150mM NaCl (0.87g) and 1ml Triton x100 in 100ml of distilled water. Protease inhibitors were added just before use. Protease inhibitors added were PMSF (100µg/ml in isopropanol), aprotinin (10µg/ml), leupeptin (10µg/ml), sodium vanadate (5mM) and sodium fluoride (50mM).

Ponceau S stain

Supplied directly by Sigma for reversible staining of protein bands after blotting.

Running buffer (10x) (for SDS-PAGE)

Ten times running buffer stock solution containing 0.25M Tris, 1.92M glycine and 1% SDS at pH8.3 was prepared by dissolving 303g of Tris, 1.44kg of glycine (Melford Laboratories Ltd, Suffolk, UK) and 100g of SDS (Melford Laboratories Ltd, Suffolk, UK) in 10L of distilled water. Prior to use this solution was further diluted to a 1x concentrate using distilled water.

Transfer buffer

Fifteen point five grams of Tris and 72g of glycine were dissolved in 4L distilled water before the addition of 1L of methanol (Fisher Scientific, Leicestershire, UK) to make a final volume of 5L in distilled water.

Tris Buffered Saline (TBS) (10x)

A 10x TBS stock solution containing 0.5M Tris and 1.38M NaCl, at pH 7.4 was prepared by dissolving 24.228g of Tris and 80.06g of NaCl (Melford Laboratories Ltd, Suffolk, UK) in 1L of distilled water. The pH was then adjusted to 7.4 using HCl and stored at room temperature until use.

2.5.4 Solutions for use in tissue culture

Antibiotics (ABS) (100x)

Five grams of streptomycin, 3.3g of penicillin and 12.5mg of amphotericin B in DMSO were dissolved in 0.5L of BSS, filtered and split into 5ml aliquots which were then added directly to 500ml bottles of media.

Balanced Saline Solution (BSS)

Seventy nine point five grams of NaCl, 2.1g of KH_2PO_4, 2g of KCl and 11.g of Na_2HPO_4 were dissolved in 10L of distilled water. The pH was subsequently adjusted to 7.4 using 1M of NaOH.

Ethylenediaminetetraacetic Acid (EDTA) (0.02%)

One gram of KCl (Fisons Scientific equipment, Loughborough, UK), 5.72g of Na_2HPO_4 (BDH Chemical Ltd, Poole, England, UK), 1g of KH_2PO_4 (BDH Chemical Ltd, Poole, England, UK), 40g of NaCl and 1.4g of EDTA (Duchefa Biochemie, Haarlem, The Netherlands) were dissolved in 5L of distilled water, the pH was adjusted to 7.4, autoclaved and stored until use.

Trypsin (25mg/ml)

Five hundred milligrams of trypsin were dissolved in 20ml 0.02% EDTA, mixed and filtered through a 0.2µm ministart filter (Sartorius, Epsom, UK). The solution was then aliquoted into 250µl samples and stored at -20ºC until use. For use in cell

culture work, an aliquot was further diluted in 10ml of 0.05M EDTA and subsequently used to detach cells.

2.5.5 Specialised reagents

Bone matrix extract (BME)

Ethical approval was granted by the Bro Taf Local Research Ethics Committee (Panel B) for the Bro Taf Health Board, Cardiff, UK. All patients gave informed and written consent. Femoral heads were collected from patients undergoing total hip replacements, placed in sterile containers and stored at -20ºC until the end of the surgery, after which they were transferred to -80ºC. The bone samples were then crushed into smaller frozen sections using a bone mill (Spierings Orthopaedics BV, Njmegen, The Netherlands), which were then further crushed using a pestle and mortar (5ml of bone fragments: 20ml BSS) whilst liquid nitrogen was applied to maintain sample temperatures. This mixture was resuspended in sterile BSS buffer and placed in a Bioruptor unit (Diagenode, Seraing, Belgium) and subjected to 5 minutes of interrupted pulses, 30 seconds on followed by 30 seconds off. Debris was removed by centrifugation at 3000rpm for 5 minutes at 4ºC. The supernatant was then transferred to a fresh tube for quantification. The protein extract was quantified using a Bio-Rad DC protein assay kit (Bio-Rad Laboratories, Hemel Hempstead, UK) and then diluted to a stock solution of 2mg/ml and stored at -80ºC until use.

Denosumab

Purchased from Amgen Limited (Cambridge, UK), a 60mg solution in a pre-filled syringe was dissolved in BSS containing 0.1%BSA to 10mg/ml and stored in 500µl aliquots at -20ºC until use.

Hepatocyte growth factor (HGF)

HGF was a kind gift from Professor Kunio Matsumoto (Kanazawa University), aliquoted into 10µg/ml with sterile BSS containing 0.1% BSA and stored at -20ºC until use.

Recombinant human OPG

Was purchased from PeproTech (Rocky Hill, New Jersey, USA), and diluted to 10µg/ml using sterile BSS: 0.1% BSA stored at -20ºC until use.

2.6 Cell maintenance, culture and storage

2.6.1 Preparation of growth medium for maintenance of cells

All cell lines unless listed below, were cultured in DMEM/Ham's F12 with L-glutamine medium (Sigma, Dorset, UK) supplemented with ABS (as described in section 2.5.4) and 10% Foetal Calf serum (FCS).

LNCaP cells were cultured in RPMI 1640 medium (Sigma, Dorset, UK) supplemented with ABS and 10% FCS.

MDA-PCa-2b cells were maintained in ATCC formulated F-12K medium supplemented with ABS, 20% FCS, 25ng/ml cholera toxin, 10ng/ml mouse EGF (Santa-Cruz, sc-4552), 0.005mM phosphoethanolamine, 45nM selenious acid, 100pg/ml hydrocortisone and 0.005mg/ml bovine insulin.

Transfected cells, containing the pEF6 plasmid, were cultured initially in appropriate "selection" medium containing 5µg/ml Blasticidin S (Melford Laboratories Ltd, Suffolk, UK), for up to 2 weeks. Resulting transfectants were then routinely cultured in an appropriate "maintenance" medium supplemented with 0.5µg/ml Blasticidin S so mammalian cells would continue to retain the plasmid vector for verification and use in subsequent *in vitro* studies.

2.6.2 Cell Maintenance

Cells were maintained and grown in $25cm^2$ or $75cm^2$ tissue culture flasks (Greiner Bio-One Ltd, Gloucestershire, UK), in an incubator at 37ºC, 5% CO_2 and 95% humidity. hFOB 1.19 cells were cultured in an incubator at 34ºC, 5% CO_2 and 95% humidity. All tissue culture techniques were carried out using aseptic techniques with autoclaved and sterile equipment inside a class II laminar flow cabinet. Cells

were maintained in the supplemented media as described in section 2.6.1 and routinely sub-cultured upon reaching 80-90% confluence. Confluence was gauged visually by assessing the appropriate coverage of cells over the surface of the tissue culture flask under a light microscope.

2.6.3 Detachment of adherent cells

Upon reaching confluence, medium was aspirated; cells were briefly washed in sterile EDTA-BSS buffer to remove any remaining serum which would have an inhibitory effect on the action of trypsin. Adherent cells were detached from the tissue culture flask by incubating with 2 - 5ml of trypsin: EDTA (0.01% trypsin: 0.02% EDTA in BSS buffer) for several minutes at 37ºC. Once detached the cell suspension was placed in a 30ml universal container (Greiner Bio-One Ltd, Gloucestershire, UK) and centrifuged at 1600rpm for 5 minutes to pellet cells. The supernatant was removed and the cell pellet was resuspended in an appropriate amount of pre-warmed medium. Cells were either counted for immediate use in experiments or transferred into a fresh tissue culture flask for sub-culturing.

2.6.4 Cell counting

Throughout this study a Neubauer haemocytometer counting chamber (Mod-Fuchs Rosenthal, Hawksley, UK) was used. A haemocytometer counting chamber allows for the number of cells in a previously determined volume to be calculated, to obtain the quantity of cells per millilitre. Cells were counted using an inverted light microscope under 10 x 10 magnification (Reichert, Austria). The chamber contains 9 large squares (1mm x 1mm x 0.2mm) each subdivided into 16 square areas, of

which three of the large squares were counted as a representation of the chamber on each occasion to determine cell numbers using the following equation:-

Cell number/ml = (number of cells counted in each 16 squares/2) x ($1x10^4$)

This allowed the accurate estimation of cell densities to be seeded during *in vitro* and *in vivo* cellular functional assays.

2.6.5 Storage of cell stocks in liquid nitrogen

Stocks of low passage cells and transfected cells were stored in liquid nitrogen. Cells were first detached from a large 75cm^2 flask using trypsin:EDTA as described in section 2.6.3. These cells were resuspended in the required volume (dependent on the number of samples to be frozen and recommended density) of a cyro-protective solution consisting of the suppliers' recommended percentage of dimethyl sulphoxide (DMSO) in growth medium (typically 5-10%). Following resuspension cells were aliquoted into 1ml volumes in pre-labelled 1.8ml cryotubes (Greiner Bio-One, Germany), wrapped loosely in tissue paper and stored overnight in a -80ºC freezer. Cells were transferred the following day to liquid nitrogen tanks for long term storage.

2.6.6 Cell revival from liquid nitrogen

When required, cells were removed from liquid nitrogen and revived. Following their removal from liquid nitrogen, cells were thawed rapidly by placing them in a water bath at 37ºC. Once thawed, the content of the cryotube was placed in a universal container containing 10ml of pre-warmed medium to immediately dilute the DMSO present. To pellet the cells the universal containers were centrifuged at 1600rpm for

5 minutes. The supernatant was aspirated, the cell pellet was resuspended in 5ml of pre-warmed medium and placed into a fresh 25cm^2 tissue culture flask and then incubated at 37ºC.

After 24 hours the flask was examined under the microscope to visually confirm a sufficient number of healthy adherent cells had survived. The medium was aspirated to remove any dead cells and residual DMSO. Fresh pre-warmed medium was added, the flask returned to the incubator and standard sub-culture techniques, as previously described, carried out when necessary.

2.7 Synthesis of complementary DNA for use in PCR analysis

2.7.1 Total RNA isolation

RNA isolation was completed using the TRI Reagent protocol from Sigma-Aldrich as summarised below. Cells were grown to a confluent monolayer, the medium was aspirated and replaced with TRI Reagent (1ml per 5-10 x 10^5 cells) to induce cell lysis. The cell lysate was transferred into a 1.8ml microfuge tube and incubated at 4ºC for 5 minutes. This was followed by the addition of 0.2ml chloroform (per 1ml of TRI Reagent), the sample being vigorously shaken for 15 seconds, and subsequently incubated at 4ºC for 5 minutes. The resulting homogenate was centrifuged at 12,000rpm for 15 minutes at 4ºC (Boeco, Wolf Laboratories, York, UK). Following centrifugation, the upper aqueous phase containing RNA was carefully removed and added to a pre-labelled microfuge tube to which an equal volume (~500µl) of isopropanol was also added. The samples were then incubated for 10 minutes at 4ºC before centrifuging at 12,000rpm for 10 minutes at 4ºC. At this stage, RNA present in the sample precipitated out of solution and was visible as a

pellet at the bottom of the microfuge tube. The supernatant was discarded and the RNA pellet washed twice in 75% ethanol (Fisher Scientific, Leicestershire, UK), prepared in a 3:1 ratio of absolute ethanol:DEPC water. Each wash consisted of the addition of 1ml of 75% ethanol, vortexing and subsequent centrifugation at 7,500rpm for 5 minutes at 4ºC. Following the final wash, the ethanol was removed and the RNA pellet was dried at 55^0C for 5-10 minutes in a drying oven (Techne Hybridiser HB-1D, Wolf Laboratories, York, UK). The pellet was dissolved in 50-100µl (dependent on pellet size) of DEPC water by vortexing, prior to quantification.

2.7.2 RNA quantification

Following RNA extraction, the concentration and purity of the resulting RNA was measured using an Implen Nanophotometer (Munchen, Germany) which had been configured to detect single strand RNA (µg/µl) in a 1 in 10 dilution, measuring the difference in absorbance at 260nm between the total RNA isolated sample and DEPC water (blank).

2.7.3 RNA extraction from tissues.

Breast sections were mixed and homogenised using a hand-held homogeniser in ice-cold RNA extraction solution (Sigma, Dorset, England, UK). The concentration of RNA was determined using UV1101 Biotech Photometer (WPA, Cambridge, UK). The photometer was set to detect single stranded RNA (µg/µl) at 1:10 dilution of the blank. Samples were measured using Stama glass cuvettes (Optiglass Limited, Essex, UK).

2.7.4 Reverse transcription of RNA

Following RNA isolation and quantification, 250ng of RNA was converted into complementary DNA (cDNA) using a high capacity cDNA reverse transcription kit (Applied Biosystems, Manchester UK) following the protocol outlined below.

A sufficient volume of RNA suspended in DEPC water (isolated previously) to supply the desired final quantity of RNA was added to a thin-walled 200µl PCR tube, additional PCR water was added to make a total volume of 10µl. An additional 10µl of mastermix was added containing:

Component	*Volume (µl)*
10x RT buffer	2
25x dNTP mix (100mM)	0.8
10x RT random primers	2
MultiScribe Reverse transcriptase	1
RNase inhibitor	1
Nuclease-free water	3.2
Total	***10***

The tubes were placed in a T-Cy thermocycler (Creacon Technologies Ltd, Netherlands), under the following conditions:-

Step 1 - 25ºC for 10 minutes

Step 2 - 37ºC for 120 minutes

Step 3 - 85ºC for 5 minutes

Once completed the cDNA generated was diluted 1:4 with PCR water and tested using conventional PCR probing for GAPDH expression to confirm successful ubiquitous reverse transcription amongst standardised samples. Samples were stored at -20ºC until needed.

2.7.5 Polymerase chain reaction (PCR)

RT-PCR was carried out using a GoTaq Green master mix (Promega, Madison, USA). Reactions were set up for each sample as follows:-

Component	*Volume (µl)*
2x GoTaq Green master mix	8
Forward primer (10pmol)	1
Reverse primer (10pmol)	1
Nuclease-free water	5
cDNA template	1
Total	***16***

All reactions were run alongside a negative control replacing the cDNA template with nuclease-free water to ensure there was no contamination.

The RT-PCR reaction was set up in 200µl PCR tubes or a 96 well plate (Bio-Rad Laboratories, Hemel Hampstead, UK) (dependent on sample numbers), mixed briefly and centrifuged before being placed in a T-Cy Thermocycler and subjected to the follow temperature shifts:-

Step 1: Initial denaturing period - 94ºC for 5 minutes

Followed by 30-36 cycles of:

Step 2: Denaturing step - 94ºC for 1 minute

Step 3: Annealing step – reaction specific temperature for 40-60 seconds

Step 4: Extension step - 72ºC for 40 seconds

And finally:

Step 5: Final extension period - 72ºC for 10 minutes

Specific reaction annealing temperatures together with primer sequence data and predicted product size is detailed in table 2.2. Primer binding sites and predicted product sizes were verified using the Primer3 software available online. RT-PCR products were run using agarose gel electrophoresis and stained.

2.7.6 Agarose gel electrophoresis

DNA was separated according to size using agarose gel electrophoresis. Dependent on the predicted size of the DNA produced, the samples were loaded onto either 0.8% (for DNA fragments 1-10kb), or 2% (for DNA fragments less than 500bp) agarose gels. Agarose gels were made by adding the required amount of agarose (Melford Chemicals, Suffolk, UK) to 1xTBE solution. This was then heated to fully dissolve the agarose after which SYBR safe DNA gel stain (Invitrogen, Manchester, UK) diluted 1:10000 was added. The agarose was poured into the electrophoresis cassette and allowed to set around a plastic comb creating loading wells. Once set, the gel was submerged in 1xTBE buffer, the comb removed and 8µl of a 1Kb DNA ladder (Cat No. M106R; GenScript USA Inc), or 10µl of sample was loaded per well. The samples were then run electrophoretically using a power pack

(Gibco BRL, Life technologies Inc) at a constant voltage of ~100V for 30-50 minutes (dependent on predicted product size).

2.7.7 DNA visualisation

Gels were visualised and images captured using a blue light illuminator in the Syngene U:Genius 3 closed system (Geneflow, Elmhurst, Lichfield Staffs).

Each RT-PCR was repeated three independent times and representative images illustrating the expression patterns are presented in this study.

2.7.8 Quantitative RT-PCR (qPCR)

qPCR is a sensitive technique that is capable of detecting very small quantities of cDNA within a sample whilst determining an accurate and reliable value of the template copy number. This current study used a molecular beacon method for quantitative PCR using the Amplifluor Uniprimer Universal system (Intergen Company, New York, USA) to quantify transcript copy number. The amplifluor probe consists of a 3' region specific to the Z-sequence (ACTGAACCTGACCGTACA) present on the target specific primers (Table 2.2) and a 5' hairpin structure labelled with a fluorophore (FAM). When the fluorophore hairpin structure is linked to an acceptor moiety (DABSYL) it acts as a fluorescence quencher which prevents any signal from being detected. During the qPCR reaction, the probe (Uniprobe, Millipore, Watford, UK) becomes incorporated and acts as a template for DNA polymerisation, in which DNA polymerase uses its 5'-3' exonuclease activity to degrade and unfold the hairpin structure, thereby disrupting the energy transfer between the fluorophore and quencher, allowing sufficient fluorescence to be

emitted and hence detected. The fluorescent signal emitted during each qPCR cycle can then be directly correlated to the amount of DNA that has been amplified.

The cDNA used in qPCR was generated as described in section 2.7.3; this cDNA was then used to make up a reaction mixture outlined below:

Component	*Volume (µl)*
2x iQ Supermix (Bio-Rad)	5
Forward primer (10pmol)	0.3
Reverse Z primer (1pmol)	0.3
Amplifluor probe (10pmol)	0.3
cDNA and Nuclease free water	4
Total	***10***

The degree of fluorescence within each sample was compared to a range of standards of known transcript copy number (Figure 2.1), allowing for the calculation of transcript copy number within each sample. Detection of GAPDH copy number within these samples was subsequently used to allow further standardisation and normalisation of the samples.

Each sample was loaded into a 96 well plate (Bio-Rad Laboratories, Hemel Hampstead, UK) alongside standards (ranging from copy numbers of 10^1 – 10^8), covered and sealed with optically clear Microseal (Bio-Rad Laboratories, Hemel Hampstead, UK) and this was placed in an iCyclerIQ thermal cycler (Bio-Rad Laboratories, Hemel Hampstead, UK). Sample cDNA was amplified and quantified over a large number of shorter cycles using an iCycler thermal cycler and detection software and experimental conditions are outlined below:-

Step 1: Initial denaturing period - 94ºC for 5 minutes

Step 2: Denaturing step - 94ºC for 10 seconds

Step 3: Annealing step - 55ºC for 15 seconds

Step 4: Extension step - 72ºC for 20 seconds

Steps 2 - 4 were repeated over 80 cycles. In this established method, approximately 20 cycles are required for the generation of Z-tagged products. The camera used in this system is set to detect signal during the annealing stage, its geometric increase directly correlates with the exponential increase of product.

Subsequently, calculation of the sample copy number was dependent on the point at which the sample reached threshold cycle in comparison to the standards, automatically generated by the instrument software. Specific qPCR primers were verified using a positive control known to express the molecule of interest and a negative control, where PCR water replaced cDNA in a reaction, to rule out contamination before use. The experimental procedure was repeated independently three times and representative data of the expression trends is presented.

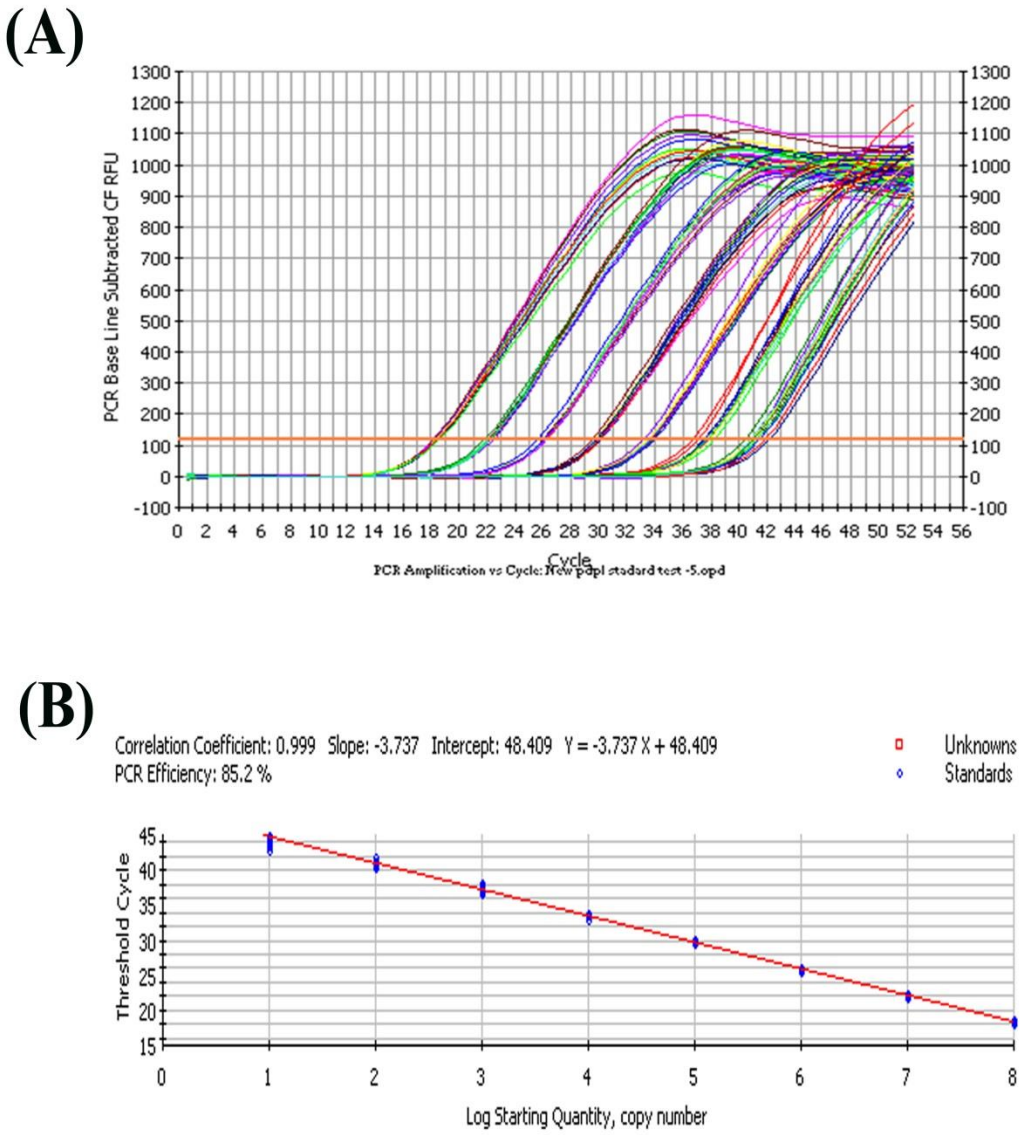

Figure 2.1: qPCR Standards

(A) The detection range of the qPCR PDPL standards used throughout this study. Each standard was tested multiple times (n=12, representative data shown) and used to generate a standard curve (B).

2.8 SDS-PAGE and Western blotting

2.8.1 Protein extraction and preparation of cellular lysates

Upon reaching sufficient confluence, the cell monoloayer was detached from the flask using a sterile cell scraper, both the detached cells and medium were then transferred to a universal container. The cell suspension was centrifuged for 5 minutes at 1,800rpm to pellet cells and protein at the bottom of the universal container. Following centrifugation, the supernatant was aspirated and the cells were lysed in 200 - 250µl of lysis buffer (depending on pellet size), before being transferred to a 1.8ml microfuge tube and placed on a Labinco rotating wheel (Wolf Laboratories, York, UK) for 1 hour at room temperature. The resulting suspension was then centrifuged at 13,000rpm for 15 minutes to remove any unwanted cell debris. The supernatant was transferred to a fresh microfuge tube to await quantification for SDS-PAGE or stored at -20ºC until further use.

2.8.2 Protein quantification

Protein quantification was undertaken to standardise the concentrations of the protein samples prior to their use in SDS-PAGE and Western blotting. Protein concentration was determined using a Bio-Rad DC protein assay kit (Hemel Hampstead, UK) following the microplate method as outlined here.

To set up a standard curve, in a 96 well plate, 50mg/ml of bovine serum albumin (BSA) was serially diluted from 10mg/ml to 0.005mg/ml in lysis buffer. Five microlitres of either the sample or standard was pipetted into a fresh well before adding 25µl of 'working Reagent A' (prepared by adding 20µl of Reagent S per millilitre of Reagent A), followed by 200µl of Reagent B. Following addition of Reagent B, samples were mixed briefly and then left for approximately 45 minutes

to allow the colorimetric reaction to occur. Once this was complete, the absorbance of each sample was measured at 620nm using an ELx800 plate reading spectrophotometer (Bio-Tek, Wolf Laboratories, York, UK). A standard curve was constructed based on the absorbance of the BSA standards and used to determine sample concentration. An equation to calculate protein concentration based on the absorbance was established using the scatter line graph in Microsoft Excel. Protein concentration of each sample was determined using the corresponding absorbance and the equation of the standard curve. All samples were then normalised to the desired final concentration of between 1.0 – 1.5mg/ml through dilution in an appropriate amount of lysis buffer and further diluted in a 1:1 ratio with 2xLamelli sample buffer concentrate. Samples were then boiled at 100ºC for 5-10 minutes and stored at -20ºC until further use.

2.8.3 Sodium dodecyl sulphate polyacrylamide gel electrophoresis (SDS-PAGE)

SDS-PAGE was undertaken using an OmniPAGE VS10 vertical electrophoresis system (Wolf Laboratories, York, UK). Resolving gels of a required percentage (depending on the predicted protein size) were made up in a universal container. The amount of each ingredient required to make up 15ml (enough for two gels) for both 8% (for proteins > 100kDa) and 10% (for proteins < 100kDa) resolving gels is indicated below:-

Component	*8% gel (ml)*	*10% gel (ml)*
Distilled water	6.9	5.9
30% acrylamide mix	4.0	5.0
1.5M Tris (pH8.8)	3.8	3.8
10% SDS	0.15	0.15
10% ammonium persulphate	0.15	0.15
TEMED	0.009	0.006
Total	**15**	**15**

The resulting mixture was then poured between glass plates, held in place in a loading cassette, until at a level 1.5cm below the top edge of the plate. To prevent gel oxidation the top of the resolving gel was covered with a 0.1% SDS solution.

Once the resolving gel had polymerised (~30 minutes at room temperature), the excess SDS solution was poured off and replaced with a sufficient amount of stacking gel. The components and quantities required to prepare 5ml of stacking gel solution (enough for two gels) are shown below:-

Component	*Stacking gel (ml)*
Distilled water	3.4
30% acrylamide mix	0.83
1.0M Tris (pH 6.8)	0.63
10% SDS	0.05
10% ammonium persulphate	0.05
TEMED	0.005
Total	**5**

A well forming Teflon comb was placed in the unset stacking gel and the mixture was left to polymerise (~20 minutes at room temperature). Once both resolving and stacking gels had set, the loading cassette was transferred into an electrophoresis tank and covered with 1x running buffer before the well comb was removed. Eight-ten microlitres of broad range molecular weight marker (Santa Cruz Biotechnology, supplied by Insight Biotechnologies Inc, Surrey, England, UK) or 18µl of protein samples were loaded into the wells. The proteins were then separated according to molecular weight using electrophoresis at 100 - 125V, 50mA and 50W for varying lengths of time (dependent on protein size and gel percentage).

2.8.4 Western blotting

Following SDS-PAGE protein samples were transferred to a PVDF membrane by Western blotting. Electrophoresis equipment was disassembled, gels were removed from the loading cassette and the stacking gel cut away. Pieces of filter paper were pre-soaked in 1x transfer buffer (Whatman International Ltd, Maidstone, UK) and the PVDF membrane (Santa Cruz Biotechnology Inc, UK) was pre-soaked in methanol and 1x transfer buffer before being arranged in an SD10 SemiDry Maxi System blotting unit (SemiDRY, Wolf Laboratories, York, UK) as outlined below:-

Negative electrode: 3x pre-soaked filter paper: PVDF membrane: gel: 3x pre-soaked filter paper: positive electrode

Electroblotting was undertaken at 15V, 500mA, 8W for 20-60 minutes (depending on protein size).

2.8.5 Protein probing

Protein probing was carried out using the Millipore SNAP i.d. protein detection system (Watford, UK) as outlined below. The blotted membrane was placed in the centre of a pre-wet blot holder and rolled gently to remove any air bubbles. A spacer was then added on top of the membrane and rolled again before the holder was securely closed and placed within the system. Blocking solution (10-30ml dependent on holder size) was added and a vacuum applied, after which the primary antibody solution (1-3ml dependent on holder size) was left to incubate for 10 minutes at room temperature. The vacuum was then re-applied and the holder washed 3 times with wash buffer (10-30ml dependent on holder size). The secondary antibody solution was then added and left to incubate for 10 minutes at room temperature, after which the vacuum was then used again and the system was again flushed three times under vacuum with wash buffer. The membrane was then removed and stained for protein detection.

2.8.6 Staining of proteins

2.8.6.1 Polyacrylamide gel staining

Coomassie blue was used to stain polyacrylamide gels following SDS-PAGE and electroblotting to verify transfer. The gel was immersed in Coomassie blue stain solution for approximately 30 minutes before being repeatedly washed in destaining solution until background staining disappeared, and the protein(s) of interest appeared as blue bands.

2.8.6.2 Chemiluminescent protein detection

This technique was carried out using the chemiluminescence detection kit (Luminata, Millipore), consisting of a highly sensitive chemiluminescent substrate that detects the horseradish peroxidase (HRP) used during the western blot procedure.

One millilitre of reagent was added onto the membrane and incubated for 5 minutes at room temperature with constant agitation. Excessive solution on the membrane was then drained over a piece of tissue paper and the membrane was transferred to a plastic tray. The chemiluminescent signal was detected using an UVITech Imager (UVITech Inc, Cambridge, UK), which contains both an illuminator and a camera. Each membrane was subjected to varying exposure times until the protein bands were sufficiently visible. These images were then captured and further analysed with the UVI band software package (UVITEC, Cambridge, UK), which allows for protein band quantification.

Throughout this study GAPDH was used a loading control and run alongside all other proteins being detected, allowing for additional normalisation of samples to occur. In order to verify the results, each western blot was carried out three times.

2.9 Manipulation of gene expression in prostate and breast cell lines

To alter gene expression profiles in the mammalian cell lines hammerhead ribozyme transgenes were used (sequences detailed in Table 2.4). These primers were designed based on the predicted secondary structure of each gene transcript (Figure 2.2 and 2.3 respectively).

2.9.1 Production of ribozyme transgenes sequences

Hammerhead motifs contain a conserved secondary structure that consists of three helical stems (I, II and III), enclosing a junction known as the catalytic core, typified by various invariant nucleotides. The best codons demonstrated to be suitable for cleavage are AUC, GUC and UUC. In order to generate ribozyme transgenes specific to the molecules of interest, sequences were designed based on secondary structure of the target molecule predicted by Zuker's RNA mFold programme (Zuker, 2003) (Figures 2.2 and 2.3). Subsequently, appropriate ribozyme target sites were chosen according to the secondary structure of each mRNA molecule.

The ribozyme was created to specifically bind the sequence adjacent to the suitable target codon sequence, located within a loop structure of the transcript. This made it possible for the hammerhead catalytic region of the ribozyme to bind to and specifically cleave the codon sequence within the target mRNA transcript. Following ribozyme design, the sequences were ordered from Sigma-Aldrich as sense/antisense strands and the transgenes were then synthesised using touchdown PCR (Figure 2.5 A), reaction mix and conditions as below:-

Component	*Volume (µl)*
2x REDtaq ready mix PCR reaction with $MgCl_2$	10
Forward Ribozyme sequence (pM)	2
Reverse Ribozyme sequence (pM)	2
Nuclease free water	6
Total	**20**

Conditions as follows:-

Step 1: Initial denaturing period, 94ºC for 5 minutes

Step 2: Denaturing step, 94ºC for 10 seconds

Step 3: Various annealing steps, 70ºC for 15 seconds, 65ºC for 15 seconds, 60ºC for 15 seconds, 57ºC for 15 seconds, 55ºC for 15 seconds and 50º for 15 seconds

Step 4: Extension step, 72ºC for 20 seconds

Step 5: Final extension period, 72ºC for 7 minutes.

Steps 2-4 were repeated over 48 cycles, each different annealing temperature comprising 8 cycles.

Once combined, the transgenes were electophoretically run on a 2% agarose gel to confirm presence and correct size before being inserted into the pEF6 plasmid (Figure 2.4) in the TOPO cloning reaction (representative in Figure 2.5 A).

Table 2.4: Primers designed for ribozyme synthesis

Target	Ribozyme	Primer Name	Primer Sequence (5'-3')
		T7F	TAATACGACTCACTATAGGG
		RBBMR	TTCGTCCTCACGGACTCATCAG
		RBTPF	CTGATGAGTCCGTGAGGACGAA
OPG	**OPG ribozyme 1**	OPGRIB1F	CTGCAGCTCCTTGCACACGGGGCTGCAGTATACT GATGAGTCCGTGAGGA
		OPGRIB1R	ACTAGTACACAGACAGCTGGCACACCAGTGACGA GTGTTTCGTCCTCACGGACT
	OPG ribozyme 2	OPGRIB2F	CTGCAGACACTGCAATTTGTGTGTTTTCTACTGGG TGCTTTACTGATGAGTCCGTGAGGA
		OPGRIB2R	ACTAGTTCTTCTCAAATGAGACGTCATTTCGTCCT CACGGACT
	OPG ribozyme 3	OPGRIB3F	CTGCAGGGTAACATCTATTCCACATTTTGAGTTCT GATGAGTCCGTGAGGA
		OPGRIB3R	ACTAGTTCCGGAAACAGTGAATTTCGTCCTCACGG ACT
RANK	**RANK ribozyme 1**	RANKRIB1F	CTGCAGCGCGCGGGGCCATGGCGCGGCTGATGA GTCCGTGAGGA
		RANKRIB1R	ACTAGTGCCGCGGCGCCGCCAGCCTGTTTCGTCC TCACGGACT
	RANK ribozyme 2	RANKRIB2F	CTGCAGCTCATAATGCTTCTCACTGGCTGATGAGT CCGTGAGGA
		RANKRIB2R	ACAGTCTTTGCAGATCGCTCCTCCATGTTTCGTCC TCACGGACT
	RANK ribozyme 3	RANKRIB3F	CTGCAGGTACTTTCCTGGTTCACATTTGTCTGATG AGTCCGTGAGGA
		RANKRIB3R	ACTAGTAGCATTATGAGCATCTGGGACGGTGCTGT TTCGTCCTCACGGACT
	RANK ribozyme 4	RANKRIB4F	CTGCAGTGCTGACCAAAGTTTGCCGTGTGTGCTG ATGAGTCCGTGAGGA
		RANKRIB4R	ACTAGTGGAGTCCTCAGGTGACAGTTGTGTCAGTT TCGTCCTCACGGAC
	RANK ribozyme 5	RANKRIB5F	CTGCAGCTGGCATCTTCGCCTTGTGCGTAGGCTG ATGAGTCCGTGAGGA
		RANKRIB5R	ACTAGTGTCAGGGCACATGTGTAGGAGGTGGTTT CGTCCTCACGGACT

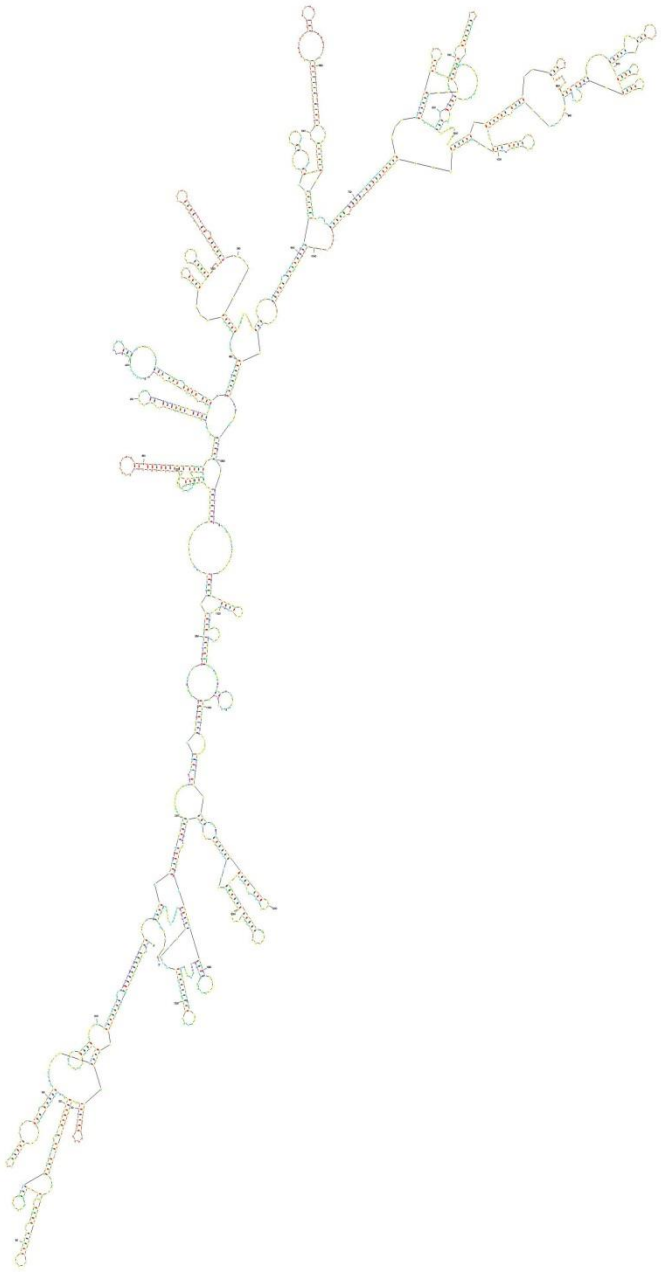

Figure 2.2: Secondary structure of OPG transcript

(As predicted Zuker's RNA mFold programme)

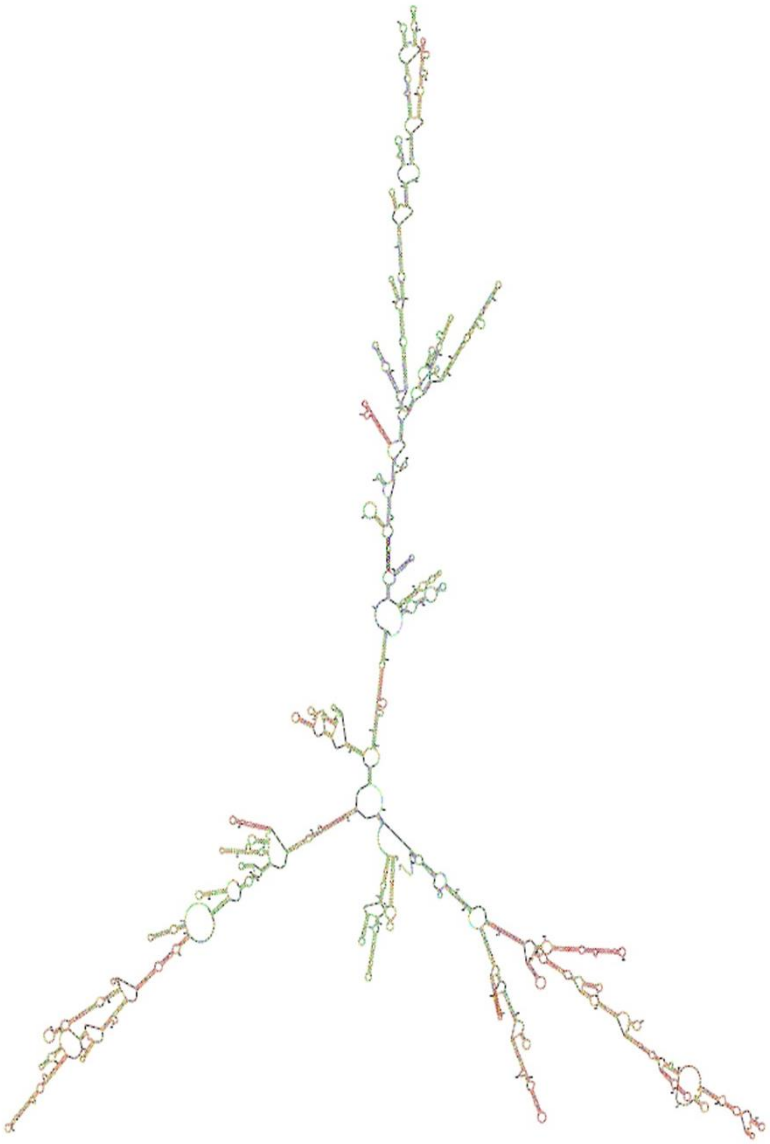

Figure 2.3: Secondary structure of RANK transcript

(As predicted by Zuker's RNA mFold programme)

2.9.2 TOPO TA cloning reaction

The TOPO TA expression system provides a highly efficient and simple one step cloning approach without the requirement of ligases, specific PCR primers, or any post PCR procedures. The process involves the effective cloning and direct insertion of *Taq* polymerase amplified PCR products into plasmid vectors for expression in mammalian cells following transfection.

Cloning of all ribozyme transgenes was completed using the pEF6/V5-His TOPO TA expression kit (Life Technologies, Paisley, UK), in accordance with the protocol provided. This kit allows linearisation with a single 3' Thymidine (T) overhang for TA cloning, and a covalently bound Topoisomerase. Due to its template independent terminal transferase activity, Taq polymerase catalyses the addition of a single deoxyadenosine (A) to the ends of PCR products allowing for efficient ligation of the PCR product into the plasmid vector due to its 3' T overhang. The manufacturer's protocol is outlined over the next few sections.

The following TOPO cloning reaction was set up in a pre-labelled microfuge tube and mixed gently before being incubated for 5 minutes at room temperature:

Component	*Volume (µl)*
Ribozyme PCR product	4
Salt solution	1
TOPO vector	1
Total	**6**

This mixture was added and gently stirred (pipetting up and down could damage the bacteria) to a vial of chemically competent One Shot TOP10 *Escherichia coli (E. coli)*, after which it was incubated on ice for 30 minutes.

2.9.3 Transformation of chemically competent E. coli

To transform the *E.coli* bacteria, the mixture was heat shocked at 42ºC for 30 seconds and immediately placed back onto ice. SOC medium (250µl pre-warmed to room temperature) was added to each cell suspension and left to shake horizontally at 200rpm on a horizontal orbital shaker (Bibby Stuart Scientific, UK), at 37ºC for 1 hour. Following this incubation period, the *E.coli* mixture was spread onto two pre-warmed selective LB-agar plates (containing 100µg/ml ampicillin), at high and low seeding densities, before being incubated at 37ºC overnight. The pEF6 plasmid contains antibiotic resistance genes that allow cells containing the plasmid to grow in the presence of ampicillin and /or Blasticidin S selection, a schematic of the plasmid is shown in Figure 2.4. Any colonies which grew on the selective plates are positive for the pEF6 plasmid. However, to confirm that the ribozyme sequence has been inserted in the correct orientation to allow transcription, further testing was needed.

2.9.4 Colony selection and orientation analysis

Correct insertion and orientation of the ribozyme sequences in the plasmid were analysed to ensure that the resulting product would be viable. For each colony two RT-PCR reactions were performed. The colonies were tested using primers specific to either the plasmid (T7F, BGHR), or the ribozyme sequence (RbToPF, RbBMR). Whilst T7F vs BGHR will give an indication of whether the complete sequence had

inserted without degradation, it cannot be used to indicate the orientation of the sequence. There are approximately 90bp between the T7F promoter and the beginning of the insert whilst the reverse primer specific for the plasmid vector (BGHR) ends around 173bps downstream of the insertion site.

In order to check the correct size and orientation of the sequence, a mixture of plasmid specific and sequence specific primers were used. RbToP and RbBMR recognise and bind to sequences within the ribozyme transgene common to all the ribozymes used in this study (See table 2.4). To check the ribozyme sequences a combination of T7F vs RbToPF was used, if this reaction was positive (~140bp), it indicated the insert has ligated in the wrong orientation. A band in the T7F vs RbBMR reaction, a reverse primer specific for the ribozyme transgene was indicative of the insert ligated in the correct orientation. If bands were seen for both reactions then the colonies contained a mixture of plasmids with both insert orientations. Examples of each of the orientation results are shown in Figures 2.5 B and C.

The protocol used was:

Following overnight incubation, the plates were examined for colony growth. Eight individual colonies were randomly selected for orientation analysis and marked and labelled on the plates. For each colony, using a sterile pipette tip, a sample of the colony was use to inoculate both reactions before the addition of the primers. The two PCR reactions were carried out as follows (full primer sequences are given in table 2.4).

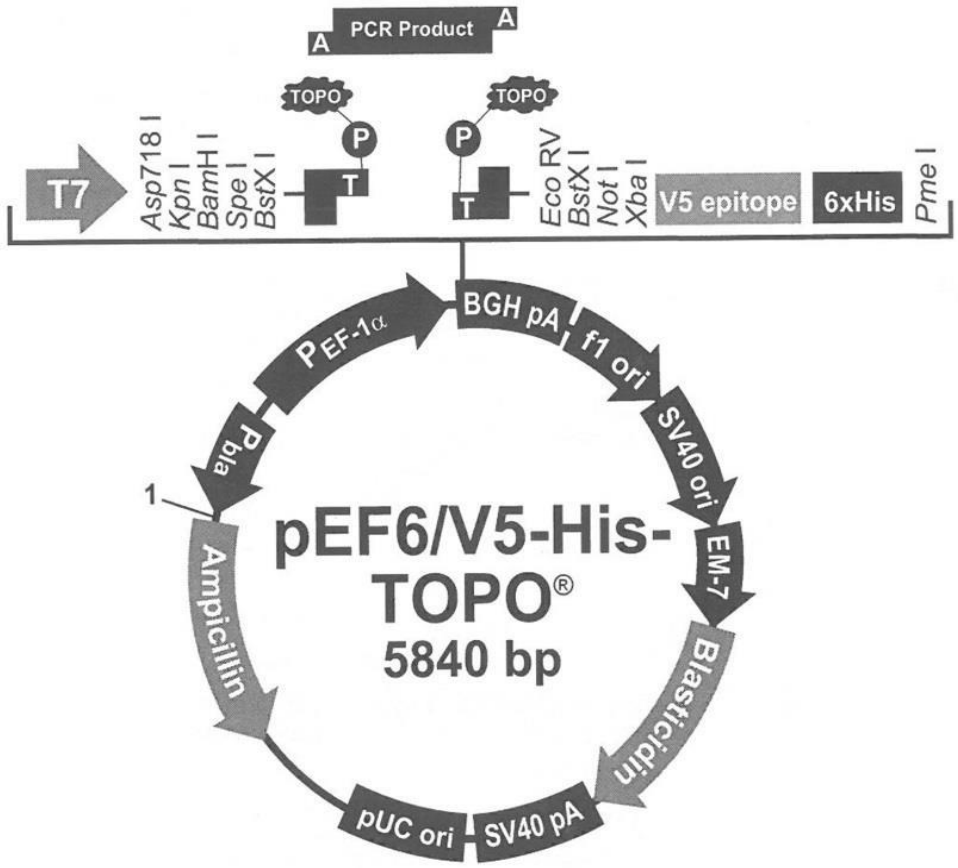

Figure 2.4: Schematic of the pEF6 plasmid

Copied from the manufacturer's handbook to show multiple insertion sites and orientation of the promoter sequence.

Component	*Volume (µl)*
Reaction 1	
2x GoTaq Green Master mix	8
Plasmid specific T7F	1
Ribozyme specific RbToP	1
Nuclease-free water	6
Reaction 2	
2x GoTaq Green Master mix	8
Plasmid specific T7F	1
Ribozyme specific RbBMR	1
Nuclease-free water	6

Each reaction mix was then placed in a thermal cycler and subjected to the following conditions:-

Step 1: Initial denaturing period - 95ºC for 10 minutes

Followed by 35 cycles of:

Step 2: Denaturing step - 94ºC for 1 minute

Step 3: Annealing step - 55ºC for 1 minute

Step 4: Extension step - 72ºC for 1 minute

And finally

Step 5: Final extension period - 72ºC for 10 minutes

The mixture was run on a 2% agarose gel using electrophoresis and visualised as previously described in Section 2.7.6.

2.9.5 Plasmid amplification, purification and quantification

Following colony orientation analysis, colonies showing correct insert orientation were removed from the LB-agar plate using a sterile pipette tip, used to inoculate 10ml of ampicillin selective LB broth and incubated at 37ºC overnight under constant agitation (at 220rpm). The amplified *E.coli* were then pelleted by centrifugation at 4ºC for 15 minutes at 3000rpm and used for plasmid extraction. Plasmid extraction was carried out using the Sigma GenElute Plasmid Miniprep Kit according to the provided protocol outlined below.

The supernatant was discarded and the bacterial pellet was resuspended in 200µl of re-suspension solution (containing RNase A), before being thoroughly mixed and transferred to a collection tube provided. This was followed by the addition of 200µl of lysis solution, and gentle mixing by inverting 5-6 times. The addition of 350µl of neutralising solution within 5 minutes of the addition of lysis buffer prevented DNA damage. The tubes were inverted 4-6 times and then centrifuged at 12,000rpm for 10minutes. The resulting supernatant was then transferred into a fresh collection tube containing a Mini Spin Column, plasmid DNA bound to the column, after which it was spun at 12,000rpm for 1 minute, and the flow through was discarded. The column was washed with 750µl of wash solution (containing ethanol) and the column spun at 12,000rpm for 1 minute, with the flow through discarded. To dry the column it was spun again at 12,000rpm for 1 minute, before being transferred to a fresh collection tube. Plasmid DNA was eluted by the addition of 100µl of elution solution and spinning the column at 12,000rpm for 1 minute. The eluted plasmid solution was quantified and then an aliquot run on a 0.8% agarose gel using electrophoresis to confirm the presence and size of each of the plasmids of interest (Figure 2.5 D).

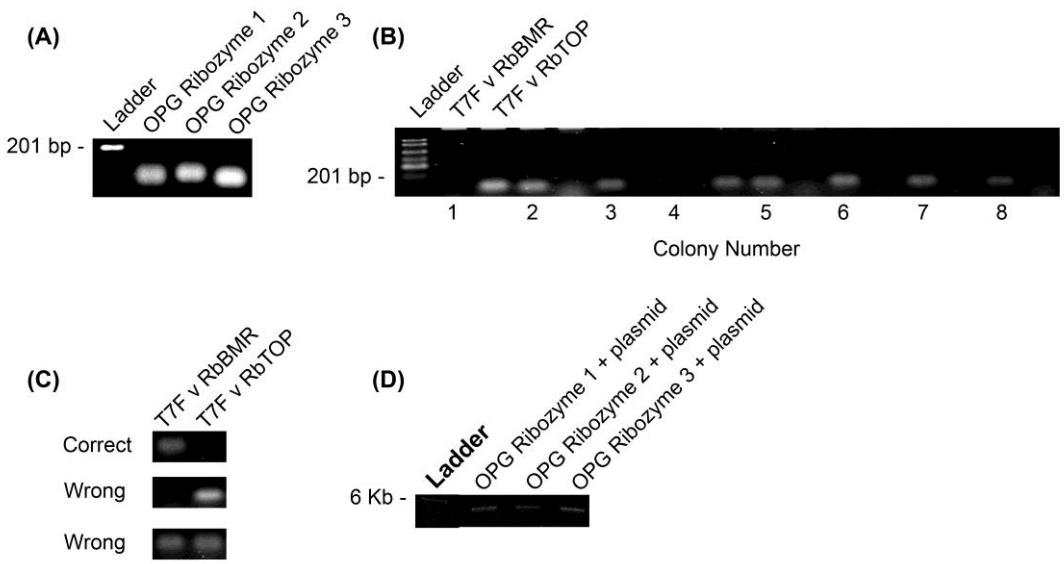

Figure 2.5: Orientation checking of ribozyme transgenes

Initially ribozyme transgenes were screened after touchdown PCR (A). To verify that the ribozyme transgenes had been inserted in the correct orientation RT-PCRs were run (B and C). Once plasmid had been amplified and purified it was confirmed using gel electrophoresis and visualisation (D)

2.9.6 Transfection of mammalian cells using electroporation

Following plasmid purification and quantification, 1-3 µg of the extracted empty control plasmid and ribozyme transgenes for OPG and RANK were used to transform the PC-3 prostate cancer cell line and the MDA-MB-231 breast cancer cell line used for this study, using the following protocol:-

Confluent low passage wild type cells were detached from tissue culture flasks as described in section 2.6.3. Approximately $1x10^6$ cells in 800µl per transfection were added to an electroporation cuvette (Eurenetech, Southampton, UK) together with 3-5µl of purified plasmid, mixed briefly and left to stand at room temperature for 5 minutes. This cell and plasmid suspension was then subjected to an electrical pulse from an electroporator (Easyject, Flowgene, Surrey, UK).

Cell line	Voltage (V)	Capacitance
PC-3	310	1500
MDA-MB-231	310	1500

Following this pulse, the cell and plasmid suspension was quickly transferred into 10ml of pre-warmed medium added to a $25cm^2$ tissue culture flask and left in an incubator at 37ºC overnight to allow cells to recover and adhere.

2.9.7 Establishment of stable transfected mammalian cell lines

Following transfection, in order to obtain a stable cell line carrying the constructed vector, the electroporated and cultured cells needed to be selected. The pEF6 TOPO plasmid used to transform the cell, encodes two antibiotic resistance genes. As previously described, the ampicillin resistance gene allows initial selection of prokaryotic bacterial colonies containing the plasmid (Section 2.9.4). The plasmid also contains a Blasticidin S resistance gene. Blasticidin S is a potent microbial antibiotic that inhibits protein synthesis in both prokaryotes and eukaryotes and therefore, for this study was used to specifically select the mammalian cells containing the pEF6 TOPO plasmid.

Following overnight incubation, the cells were subjected to an initial 5 day period of intense selection, by incubating them in medium supplemented with 5µg/ml of the Blasticidin S. After this initial intense selection, to ensure the cells maintained the plasmid and therefore long term transformation, cells were maintained in maintenance medium containing 0.5µg/ml of Blasticidin S.

All cells were tested initially and routinely following revival to verify the efficacy and stability of ribozyme transformation cell lines using RT-PCR, qPCR and Western blot analysis. Once the cells had been verified to stably express the desired molecule; they were subjected to various *in vitro* function assays in order to test the effect altered expression of the molecule of interest had on biological cancer cell properties.

2.10 Tumour cell functional assays

For all the cell function assays, final volume per well or insert was 200µl of Blasticidin S free media. Cell volumes were calculated in 100µl, the additional 100µl was a 2x concentrate of any additional treatment made in medium or medium alone.

2.10.1 In vitro tumour cell growth assay

Cells were detached and cell concentration (per millilitre) was established as previously described (Section 2.6.3 and 2.6.4 respectively). Cells were then seeded into three 96 well plates at a seeding density of $3x10^3$ cells/100µl, supplemented with an additional 100µl of Blasticidin S free medium or treatment and incubated for 1, 3 and 5 day periods respectively at 37ºC with 5% CO_2. Following the appropriate incubation period, medium was removed and cells were fixed in 4% formaldehyde (v/v) in BSS for 10 minutes before being subsequently stained in 0.5% crystal violet (w/v) in distilled water, for 10 minutes. The stain was washed off with water and the plates left to dry at room temperature for 24 hours. For analysis the dye was solubilised using 200µl 10% acetic acid and cell density determined by measuring the absorbance at 540nm on a plate reading spectrophotometer (BIO-TEK, Elx800, UK). Cell growth rates were initially presented, from the individual repeats, as a percentage increase calculated by comparing the absorbance obtained for each incubation period against the absorbance taken after day 1 as a baseline, using the following equation:

Percentage increase = ((day 3 or 5 absorbance) – day 1 absorbance/ day 1 absorbance x100)

Within each experiment triplicate wells were set up and the entire experimental protocol was repeated at least three independent times. Data from all the repeats were combined and presented as mean percentage control with SEM.

2.10.2 In vitro tumour cell Matrigel adhesion assay

The ability of tumour cells to adhere to an artificial Matrigel basement membrane was examined using an *in vitro* Matrigel adhesion assay technique modified from Jiang *et al*, 1995a.

Wells in a 96 well plate were coated with 5µg of Matrigel in serum free medium and left to dry for 2 hours at 55ºC in a drying oven. This membrane was then rehydrated in 100µl of serum free medium for 40 minutes at room temperature. The medium was aspirated and $4.5x10^4$ cells/100µl were seeded into each well and supplemented with a further 100µl of Blasticidin S free medium or treatment. Cells were left to adhere to the Matrigel for 40 minutes at 37ºC with 5% CO_2. After incubation, the medium was removed and the wells washed with 150µl of BSS solution to remove any non-adherent cells. Adherent cells were then fixed in 4% formaldehyde (v/v) in BSS for 10 minutes before being stained in 0.5% crystal violet solution (w/v) in distilled water for 10 minutes. Crystal violet was then washed off with distilled water and the plates left to dry for 24 hours at room temperature. Adherent cells were then visualised under the microscope under x20 objective magnification and 4 random fields per well were captured and counted.

Within each experiment all wells were prepared in triplicate per sample and the entire experimental procedure was repeated at least three independent times. Data from all the repeats were combined and presented as mean percentage control with SEM.

2.10.3 In vitro tumour motility assays

Cellular motility was assessed using one of two methods as described below based on tumour cell behaviour.

2.10.3.1 Cytodex-2 bead motility assay

Cellular motility was assessed using a cytodex-2 bead motility assay as described previously (modified from Jiang *et al* 1995b; Rosen *et al* 1990).

Overnight, $1x10^6$ cells in 10ml of growth medium and 100µl of cytodex-2 beads (20mg/ml) were incubated at 37ºC and 5% CO_2, to allow cells to adhere to the beads. The beads were then washed twice in 5ml of growth medium to remove any non-adherent cells and resuspended in 1ml of growth medium. One hundred microliters of the bead suspension was then added, in triplicate, to a 96 well plate containing a further 100µl of Blasticidin S free medium, or treatment, and incubated for 4 hours at 37ºC and 5% CO_2. Following incubation, the medium was removed and the wells washed with 150µl BSS to remove any remaining beads or non-adherent cells. Adherent cells were fixed in 4% formaldehyde (v/v) in BSS for 10 minutes and then stained with 0.5% crystal violet (w/v) in distilled water for 10 minutes. The crystal violet was washed off with distilled water and the plates left to dry for 24 hours at room temperature. Stained cells were then visualised under x20 objective magnification, where at least 4 random fields were captured and counted per well.

Within each experiment each sample was prepared in triplicate. The entire experimental procedure was repeated a minimum of three independent times. Data from all the repeats were combined and presented as mean percentage control with SEM.

2.10.3.2 Electric Cell-substrate Impedance Sensing (ECIS)

ECIS is a technique designed and licensed by Applied Biophysics which monitors cell attachment and migration, on gold electrodes in 96 well arrays, using changes in resistance and impedance over time.

This study used 96W1E arrays (ECIS cultureware, Applied Biophysics Inc, NY, USA) which were stabilised by adding 200µl of stabilising solution (Applied Biophysics Inc, NY, USA) to each well and leaving them at room temperature for 20 minutes. This medium was aspirated off and replaced with $8x10^4$ cells/100µl of HEPES buffered medium and 100µl of treatments. The array was then placed in the ECIS incubator at 37ºC connected to the Theta ECIS controller system (Applied Biophysics Inc, NY, USA). The software was configured so resistance of the current flow was measured at 4000Hz. Data was normalised using resistance from the first time point.

Within each experiment each sample was prepared in triplicate. The entire experimental procedure was repeated a minimum of three independent times. Data from all the repeats were combined and presented as change in resistance over a 4 hour period with SEM.

2.10.4 In vitro tumour cell Matrigel invasion assay

The invasive capacity of the cells used in this study was determined using an *in vitro* Matrigel invasion assay (modified from Albini *et al* 1987, Parish *et al* 1992), measuring the cells ability to degrade and invade through an artificial basement membrane and migrate through 8µm pores. Transwell inserts containing 8µm pores (Falcon, pore size 8.0µm, 24 well format, Greiner Bio-One, Germany) were placed into wells of a 24 well plate (NUNC, Greiner Bio-One, Germany) using sterile

forceps in order to prevent contamination. Each insert was subsequently coated in 50µg of Matrigel (BD Matrigel Matrix, Matrigel Basement Membrane Matrix, Biosciences) in a serum free medium solution and left to dry for 2 hours at 55ºC. The Matrigel artificial membrane was rehydrated in 100µl of serum free medium for approximately 40 minutes at room temperature. Once rehydrated, the serum free medium was removed and 1ml of Blasticidin S free medium was added to the bottom of the well containing the insert in order to sustain any cells that invaded through the insert. Subsequently, 2 - 3 x 10^4 cells/100µl and 100µl of Blasticidin S free medium or treatment were added into the Matrigel coated insert and incubated for 72 hours at 37ºC, 5% CO_2 and 95% humidity.

After 72 hours, the inserts were removed from the plate and any non-invaded cells and the Matrigel were cleaned thoroughly with tissue paper, prior to fixing. The underside of the insert was fixed in 4% formaldehyde (v/v) in BSS for 10 minutes before being stained in 0.5% crystal violet solution (w/v) in distilled water for 10 minutes. The crystal violet solution was washed off using distilled water and the inserts left to dry at room temperature for 24 hours. Cells were visualised under a light microscope under x20 objective magnification and at least 5 random fields per insert were captured and counted. This experimental procedure was repeated a minimum of three independent times. Data from the independent repeats were combined and are presented as percentage control with SEM.

2.11 *In vivo* tumour growth and development model

The project license (PPL 30/2591) under which all *in vivo* work was carried out was approved by both the Cardiff University School of Medicine JBIOS Committee and the UK Home Office under the Animals (Scientific Procedures) Act 1986, as issued by the Secretary of State for the UK Home Office. *In vivo* work was carried out

under the strict guidelines of the UK Home Office to ensure that the 3R's were strictly adhered to. Thus, the minimum number of animals was used in the experiment, with a minimum of suffering and maximum attention to animal welfare. The maximum severity band allowed was moderate, although the procedures carried out in this work were ostensibly only mild. Animals were checked daily and their behaviour and health monitored. Animals were weighed and measured twice weekly to ascertain loss of health (as determined by weight loss greater than 20% or tumour burden greater than $1cm^3$). Adverse effects resulted in sacrifice via UK Schedule One procedures.

The *in vivo* tumour progression model was adapted from similar previously described protocols (Jiang *et al* 2005a; Kuba *et al* 200; Martin *et al* 2003). A suspension of 100µl containing one million breast cancer cells and 0.5mg/ml Matrigel was subcutaneously injected into the left and right flanks of 4-6 week old athymic nude mice (CD-1) and allowed to develop. The mice were maintained in filter top units according to House Office regulations. The mice were weighed and the size of the developing tumour measured using vernier callipers under sterile conditions each week. At the conclusion of the experiment animals were weighed, humanely killed under Schedule One and tumours were dissected out if sufficiently sized. Thus, tumour volume was determined, at each time point, using the following formula:-

$$\text{Tumour volume} = 0.523 \times \text{width}^2 \times \text{length}$$

2.12 Statistical analysis

For statistical analysis experiments were repeated at least three independent times. Resultant data was then analysed using the Sigma plot 11.0 statistical software package. In ribozyme transgene manipulated cell lines, data was compared to the

pEF6 control cell line (cells containing a closed pEF6 plasmid only); as this control confirmed that it was the ribozyme/expression sequence that was responsible for any changes seen and not the pEF6 plasmid itself. Where appropriate non-manipulated cell lines were compared to untreated cells. The statistical comparisons between the test and control cell lines were made using either a Students two tailed *t*-test if the data was found be normalised and have equal variances or a non-parametric Mann-Whitney test if the data was not normalised. In all cases p-values of ≤0.05 were regarded as being significant.

Cytotoxicity assays and ECIS were assessed using ANOVA tests with post hoc analysis (Holm-Sidak method). In all cases p-values of ≤0.05 were regarded as being significant.

Chapter 3

Expression profile of OPG, RANK and RANKL

in breast and prostate cancer

3.1 Introduction

The complexity of the dysregulated bone response in breast and prostate cancer is underpinned by the vast number of soluble factors, signalling pathways and transcription regulators involved. In order to clarify the dysregulation that occurs to both extremes, osteoblastic and osteoclastic, of the bone remodelling process, particular focus must be given to each individual aspect in turn. Elucidation of this process will hopefully result in improved therapeutic intervention and patient management.

The OPG/RANK/RANKL system has already been linked to cancer cells through the inhibition of TRAIL-apoptosis (Holen *et al* 2002). However, much still remains unknown about the interplay and influence tumour cells, the factors they produce and bone have on each other during osteotropic cancer progression.

In the literature it has been well characterised that unlike most other osteotrophic cancers, prostate cancer presents with a predominantly osteoblastic phenotype though osteolytic activity is also present (Lynch *et al* 2005, Lu *et al* 2009). In contrast, it is mainly the osteolytic phenotype which is associated with breast cancer (Roodman 2001). It has been shown that prostate and breast cancer cells produce a variety of factors which influence the bone environment, including OPG, RANK and RANKL, all of which can affect bone re-modelling. OPG, RANK and RANKL have also been linked to signalling cascades which can also initiate cell proliferation, differentiation and survival.

The aim of this section of the study was to determine the expression levels of OPG, RANK and RANKL in the available prostate and breast cancer cell lines. Additionally the aim was to characterise the proliferative response of the prostate and breast cancer cells to exogenous HGF stimulation and isolated bone proteins (BME) and how these factors affected OPG and RANK transcript expression levels.

3.2 Transcript expression profiles in prostate cancer cell lines

Six prostate cancer cell lines were screened during the course of this study. PZHPV-7 is considered an immortalised cell line which is representative of normal prostate epithelium. CAHPV-10, is an immortalised cell line derived from primary prostate cancer. PC-3, DU-145, LNCaP and MDA-PCa-2b are all cell lines derived from metastatic sites associated with prostate cancer, all of which have differing tumourigenic potential in *in vivo* models. The most aggressive of these cell lines is considered to be the PC-3 cell line, which *in vivo* presents with osteolytic bone lesions. DU-145 cells also generate osteolyic bone lesions in pre-clinical models. In contrast, MDA-PCa-2b cells are one of the few commercially available cell lines which result in osteoblastic bone lesions whilst LNCaP cells generate mixed osseous (osteoblastic and osteolytic) bone lesions.

3.2.1 Transcript expression of OPG, RANK and RANKL in prostate cancer cell lines

OPG transcript expression was detected in all the available cell lines tested (Figure 3.1). It appeared to be strongest in the normal prostate epithelium cell line (PZHPV-7) and primary cancer cell line (CAHPV-10), and weakest in the mixed osteoblastic-osteolytic androgen dependent LNCaP cell line, where only minimal expression was detected. RANK transcript was also detected in all the prostate cancer cell lines tested but appeared strongest in the osteolytic PC-3 and DU-145 cell lines. In contrast RANKL transcript expression was only detected in the DU-145 and LNCaP cell lines, whilst a very weak expression was detected in the CAHPV-10 cells.

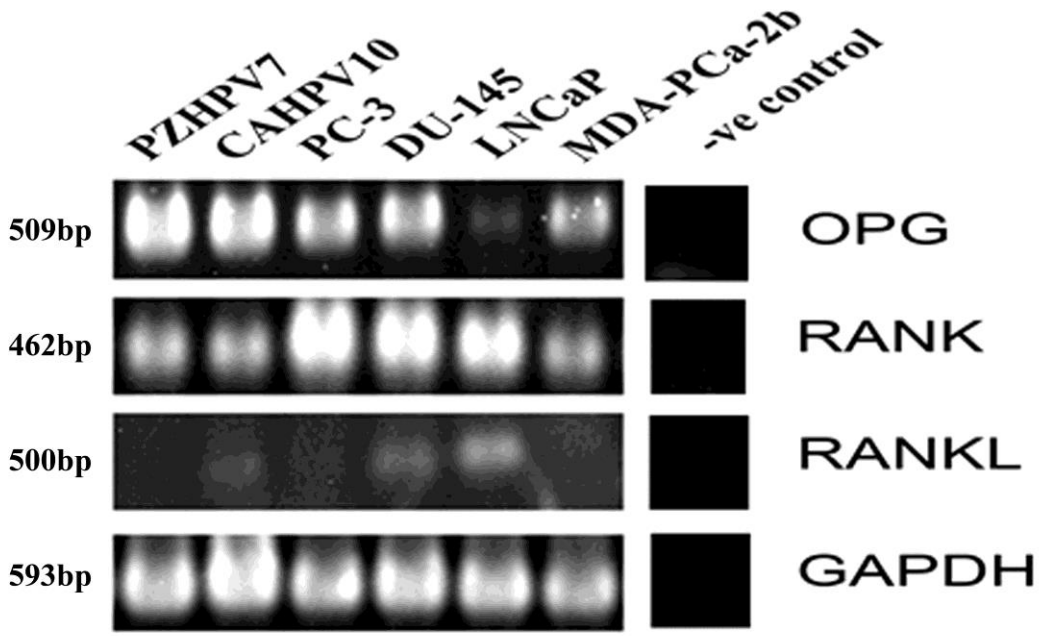

Figure 3.1: Transcript expression levels of OPG, RANK and RANKL

Control = Nuclease free water and all gels were ran with a molecular weight marker used to identify band sizes.

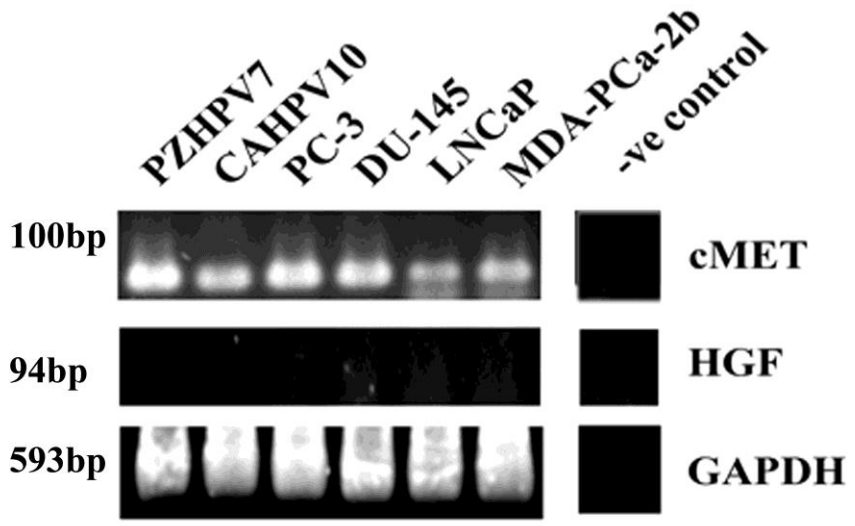

Figure 3.2: Transcript expression levels of HGF and its receptor c-MET

Control = Nuclease free water and all gels were ran with a molecular weight marker used to identify band sizes.

3.2.2 Transcript expression of HGF and its receptor, c-MET in prostate cancer cell lines

All the prostate cancer cell lines were also screened for HGF transcript and its receptor c-MET. None of the prostate cancer cell lines produced any detectable HGF transcript levels. In contrast all were positive for its receptor c-MET (Figure 3.2). c-MET expression appeared particularly strong in the PC-3, DU-145 and PZHPV-7 cell lines. In contrast the weakest transcript expression was seen in the mixed osteoblastic-osteolytic androgen dependent LNCaP cell line.

For the purposes of this study PC-3 and LNCaP cell lines were chosen for further investigation.

3.3 Impact of HGF treatment on prostate cancer cell proliferation

3.3.1 Effect of HGF treatment on PC-3 cell proliferation

PC-3 cells were treated with 3 concentrations of HGF (10ng/ml, 40ng/ml or 80ng/ml) and proliferation rates were assessed over both 3 and 5 days incubation (Figure 3.3). Treatment of PC-3 cells with HGF, after 3 day incubation, appeared to bring about an initial enhancement of PC-3 cell proliferation at the higher concentrations (40ng/ml and 80ng/ml), though none of these changes reached significant levels (Figure 3.3 A). This trend did not continue over the 5 day incubation period, in which similar PC-3 cell proliferation levels were seen between the control and treated cells (Figure 3.3 B).

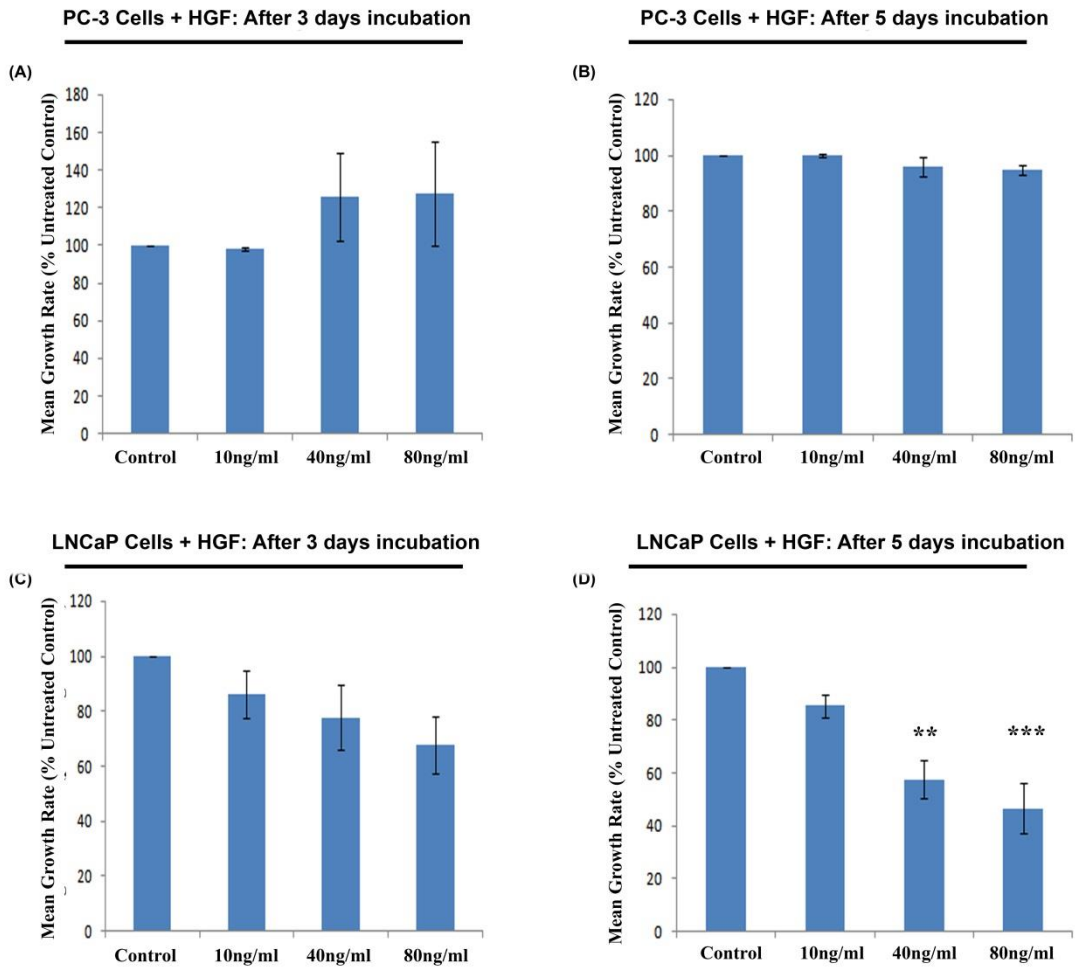

Figure 3.3: Impact of HGF treatments on prostate cancer cell proliferation

Impact of HGF treatment was assessed on PC-3 cells (A and B) and LNCaP cells (C and D) over both 3 and 5 days incubation. Data represents mean of 3 independent repeats, error bars represent SEM. * - p=<0.05, ** - p=<0.01 and *** - p=<0.001.

3.3.2 Effect of HGF treatment on LNCaP cell proliferation

In LNCaP cells, treatment with HGF brought about a reduction in cell proliferation after both 3 days incubation (Figure 3.3 C) and 5 days incubation (Figure 3.3 D). No significant differences were seen after 3 days incubation with each of the HGF concentrations compared to the untreated control. However, after 5 days incubation, both the 40ng/ml HGF treatment ($p=0.002$) and 80ng/ml treatment ($p<0.001$) resulted in a significant decrease in LNCaP cell proliferation compared to the untreated control.

3.4 Impact of BME treatment on prostate cancer cell proliferation

3.4.1 Effect of BME treatment on PC-3 cell proliferation

Treatment of PC-3 cells with BME (1µg/ml, 10µg/ml and 50µg/ml) did not greatly impact PC-3 cell proliferation after 3 days incubation (Figure 3.4 A). After 5 days incubation PC-3 cell proliferation was significantly increased at all the concentrations tested (Figure 3.4 B, $p=0.012$, <0.001 and 0.015 respectively vs untreated control). Whilst these changes were deemed to be significant, changes were only approximately increased 10% compared to the control cells.

3.4.2 Effect of BME treatment on LNCaP cell proliferation

LNCaP cells treated with BME showed no difference in cell proliferation after 3 days incubation compared to the untreated control (Figure 3.4 C). However, after 5 days incubation LNCaP cell proliferation was increased at the higher concentrations compared to the untreated control (Figure 3.4 D, 10µg/ml and 50µg/ml), though this did not reach statistical significance.

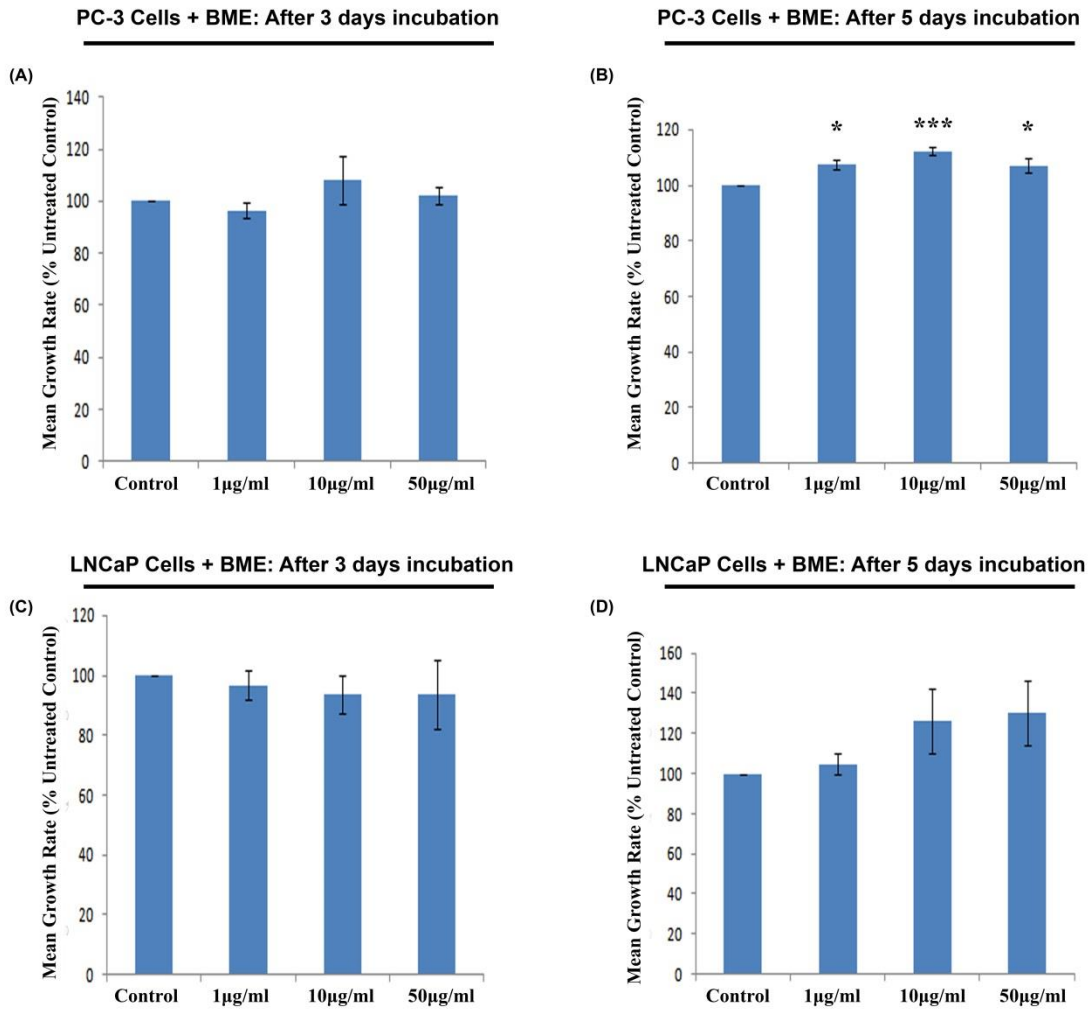

Figure 3.4: Impact of BME treatments on prostate cancer cell proliferation

Impact of BME treatment was assessed on PC-3 cells (A and B) and LNCaP cells (C and D) over both 3 and 5 days incubation. Data represents mean of 3 independent repeats, error bars represent SEM. * - p=<0.05, ** - p=<0.01 and *** - p=<0.001.

Based on these observations for the remainder of this study all subsequent treatments were carried out with 40ng/ml HGF and 50µg/ml BME.

3.5 Prostate cancer cell transcript expression of OPG and RANK after treatment with HGF and BME treatment in a time course

OPG and RANK transcript expression levels were examined in PC-3 and LNCaP prostate cancer cells, in response to 40ng/ml HGF, 50µg/ml BME and combined 40ng/ml HGF and 50µg/ml BME over a 2 hour period by qPCR.

3.5.1 Transcript analysis of OPG expression in PC-3 prostate cancer cells following treatment with HGF and BME

Treatment of PC-3 cells with 40ng/ml HGF increased OPG transcript expression levels after 1 hour incubation and this was increased further after 2 hours incubation, however both of these increases did not reach statistical significance compared to the untreated control (Figure 3.5 A).

In the PC-3 cells, peak OPG transcript levels were seen in cells treated with 50µg/ml BME for 1 hour, however this did not reach significance compared to the untreated control (Figure 3.5 B). However, after 2 hours incubation with 50µg/ml BME, OPG transcript levels appeared to have been restored to similar levels seen in the untreated control.

When HGF and BME were administered in combination, OPG transcript levels appeared to increase, peaking after 2 hours incubation, though again this increase failed to reach significance compared to the untreated control (Figure 3.5 C).

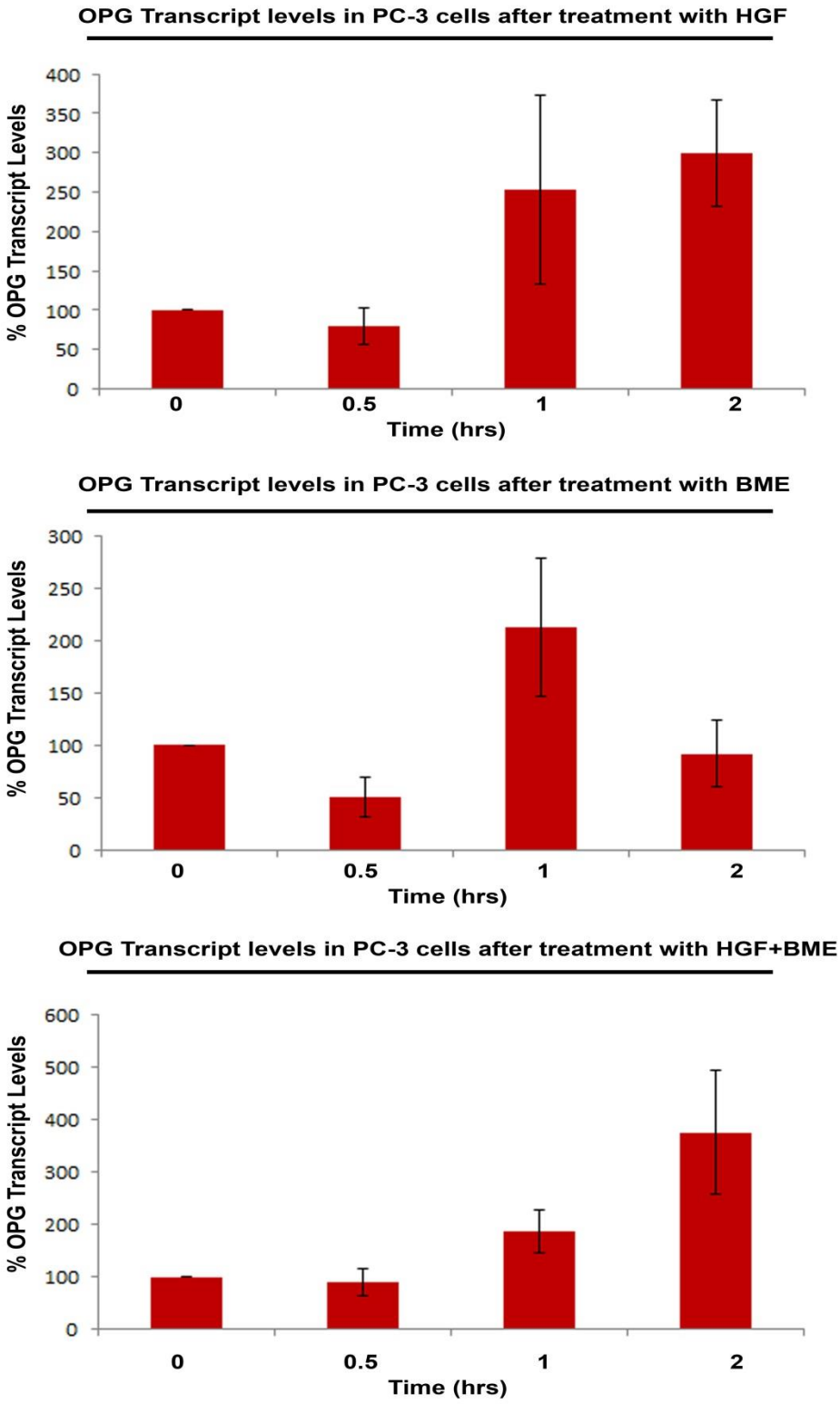

Figure 3.5: OPG transcript analysis following treatment with HGF and BME in PC-3 cells

Response of OPG transcript expression following time course treatment with 40ng/ml HGF (A), 50µg/ml BME (B) or combined 40ng/ml HGF and 50µg/ml BME (C). Data represents mean values of 3 independent repeats normalised against GAPDH, error bars represent SEM. * - p=<0.05, ** - p=<0.01 and *** - p=<0.001.

3.5.2 Transcript analysis of OPG expression in LNCaP prostate cancer cells following treatment with HGF and BME

In the androgen dependent LNCaP cell line, when incubated with HGF, OPG transcript levels increased after 1 hour (Figure 3.6 A). However at both of the other time points analysed (30 minutes and 2 hours) OPG transcript levels appeared reduced in comparison to the control levels. None of these results reached statistically significant levels and due to the large standard deviation bars these must be interpreted with caution.

When the LNCaP cells were treated with BME, OPG transcript levels were found to be reduced at all the time points assessed compared to the untreated control (Figure 3.6 B). However, none of these reductions in OPG transcript levels were found to be statistically significant.

When HGF and BME were combined as a treatment, OPG transcript levels in LNCaP cells appeared to reduce at all the time points analysed (Figure 3.6 C).

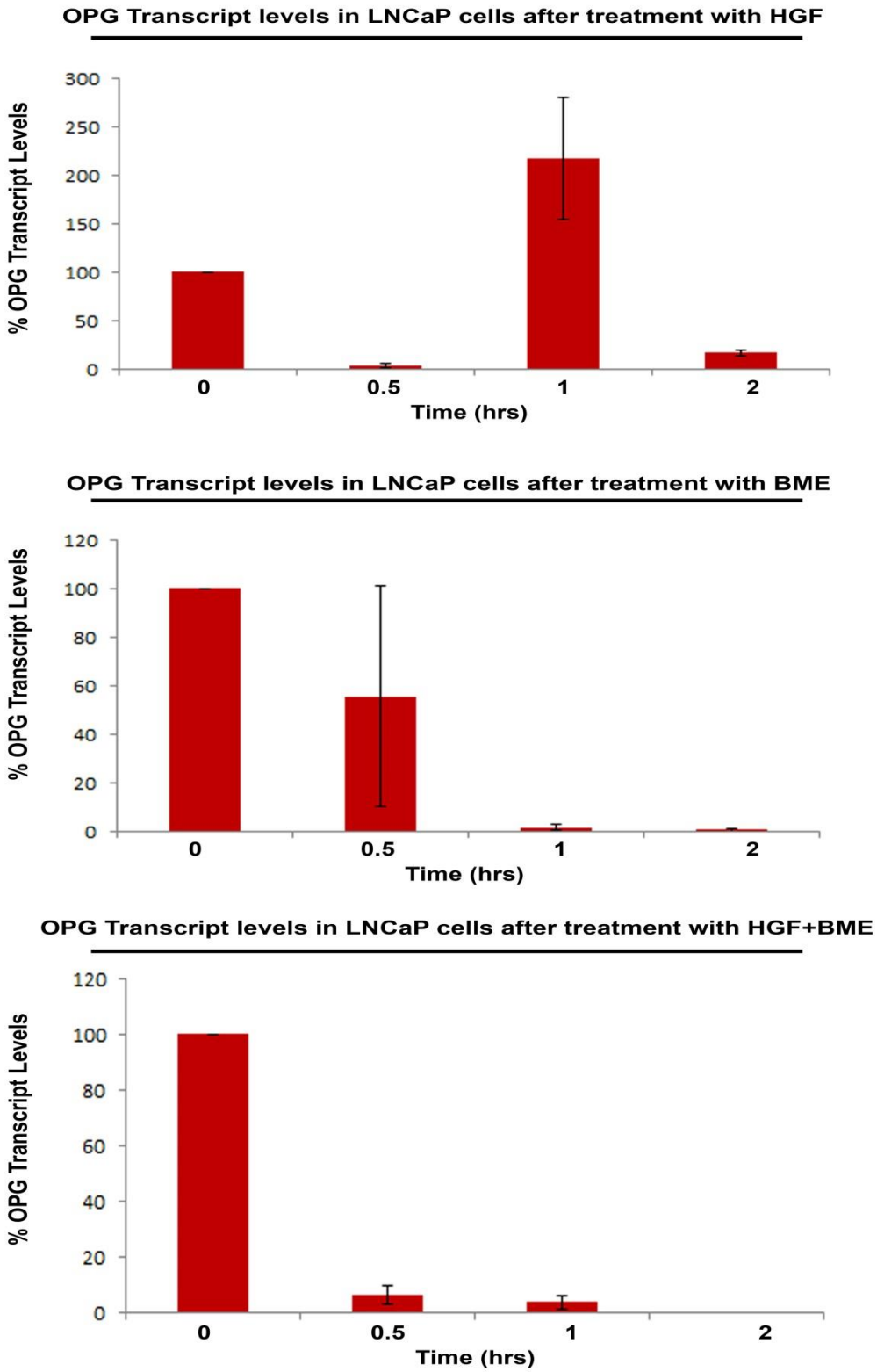

Figure 3.6: OPG transcript analysis following treatment with HGF and BME in LNCaP cells

Response of OPG transcript expression following time course treatment with 40ng/ml HGF (A), 50µg/ml BME (B) or combined 40ng/ml HGF and 50µg/ml BME (C). Data represents mean values of 3 independent repeats normalised against GAPDH, error bars represent SEM. * - p=<0.05, ** - p=<0.01 and *** - p=<0.001.

3.5.3 Transcript analysis of RANK expression in PC-3 prostate cancer cel ls following treatment with HGF and BME

Treatment of PC-3 cells with 40ng/ml HGF, increased RANK transcript expression levels after 2 hour incubation, however this increase did not reach statistical significance compared to the untreated control (Figure 3.7 A).

In the PC-3 cells, peak RANK transcript levels were seen in cells treated with BME for 1 hour, which was a significant increase compared to the untreated control (Figure 3.7 B, $p<0.001$). However, after 2 hours incubation with BME, RANK transcript levels appeared to have been restored to similar levels seen in the untreated control.

When HGF and BME were administered in combination, RANK transcript levels appeared to increase, peaking after 1 hour incubation which reached significance compared to the untreated controls ($p<0.001$) (Figure 3.7 C). However, RANK transcript levels returned to control levels after 2 hours incubation.

3.5.4 Transcript analysis of RANK expression in LNCaP prostate cancer cells following treatment with HGF and BME

HGF treatment of LNCaP cells appeared to have no impact on RANK transcript levels at each of the time points analysed (Figure 3.8 A). In contrast, when treated with BME, RANK transcript expression in LNCaP cells appeared to increase compared to the untreated cells, peaking after 1 hour incubation, though this increase did not reach statistical significance (Figure 3.8 B). This increase in RANK transcript was sustained after 2 hours incubation with BME.

When HGF and BME were added in combination, increases in RANK transcript levels were seen after both 30 minutes and 1 hour incubation periods compared to

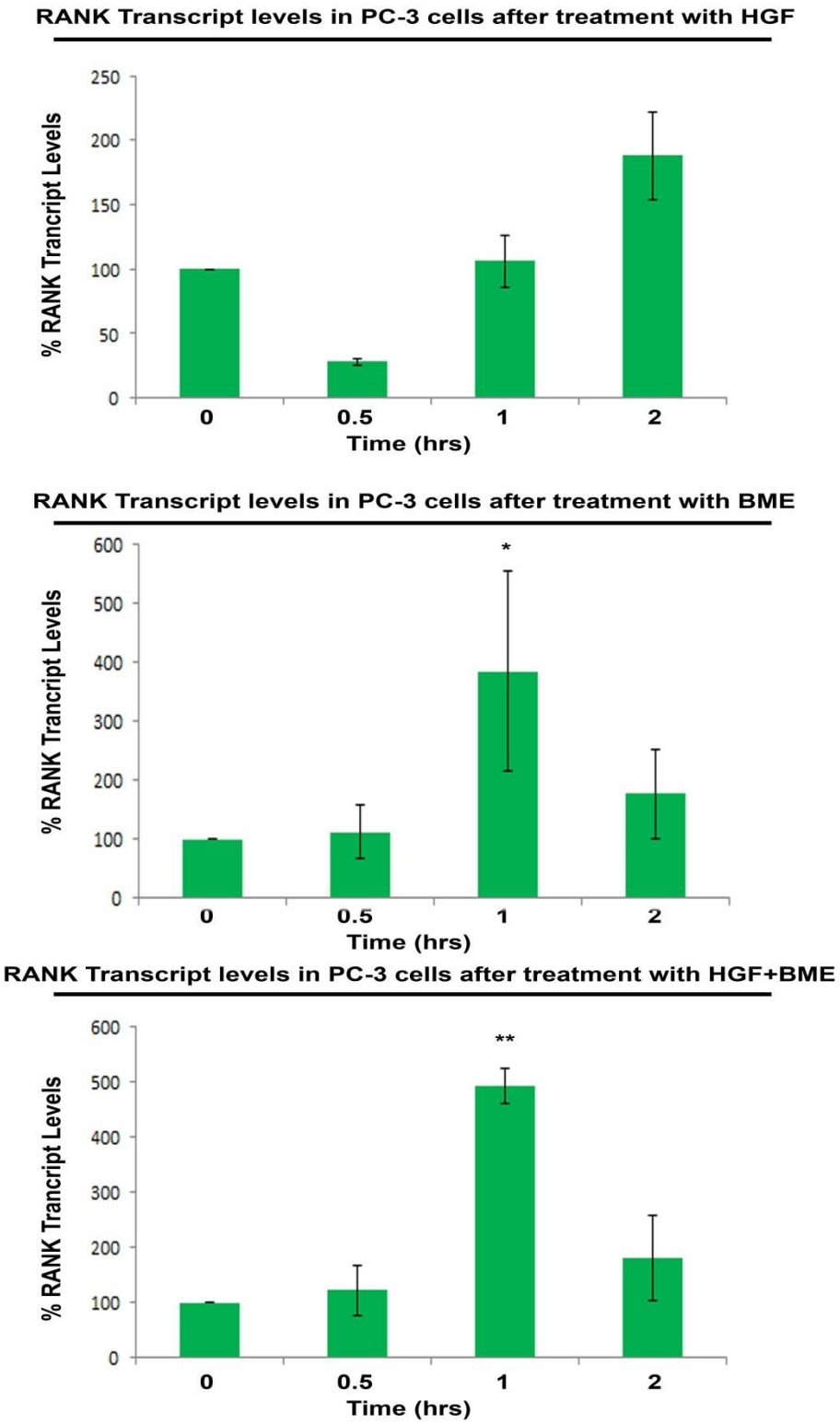

Figure 3.7: RANK transcript analysis following treatment with HGF and BME in PC-3 cells

Response of RANK transcript expression following time course treatment with 40ng/ml HGF (A), 50µg/ml BME (B) or combined 40ng/ml HGF and 50µg/ml BME (C). Data represents mean values of 3 independent repeats normalised against GAPDH, error bars represent SEM. * - p=<0.05, ** - p=<0.01 and *** - p=<0.001.

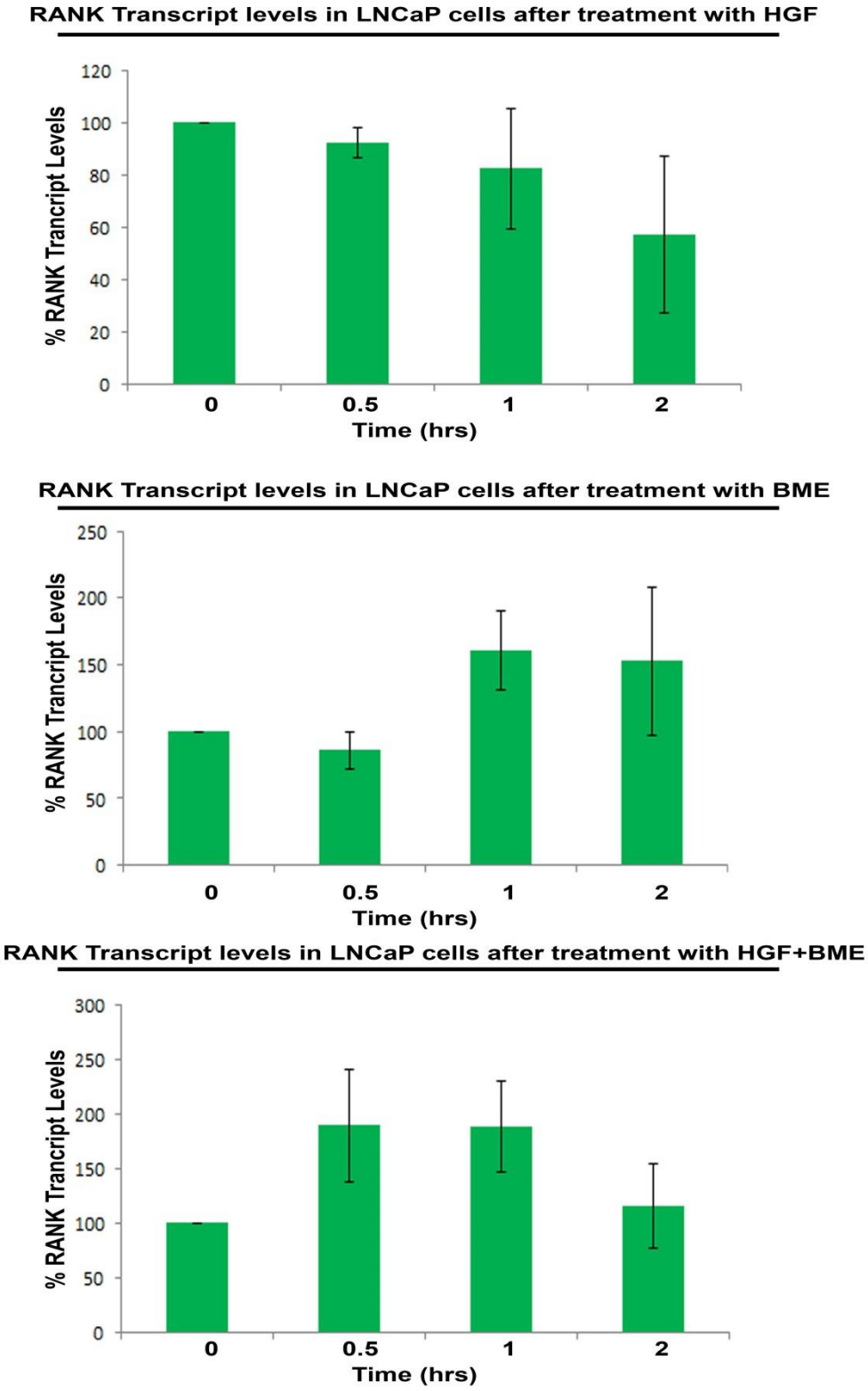

Figure 3.8: RANK transcript analysis following treatment with HGF and BME in LNCaP cells

Response of RANK transcript expression following time course treatment with 40ng/ml HGF (A), 50µg/ml BME (B) or combined 40ng/ml HGF and 50µg/ml BME(C). Data represents mean values of 3 independent repeats normalised against GAPDH, error bars represent SEM. * - p=<0.05, ** - p=<0.01 and *** - p=<0.001.

the untreated controls, however neither of these reached significance (Figure 3.8 C). After 2 hours incubation with a combination of HGF and BME, RANK transcript levels appeared to be at similar levels to those observed in the untreated cells.

3.6 Transcript expression profiles in breast cancer cell lines

3.6.1 Expression profiles of OPG, RANK and RANKL in breast cancer cell lines

In the laboratory, ZR-75-1, MCF-7 and MDA-MB-231 cells were available. Therefore, as an initial step, all 3 of the breast cancer cell lines were screened using RT-PCR (Figure 3.9). All three cell lines showed strong expression of RANK transcript, however only the metastatic and ER negative MDA-MB-231 cell line showed RANKL transcript expression. All the cell lines were also positive for OPG expression, although, the weakly tumourigenic ZR-75-1 cell line displayed weak expression levels compared to the more aggressive MCF-7 and MDA-MB-231 cell lines.

3.6.2 Expression profiles of HGF and c-MET receptor in breast cancer cell lines

As was seen in the prostate cancer cell lines, all three breast cancer cell lines did not express the HGF transcript at detectable levels, however they were all found to be positive for the HGF receptor, c-MET (Figure 3.10).

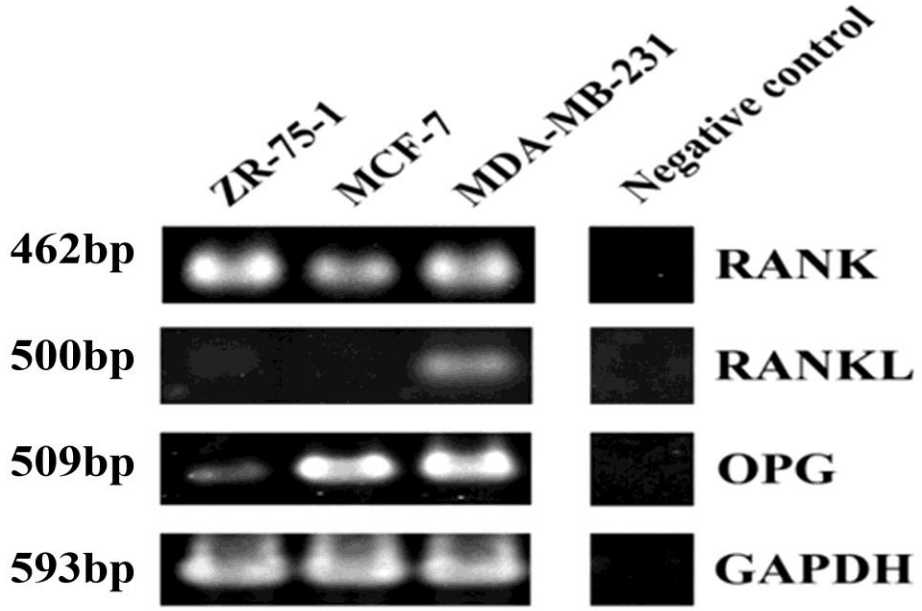

Figure 3.9: Expression of RANK, RANKL and OPG in breast cancer cell lines

Control = Nuclease free water and all gels were ran with a molecular weight marker used to identify band sizes.

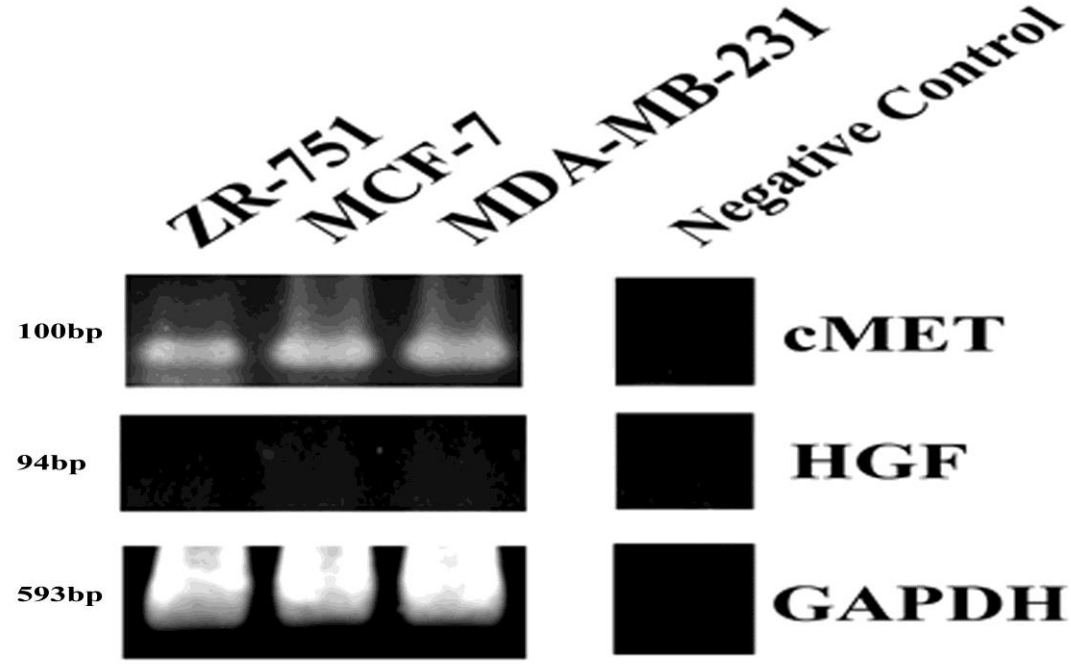

Figure 3.10: Expression of HGF and c-MET in breast cancer cell lines

Control = Nuclease free water and all gels were ran with a molecular weight marker used to identify band sizes.

3.7 Impact of HGF and BME on MDA-MB-231 cell proliferation

Treatment of MDA-MB-231 breast cancer cells with HGF (10ng/ml, 40ng/ml and 80ng/ml) did not result in any significant changes in cell proliferation after 3 days incubation (Figure 3.11 A). After 5 days incubation all of the HGF treatment concentrations tested resulted in increased cell proliferation though none of these reached significance (Figure 3.11 B).

Following incubation of MDA-MB-231 cells with BME (1µg/ml, 10µg/ml and 50µg/ml) for 3 days, no significant effects were seen on cell proliferation (Figure 3.11 C). After 5 days incubation at the higher concentrations (10µg/ml and 50µg/ml) MDA-MB-231 cell proliferation increased, though again this did not reach significance (Figure 3.11 D).

3.8 Transcript analysis of OPG and RANK expression in MDA-MB-231 breast cancer cells following treatment with HGF and BME over a time course

OPG and RANK expression were assessed in MDA-MB-231 breast cancer cells in response to 40ng/ml HGF, 50µg/ml BME and combined 40ng/ml HGF and 50µg/ml BME over a 2 hour period by qPCR.

3.8.1 Transcript analysis of OPG expression in MDA-MB-231 breast cancer cells following treatment with HGF and BME

OPG transcript levels were significantly reduced after 30 minutes ($p=0.02$) and 2 hours ($p<0.001$) incubation with 40ng/ml HGF compared to control cells (Figure 3.12 A).

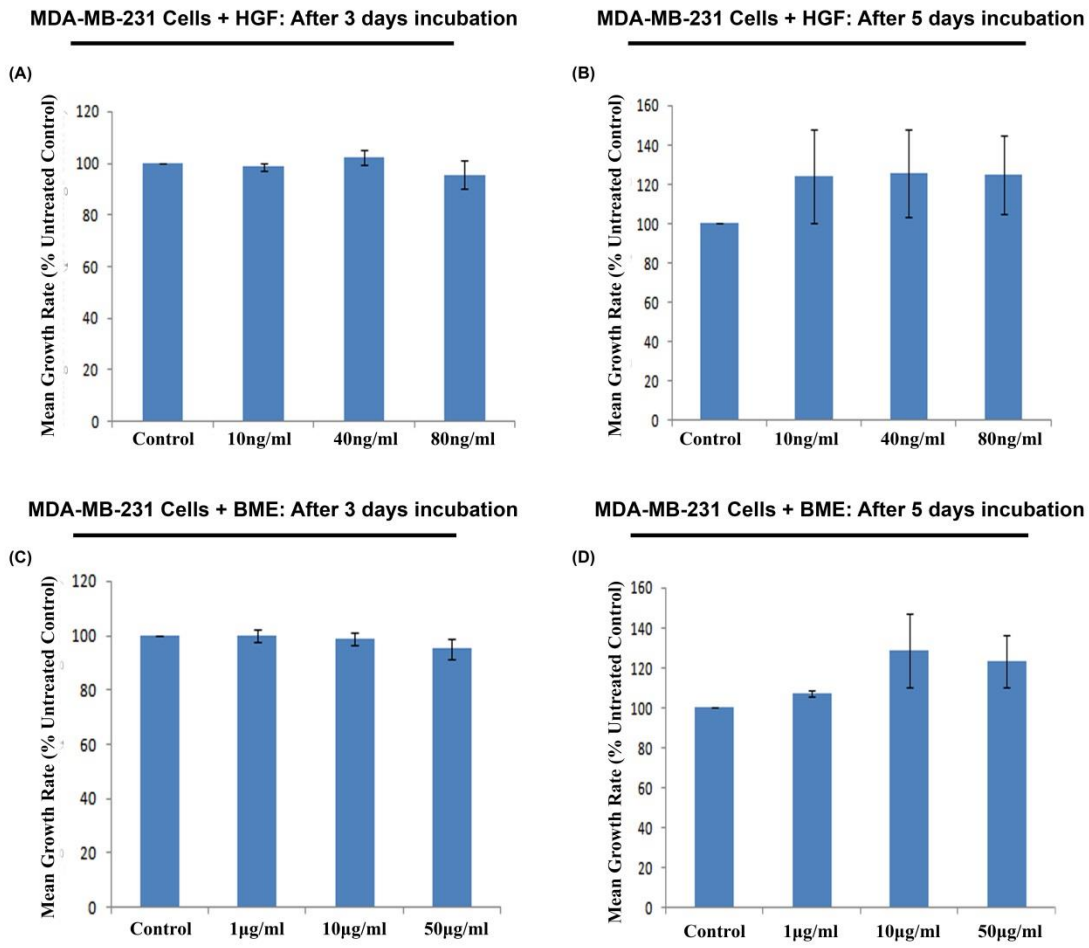

Figure 3.11: Impact of HGF and BME treatments on MDA-MB-231 cell proliferation

MDA-MB-231 cells were incubated with 10ng/ml, 40ng/ml and 80ng/ml HGF for 3 and 5 days (A and B).Treatment of MDA-MB-231 cells with 1µg/ml, 10µg/ml and 50µg/ml BME for 3 and 5 days (C and D). Data represents mean of 3 independent repeats, error bars represent SEM. * - p=<0.05, ** - p=<0.01 and *** - p=<0.001.

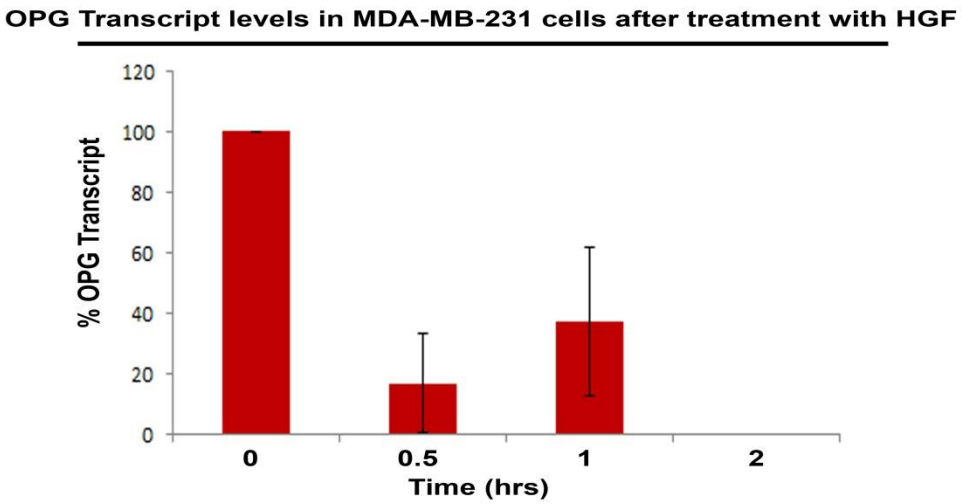

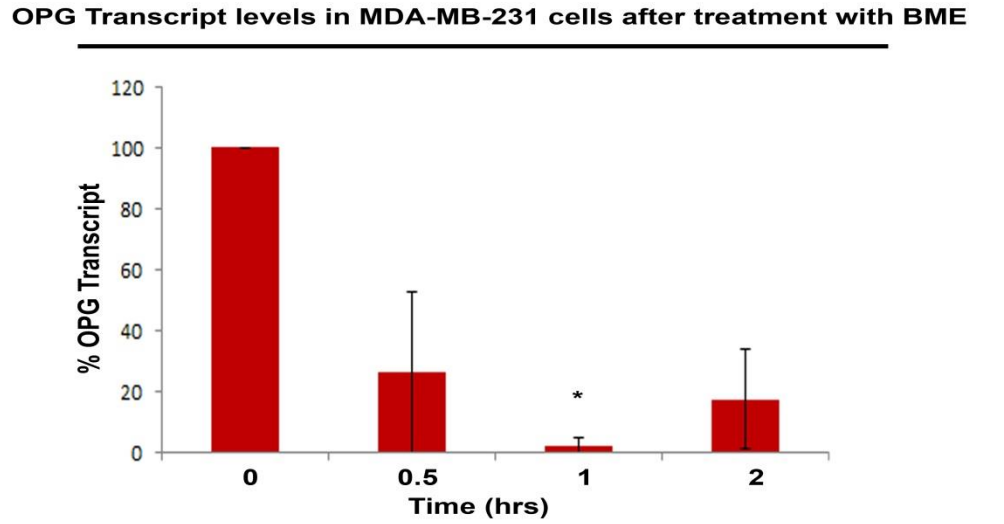

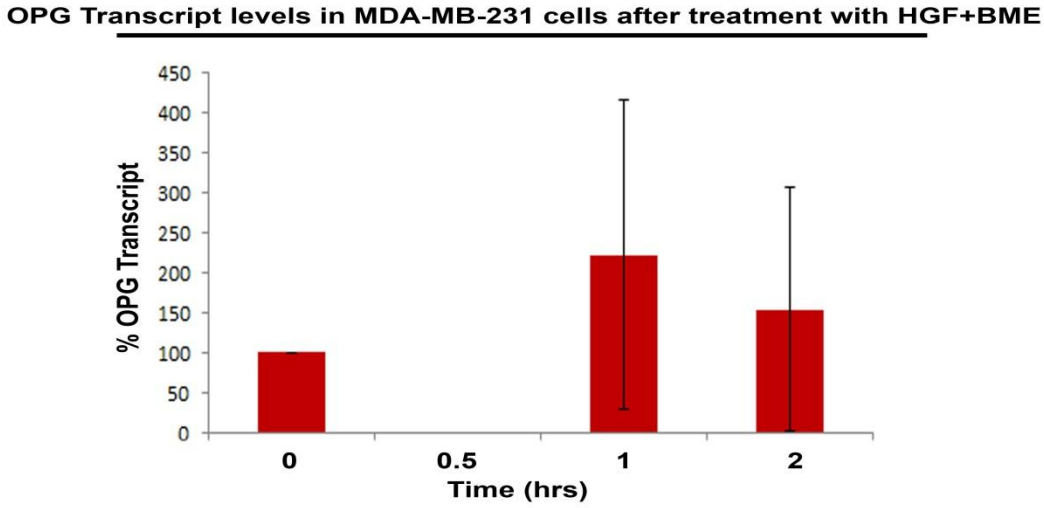

Figure 3.12: OPG transcript analysis following treatment with HGF and BME in MDA-MB-231 cells

Response of OPG transcript expression following time course treatment with 40ng/ml HGF (A), 50µg/ml BME (B) or combined 40ng/ml HGF and 50µg/ml BME (C). Data represents mean values of 3 independent repeats normalised against GAPDH, error bars represent SEM. * - p=<0.05, ** - p=<0.01 and *** - p=<0.001.

A general reduction in OPG expression was also seen in response to 50µg/ml BME treatment (Figure 3.12 B). The largest reduction was seen after 1 hour incubation with BME which also reached significance (p=0.02).

When HGF and BME were combined as a treatment, initially after 30 minutes incubation a significant decrease in OPG transcript levels was seen compared to the untreated cells (p=0.02) (Figure 3.12 C). However, after 1 hour incubation OPG transcript levels were increased in comparison to the untreated cells, a response which was maintained over the 2 hour incubation period, though neither reached significant levels compared to the untreated control.

3.8.2 Transcript analysis of RANK expression in MDA-MB-231 breast cancer cells following treatment with HGF and BME

Treatment of MDA-MB-231 cells with 40ng/ml HGF resulted in increased RANK transcript expression at every time point assessed compared to the untreated control, however none of these increases reached statistical significance (Figure 3.13 A). A similar response in RANK transcript expression was observed following 2 hours incubation with the BME treatment (Figure 3.13 B).

In contrast, when HGF and BME were combined as a treatment, an initial increase in RANK transcript levels was seen after 30 minutes. This appeared to return to control levels after 1 hour, before another increase, though not as big as the 30 minute response, was noted after 2 hours incubation (Figure 3.13 C). However, none of these alterations in RANK transcript levels reached statistical significance and due to the large standard deviation bars these trends must be interpreted with caution.

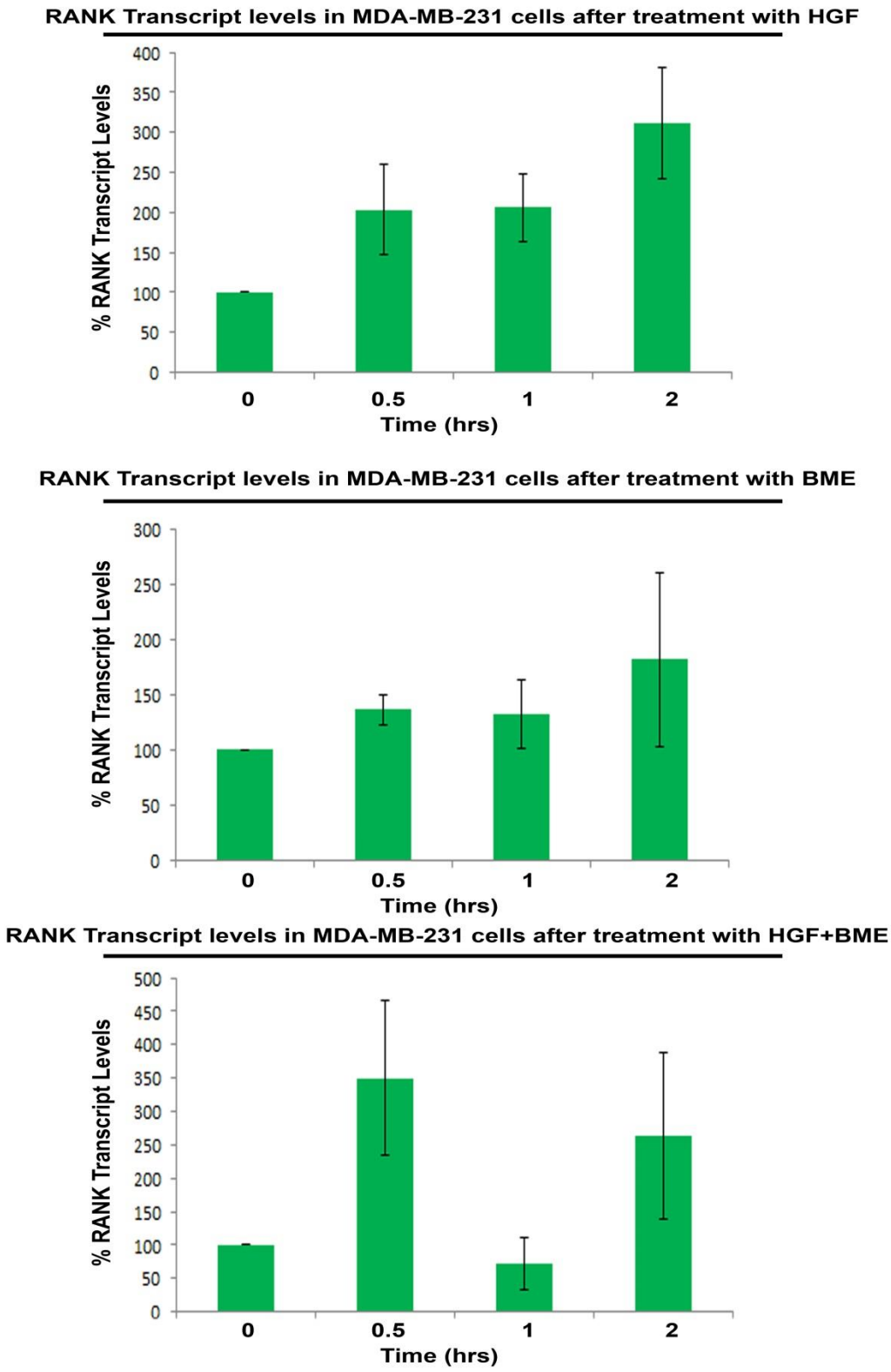

Figure 3.13: RANK transcript analysis following treatment with HGF and BME in MDA-MB-231 cells

Response of RANK transcript expression following time course treatment with 40ng/ml HGF (A), 50µg/ml BME (B) or combined 40ng/ml HGF and 50µg/ml BME (C). Data represents mean values of 3 independent repeats normalised against GAPDH, error bars represent SEM. * - p=<0.05, ** - p=<0.01 and *** - p=<0.001.

3.9 Discussion

Tumours secrete factors which can influence the bone environment, whilst cells and factors within the bone environment reciprocally influence the tumour cells themselves, thus contributing to the 'vicious cycle' described in bone metastases. OPG, RANK and RANKL as integral regulators of the bone remodelling process have been shown to be affected by the presence of tumour cells, however little is understood on how the bone environment might influence these factors produced by tumour cells themselves, or how these may impact cellular function of cancer cells.

3.9.1 Expression profiles of OPG, RANK and RANKL in breast and prostate cancer cell lines

Of the six prostate cancer cell lines available for this study, all expressed OPG transcript levels, to varying degrees. This correlates with the literature which has also highlighted that the androgen dependent, weakly metastatic LNCaP cell line produced approximately 10 fold less OPG than the more aggressive androgen independent cell line, PC-3 (Holen *et al* 2002).

RANK expression has also been shown to be ubiquitously expressed in all cell lines both, in this study, and in the literature (Armstrong *et al* 2008). Interestingly, expression was strongest in the aggressive osteolytic PC-3 and DU-145 cell lines and the LNCaP cell line, which forms mixed osteoblastic and osteolytic bone lesions. This is also of interest because all three cell lines originate from different prostate associated metastatic sites (DU-145 from the brain, LNCaP from the lymph node and PC-3 from the bone).

RANKL transcript expression levels were only detected in the DU-145 and LNCaP cell lines in the course of this study, both of which have been shown to have strong

osteolytic components in associated bone lesions. In the literature, LNCaP cells have also been shown to produce membrane bound and soluble forms of RANKL making it an interesting model for further study (Zhang *et al* 2001). It is therefore surprising that the aggressive osteolytic PC-3 cell line studied here did not also express detectable levels of RANKL. The literature does suggest that RANKL transcript levels and protein expression have been detected in prostate cancer samples and in the PC-3 cell line, the exact reason for this discrepancy is unknown (Chen *et al* 2006, Brown *et al* 2001). To ensure that all the products seen were the expected molecules of interest placenta cDNA could potentially be used as a positive control for future experiments.

Unfortunately, there are very few purely osteoblastic prostate cancer cell lines commercially available. Unlike PC-3 and LNCaP prostate cancer cells, MDA-PCa-2b cells are difficult to culture due to their growth in sparse colonies with loose adherence to culture flasks. Routine culture of this cell line to generate sufficient numbers for subsequent study has proved problematic and time consuming.

In the 3 breast cancer cell lines tested, ZR-75-1, MCF-7 and MDA-MB-231, all expressed transcript levels of RANK and OPG. RANK transcript levels appeared to be consistent throughout the cell lines irrespective of oestrogen receptor status and metastatic potential. OPG transcript levels appeared strongest in the osteolytic metastatic MDA-MB-231 cell line and weakest in the primary breast cancer cell line (ZR-75-1). RANKL expression was only detected in the aggressive osteolytic breast cancer cell line MDA-MB-231.

3.9.2 Expression profiles of OPG and RANK in breast and prostate cancer cell lines treated with HGF and BME

In the first two hours tested in this study, OPG and RANK transcript levels appeared to be influenced by both HGF and BME to varying degrees in the PC-3 and LNCaP prostate cancer cell lines and the MDA-MB-231 breast cancer cell line.

In the PC-3 prostate cancer cell line HGF treatment appeared to increase OPG and RANK transcript levels, with the highest levels observed after 2 hours incubation. In contrast, BME treatment of PC-3 cells resulted in peak OPG and RANK transcript levels after 1 hour incubation, with restoration to normal levels observed after 2 hours incubation. OPG transcript levels appeared to fluctuate in the LNCaP cell line under stimulation from HGF for 2 hours. However, a similar trend was not seen in the RANK transcript levels. BME treatment also appeared to result in differing transcript level responses. Under the influence of BME, OPG transcript levels decreased and did not show any sign of recovery after 2 hours incubation. However, BME appeared to induce RANK transcript expression after 1 hour incubation, a response which was also maintained after 2 hours incubation.

In the MDA-MB-231 breast cancer cells, OPG transcript levels significantly decreased under the influence of HGF, particularly after 2 hours incubation, a pattern which was also mimicked when these cells were incubated with BME. In contrast, RANK transcript levels appeared to increase after treatment with HGF or BME.

Thus, our current data suggests that OPG and RANK expression may be influenced by the presence of HGF or bone like proteins which may have implications in the metastatic process, particularly concerning the potential involvement of these molecules in the homing and colonisation of cancer cells to the bone. However, further work is required to fully establish this theory. If subsequent work from this

study suggests that BME, as a protein rich factor, influences cell behaviour to isolate the component(s) which may result in these observations, further work could be carried out by using synthetic cocktail of growth factors and proteins or conditioned medium from a range of cell types in the bone environment to fully understand these complex and multifaceted interactions.

Preliminary work in this chapter was conducted over an initial 2 hour time period because HGF has previously been demonstrated to have phosphorylation and transcriptional changes 30 minutes after exposure. Some bi-directional changes in expression were observed over this period, further investigation, without time constraints, would have allowed this to be extended for up to a 24hour period, providing information on the long term alterations which may be induced. It would therefore be of interest to test longer time points (possibly up to 24hours) to fully evaluate the long term effects that exposure to these external cell factors and proteins may have on OPG and RANK transcript expression profiles. Additionally, further repeats are required to clarify some of the trends, as in some of the experiments (particularly the LNCaP model) there is a high degree of standard error, therefore further repeats are necessary.

Based on the data obtained in these early experiments the following model systems were chosen for further investigation. Given the strong expression of OPG and RANK in the PC-3 and MDA-MB-231 cell lines, ribozyme targeting of these molecules were chosen to assess their impact on these osteolytic prostate and breast cancer cells. The LNCaP cell line showed strong expression for RANKL but only weak expression for OPG therefore the addition of a recombinant form of OPG and a neutralising antibody for RANKL were chosen to assess their impact on the mixed osseous prostate cancer cell line. These findings will be presented in full in the following results chapters.

Chapter 4

Role of OPG and RANK in osteolytic prostate cancer

4.1 Introduction

Treatment of localised prostate cancer has significantly improved in recent years, despite this, once metastases have been detected patient prognosis still remains poor (Lee *et al* 2011). Although prostate cancer is initially an androgen dependent disease, the tumour ultimately becomes hormone refractory and resistant to therapy (Feldman and Feldman 2001). Generally it is this androgen independent phenotype which develops at metastatic sites. The main metastatic site associated with prostate cancer is the bone, of which the osteoblastic phenotype is most commonly reported (Roudier *et al* 2004). However, there is strong evidence to suggest that bone resorption may play a vital role in the establishment of the micro-metastases in the bone (Lynch *et al* 2005). What remains unclear is whether, in prostate cancer, bone turnover shifts to favour bone formation or if the 'vicious' bone cycle, created in prostate cancer bone metastases, helps nullify the bone resorption process.

The links between OPG and RANK and their roles in bone turnover are well established. Since their discoveries in the late 1990's, the understanding of bone physiology has led to some major therapeutic interventions in several chronic orthopaedic and rheumatologic conditions, including rheumatoid arthritis and osteoporosis (Lacey *et al* 2012). However, despite the elucidation of their potential roles in several other cancers, particularly breast and melanoma, there remains poor understanding of the roles and mechanisms by which OPG and RANK can influence other osteotrophic cancer cell behaviour, particularly in the prostate. There are several articles in the literature which clinically link OPG and RANK to prostate cancer progression and the presence of bone metastases, however the potential mechanisms by which this occurs have yet to be fully explained, and therefore possible exploitation of these changes therapeutically has never been explored (Brown *et al* 2001, Corey *et al* 2002).

Despite the predominance of osteoblastic bone metastases in prostate cancer, few established osteoblastic models exist. One of the most common prostate cancer cell lines used for *in vitro* studies is the osteolytic PC-3 cell line. Given that it is predominantly castrate resistant cells which are associated with bone metastases, and that the cell line is derived from a metastatic bone site, it provided an interesting model to investigate the potential implications targeting OPG and RANK expression may have on prostate cancer cell behaviour.

Given previous observations that the aggressive osteolytic prostate cancer cell line PC-3 produces 10 fold more OPG than LNCaP cells (Holen *et al* 2002), we aimed to explore the potential implications targeting OPG and RANK expression might have on PC-3 cancer cell behaviour. This section of the study therefore aimed to establish if targeting OPG or RANK, using hammerhead ribozyme transgenes, influenced PC-3 prostate cancer cell behaviour *in vitro*. Subsequently, this section also aimed to explore the potential effects treatment with exogenous HGF or BME might further impose on the manipulated cancer cell behaviour.

4.2 Materials and Methods

4.2.1 Cell line

In this study, the PC-3 prostate cancer cell line was used to generate empty plasmid control cells (PC-3^{pEF6}) and transfectants for either OPG or RANK knockdown (PC-3^{OPGKD}, PC-3^{RANKKD}). Cells were maintained in DMEM medium supplemented with 10% FCS and ABS as described previously (Section 2.6.1). All transfectants were initially exposed to selection medium (DMEM complete medium supplemented with 5µg/ml Blasticidin S) for 10 days. All transfectants were subsequently maintained in DMEM complete medium supplemented with 0.5µg/ml Blasticidin S, to ensure the plasmid vector was retained.

All *in vitro* function assays were conducted in Blasticidin S free medium.

4.2.2 Treatment(s)

Transfectants were treated with 40ng/ml HGF and/or 50µg/ml BME. For experimental purposes all treatments were prepared at a 2x concentrate and added in 100µl volumes in each *in vitro* function assay carried out.

4.2.3 Generation of OPG and RANK ribozyme transgenes, cloning into pEF6 plasmid vectors, PC-3 cell transfection and generation of stable transfectants

Hammerhead ribozymes targeting OPG and RANK were designed and generated as previously described in Section 2.9.1 and Table 2.4. Following verification of the touchdown PCR, OPG and RANK transgenes were cloned into pEF6 plasmid vectors and subsequently transformed into *E.coli* (Section 2.9.3 and 2.9.4). Correctly oriented constructs were then amplified, purified and verified (Section 2.9.5) before being transfected into PC-3 prostate cancer cells using electroporation (Section 2.9.6).

4.2.4 RNA isolation, cDNA synthesis, RT-PCR and qPCR

RNA isolation was carried out using the TRI reagent kit as described in Section 2.7 after which reverse transcription was completed using a high capacity RT kit (full details Section 2.7.3). Following RT-PCR, products were separated electrophoretically on an agarose gel and representative images, normalised against GAPDH, are shown. All qPCRs were performed and normalised against

GAPDH as described in Section 2.7.7. Data presented represents results from at least 3 independent repeats.

4.2.5 Protein isolation, SDS-PAGE, Western blotting and ICC

Protein lysates were isolated and quantified as described previously (Section 2.8). After SDS-PAGE, protein was transferred onto PVDF membrane and subsequently probed with specific primary antibody (anti-GAPDH, anti-OPG, anti-RANK) and corresponding peroxidase conjugated secondary antibodies (1:1000). Protein bands were visualised using the chemiluminescent protein detection kit. At least 3 independent repeats were carried out of which a representative image is shown.

4.2.6 *In vitro* cell proliferation assay

PC-3 transfectant(s) were seeded at $3x10^3$ cells/well into triplicate 96 well plates and incubated for 1, 3 and 5 days with treatments as described in Section 2.10.1. Following incubation, cells were fixed in 4% formalin (v/v) and stained with 0.5% crystal violet (v/v). Subsequently, crystal violet stain was extracted from the cells using 10% acetic acid (v/v) and the absorbance at 540nm was determined using a spectrophotometer. Data presented is mean percentage control of a minimum of 4 independent repeats with SEM.

4.2.7 *In vitro* cell Matrigel adhesion assay

A 96 well plate was coated with 5ug/well of Matrigel and left to dry as described in Section 2.10.2. PC-3 transfectant(s) were seeded at $4.5x10^4$ cells/well and left to adhere for 45 minutes before being fixed in 4% formalin (v/v) and stained with 0.5%

crystal violet (v/v). Four representative images were captured for each well and subsequently counted using Image J software. Data presented is mean percentage control of a minimum of 3 independent repeats with SEM.

4.2.8 *In vitro* cell migration assay

The cytodex bead motility assay was used to assess PC-3 cell motility (Section 2.10.3) where briefly, $1x10^6$ cells in 10ml were left to incubate with cytodex beads (100µl) overnight. The following day, cells were washed twice with fresh medium before being re-suspended in 1.5ml and added to a 96 well plate in triplicate (100µl/well) and the necessary treatments added. Cells were incubated for 4 hours after which the plate was washed, fixed in 4% formalin (v/v) and stained with 0.5% crystal violet (v/v). Four representative images were captured for each well and subsequently counted using Image J software. Data presented is the mean percentage control of a minimum of 3 independent repeats with SEM.

4.2.9 *In vitro* Matrigel cell invasion assay

Transwell inserts were coated with 50µg/insert of Matrigel and dried before PC-3 cell transfectants were seeded ($2x10^4$/100µl) into each insert and incubated for 3 days with respective treatments (100µl), as described in Section 2.10.4. Following incubation, invaded cells were fixed in 4% formalin (v/v) and stained with 0.5% crystal violet (v/v). Five representative images were captured per transwell insert and subsequently counted using Image J software. Data presented is the mean percentage control of a minimum of 3 independent repeats with SEM.

4.3 Results

4.3.1 Role of OPG in PC-3 Prostate Cancer Cells in vitro

4.3.1.1 Confirmation of ribozyme transgene knockdown of OPG expression in PC-3 prostate cells

Expression of OPG was successfully targeted in PC-3 prostate cancer cells following transfection with an anti-OPG ribozyme transgene contained within a pEF6 plasmid. Following RNA isolation, RT-PCR and qPCR showed significantly reduced OPG transcript expression in PC-3^{OPGKD} cells compared to the PC-3^{pEF6} control cells (Figures 4.1 A and B respectively). Western blot subsequently confirmed the knockdown of OPG at a protein level in comparison to the PC-3^{pEF6} cells (Figures 4.1 C).

4.3.1.2 OPG suppression enhances PC-3 cell proliferation

Reduced OPG expression in PC-3 prostate cancer cells resulted in increased cell proliferation after 3 days incubation (232% compared to control) (Figure 4.2A) and significantly so after 5 days incubation (205% compared to control) (Figure 4.2 B, $p=0.008$) compared to the control PC-3^{pEF6} cells.

The impact of reduced OPG expression in PC-3 prostate cancer cells was further examined following treatment with 40ng/ml HGF, 50µg/ml BME or a combination of 40ng/ml HGF and 50µg/ml BME. In the PC-3^{pEF6} control cells, treatment with 40ng/ml HGF, 50µg/ml BME or a combination of 40ng/ml HGF and 50µg/ml BME all resulted in increases in PC-3^{pEF6} cell proliferation, after both 3 day incubation (112%, 132% and 132% of untreated control respectively) (Figure 4.2 C) and 5 days incubation (122%, 136% and 139% of untreated control respectively) (Figure 4.2 D). Treatment of PC-3^{pEF6} cells with 50µg/ml BME reached significant levels after 3 days

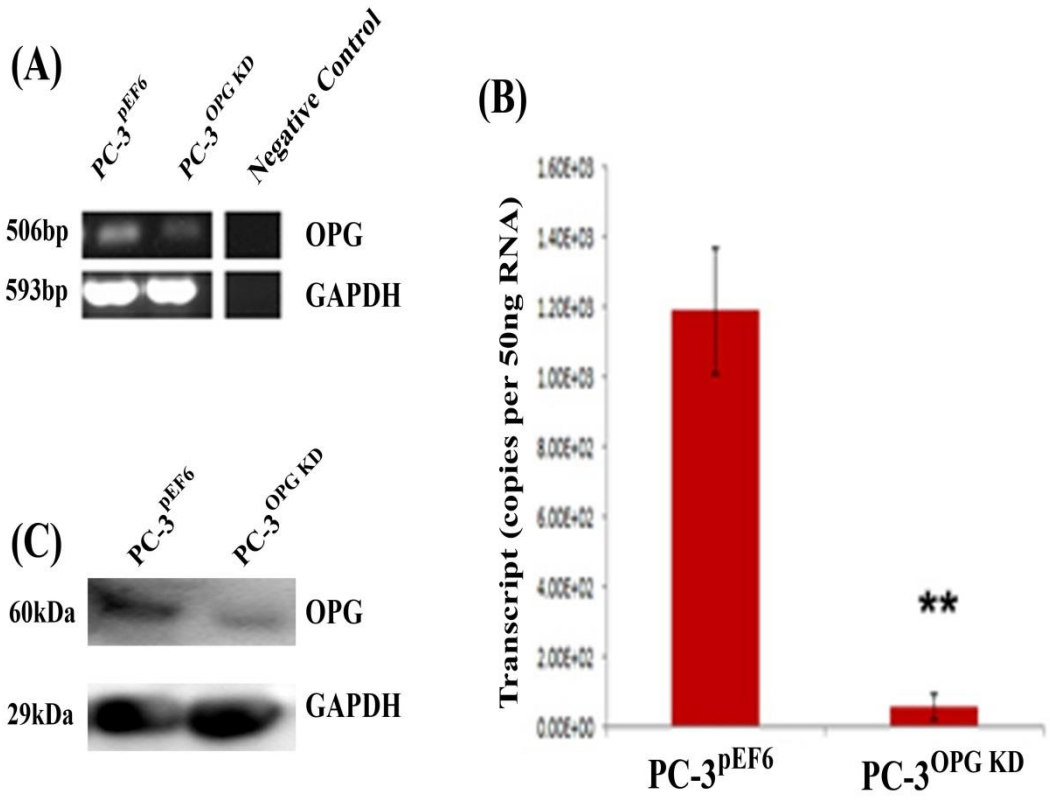

Figure 4.1: Verification of ribozyme transgene knockdown of OPG in PC-3 cells

Reduced expression of OPG was confirmed at a transcript level using RT-PCR (A) and qPCR (B) compared to the control cell line. Western blot (C) was used to confirm knockdown of OPG at a protein level. PCR and Western blot were normalised against GAPDH. Control = Nuclease free water and all gels were ran with a molecular weight marker used to identify band sizes. Representative images and data shown. * - p=<0.05, ** - p=<0.01 and *** - p=<0.001.

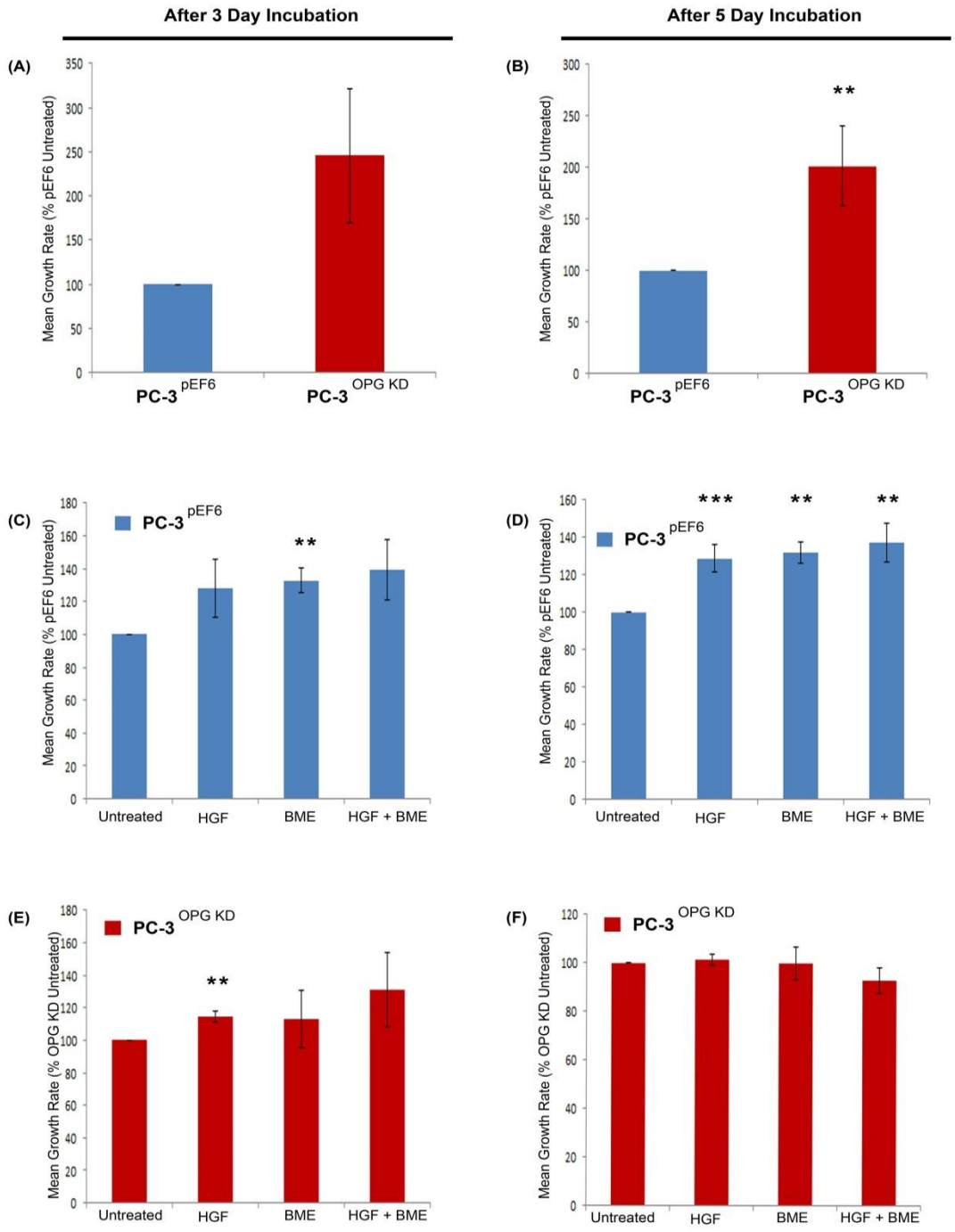

Figure 4.2: Impact of OPG knockdown on PC-3 cell proliferation in v*itro*
Reduced OPG expression resulted in increased PC-3 cell proliferation after 3 days (A) and 5 days incubation (B) compared to control cells. Treatment of the PC-3^{pEF6} control cell line with 40ng/ml HGF, 50µg/ml BME or a combination of 40ng/ml HGF and 50µg/ml BME resulted in an increase in cell proliferation after 3 days incubation, the BME treatment resulted in a significant increase in cell proliferation (C), all other treatments reached significant levels after 5 days incubation in comparison to untreated PC-3 ^{pEF6} cells (D). Treatment of PC-3^{OPGKD} cells with 40ng/ml HGF, 50µg/ml BME or a combination of 40ng/ml HGF and 50µg/ml BME resulted in further increases in cell proliferation after 3 days (E) which were not seen after 5 days (F). Data represents mean of 5 independent repeats, error bars represent SEM. * - p=<0.05, ** - p=<0.01 and *** - p=<0.001.

incubation (p=0.008 vs untreated PC-3^{pEF6} control cells) and this trend was maintained after 5 days incubation (p=<0.001 vs untreated PC-3^{pEF6} control cells). Treatments with 40ng/ml HGF or combined 40ng/ml HGF and 50µg/ml BME did not result in significant increases in PC-3^{pEF6} cell proliferation until 5 days incubation (p=0.004 and 0.008 respectively vs untreated PC-3^{pEF6} control cells). Similar patterns of cell proliferation were seen in PC-3^{OPGKD} under treatment with 40ng/ml HGF, 50µg/ml BME or a combination of 40ng/ml HGF and 50µg/ml BME, all of which appeared to initially further enhance cell proliferation. After 3 days incubation (Figure 4.2 E), the effect of 40ng/ml HGF treatment, resulted in an increase in PC-3^{OPGKD} cell proliferation which reached significance (114% of untreated PC-3^{OPGKD} cells, p=0.001). However, after 5 days incubation, treatments with 40ng/ml HGF, 50µg/ml BME or a combination of 40ng/ml HGF and 50µg/ml BME were not found to have any significant effects and the initial increases in PC-3^{OPGKD} cell proliferation following treatment appeared to have been negated (99%, 100% and 92% of untreated PC-3^{OPGKD} cells). Under the influence of the combined 40ng/ml HGF and 50µg/ml BME treatment, PC-3^{OPGKD} cell proliferation decreased in comparison to the untreated cells, though this trend was not significant (change of less than 10%) (Figure 4.2 F).

4.3.1.3 Exogenous stimuli can influence cell-matrix adhesion of PC-3^{OPGKD} cells

Reduced OPG expression in PC-3 prostate cancer cells appeared to have little impact on cell-matrix adhesion *in vitro* compared to the PC-3^{pEF6} control cells (less than 5% change from control) (Figure 4.3 A).

Treatment of PC-3^{pEF6} control cells with 40ng/ml HGF appeared to marginally reduce cell-matrix adhesion (less than 5% of control), whilst treatment with 50µg/ml

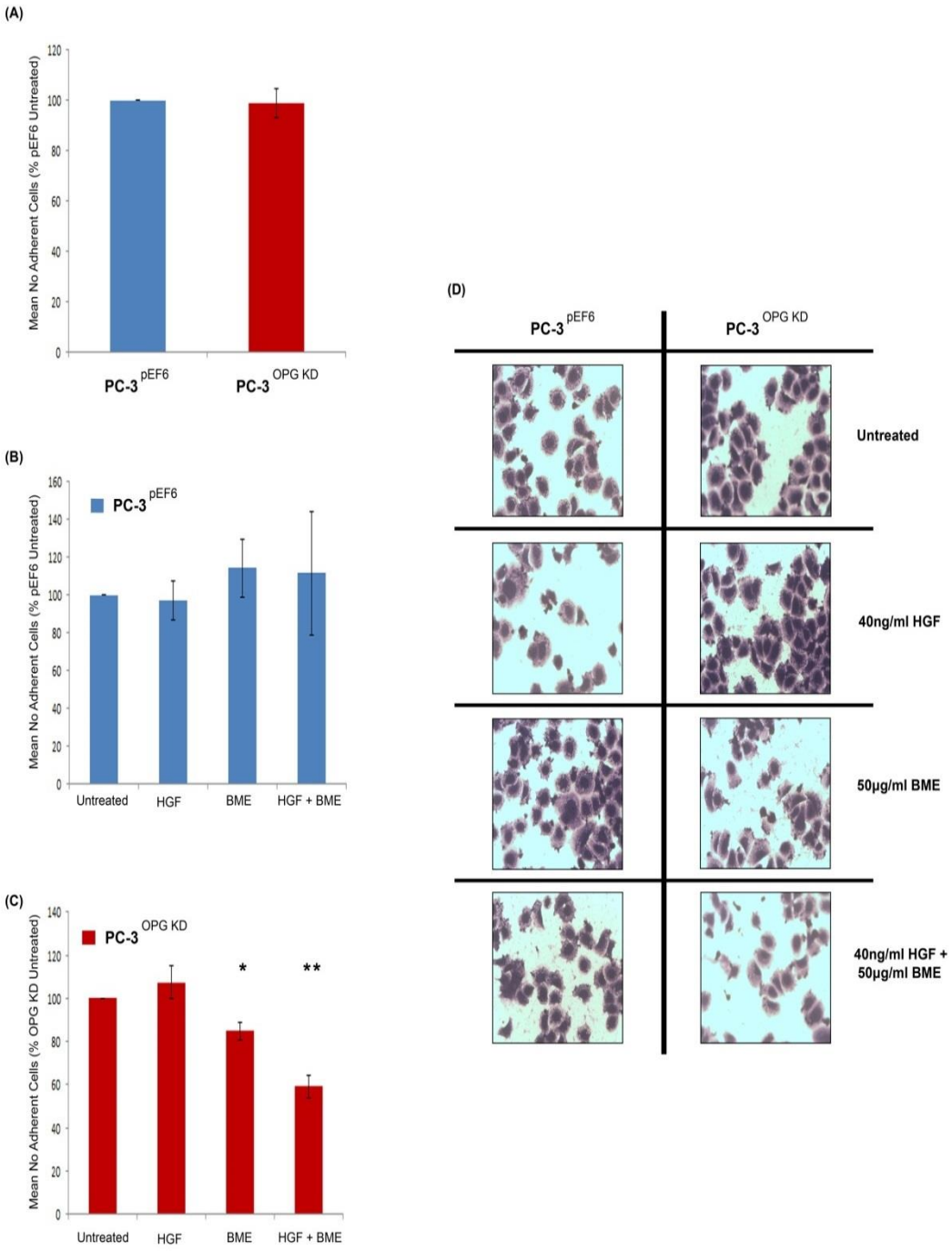

Figure 4.3: Impact of reduced OPG expression in PC-3 cells on cell-matrix adhesion *in vitro*

Reduced OPG expression resulted in no noticeable effect on PC-3 cell-matrix adhesion compared with control cells (A). When PC-3^{pEF6} control cells were treated with 50µg/ml BME or 50µg/ml BME and 40ng/ml HGF small increases in cell-matrix adhesion were seen (B), however 40ng/ml HGF resulted in no notable change in cell-matrix adhesion. In the PC-3^{OPGKD} cells treated with 40ng/ml HGF cell-matrix adhesion increased, however under 50µg/ml BME or combined HGF and BME treatment cell matrix adhesion decreased (C). Representative images from one repeat (D). Data represents mean of a minimum 3 independent repeats, error bars represent SEM. * - p=<0.05, ** - p=<0.01 and *** - p=<0.001.

BME or combined treatment of 40ng/ml HGF and 50µg/ml BME increased cell-matrix adhesion compared to the untreated PC-3^{pEF6} control cells, these trends were not significant (114% and 111% change from untreated control respectively) (Figure 4.3 B). When PC-3^{OPGKD} cells were treated with 40ng/ml HGF, a slight increase in cell-matrix adhesion was observed compared to the untreated PC-3^{OPGKD} cells (107% of untreated control), however as in the PC-3^{pEF6} cells this change was not significant. Interestingly, when PC-3^{OPGKD} cells were treated with 50µg/ml BME a significant decrease in cell-matrix adhesion was observed (84% of untreated control) (Figure 4.3 C, p=0.031). Of greater interest was the observation that under the combined treatment of 40ng/ml HGF and 50µ/ml BME an even greater reduction in cell-matrix adhesion was seen compared to the untreated PC-3^{OPGKD} cells (59% of untreated control, p=0.003). Representative images for these changes are shown in Figure 4.3 D.

4.3.1.4 Effect of OPG suppression on PC-3 prostate cell motility

Knockdown of OPG in PC-3 cells appeared to produce a non-significant decrease in cell motility compared to the PC-3^{pEF6} control cells (less than 5% decrease compared to control) as shown in the representative images (Figure 4.4 A and 4.4 D respectively).

When PC-3^{pEF6} control cells were treated with 40ng/ml HGF, 50µg/ml BME or a combination of 40ng/ml HGF and 50µg/ml BME, PC-3 cell motility from the cytodex beads was increased compared to the untreated PC-3^{pEF6} control cells (134%, 149% and 181% compared to untreated control respectively) (Figure 4.4 B). Though none of these changes in motility reached significance, the 40ng/ml HGF treatment was close to the threshold (p=0.081).

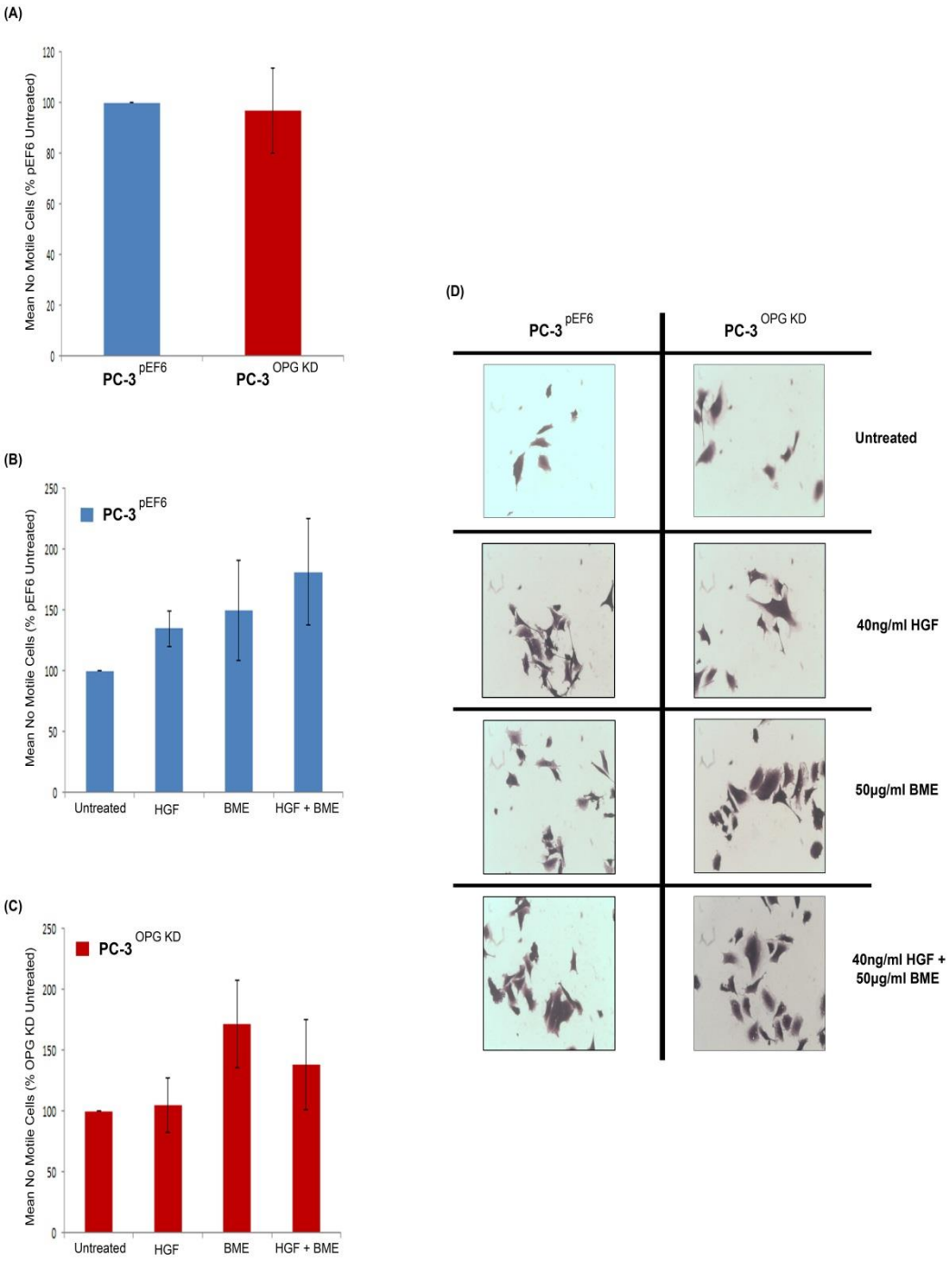

Figure 4.4: Effect of OPG knockdown on PC-3 cell motility
PC-3^{OPGKD} cells showed no noticeable changes in motility compared with PC-3^{pEF6} control cells (A). Treatment of PC-3^{pEF6} control cells with 40ng/ml HGF, 50µg/ml BME or a combination of 40ng/ml HGF and 50µg/ml BME increased cell motility (B). Treatment of PC-3^{OPGKD} cells with 40ng/ml HGF appeared to have no effect on cell motility (C). However, treatment with 50µg/ml BME or 40ng/ml HGF and 50µg/ml BME resulted in an increase in cell motility. Representative images from one repeat (D). Data represents mean of 3 independent repeats, error bars represent SEM. * - p=<0.05, ** - p=<0.01 and *** - p=<0.001.

The same effect was not seen when PC-3^{OPGKD} cells were treated with 40ng/ml HGF, there appeared to be no notable additional response to HGF in these cells (less than 5% increase compared to untreated control) (Figure 4.4 C). Interestingly, the 50µg/ml BME treatment appeared to increase PC-3^{OPGKD} cell motility compared to the untreated PC-3^{OPGKD} cells, a change which almost reached significance (172% compared to untreated control, p=0.084). The combined treatment of 40ng/ml HGF and 50µg/ml BME also resulted in an increase in PC-3^{OPGKD} cells (138% of untreated control); however this was not as notable as the individual 50µg/ml BME treatment. Representative images of these trends are shown in Figure 4.4 D.

4.3.1.5 OPG suppression significantly increases PC-3 cell invasion

Suppression of OPG in PC-3 prostate cancer cells resulted in a significant increase in *in vitro* cell invasion compared to PC-3^{pEF6} control cells (Figure 4.5 A, 210% compared to control, p=0.02).

When PC-3^{pEF6} control cells were treated with 40ng/ml HGF a significant increase in PC-3 cell invasion was observed (Figure 4.5 B, 117% of untreated control, p=0.02). The 50µg/ml BME treatment resulted in a negligible increase in PC-3^{pEF6} control cell invasion however; this trend was not significant (106% of untreated control). When 40ng/ml HGF and 50µg/ml BME treatments were combined, PC-3^{pEF6} control cell invasion was generally decreased compared to the untreated control cells (81% of untreated control), though this did not reach significance (Figure 4.5 B).

In contrast to the PC-3^{pEF6} control cell response to 40ng/ml HGF treatment, PC-3^{OPGKD} cells, when treated with 40ng/ml HGF, resulted in a decrease in cell invasion, a trend which was very close to significance (Figure 4.5 C, 81% of untreated control,

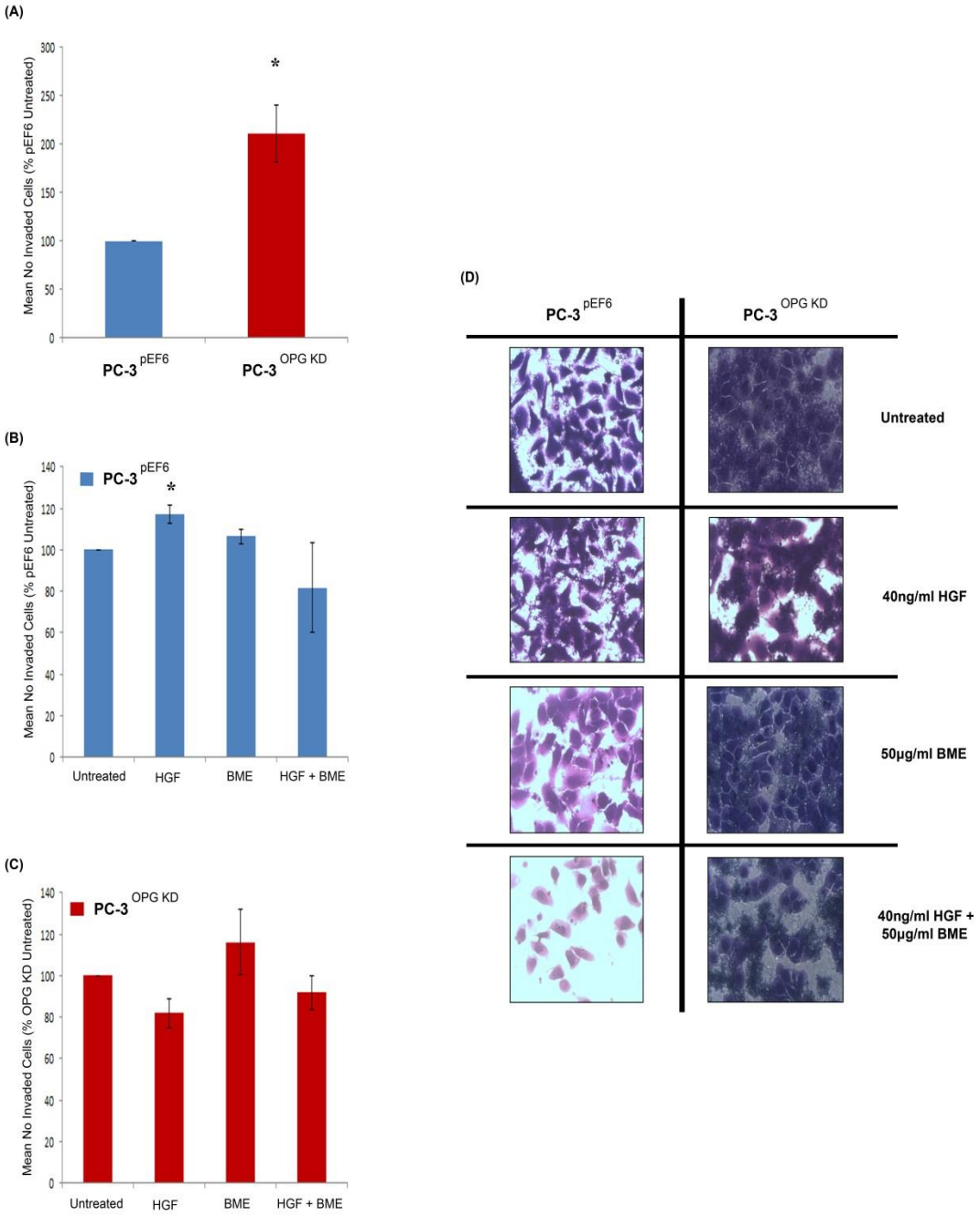

Figure 4.5: Impact of reduced OPG expression on PC-3 cell invasion *in vitro*

PC-3^{OPGKD} cells showed significantly increased cell invasion compared with PC-3^{pEF6} control cells (A). Treatment of PC-3^{pEF6} control cells with 40ng/ml HGF or 50µg/ml BME increased cell invasion, HGF significantly so, but a combination of 40ng/ml HGF and 50µg/ml BME resulted in a general decrease in cell invasion in comparison to untreated PC-3^{pEF6} control cells (B). Treatment of PC-3^{OPGKD} cells with 40ng/ml HGF or combined 40ng/ml HGF and 50µg/ml BME resulted in a decrease in cell invasion (C). Treatment with 50µg/ml BME resulted in an increase in cell invasion. None of these effects were found to be significant. Representative images from one repeat (D). Data represents mean of 3 independent repeats, error bars represent SEM. * - p=<0.05, ** - p=<0.01 and *** - p=<0.001.

p=0.065). Treatment of PC-3^{OPGKD} cells with 50µg/ml BME resulted in an increase in cell invasion, however this enhancement in invasion was slight and did not reach significance (116% of untreated control). Surprisingly, when 40ng/ml HGF and 50µg/ml BME were combined, PC-3^{OPGKD} cells appeared to show a reduced invasive ability compared to untreated PC-3^{OPGKD} cells (91% of untreated control), however, this was less notable than that which had been observed under the individual 40ng/ml HGF treatment.

4.3.2 Role of RANK in PC-3 Prostate Cancer Cells in vitro

4.3.2.1 Confirmation of ribozyme transgene knockdown of RANK expression in PC-3 prostate cells

Expression of RANK was successfully targeted in PC-3 prostate cancer cells following transfection with an anti-RANK ribozyme transgene contained within a pEF6 plasmid. Following RNA isolation, RT-PCR and qPCR showed significantly reduced RANK transcript expression in PC-3^{RANKKD} cells compared to the PC-3^{pEF6} control cells (Figures 4.6 A and B respectively). Western blot analysis subsequently confirmed the knockdown of RANK at a protein level in comparison to the PC-3^{pEF6} control cells (Figures 4.6 C).

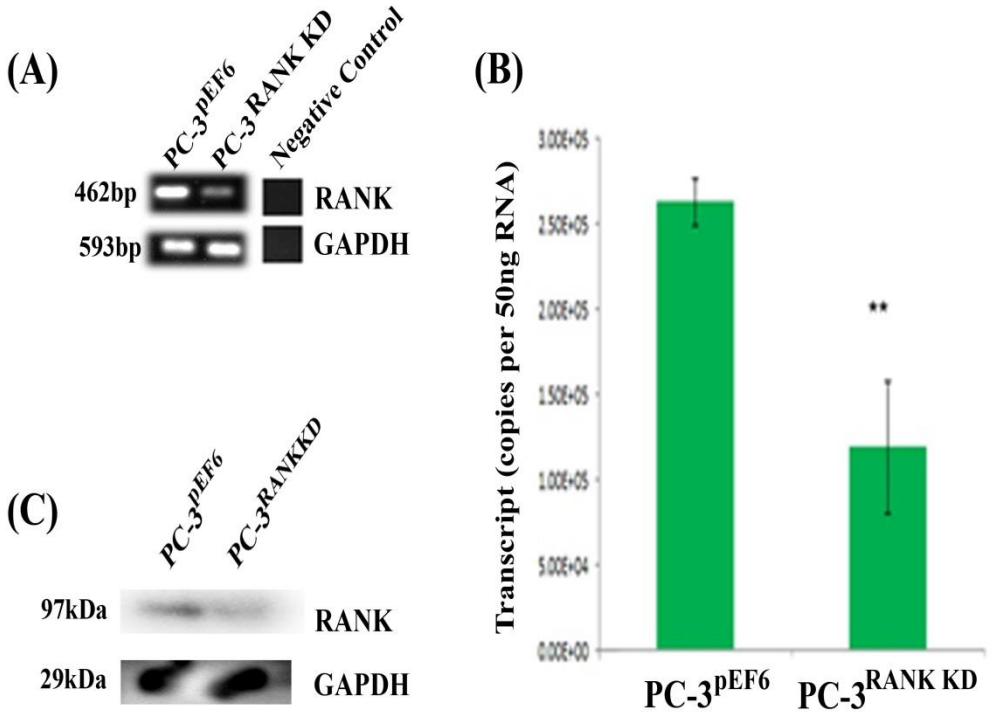

Figure 4.6: Verification of successful ribozyme transgene knockdown of RANK expression in PC-3 cells

Reduced expression of RANK was confirmed at a transcript level using RT-PCR (A) and qPCR (B) compared to the control cell line. Western blot (C) was used to confirm knockdown of RANK at a protein level. PCR and Western blot were normalised against GAPDH. Control = Nuclease free water and all gels were ran with a molecular weight marker used to identify band sizes. Representative images and data shown. * - p=<0.05, ** - p=<0.01 and *** - p=<0.001.

4.3.2.2 RANK suppression enhances PC-3 cell proliferation

Suppression of RANK expression significantly enhanced PC-3 prostate cancer cell proliferation after 3 days incubation (Figure 4.7 A, 166% compared to control, p=0.008) and after 5 days incubation (Figure 4.7 B, 124% compared to control, p=0.008) compared to PC-3^{pEF6} control cells.

Treatment of PC-3^{pEF6} control cells with 40ng/ml HGF, 50µg/ml BME or combined 40ng/ml HGF and 50µg/ml BME resulted in increases in PC-3^{pEF6} control cell proliferation compared to untreated cells after 3 days incubation (112%, 132% and 132% respectively of untreated control) (Figure 4.7 C) and 5 days incubation (122%, 136% and 139% respectively of untreated control) (Figure 4.7 D). The 50µg/ml BME treatment resulted in a significant increase in PC-3^{pEF6} control cell proliferation after 3 days incubation (p=0.008) which was maintained after 5 days incubation (p=<0.001). PC-3^{pEF6} control cell proliferation under the influence of treatment with 40ng/ml HGF or a combination of 40ng/ml HGF and 50µg/ml BME reached a significant level after 5 days incubation compared to the untreated PC-3^{pEF6} control cells (p=0.004 and 0.008 respectively).

When PC-3^{RANKKD} cells were incubated for 3 days with 40ng/ml HGF or 50µg/ml BME, no further increases in cell proliferation were observed, trends suggested very small insignificant decreases (97% and 94% of untreated control respectively) (Figure 4.7 E). The combined treatment of 40ng/ml HGF and 50µg/ml BME did result in a notable increase in cell proliferation after 3 days incubation (178% of untreated control); however, this did not reach a significant level. After 5 days incubation a slight increase in PC-3^{RANKKD} cell proliferation was observed in the 40ng/ml HGF treated cells however no difference was seen in the 50µg/ml BME treated PC-3^{RANKKD} cells compared to the untreated PC-3^{RANKKD} cells (110% and 103% of untreated control respectively) (Figure 4.7 F). However combined

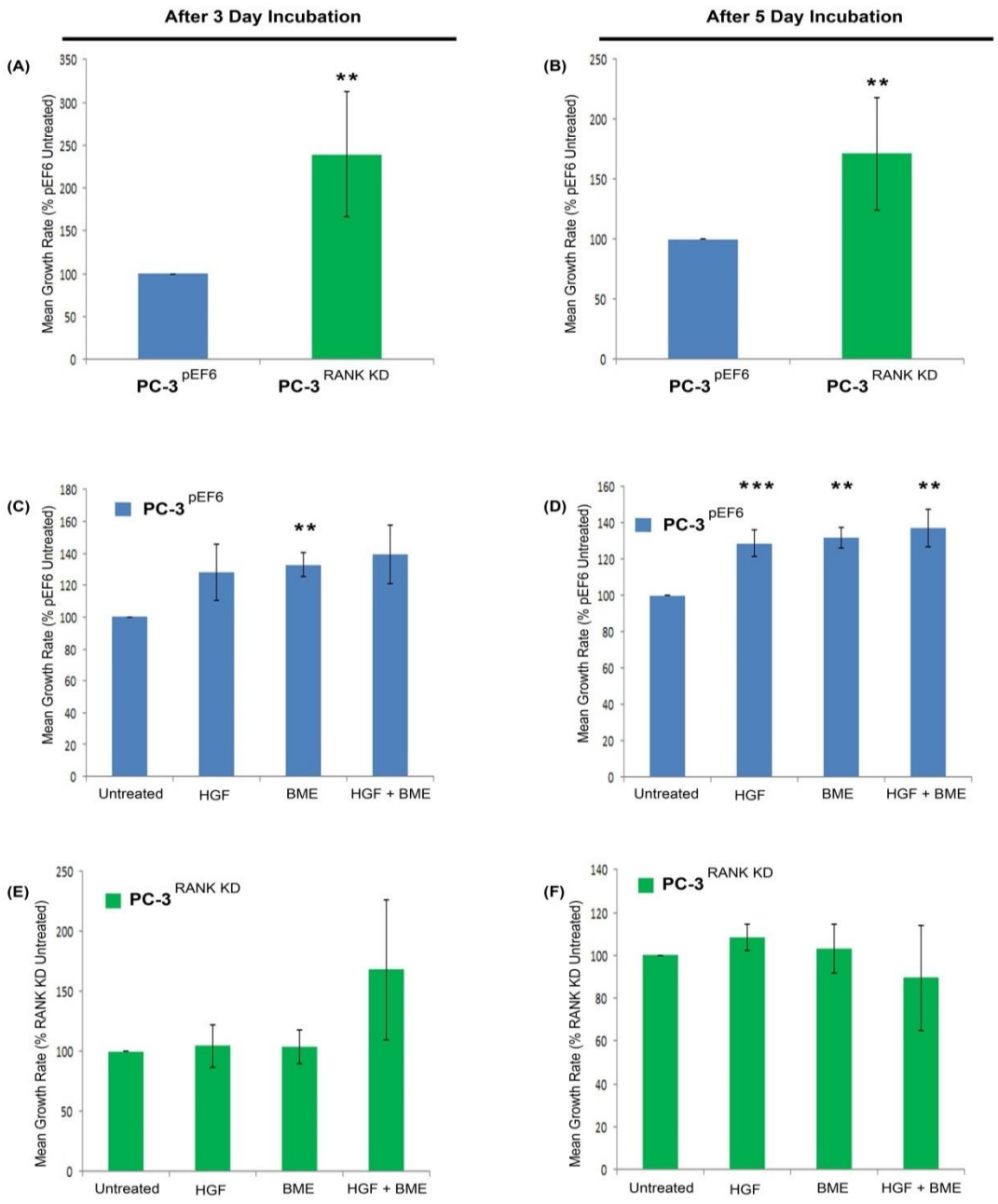

Figure 4.7: Effects of reduced RANK expression on PC-3 cell proliferation *in vitro*

Reduced RANK expression in PC-3 cells resulted in a significant increase in cell proliferation after 3 days (A) and 5 days incubation (B) compared with control cells. Treatment of the PC-3^{pEF6} control cell line with 40ng/ml HGF, 50µg/ml BME or a combination of 40ng/ml HGF and 50µg/ml BME resulted in an increase in cell proliferation after 3 days, the BME treatment significantly so (C) and 5 days incubation at which all treatments resulted in significant increases (D). Treatment of PC-3^{RANKKD} cells with 40ng/ml HGF or 50µg/ml BME resulted in negligible increases in cell proliferation over 3 and 5 day incubations (E and F respectively). A combination of 40ng/ml HGF and 50µg/ml BME resulted in an increase in cell proliferation after 3 days incubation (E), however this trend was not maintained over a 5 day incubation period (F). Data represents mean of 5 independent repeats, error bars represent SEM. * - p=<0.05, ** - p=<0.01 and *** - p=<0.001.

treatment with 40ng/ml HGF and 50µg/ml BME resulted in a slight decrease in PC-3^{RANKKD} cell proliferation compared to the untreated PC-3^{RANKKD} cells though again this did not reach significance (88% of untreated control).

4.3.2.3 RANK suppression enhances cell-matrix adhesion in PC-3 prostate cancer cells

Suppression of RANK expression in PC-3 prostate cancer cells significantly increased cell-matrix adhesion compared to PC-3^{pEF6} control cells (Figure 4.8 A, 171% of control, p=0.02).

Treatment of PC-3^{pEF6} control cells with 40ng/ml HGF, 50µg/ml BME or a combination of 40ng/ml HGF and 50µg/ml BME all resulted in increases in cell-matrix adhesion (119%, 144% and 143% of untreated control respectively); however none of these changes were deemed significant (Figure 4.8 B).

Cell-matrix adhesion in the PC-3^{RANKKD} cells was further increased following treatment with 40ng/ml HGF (119% of untreated control), however, this did not reach significance compared to the untreated PC-3^{RANKKD} cells. In contrast, when PC-3^{RANKKD} cells were treated with 50µg/ml BME there appeared to be no further impact on PC-3 cell-matrix adhesion (103% of untreated control). When PC-3^{RANKKD} cells were treated with 40ng/ml HGF and 50µg/ml BME cell-matrix adhesion was reduced compared to the untreated PC-3^{RANKKD} cells (93% of untreated control) however again this change did not reach significance (Figure 4.8 C). Representative images are shown in Figure 4.8 D.

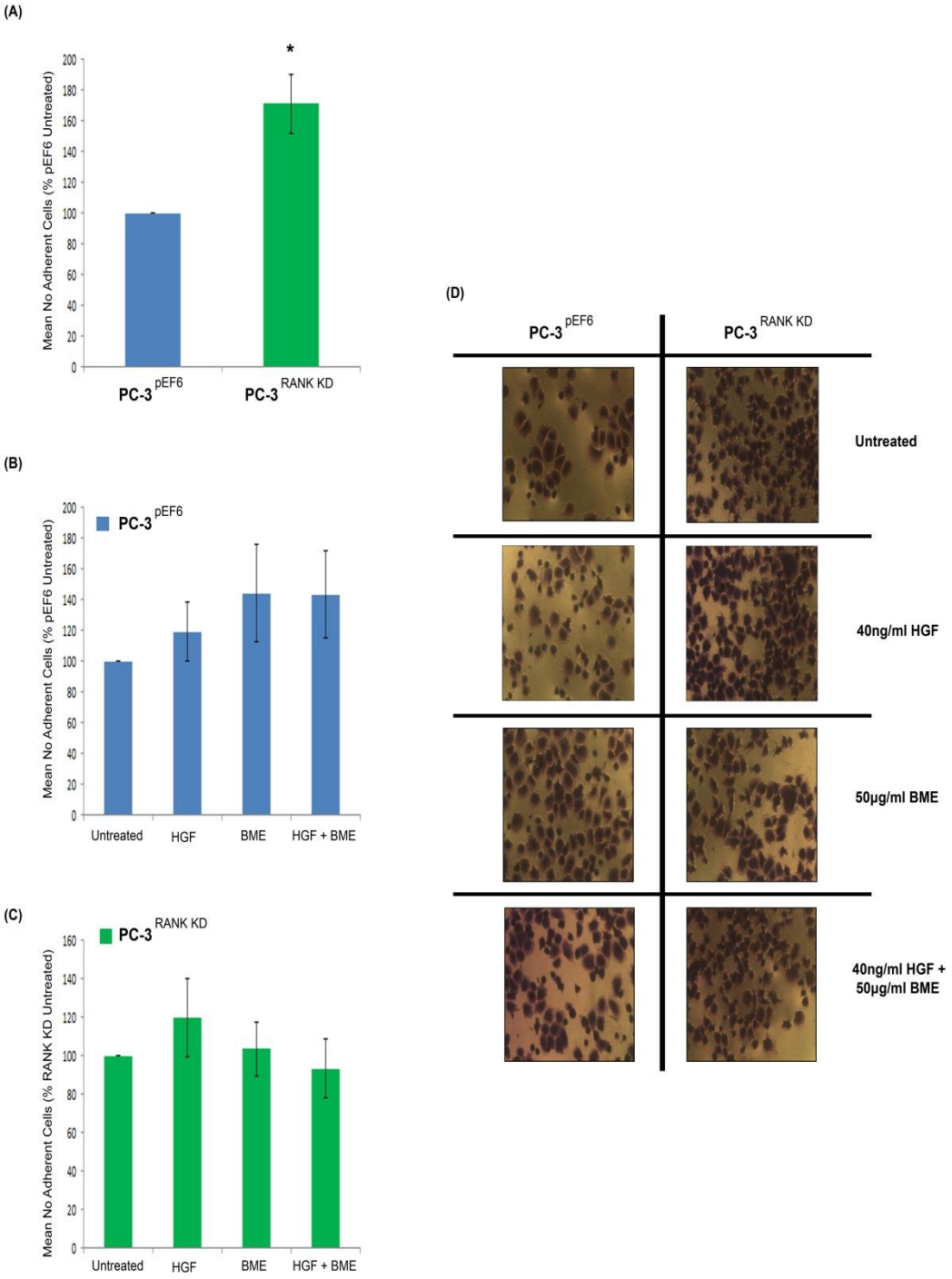

Figure 4.8: Effect of RANK knockdown on cell-matrix adhesion in PC-3 cells *in vitro*

Reduced RANK expression resulted in a significant increase in PC-3 cell-matrix adhesion compared with control cells (A). When PC-3^{pEF6} control cells were treated with 40ng/ml HGF or 50µg/ml BME or a combination of these treatments increases in cell-matrix adhesion were seen (B). PC-3^{RANKKD} cells treated with 40ng/ml HGF resulted in a further increase in cell-matrix adhesion. Treatment with 50µg/ml BME appeared to have little influence on PC-3^{RANKKD} cell-matrix adhesion. The combined HGF and BME treatment resulted in a small decrease in cell-matrix adhesion compared with untreated PC-3^{RANKKD} cells (C). Representative images from one repeat (D). Data represents mean of a minimum of 3 independent repeats, error bars represent SEM. * - p=<0.05, ** - p=<0.01 and *** - p=<0.001.

4.3.2.4 RANK suppression enhances PC-3 prostate cancer cell motility

The cytodex bead assay was used to quantify the impact RANK suppression had on PC-3 prostate cell motility. PC-3 cells with suppressed RANK expression exhibited increased cell motility compared to the PC-3^{pEF6} control cells (Figure 4.9 A, 206% of control). This increase almost reached a significant level (p=0.057).

The most notable change observed in the PC-3^{RANKKD} cells was how aggregated they appeared to be compared to the control PC-3^{pEF6} cells (Representative images shown in Figure 4.9 D). When PC-3^{pEF6} control cells were treated with 40ng/ml HGF, 50µg/ml BME or a combination of 40ng/ml HGF and 50µg/ml BME, PC-3 cell motility was increased compared to the untreated PC-3^{pEF6} control cells (136%, 164% and 185% of untreated control) (Figure 4.9 B), though none of these trends reached significance the 40ng/ml HGF treatment was close (p=0.057).

When RANK suppressed PC-3 cells were exposed to treatment with 40ng/ml HGF, PC-3 cell motility was further enhanced (131% of untreated control); however, this trend did not reach a significant level (Figure 4.9 C). When PC-3^{RANKKD} cells were treated with 50µg/ml BME or a combined treatment of 40ng/ml HGF and 50µg/ml BME, cell motility was increased though not significantly or as dramatically as had been observed under the 40ng/ml HGF treatment (112% and 106% of untreated control respectively).

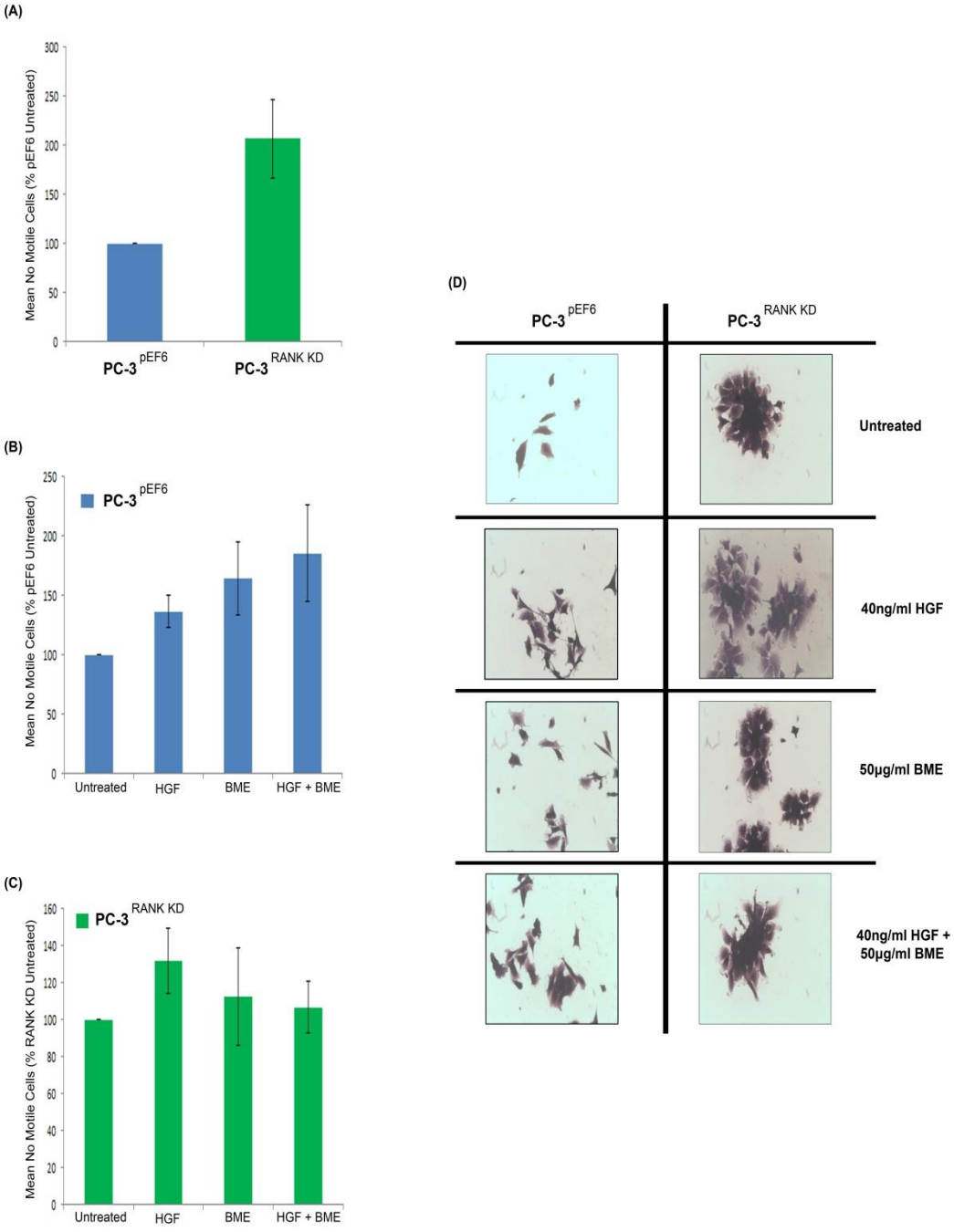

Figure 4.9: Effect of reduced RANK expression on PC-3 cell motility
Reduced RANK expression resulted in an increase in PC-3 cell motility compared to PC-3^{pEF6} control cells (A). PC-3^{pEF6} control cells treated with 40ng/ml HGF, 50µg/ml BME or a combination of 40ng/ml HGF and 50µg/ml BME resulted in increased cell motility (B). A similar response was observed when PC-3^{RANKKD} cells were treated with 40ng/ml HGF but not with 50µg/ml BME or a combination of 40ng/ml HGF and 50µg/ml BME (C). Representative images from one repeat (D). Data represents mean of a minimum of 3 independent repeats, error bars represent SEM. * - p=<0.05, ** - p=<0.01 and *** - p=<0.001.

4.3.2.5 RANK suppression enhances PC-3 prostate cell invasion

When RANK expression was reduced in PC-3 prostate cancer cells their *in vitro* invasive potential was increased (197% of control) (Figure 4.10 A), however this trend did not reach a significant level.

PC-3^{pEF6} control cells treated with 40ng/ml HGF showed a significant increase in cell invasion compared to the untreated cells (Figure 4.10 B, 117% of untreated control, p=0.02). The 50µg/ml BME treatment also resulted in a slight increase in PC-3^{pEF6} control cell invasion (106% of untreated control) however this did not reach significance. When 40ng/ml HGF and 50µg/ml BME were combined, PC-3^{pEF6} control cell invasion was decreased compared to the untreated control cells (81% of untreated control), though again this trend did not reach a significant level (Figure 4.10 B).

Treatment of PC-3^{RANKKD} cells with 40ng/ml HGF resulted in a small non-significant decrease in cell invasion (95% of untreated control) (Figure 4.10 C and representative images Figure 4.10 D). Treatment with 50µg/ml BME resulted in no change in PC-3^{RANKKD} cell invasion (101% of untreated control) and therefore did not reach significance. As was seen with the PC-3^{pEF6} control cells the combined treatment of 40ng/ml HGF and 50µg/ml BME reduced PC-3^{RANKKD} cell invasion compared to the untreated PC-3^{RANKKD} cells (76% of untreated control), though again this trend did not reach significance.

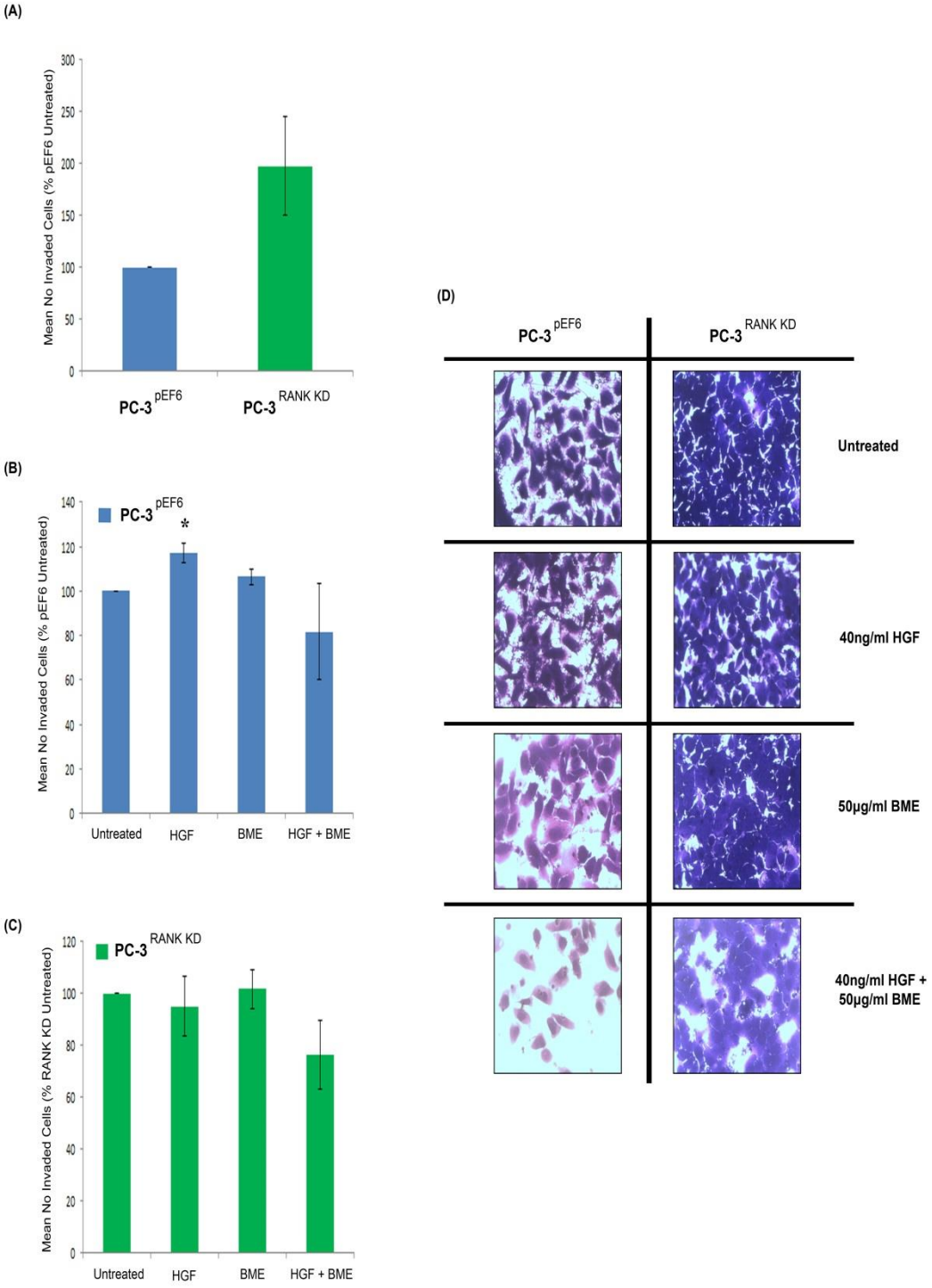

Figure 4.10: Effect of RANK knockdown on PC-3 cell invasion *in vitro*
PC-3^{RANKKD} cells showed increased cell invasion compared with PC-3^{pEF6} control cells (A). When PC-3^{pEF6} control cells were treated with 40ng/ml HGF or 50µg/ml BME cell invasion increased, under the influence of HGF significantly so, however the combined 40ng/ml HGF and 50µg/ml BME treatment decreased cell invasion (B). PC-3^{RANKKD} cells treated with 40ng/ml HGF or combined 40ng/ml HGF and 50µg/ml BME showed small decreases in cell invasion compared to untreated PC-3^{RANKKD} cells (C), however the 50µg/ml BME treatment resulted in a marginal increase in cell invasion. Representative images from one repeat (D). Data represents mean of a minimum of 3 independent repeats, error bars represent SEM. * - p=<0.05, ** - p=<0.01 and *** - p=<0.001.

4.4 Discussion

OPG and RANK are part of the TNFRSF and have been clinically implicated in prostate cancer progression, where increased transcript and protein levels have correlated with increasing tumour burden, metastatic bone involvement and androgen status. Elevated serum OPG levels have also been frequently reported in metastatic or relapsed prostate cancer patients. However, the potential explanations for these have never been well explored.

4.4.1 Effect of reduced OPG expression on PC-3 prostate cancer cell behaviour

The impact of targeting OPG was assessed using several *in vitro* function assays after successful knockdown of OPG using ribozyme transgenes. In the PC-3 cell line, reduced OPG expression resulted in increased cell proliferation after 3 days, a trend which reached significance after 5 days incubation. However, reduced OPG expression did not appear to have an impact on PC-3 cell matrix adhesion or motility *in vitro*. PC-3^{OPGKD} cells were also found to have significantly increased invasive properties. Therefore based on these observations it appears that OPG plays a role in PC-3 cell proliferation and invasion.

There is mixed evidence on the potential roles OPG may have in prostate tumour growth, though there is currently little doubt that it plays a role in prostate cancer progression and bone metastases. Therefore the current hypothesis remains that proposed by Corey *et al* (2005), that altered OPG expression may not be a direct causation factor in prostate cancer development, but it is one which may define the disease progression.

Brown *et al* (2001) have previously shown that OPG is detectable in normal prostate epithelium; however this expression is lost during primary prostate cancer. Of greater interest, it appeared that in the small cohort studied, the bone metastases associated with prostate cancer appeared to show re-established OPG expression. A further observation by Brown *et al* (2001) was that in the stained bone metastases sections OPG appeared to be co-localised to both the cell nucleus and the cytoplasm, suggesting there may be further alterations to OPG itself. In this study, though PC-3 cells are not a representative primary prostate cancer cell model, reducing OPG expression in these cells resulted in increased cell proliferation and cell invasion, both characteristics which are associated with cancer progression and metastases. Corey *et al* (2005) have speculated that loss of OPG itself may not have a direct impact on prostate cancer cell proliferation, but may affect other pathway(s) and molecules which in turn influence this particular cancer cell behaviour trait. This study might speculatively support this theory, since after 3 days incubation there was an increase in PC-3^{OPGKD} cell proliferation however this trend did not reach significance until after 5 days incubation. This trend might be as a result of alterations in other signalling cascades of which the net outcome may not be evident until after 5 days incubation.

Given the rich microenvironment which is associated with bone, it is possible that other factors, such as BMPs, are pivotal to disseminating prostate cancer cells settling in the bone. Brubaker *et al* (2003) have also previously demonstrated that OPG expression can be up-regulated in PC-3 cells by BMPs. The observations in this study, whereby reducing OPG expression in its own right promotes PC-3 cell proliferation is interesting in itself but, of further note is the observation that no further significant increase in this response was seen when cells were treated with 50µg/ml BME, as had been observed with the PC-3^{pEF6} control cell line. This again supports the idea that OPG may be pivotal to prostate cancer cells homing to the

bone therefore influencing disease progression, particularly bone metastases. This is potentially supported by results in this study, including the significantly reduced cell-matrix adhesion and greater (almost significant) motility which was observed in the PC-3^{OPGKD} cells treated with 50µg/ml BME.

The other main observation that may support this theory is the increased invasion which was seen in the PC-3^{OPGKD} cells. Though these cells are not the ideal model to explore the EMT process, it does support the idea that OPG may be important to the EMT process at the bone site. Though none of the subsequent treatments yielded significant results, the trends in themselves generate interest. It appeared that in PC-3^{OPGKD} cells under the influence of 40ng/ml HGF, cell invasion was decreased. This trend was very near to being a significant result ($p=0.065$) and was of particular interest as the change in response was from an increase to a decrease compared to the PC-3^{pEF6} control. Given the strong wealth of evidence that HGF is such a pleiotropic growth factor, more investigation is required to determine why this unexpected response has occurred. A further increase in PC-3^{OPGKD} cell invasion, under the 50µg/ml BME treatment was somewhat anticipated due to the potential restoration of some exogenous OPG, since the complete composition of the in-house bone mix (BME) has never been quantified. Therefore, this may, in an *in vitro* model, be one of the best ways of representing physiological conditions. Further work could focus on isolating the signalling pathway(s) in which these stimuli exert their effects.

4.4.2 Effect of reduced RANK expression on PC-3 prostate cancer cell behaviour

Reduced RANK expression was successfully achieved in PC-3 cells using ribozyme transgene. Reduced RANK expression resulted in significant increases in PC-3 cell

proliferation and cell-matrix adhesion. However, when PC-3^{RANKKD} cells were exposed to HGF or BME no further increases in cell proliferation were seen, unlike those which were seen in the PC-3^{pEF6} control cells. In contrast, PC-3^{RANKKD} cells under the influence of HGF appeared to have further enhanced cell-matrix adhesion, a pattern which was not mirrored under the influence of BME. Though increases were seen in both PC-3^{RANKKD} cell motility and invasion compared to the PC-3^{pEF6} control cells, these trends did not reach a statistically significant level. These findings agree with data from Casimiro *et al* (2013), who showed that knocking down RANK using siRNA inhibited RANKL induced JNK phosphorylation. Despite this it was interesting to observe that the PC-3^{RANKKD} cells appeared to be more aggregated during the motility assay compared to the PC-3^{pEF6} control cells, though more investigation is needed to understand this observation.

Much of the previous work studying the role of RANK in PC-3 prostate cancer cells has focused on its interaction with stromal RANKL (Armstrong *et al* 2008). This has led many to hypothesise that the rich soil of RANKL in the bone microenvironment attracts RANK expressing tumour cells (Armstrong *et al* 2008). In the current study, though reduced RANK expression in the PC-3 cells did result in enhanced tumourigenic behaviour *in vitro*, when these cells were exposed to a bone like environment (BME), no further effect was seen, suggesting that RANK expression may also be integral to the bone homing phenotype associated with prostate cancer cells. In this study, by targeting RANK expression in PC-3 cells, interesting increases in tumourigenic cell behaviour were seen. This poses the question of what advantageous influence RANK expression might also have on prostate cancer itself? This appears particularly apt given the aggregated appearance which was observed in the motility assay. Further work might focus on looking at several surface markers which may affect such cell behaviour.

Chapter 5

Role of OPG and RANKL in mixed osseous prostate cancer

5.1 Introduction

In the unravelling of the complex interactions which occur between prostate cancer cells and the bone environment, *in vitro* and *in vivo* studies have highlighted the roles of both direct and indirect interactions which contribute to prostate cancer progression (Blaszczyk *et al* 2004, Dai *et al* 2004, Dai *et al* 2005, Bryden *et al* 2002a). However it remains unclear if disseminating prostate cancer cells already possess osteomimetic properties or if molecular characteristics are induced by factors in the bone microenvironment which allow the disseminated cancer cells to colonise and invade into the bone. Androgen ablation therapy, the mainstay of current prostate cancer therapy, has been associated with increased risk of osteoporosis, decreased bone mineral density and increased bone resorption (Orwoll and Klein 1995). This coupled with *in vitro* evidence that androgens play a role in the regulation of pro- and anti- resorptive bone factors, further highlights some of the clinical challenges in this area (Bellido *et al* 1995, Hofbauer and Khosla 1999, Hofbauer *et al* 2004, Pederson *et al* 1999).

There have been several *in vivo* studies which have shown that the mildly tumourigenic prostate cancer cell line LNCaP, can acquire androgen independence and progress to develop a mixed osseous phenotype metastasis, therefore providing a more representative experimental model of metastatic prostate cancer disease progression (Wu *et al* 1994, Thalmann *et al* 1994, Gleave *et al* 1991, Thalmann *et al* 2000). In agreement with the literature, it has been previously shown in this study (Figure 3.1) that the majority of prostate cancer cell lines strongly express OPG but the androgen dependent LNCaP cell line only weakly expresses OPG (Penno *et al* 2002, Holen *et al* 2002).

This section of the study aimed to investigate the impact of treating LNCaP cells with rhOPG and/or nRANKL had on prostate cancer cell behaviour *in vitro*, before

subsequently investigating the potential roles HGF and/or BME may have in enhancing or negating these responses. Based on our LNCaP cell line observations and given the secreted nature of OPG, a recombinant protein form was purchased after initial efforts to produce a stable expression model proved problematic. Generation of reduced RANKL expression in LNCaP cells was also unsuccessful and, given the time sensitivity of this study, the recently licensed neutralising RANKL antibody, Denosumab, was also subsequently purchased.

5.2 Materials and Methods

5.2.1 Cell line

The LNCaP (FGC clone) cell line was purchased from the ATCC and was maintained in RPMI 1640 medium supplemented with 10% FCS and ABS as described in Section 2.6.

5.2.2 Treatments

Denosumab was sourced from Amgen Limited, recombinant human OPG was sourced from PeproTech. LNCaP cells throughout this section were treated with 25ng/ml rhOPG and/or 100ng/ml nRANKL, 40ng/ml HGF and/or 50µg/ml BME. All treatments were prepared initially at a 4x concentrate and added to each experiment in 50µl volumes.

5.2.3 *In vitro* cell proliferation assay

LNCaP cells were seeded at $3x10^3$/well in triplicate 96 well plates and incubated for 1, 3 and 5 days respectively as described in Section 2.10.1. Following incubation, cells were fixed in 4% formalin (v/v) and stained with 0.5% crystal violet (v/v). Subsequently, crystal violet stain was extracted from the cells using 10% acetic acid (v/v) and the absorbance at 540nm was determined using a spectrophotometer. Data presented is mean percentage control of a minimum of 4 independent repeats with SEM.

5.2.4 *In vitro* cell Matrigel adhesion assay

A 96 well plate was coated with 5µg/well of Matrigel and left to dry as described in Section 2.10.2. Then $4.5x10^4$ LNCaP cells/well with respective treatments (final volume 200µl) were left to adhere for 45 minutes before being fixed in 4% formalin (v/v) and stained with 0.5% crystal violet (v/v). Four representative images were captured for each well and subsequently counted using Image J software. Data presented is mean percentage control of a minimum of 3 independent repeats with SEM.

5.2.5 *In vitro* cell migration assay

For the LNCaP cell line, the cytodex bead assay was considered to be inappropriate to analyse cell motility as $LNCaP^{WT}$ cells did not migrate from the cytodex beads within the 4 hour incubation period thus being unquantifiable. Therefore an alternative method was found. Due to the number of treatments required, the traditional scratch-wounding assay was considered to be too time consuming. Fortunately, in the laboratory, the ECIS system was available.

$8x10^4$ LNCaP cells were seeded with/without treatment and left to form a monolayer and the resistance to plateau prior to wounding as described in Section 2.10.3. The resistance at 4KHz was recorded for 4 hours after wounding.

5.2.6 *In vitro* Matrigel cell invasion assay

Transwell inserts were coated with 50µg/insert of Matrigel and dried before $3x10^4$ cells/50µl were seeded into each insert and incubated for 3 days with respective treatments (Final volume 200µl), as described in Section 2.10.4. Following incubation, cells were fixed in 4% formalin (v/v) and stained with 0.5% crystal violet (v/v). Five representative images were captured per transwell insert and subsequently counted using Image J software. Data presented is the mean percentage control of 3 independent repeats with SEM.

5.3 Results

5.3.1 The effect of exogenous rhOPG and nRANKL on LNCaP cell proliferation at different concentrations

From the initial prostate cancer cDNA screen (Figure 3.1), LNCaP cells showed very weak expression of OPG but were one of the few cell lines exhibiting RANKL expression. After sourcing rhOPG and nRANKL and carrying out a literature search, cytotoxicity assays were conducted analysing LNCaP cell proliferation at a range of concentrations (Figure 5.1). After 3 days incubation with each of the individual concentrations of rhOPG, no notable cytotoxic effects were observed (Figure 5.1 A). After 5 days incubation, though no significant cytotoxic effects on LNCaP cells were seen, at the highest concentration (500ng/ml) a drop off in cell proliferation was observed (Figure 5.1 B).

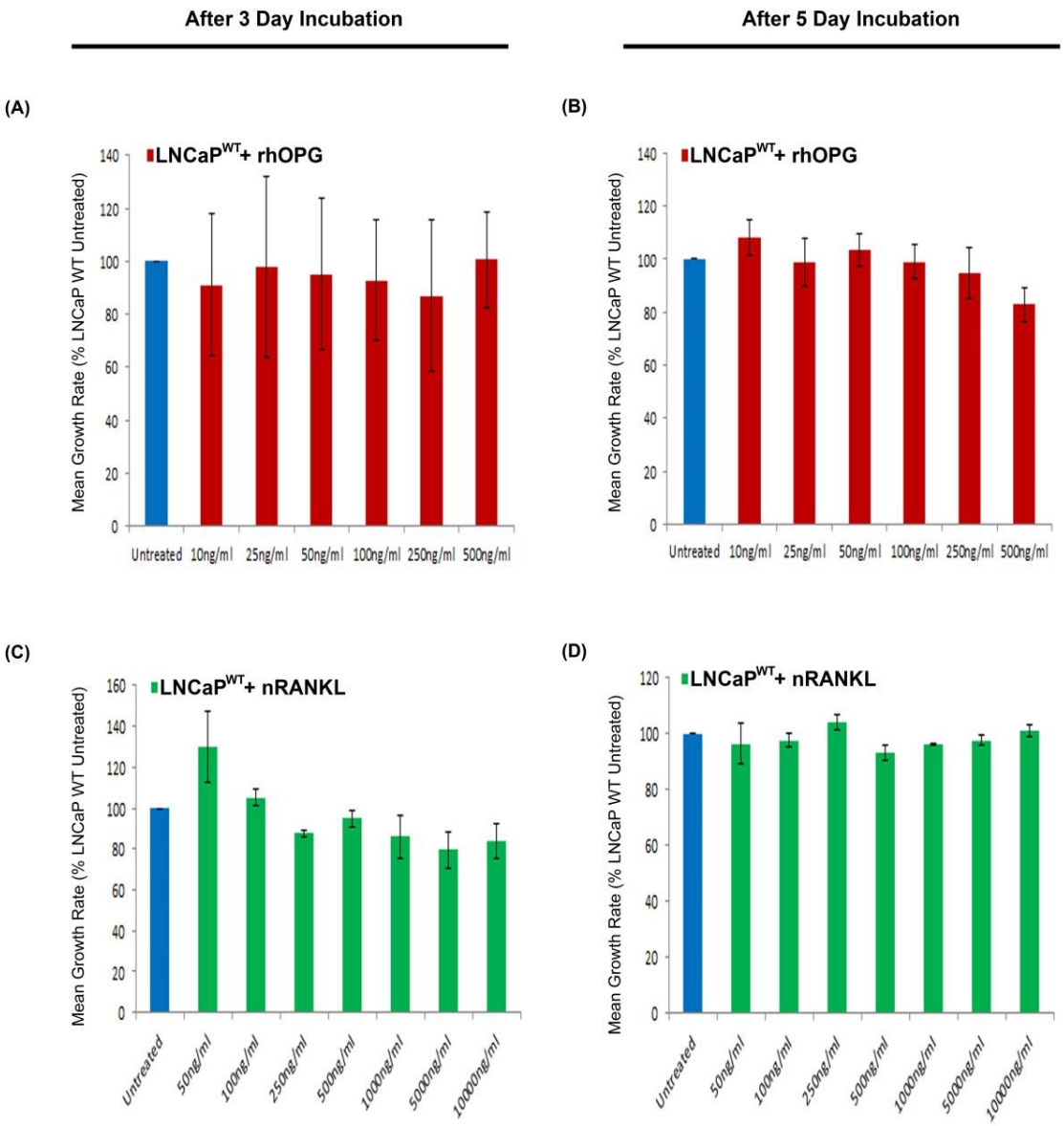

Figure 5.1: rhOPG and nRANKL concentration gradients
A range of rhOPG concentrations were tested on LNCaP cells, no noticeable cytotoxic effects were observed on LNCaP cell proliferation after 3 days incubation (A) or after 5 days incubation (B). LNCaP cells treated with a range of concentrations of nRANKL; cells treated with 50ng/ml showed a significant increase in cell proliferation compared to the untreated cells and all other nRANKL concentrations after 3 days incubation (C). This trend was not continued after 5 days incubation (D); no concentrations appeared to have significant cytotoxic effects. Data represents mean values of 3 independent repeats and error bars represent SEM. * - p=<0.05, ** - p=<0.01 and *** - p=<0.001.

After 3 days incubation with nRANKL, 50ng/ml resulted in an initial significant increase in LNCaP cell proliferation compared to all other tested concentrations and the untreated LNCaP cells (Figure 5.1 C). All other concentrations tested did not appear to have any significant cytotoxic effects. However, after 5 day incubation all nRANKL concentrations had no significant biological effects on LNCaP cell proliferation (Figure 5.1 D). The initial increase observed after 3 days incubation with 50ng/ml was no longer evident. As a result of these assays, all future experiments were carried out using 25ng/ml rhOPG and 100ng/ml nRANKL based on other literature (Lane *et al* 2012).

5.3.2 Effect of exogenous rhOPG and nRANKL treatment on LNCaP cell proliferation

LNCaP cells treated with 25ng/ml rhOPG showed an initial increase in cell proliferation compared to the untreated LNCaP cells (Figure 5.2 A, 135% of untreated cells); however this did not reach a significant level. This pattern was continued, though less pronounced, after 5 day incubation with the LNCaP cells treated with 25ng/ml rhOPG which showed slightly increased cell proliferation compared with the untreated cells (Figure 5.2 B, 109% of untreated cells).

LNCaP cells treated with 100ng/ml nRANKL showed an initial increase in cell proliferation compared to the untreated LNCaP cells (Figure 5.2 C, 174% of untreated cells), however this difference appeared to have been negated after 5 day incubation with 100ng/ml nRANKL (Figure 5.2 D, 105% of untreated cells).

LNCaP cells treated with a combination of 25ng/ml rhOPG and 100ng/ml nRANKL resulted in an increase in cell proliferation after 3 days incubation compared with untreated LNCaP cells (153% of untreated cells), though again this difference did

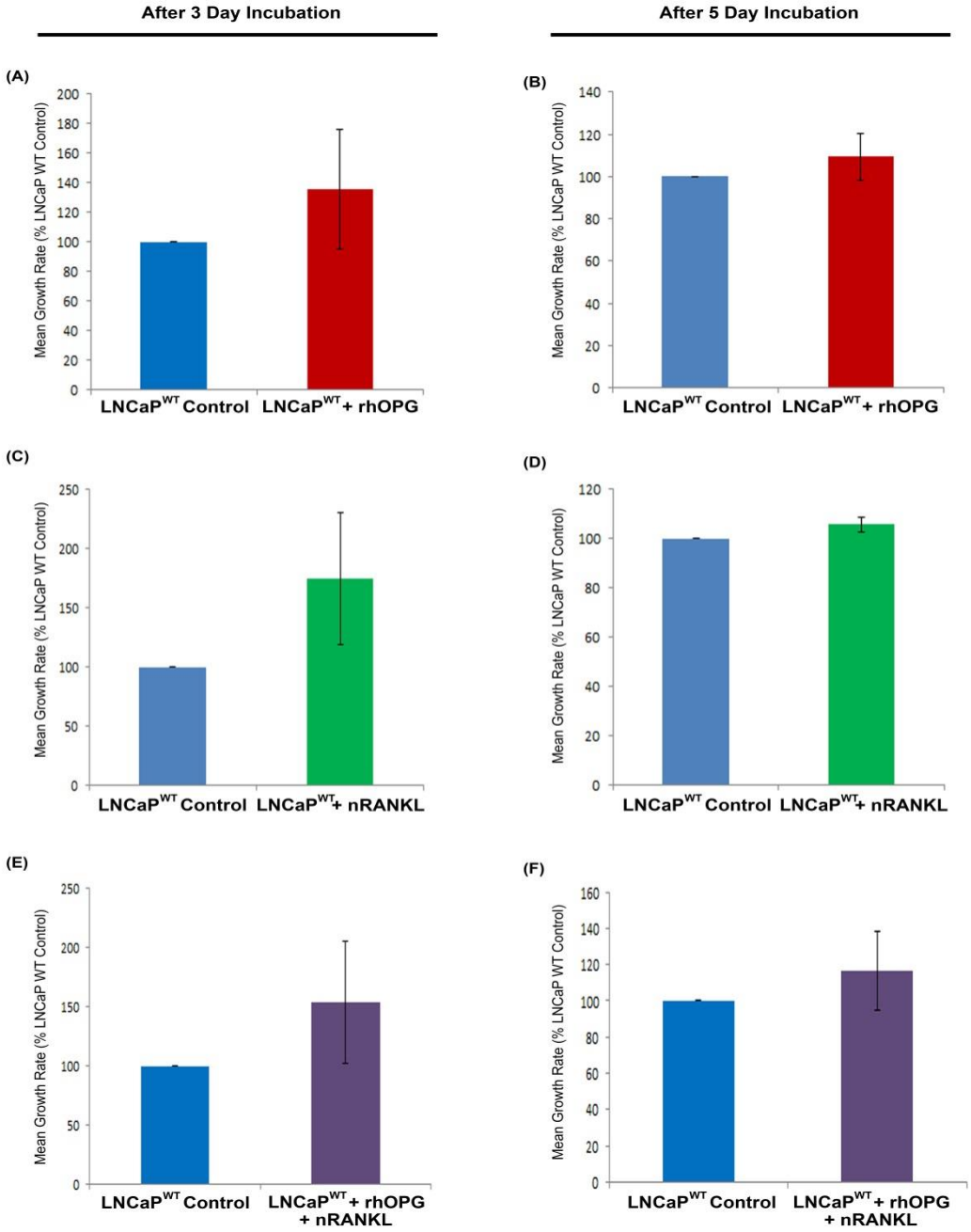

Figure 5.2: Effect of rhOPG and nRANKL on LNCaP cell proliferation

LNCaP cells incubated with 25ng/ml rhOPG showed an increase in cell proliferation compared to the untreated cells after 3 days (A) however this did not reach significance and was negated after 5 days incubation (B). When LNCaP cells were incubated for 3 days with 100ng/ml nRANKL (C) or a combination of 25ng/ml rhOPG and 100ng/ml nRANKL (E) increases in LNCaP cell proliferation were observed, though these did not reach significance. After 5 days incubation with 100ng/ml nRANKL LNCaP cell proliferation was similar to that of the untreated cells (D). LNCaP cells incubated with 25ng/ml rhOPG and 100ng/ml nRANKL still showed increased cell proliferation compared to the untreated cells, however this still did not reach significance (F). Data represents mean values of 4 independent repeats, error bars represent SEM. * - p=<0.05, ** - p=<0.01 and *** - p=<0.001.

not reach a significant level (Figure 5.2 E). As with the individual treatments this difference was less pronounced after 5 days incubation, though the combined treatment with 25ng/ml rhOPG and 100ng/ml nRANKL resulted in increased LNCaP cell proliferation (Figure 5.2 F 116% of untreated cells).

5.3.3 Effect of exogenous HGF and BME on LNCaP cell proliferation

Treatment of LNCaP cells with 40ng/ml HGF, appeared to have no impact on cell proliferation after 3 days incubation (99% of untreated cells) (Figure 5.3 A), however after 5 days incubation a significant reduction in cell proliferation was seen compared with the untreated cells (62% of untreated cells) (Figure 5.3 B, p=0.029). However, treatment of LNCaP cells with 50µg/ml BME resulted in an increase in LNCaP cell proliferation after 3 days incubation (178% of untreated cells) (Figure 5.3 A), though this increase did not reach a significant level until after 5 days incubation (120% of untreated cells) (Figure 5.3 B, p=0.029). When a combined treatment of 40ng/ml HGF and 50µg/ml BME were added to LNCaP cells an increase in cell proliferation was observed after 3 days incubation and 5 days incubation (155% and 115% of untreated cells) (Figures 5.3 A and B). These increases in cell proliferation did not reach significant levels and were not as pronounced as those observed with the individual 50µg/ml BME treatment, especially after 3 days incubation, but the combined treatment did appear to nullify the effects of the individual 40ng/ml HGF treatment.

LNCaP cells treated with 25ng/ml rhOPG and 40ng/ml HGF showed reduced cell proliferation after both 3 day and 5 day incubation (Figure 5.3 C and D respectively). After 5 days incubation this reduction in LNCaP cell proliferation reached significance (p=0.009) compared with the rhOPG treated cells (66% of 25ng/ml rhOPG treated cells). Treatment of LNCaP cells with 25ng/ml rhOPG and 50µg/ml

BME did not seem to have an initial impact on cell proliferation after 3 days incubation (Figure 5.3 C, 98% compared to 25ng/ml rhOPG treated cells). However, after 5 days incubation, LNCaP cell proliferation was increased compared to 25ng/ml rhOPG treated cells, although this did not reach a significant level (Figure 5.3 D, 120% compared to 25ng/ml rhOPG treated cells). When 40ng/ml HGF and 50µg/ml BME were used in combination with 25ng/ml rhOPG, after 3 days incubation LNCaP cell proliferation was initially increased, though not significantly compared to the rhOPG only treated cells (Figure 5.3 C, 149% compared to 25ng/ml rhOPG treated cells). However, after 5 day incubation there was no apparent difference between the combined 25ng/ml rhOPG, 40ng/ml HGF and 50µg/ml BME treated cells and the 25ng/ml rhOPG only treated cells (Figure 5.3 D).

LNCaP cells treated with 100ng/ml nRANKL and 40ng/ml HGF also resulted in a significant decrease in cell proliferation after 3 days incubation (Figure 5.3 E, 65% of nRANKL treated cells, p=0.029) and 5 days incubation (Figure 5.3 F, 49% of nRANKL treated cells, p=0.029). Combined treatment of 100ng/ml nRANKL and 50µg/ml BME, after 3 days incubation resulted in an initial non-significant decrease in LNCaP cell proliferation (Figure 5.3 E, 86% compared to nRANKL treated cells). Incubation with 100ng/ml nRANKL and 50µg/ml BME for 5 days resulted in a slight increase in LNCaP cell proliferation compared to 100ng/ml nRANKL treated cells (Figure 5.3 F, 109% compared to nRANKL cells). However, when 100ng/ml nRANKL, 40ng/ml HGF and 50µg/ml BME were used in combination to treat LNCaP cells, they appeared to have little impact on cell proliferation (Figures 5.3 E and F respectively). After 3 days incubation there was a slight reduction in LNCaP cell proliferation after treatment with 100ng/ml nRANKL, 40ng/ml HGF and 50µg/ml BME compared to the 100ng/ml nRANKL only treated cells (Figure 5.3 E, 89% of nRANKL treated cells). This decrease in LNCaP cell proliferation appeared negated

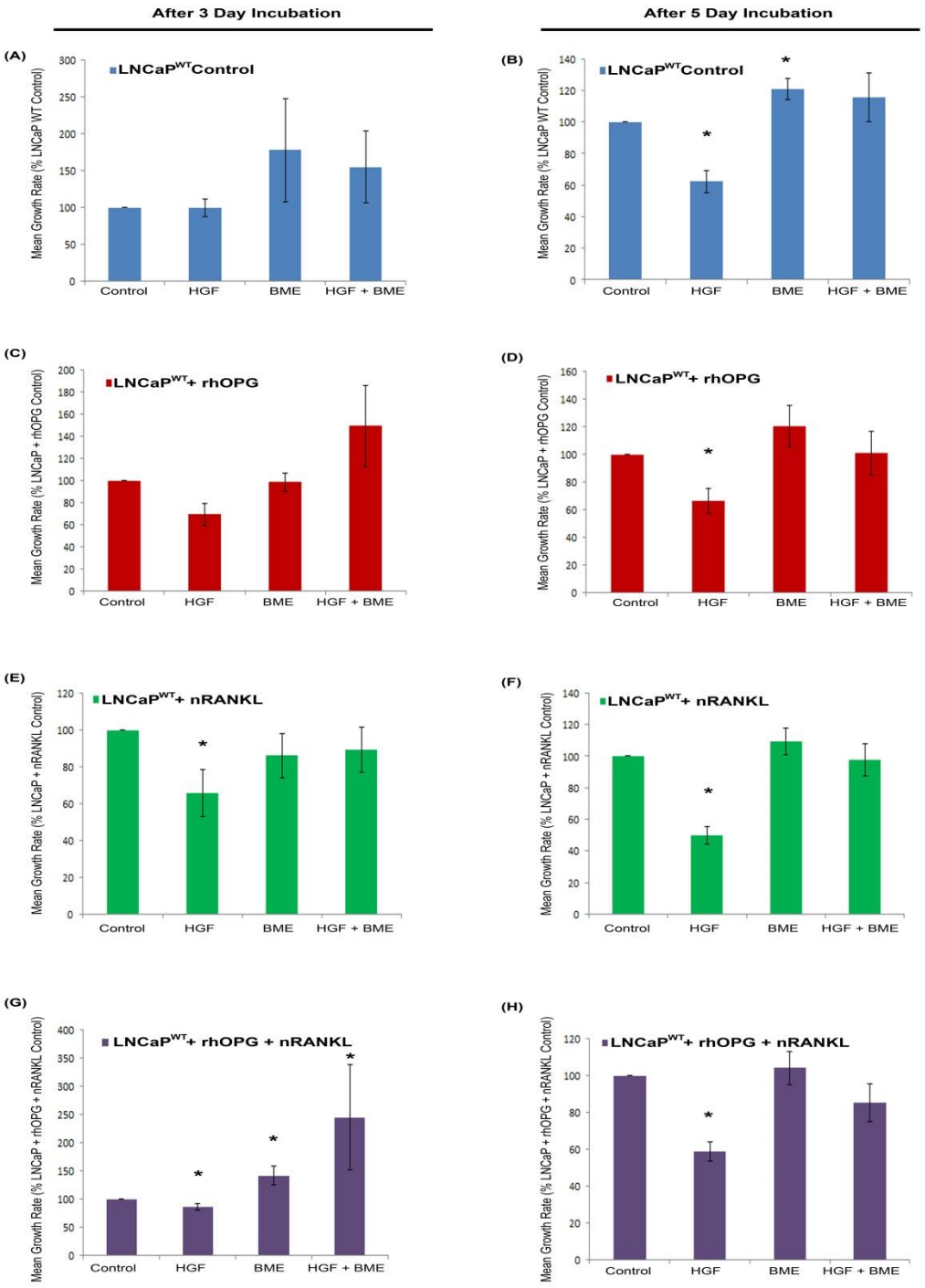

Figure 5.3: Effect of HGF and BME on LNCaP cell proliferation
LNCaP cells incubated with 40ng/ml HGF, 50µg/ml BME or 40ng/ml HGF and 50µg/ml BME after 3 days incubation (A) and after 5 days incubation (B). LNCaP cell proliferation when cells were treated with 25ng/ml rhOPG and 40ng/ml HGF, 50µg/ml BME or 40ng/ml HGF and 50µg/ml BME after 3 days incubation (C) and after 5 days incubation (D). LNCaP cell proliferation when cells were treated with 100ng/ml nRANKL and 40ng/ml HGF, 50µg/ml BME or 40ng/ml HGF and 50µg/ml BME after 3 days incubation (E) and after 5 days incubation (F). LNCaP cell proliferation when cells were treated with 25ng/ml rhOPG and 100ng/ml nRANKL and 40ng/ml HGF, 50µg/ml BME or 40ng/ml HGF and 50µg/ml BME after 3 days incubation (G) and after 5 days incubation (H). Data represents mean of 4 independent repeats, error bars represent SEM. * - p=<0.05, ** - p=<0.01 and *** - p=<0.001.

after 5 days incubation compared to the 100ng/ml nRANKL treated cells (Figure 5.3 F, 97% of nRANKL treated cells). None of these patterns reached significant levels.100ng/ml nRANKL and 25ng/ml rhOPG were also used in combination with 40ng/ml HGF on LNCaP cells. After 3 and 5 days incubation, LNCaP cell proliferation was again significantly reduced (Figure 5.3 G and H, 86% and 58% of rhOPG and nRANKL treated cells, p=0.029 and 0.029 respectively). 100ng/ml nRANKL and 25ng/ml rhOPG used in combination with 50µg/ml BME initially after 3 days incubation appeared to significantly increase LNCaP cell proliferation (Figure 5.3 G, 141% of rhOPG and nRANKL treated cells, p=0.029), however this increase was negated after 5 days incubation (Figure 5.3 H, 104% of rhOPG and nRANKL treated cells). When all 4 treatments were combined, initially LNCaP cell proliferation appeared significantly increased compared to the 25ng/ml rhOPG and 100ng/ml nRANKL treated cells (Figure 5.3 G, 245% of rhOPG and nRANKL treated cells, p=0.029). However, after 5 days incubation cell proliferation appeared to be reduced in comparison to the 25ng/ml rhOPG and 100ng/ml nRANKL treated cells, though this did not reach a significant level (Figure 5.3 H, 85% of rhOPG and nRANKL treated cells).

5.3.4 Effect of exogenous rhOPG and nRANKL treatment on LNCaP cell-matrix adhesion

LNCaP cells treated with 25ng/ml rhOPG showed increased cell-matrix adhesion compared to untreated LNCaP cells (Figure 5.4 A, 178% of untreated control), however, this trend did not achieve significance. Similar patterns for the 100ng/ml nRANKL treated cells (202% of untreated control) and combined 25ng/ml rhOPG and 100ng/ml nRANKL cells (239% of untreated control) were also seen (Figures 5.4 C and E respectively). Again, however, both of these trends failed to reach

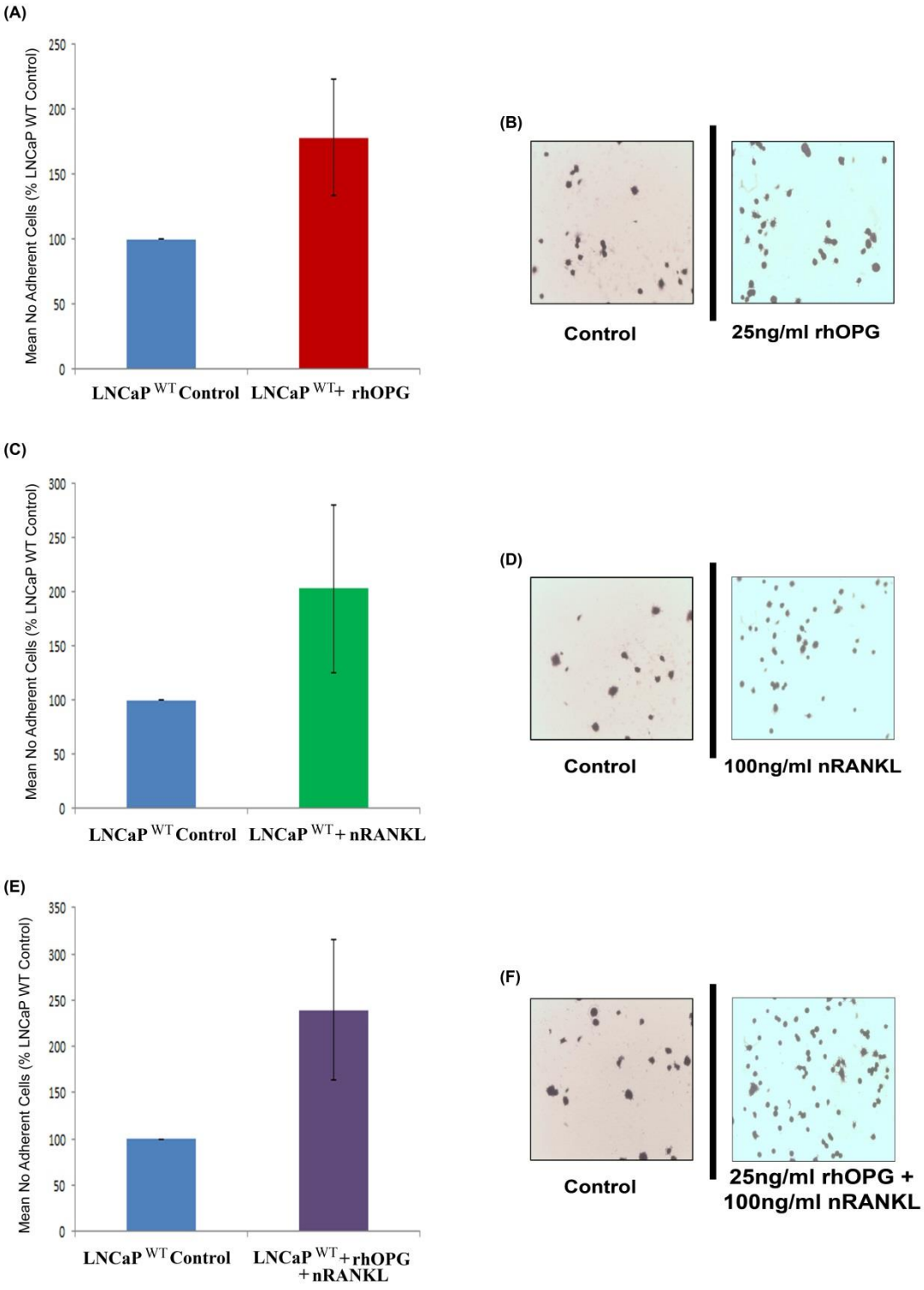

Figure 5.4: Effect of rhOPG and nRANKL on LNCaP cell-matrix adhesion
LNCaP cells treated with 25ng/ml rhOPG showed increased cell-matrix adhesion compared to untreated cells (A). Treatment with 100ng/ml nRANKL also appeared to increase LNCaP cell-matrix adhesion compared to untreated cells (C). When LNCaP cells were treated with combined 25ng/ml rhOPG and 100ng/ml nRANKL an increase in cell-matrix adhesion was observed (E). Representative images from one repeat for rhOPG, nRANKL and rhOPG and nRANKL in B, D and F respectively. Data shown is the mean of 3 independent repeats, error bars represent SEM. * - p=<0.05, ** - p=<0.01 and *** - p=<0.001.

significance. Representative images for each of the treatments compared to untreated LNCaP cells are also shown (Figure 5.4 B, D and F).

5.3.5 Effect of exogenous HGF and BME on LNCaP cell-matrix adhesion

Treatment of LNCaP cells with 40ng/ml HGF appeared to slightly increase cell-matrix adhesion *in vitro* (109% of untreated control), whereas treatment with 50µg/ml BME resulted in a more prominent increase (124% of untreated control). However, a combination of 40ng/ml HGF and 50µg/ml BME resulted in a considerable increase in LNCaP cell-matrix adhesion (165% of untreated control) (Figure 5.5 (1) A). However none of these notable changes gave significant results. (Representative images shown in Figure 5.5 (1) B).

When 40ng/ml HGF treatment was added in combination with 25ng/ml rhOPG, the cell-matrix adhesive properties of LNCaP cells appeared reduced (79% of rhOPG treated control) (Figure 5.5 (1) C, representative images shown in Figure 5.5 (1) D). Treatment with 50µg/ml BME appeared to have no additional effect when added in combination with 25ng/ml rhOPG (93% of rhOPG treated control). However, of interest was the significant reduction in cell-matrix adhesion which was observed when 25ng/ml rhOPG, 40ng/ml HGF and 50µg/ml BME were added in combination to LNCaP cells (64% of rhOPG treated control) (Figure 5.5 (1) C, representative images 5.5 (1) D, $p = 0.003$).

When 40ng/ml HGF was added in combination with 100ng/ml nRANKL to LNCaP cells there was no effect on cell-matrix adhesion (100% of nRANKL treated control) (Figure 5.5 (2) E). The 50µg/ml BME treatment or the 40ng/ml HGF and 50µg/ml BME treatment in combination with 100ng/ml nRANKL, appeared to further enhance cell-matrix adhesion (124% and 124% of nRANKL treated control respectively), however

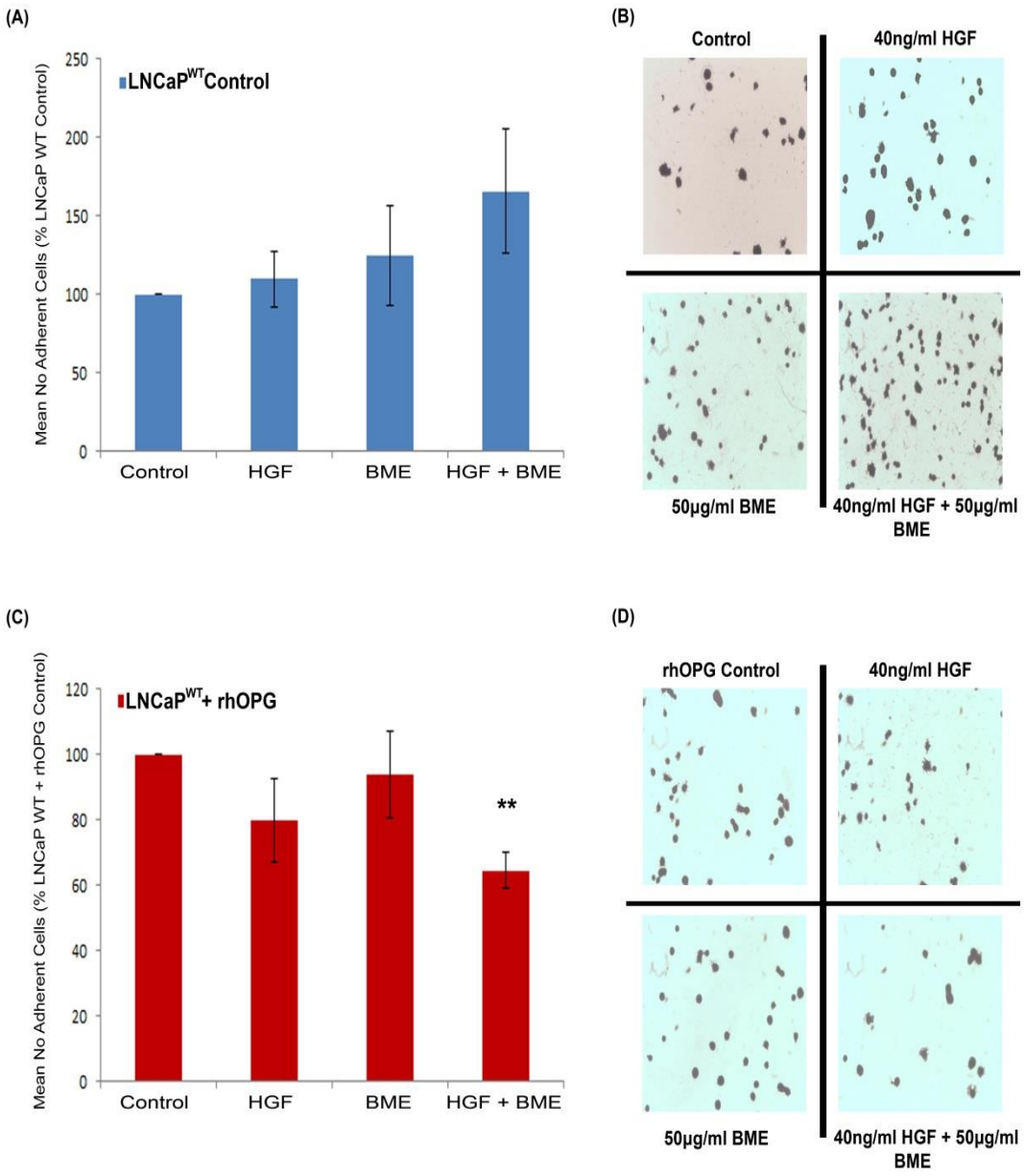

Figure 5.5 (1): Effect of HGF and BME on LNCaP cell matrix adhesion
LNCaP cells treated with 40ng/ml HGF, 50µg/ml BME or 40ng/ml HGF and 50µg/ml BME showed slight increases in cell-matrix adhesion (A, representative images B). LNCaP cells treated with 25ng/ml rhOPG and 40ng/ml HGF or 40ng/ml HGF and 50µg/ml BME showed reductions in cell-matrix adhesion whilst the 50µg/ml BME and 25ng/ml rhOPG appeared to have little effect on LNCaP cell-matrix adhesion (C, representative images D). Data represents mean of 3 independent repeats, error bars represent SEM. * - p=<0.05, ** - p=<0.01 and *** - p=<0.001.

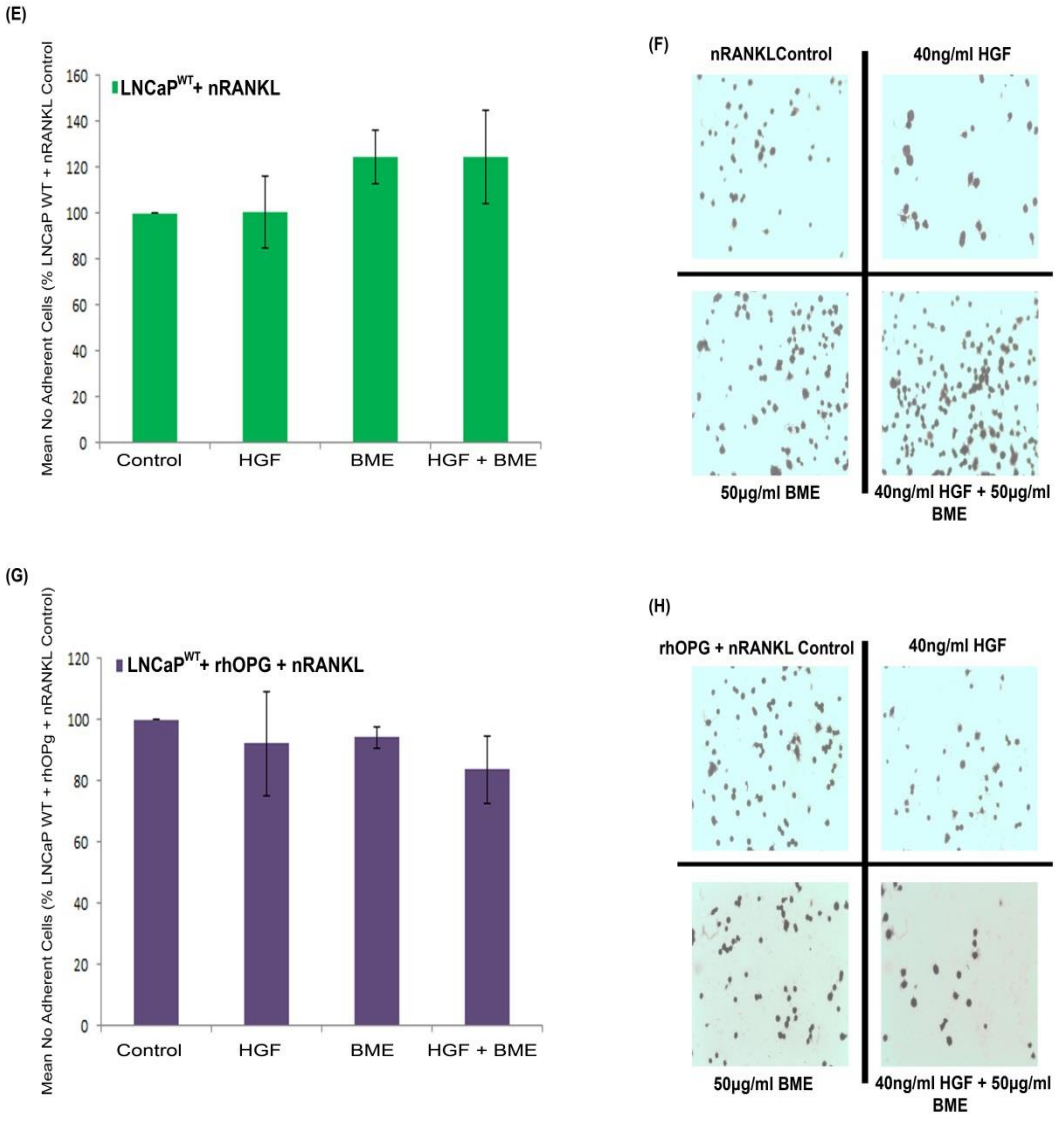

Figure 5.5 (2): Effect of HGF and BME on LNCaP cell matrix adhesion
LNCaP cells treated with 100ng/ml nRANKL and 40ng/ml HGF were added together there was no effect on cell-matrix adhesion however, when 100ng/ml nRANKL and either 50µg/ml BME or 40ng/ml and 50µg/ml BME were added non-significant increases in cell-matrix adhesion were observed (E, representative images F). LNCaP cells treated with 25ng/ml rhOPG, 100ng/ml nRANKL and 40ng/ml HGF or 50µg/ml BME had little impact on cell-matrix adhesion but a combination of 25ng/ml rhOPG, 100ng/ml nRANKL, 40ng/ml HGF and 50µg/ml BME showed a non-significant decrease in cell-matrix adhesion (G, representative images H). Data represents mean of 3 independent repeats, error bars represent SEM. * - p=<0.05, ** - p=<0.01 and *** - p=<0.001.

neither of these results reached a significant level (Figure 5.5 (2) E, representative images 5.5 (2) F).

LNCaP cell-matrix adhesion appeared slightly reduced when 25ng/ml rhOPG, 100ng/ml nRANKL and 40ng/ml HGF were added together compared to just the 25ng/ml rhOPG and 100ng/ml nRANKL treated cells (92% of rhOPG and nRANKL treated control) (Figure 5.5 (2) G), though this was not statistically significant. A similar response was seem when 50µg/ml BME was added in combination with 25ng/ml rhOPG and 100ng/ml nRANKL (94% of rhOPG and nRANKL treated control). The most noticeable effect on cell-matrix adhesion was when 25ng/ml rhOPG, 100ng/ml nRANKL, 40ng/ml HGF and 50µg/ml BME were all added in combination (83% of rhOPG and nRANKL treated control). However again this failed to reach significance (Figure 5.5 (2) G, representative images Figure 5.5 (2) H).

5.3.6 Effect of exogenous rhOPG and nRANKL treatment on LNCaP cell migration

LNCaP cells treated with 25ng/ml rhOPG had a very slight decrease in cell migration compared to untreated LNCaP cells over a 4 hour period (Figure 5.6 A). When LNCaP cells were treated with 100ng/ml nRANKL there appeared to be no difference in cell migration, over 4 hours, compared with untreated LNCaP cells, following electrical wounding using ECIS (Figure 5.6 B). However, when 25ng/ml rhOPG and 100ng/ml nRANKL treatments were combined LNCaP cell migration increased compared to untreated cells, though this was not significant after 4 hours (Figure 5.6 C).

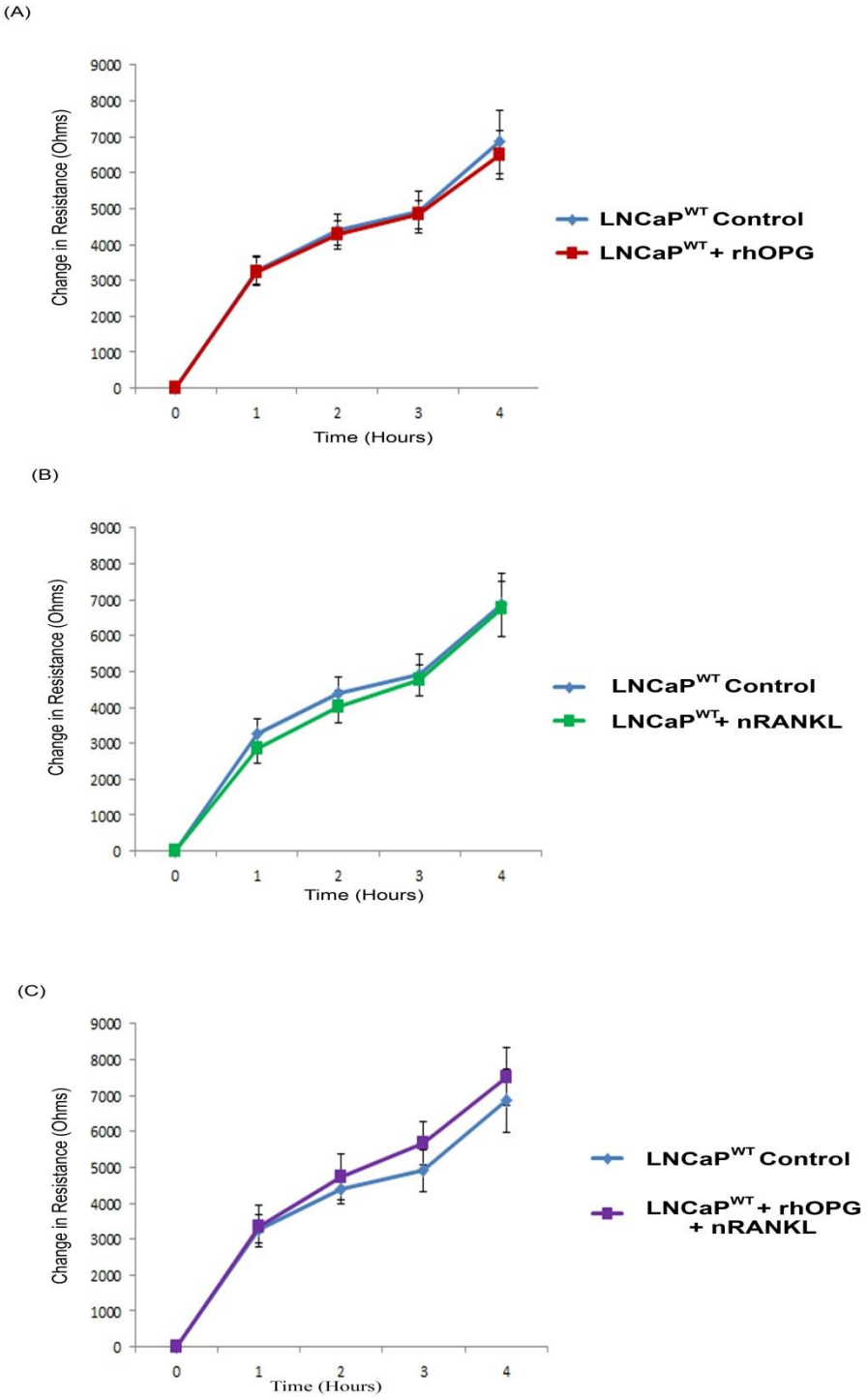

Figure 5.6: Effect of rhOPG and nRANKL on LNCaP cell migration
Using ECIS, treatments of 25ng/ml rhOPG (A), 100ng/ml nRANKL (B) or 25ng/ml rhOPG and 100ng/ml nRANKL (C) had little effect on LNCaP cell migration, after wounding, over a 4 hour period compared to untreated LNCaP cells. Data represents mean of 3 independent repeats, error bars represent SEM. * - p=<0.05, ** - p=<0.01 and *** - p=<0.001.

5.3.7 Effect of exogenous HGF and BME on LNCaP cell migration

Under the influence of 40ng/ml HGF or 50µg/ml BME, LNCaP cell migration over a 4 hour period was unaffected compared to the untreated cells. However, when a combination of 40ng/ml HGF and 50µg/ml BME was added to the LNCaP cells, a significant increase in cell migration compared to the untreated cells was observed (Figure 5.7 A, p=0.014).

When 25ng/ml rhOPG and 40ng/ml HGF were added to LNCaP cells, cell migration was significantly increased over a 4 hour period compared to 25ng/ml rhOPG treated cells (Figure 5.7 B, p=0.007). However, when 25ng/ml rhOPG and 50µg/ml BME were added in combination to LNCaP cells, cell migration was significantly decreased over a 4 hour period compared to the 25ng/ml rhOPG treated cells (Figure 5.7 B, p=<0.001). Conversely, when 25ng/ml rhOPG, 40ng/ml HGF and 50µg/ml BME were added in combination, the decreased effects of 50µg/ml BME were negated, and an increase in LNCaP cell migration was seen, however, this increase was less than that seen under the influence of the individual 40ng/ml HGF treatment.

LNCaP cells treated with 100ng/ml nRANKL and 40ng/ml HGF showed a significant increase in cell migration over a 4 hour period compared to 100ng/ml nRANKL treated LNCaP cells (Figure 5.7 C, p=0.018). When 100ng/ml nRANKL and 50µg/ml BME were added in combination to the LNCaP cells, cell migration was decreased compared to the 100ng/ml nRANKL treated cells, however this did not reach a significant level. However, when 100ng/ml nRANKL, 40ng/ml HGF and 50µg/ml BME were added in combination to LNCaP cells, cell migration was significantly increased compared to 100ng/ml nRANKL treated cells (Figure 5.7 C, p=0.019).

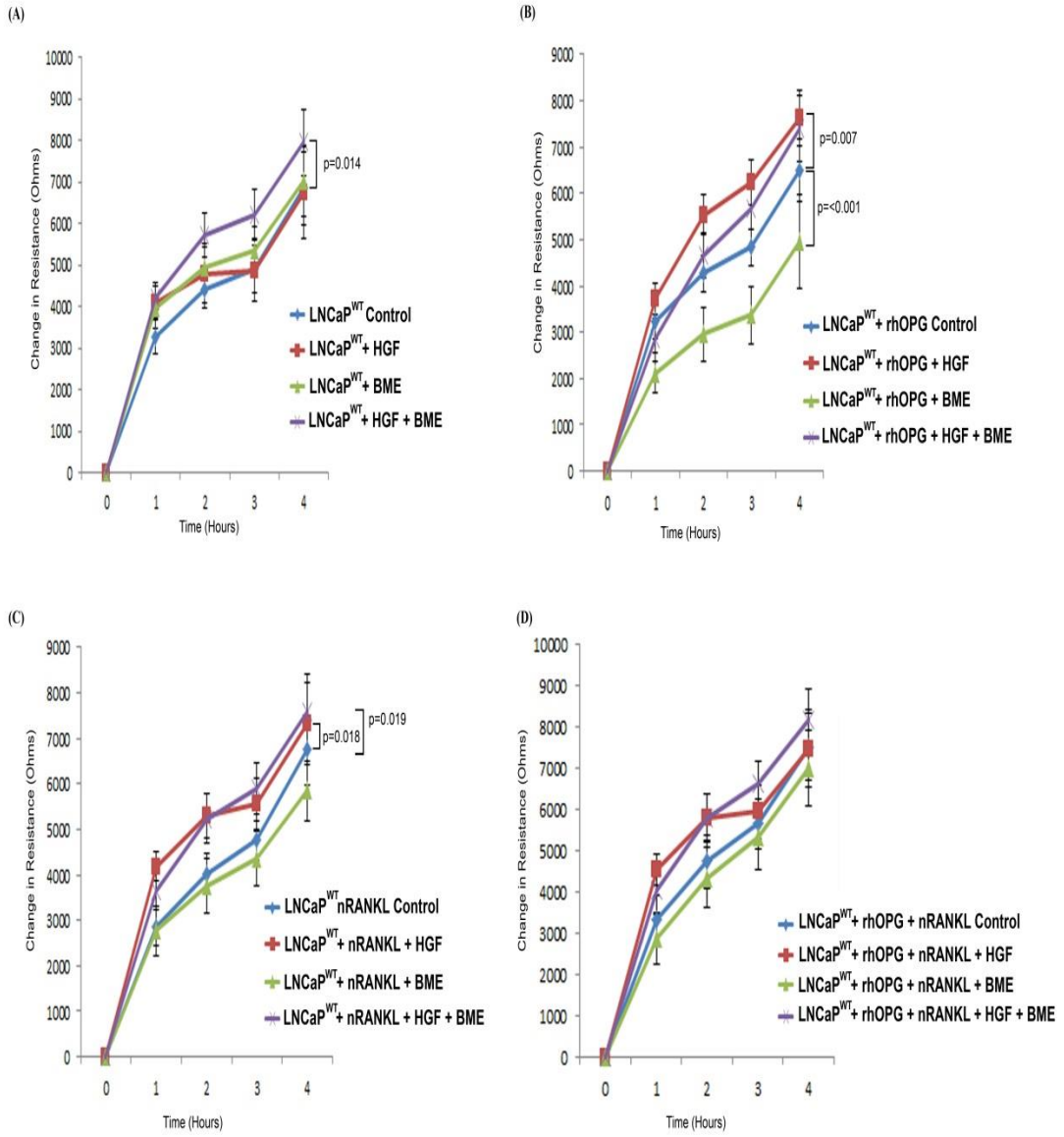

Figure 5.7: Effect of HGF and BME on LNCaP cell migration
LNCaP cell migration after treatment with 40ng/ml HGF or 50µg/ml BME showed little change but cell migration significantly increased after treatment with 40ng/ml HGF and 50µg/ml BME compared to the untreated LNCaP cells (A). LNCaP cell migration after treatment with 25ng/ml rhOPG and 40ng/ml HGF significantly increased compared to the rhOPG treated cells. Treatment with 25ng/ml rhOPG, 40ng/ml HGF and 50µg/ml BME also increased LNCaP migration however this was not significant compared to the rhOPG treated cells. Treatment with 25ng/ml rhOPG and 50µg/ml BME significantly decrease LNCaP cell migration compared to the rhOPG treated cells (B). LNCaP cell migration after treatment with 100ng/ml nRANKL and 40ng/ml HGF or 40ng/ml HGF and 50µg/ml BME significantly increased compared to the 100ng/ml nRANKL treated cells. However, treatment with 100ng/ml nRANKL and 50µg/ml BME non-significantly decreased LNCaP cell migration (C). LNCaP cell migration after being treated with 25ng/ml rhOPG, 100ng/ml nRANKL and 40ng/ml HGF or 50µg/ml BME showed little difference in cell migration compared to the 25ng/ml rhOPG and 100ng/ml nRANKL treated cells, but treatment with 25ng/ml rhOPG, 100ng/ml nRANKL, 40ng/ml HGF and 50µg/ml BME resulted in a non-significant increase in cell migration (D). Data represents mean of 3 independent repeats, error bars represent SEM. * - p=<0.05, ** - p=<0.01 and *** - p=<0.001.

When 25ng/ml rhOPG and 100ng/ml nRANKL were added in combination with 40ng/ml HGF, unlike the effects seen with the individual rhOPG or nRANKL treatments there appeared to be little effect on LNCaP cells compared to the 25ng/ml rhOPG and 100ng/ml nRANKL treated cells (Figure 5.7 D). LNCaP cell migration over a 4 hour period when treated with 25ng/ml rhOPG, 100ng/ml nRANKL and 50µg/ml BME showed a slight decrease compared to the 25ng/ml rhOPG and 100ng/ml nRANKL treated cells. This pattern was less dramatic than those seen in the individual 25ng/ml rhOPG or 100ng/ml nRANKL treated cells further treated with 50µg/ml BME. The combination of 25ng/ml rhOPG, 100ng/ml nRANKL, 40ng/ml HGF and 50µg/ml BME appears to increase LNCaP cell migration over 4 hours compared to the 25ng/ml rhOPG or 100ng/ml nRANKL treated cells. However, as was noted with the 40ng/ml HGF and 50µg/ml BME treatments these responses were not as pronounced in the combined group as seen in the individual treatment groups, and these did not reach significant levels.

5.3.8 Effect of exogenous rhOPG and nRANKL treatment on LNCaP cell invasion

LNCaP cells treated with 25ng/ml rhOPG showed significantly reduced cell invasion compared to the untreated LNCaP cells (67% of untreated cells) (Figure 5.8 A, $p = 0.017$, representative images B). LNCaP cells treated with either 100ng/ml nRANKL or a combination of 25ng/ml rhOPG and 100ng/ml nRANKL also showed reduced cell invasion compared with untreated cells (59% and 68% of untreated cells respectively); however neither of these were statistically significant (Figures 5.8 C and E respectively, representative images D and F).

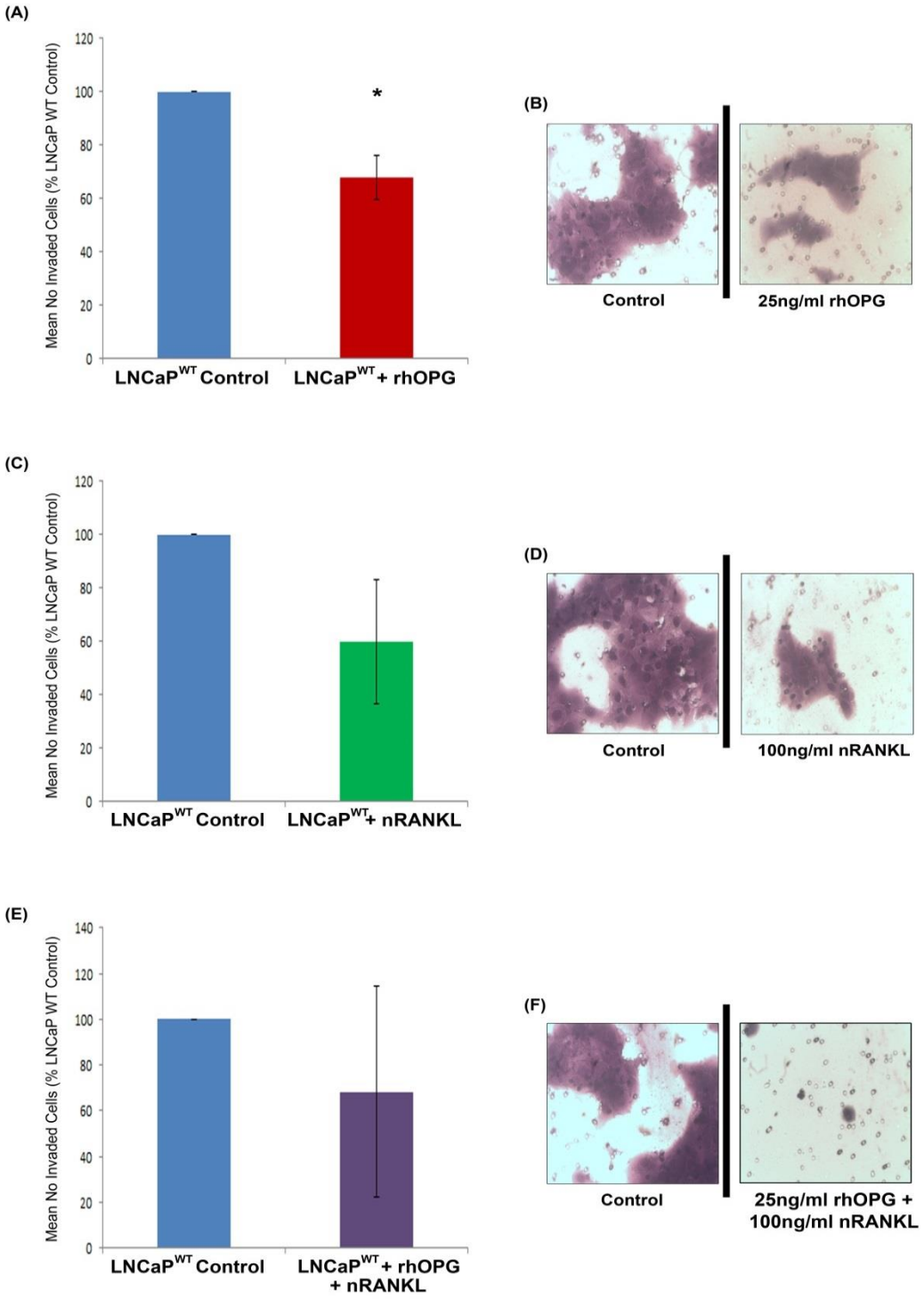

Figure 5.8: Effect of rhOPG and nRANKL on LNCaP cell invasion
Incubation of LNCaP cells with 25ng/ml rhOPG resulted in a significant decrease in cell invasiveness (A, representative images B). Treatment with 100ng/ml nRANKL (C, representative images D) and 25g/ml rhOPG and 100ng/ml nRANKL (E, representative images F) resulted in non-significant decreases in LNCaP cell invasion. Data represents mean of 3 independent repeats, error bars represent SEM. * - p=<0.05, ** - p=<0.01 and *** - p=<0.001.

5.3.9 Effect of exogenous HGF and BME on LNCaP cell invasion

Incubation of LNCaP cells with 40ng/ml HGF resulted in a significant decrease in cell invasion compared to untreated LNCaP cells (43% of untreated cells) (Figure 5.9 (1) A, p=0.015 representative images 5.9 B). Treatment with 50µg/ml BME also resulted in a decrease in LNCaP cell invasion, though this did not reach a significant level (69% of untreated cells). A combined treatment of 40ng/ml HGF and 50µg/ml BME resulted in a significant decrease in LNCaP cell invasion compared to the untreated cells (34% of untreated cells) (Figure 5.9 (1) A, p = 0.012).

Treatment of LNCaP cells with 25ng/ml rhOPG combined with 40ng/ml HGF appeared to show slightly reduced cell invasion compared to the 25ng/ml rhOPG treated cells (89% of rhOPG treated cells) (Figure 5.9 (1) C). Interestingly, a combined treatment of 25ng/ml rhOPG and 50µg/ml BME resulted in an increase in LNCaP cell invasion compared to the 25ng/ml rhOPG treated cells (157% of rhOPG treated cells), however this change did not reach significance. A combined treatment of 40ng/ml HGF and 50µg/ml BME with 25ng/ml rhOPG resulted in a significant decrease in LNCaP cell invasion (38% of rhOPG cells) (Figure 5.9 (1) C, p = 0.004, representative images 5.9 (1) D).

When LNCaP cells were treated with 100ng/ml nRANKL together with 40ng/ml HGF little effect was seen on cell invasion (97% of nRANKL treated cells) (Figure 5.9 (2) E). Treatment with 50µg/ml BME in addition to 100ng/ml nRANKL showed an increase in LNCaP cell invasion which almost reached significance (136% of nRANKL treated cells, p=0.06) (representative images shown in Figure 5.9 (2) F). Combining all the treatments, 100ng/ml nRANKL, 40ng/ml HGF and 50µg/ml BME resulted in a significant decrease in LNCaP cell invasion (42% of nRANKL treated cells) (Figure 5.9 (2) E, p = <0.001).

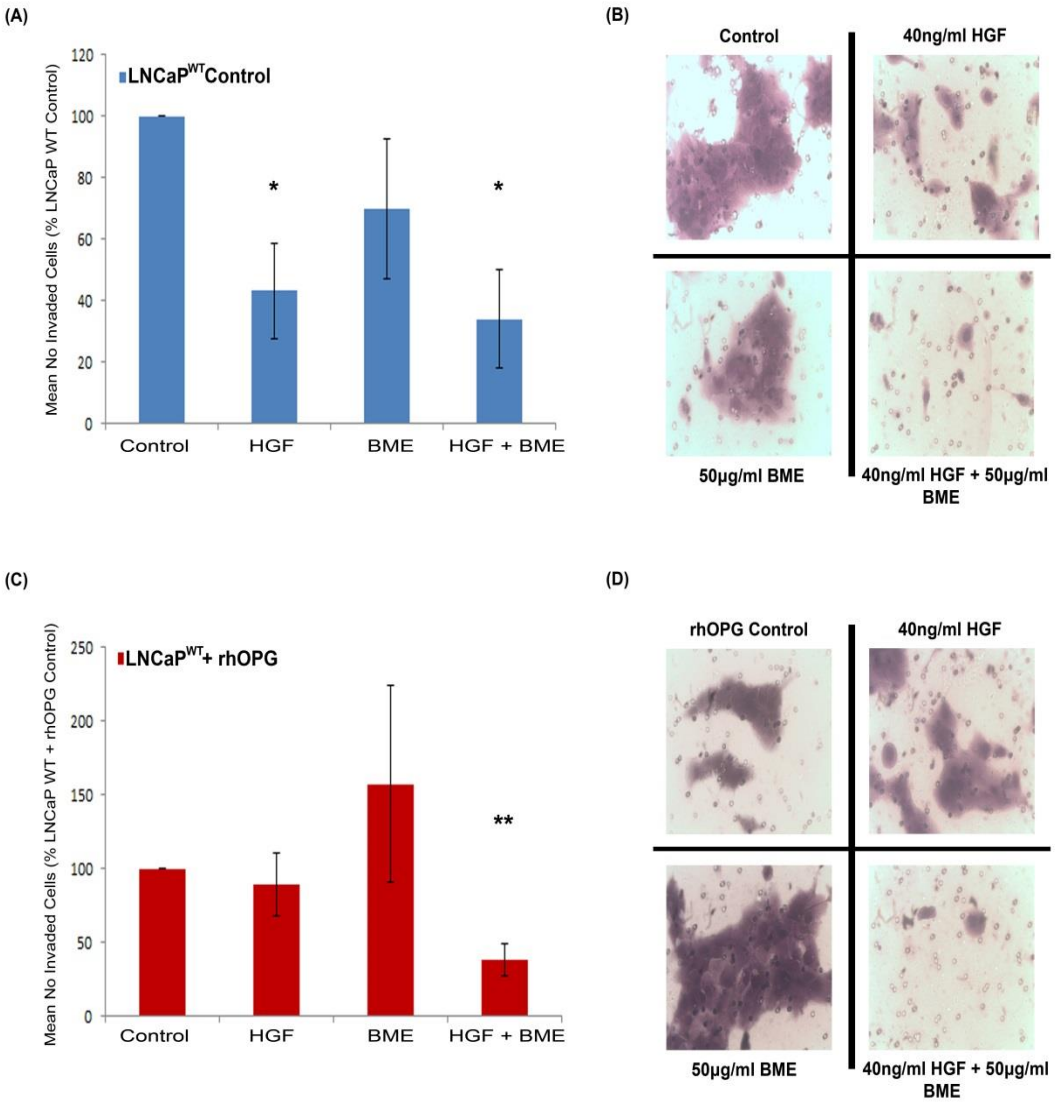

Figure 5.9 (1): Effect of HGF and BME on LNCaP cell invasion
LNCaP cells treated with 40ng/ml HGF (p=0.015), 50µg/ml BME or 40ng/ml HGF and 50µg/ml BME (p=0.012) resulted in decreased cell invasion (A, representative images B). LNCaP cells treated with 25ng/ml rhOPG and 40ng/ml HGF or 40ng/ml HGF and 50µg/ml BME resulted in decrease invasion, the latter significantly so (p=0.004) but 25ng/ml rhOPG and 50µg/ml BME treatment non-significantly increased LNCaP cell invasion (C, representative images D). Data represents 3 independent repeats, error bars represent SEM. * - p=<0.05, ** - p=<0.01 and *** - p=<0.001.

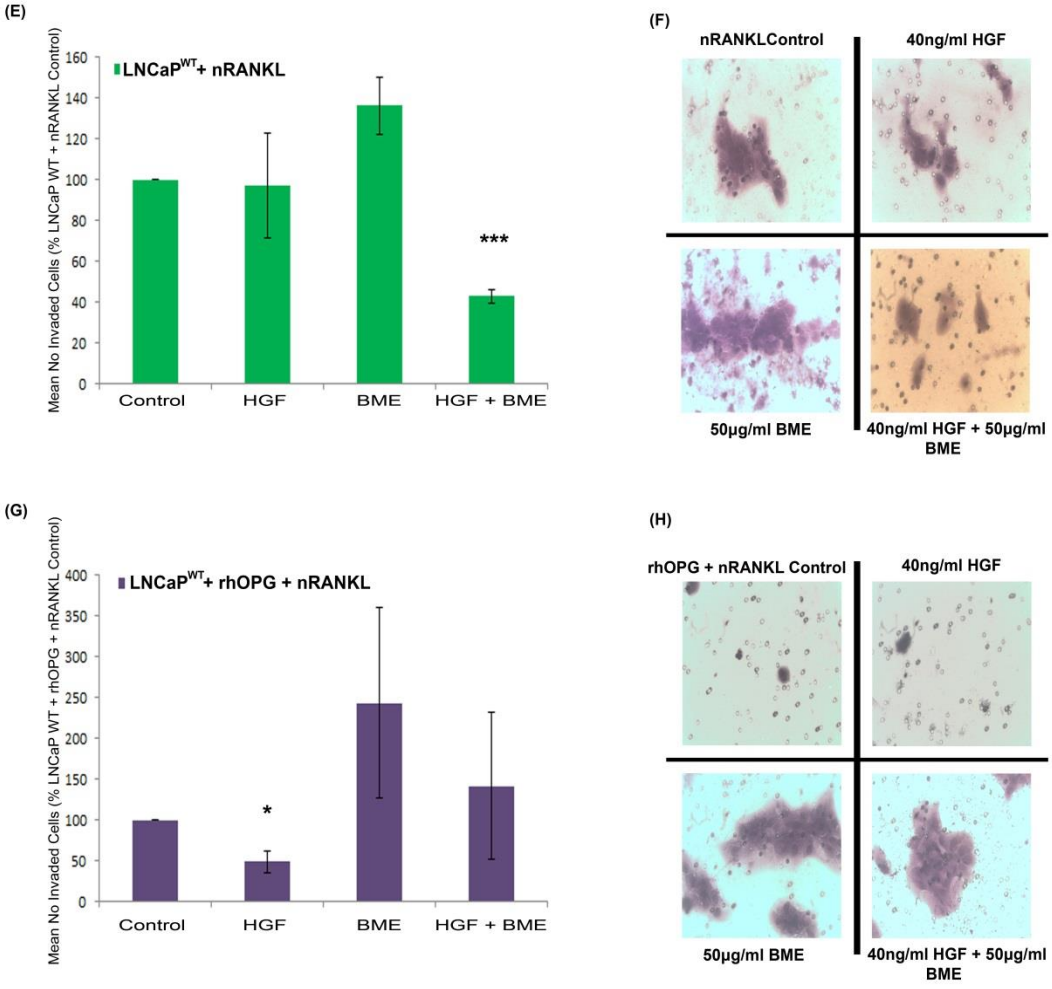

Figure 5.9 (2): Effect of HGF and BME on LNCaP cell invasion
LNCaP cells treated with 100ng/ml nRANKL together with either 40ng/ml HGF or a combination of 40ng/ml HGF and 50µg/ml BME decreased cell invasion, the latter significantly so (<0.001). Treatment with 100ng/ml nRANKL combined with 50µg/ml BME non-significantly increased LNCaP cell invasion (E, representative images F). LNCaP cells treated with a combination of 25ng/ml rhOPG and 100ng/ml nRANKL, together with 40ng/ml HGF resulted in significantly decreased cell invasion (p=0.02) whilst treatment with 25ng/ml rhOPG and 100ng/ml nRANKL together with 50µg/ml BME or both 40ng/ml HGF and 50µg/ml BME resulted in non-significant increased cell invasion (G, representative images H). Data represents mean of 3 independent repeats, error bars represent SEM. * - p=<0.05, ** - p=<0.01 and *** - p=<0.001.

Combination of both 25ng/ml rhOPG and 100ng/ml nRANKL together with 40ng/ml HGF resulted in a significant decrease in LNCaP cell invasion (48% of rhOPG and nRANKL treated cells) (Figure 5.9 (2) G, p = 0.02). The combination of 25ng/ml rhOPG and 100ng/ml nRANKL when supplemented with 50µg/ml BME resulted in an increase in LNCaP cell invasion in comparison to 25ng/ml rhOPG and 100ng/ml nRANKL treated cells, however this did not reach significance (243% of rhOPG and nRANKL treated cells). When all the treatments, 25ng/ml rhOPG, 100ng/ml nRANKL, 40ng/ml HGF and 50µg/ml BME were applied in combination the effects seen with the individual 40ng/ml HGF treatment were nullified, and invasion increased in comparison to the 25ng/ml rhOPG and 100ng/ml nRANKL treated cells. However, this increase was not as large as that seen with the individual 50µg/ml BME treatment (156% of 25ng/ml rhOPG and 100ng/ml nRANKL treated cells).

5.4 Discussion

The competing effects of androgens on prostate cancer and bone cells within the bone environment can result in a local niche which either favours bone resorption or protection of the bone. The absolute levels of OPG and RANKL expression fluctuate during the progression of many cancers, including prostate cancer. *In vivo* models have linked RANKL in bone lesion formation and progression associated with prostate cancer, with strong evidence that RANKL and RANK are integral to cancer cells homing to the bone. This therefore offers pharmacological targets for which a recombinant formation of OPG and nRANKL provide interesting potential novel therapies.

5.4.1 Effect of exogenous rhOPG treatment on LNCaP prostate cancer cells

Treating the androgen dependent prostate cancer cell line, LNCaP, with exogenous rhOPG resulted in a small initial increase in LNCaP cell proliferation which was not maintained over 5 days incubation, a similar pattern to that seen in the cytotoxicity assay. Of interest was the response of LNCaP cell proliferation, treated with rhOPG, to HGF which was similar to the cell proliferation response seen in the non-rhOPG treated LNCaP cells to HGF. However, the addition of BME with rhOPG appeared to maintain the increase in LNCaP cell proliferation however this trend did not reach statistical significance. It again highlights the possibility that OPG may not directly affect prostate cancer cell proliferation however; it may facilitate and influence other factors, particularly in the bone environment, which ultimately culminate in an increase in prostate cancer cell proliferation.

Corey *et al* (2005), with variants of LNCaP cells, demonstrated that when C4-2 prostate cancer cells, which over expressed OPG, were subcutaneously injected into mice there was no impact on tumour take rate or tumour growth rate compared to the control cells. However, when these OPG over-expressing cells were implanted in the bone, tumour volume was significantly decreased. Vandyke *et al* (2007) concluded that androgen stimulation decreased mRNA expression of OPG. Therefore, other unidentified modulations, possibly post-transcriptional, might also affect the production of OPG and may additionally affect prostate cancer progression. This is of particular interest because the C4-2 cell line is believed to be the more tumourigenic, androgen responsive, though not dependent, sub-clone of the parental LNCaP cell line. This difference in cell behaviour under the influence of OPG as the cancer cells switch between androgen dependence and independence as replicated in these sub-clones, poses more questions than answers, especially when taken into consideration with the evidence by Vandyke *et al* (2007).

Nyambo *et al* (2004) demonstrated that bone marrow stromal cells *in vitro* could produce enough OPG to protect PC-3 prostate cancer cells from TRAIL induced apoptosis. This pattern of behaviour may also be seen in this section of the study when the LNCaP cells were treated with both rhOPG and BME though further investigation with the addition of TRAIL would be required to confirm this. Based on these observations there therefore needs to be further investigation into which pathways may be affected and result in this ultimate increase in prostate cancer cell proliferation, whilst also trying to isolate the potential roles androgen sensitivity and inhibition of TRAIL apoptosis may play.

Exogenous rhOPG appeared to have little influence on LNCaP cell-matrix adhesion and migration on its own. However, when LNCaP cells were treated individually with HGF, BME or HGF and BME in combination both cell-matrix adhesion and migration appeared to be affected. HGF treatment appeared to be a pro-migratory factor for the LNCaP cell line which was further enhanced when added in addition to exogenous rhOPG. This was accompanied by the observation that rhOPG and HGF appeared to make the LNCaP cells less adhesive to the artificial matrix (Matrigel). In contrast, the more interesting observation was that the addition of rhOPG and BME together resulted in a reduced migratory response in the LNCaP cells, whilst cell-matrix adhesion appeared unaffected. Sikes *et al* (2004) investigated the interactions between bone derived cells and LNCaP and C4-2 prostate cancer cells. They concluded that there was no apparent difference between the LNCaP cells and the more tumorigenic subclone C4-2, despite the propensity for C4-2 cells to be able to spontaneously form ostoeblastic lesions *in vivo*. Though several integrins were noted to have been affected between both cell lines, no evident consequence of this was found in their study. Due to the complexity of the bone environment, paracrine factors may play a pivotal role in the metastatic process of prostate

cancer cells. This study has therefore provided some evidence to suggest OPG may be a factor involved in prostate cancer cells homing to the bone.

Though in this study, in its own right, rhOPG did not appear to affect LNCaP cell migration and resulted in increased cell-matrix adhesion our results potentially highlight that OPG could stimulate prostate cancer cell arrest in the bone microenvironment, as cells were less migratory under the influence of the inhouse bone mix (BME) which would not necessarily be favourable in all clinical settings. This has been demonstrated by Kiefer *et al* (2004) who showed that the administration of OPG decreased the growth of LuCAP23.1 cells intra-tibially however it did not prevent the establishment of prostate-derived tumours in bone. This *in vitro* and *in vivo* data may therefore present somewhat of a challenge, as there are ongoing clinical trials into the potential of recombinant OPG as a pharmaceutical intervention for prostate cancer.

The most intriguing observation from this section of the study was that the addition of rhOPG to the androgen dependent LNCaP cells resulted in a significant decrease in LNCaP invasion *in vitro*. However, this pattern was reversed under the combined influence of rhOPG and BME. Of further note was the observation that combined HGF and BME under the influence of rhOPG resulted in a significant decrease in LNCaP cell invasion *in vitro*. This pattern of observations supports that of Kiefer *et al* (2004), despite the different cell lines and the fact that this study has only used an *in vitro* model it does appear that there is parity in the overall conclusions that can be drawn. OPG may play multiple roles during the course of prostate cancer cells metastasising to the bone, influencing a variety of traits, though the impact of these treatments also appears, at least somewhat, to vary depending on environmental conditions and factors present (*e.g.* HGF, bone proteins). Therefore using rhOPG as a potential therapy may be a double edged sword, further research is required to fully understand the complete role OPG plays in prostate cancer, how such a

treatment might impact disease progression both in the immediate and long term clinical settings and the potential rhOPG may have as a combination therapy.

5.4.2 Effect of exogenous nRANKL treatment on LNCaP prostate cancer cells

Neutralising RANKL antibody, Denosumab, was licensed in October 2012 for the treatment of SREs associated with solid tumours except prostate cancer. The purpose of this study was to investigate if targeting RANKL would prevent prostate cancer cells from settling in the bone environment and establishing bone metastases *in vitro*.

The LNCaP prostate cell line used in this study expressed RANKL (Figure 3.1). Hu *et al* (2013) and Chu *et al* (2014) have demonstrated that RANKL is prevalently expressed in human prostate cancer specimens with increasing levels correlating with higher tumour grade, metastasis and association with clinical outcome. Treating the LNCaP cells with a neutralising RANKL antibody appeared to have little effect on LNCaP cell proliferation. As has been previously noted, exogenous HGF treatment appeared to result in reduced LNCaP cell proliferation, and this pattern continued irrespective of the presence of nRANKL, but was more pronounced in the presence of nRANKL. Of interest was the lack of further response in LNCaP cell proliferation when nRANKL and BME treatment were combined. There also appeared to be little impact on cell-matrix adhesion of LNCaP cells which were also under the influence of nRANKL on its own, or under the influence of HGF or BME.

In contrast, though individually nRANKL treatment appeared to have little impact on LNCaP cell migration, the addition of HGF or a combination of HGF and BME both resulted in a pro-migratory response in the LNCaP cells. Despite observations that the individual HGF treatment in this study was anti-proliferative, its pro-migratory response remained present, especially under the influence of nRANKL. This also

appeared the case when HGF and BME were added in combination with nRANKL to LNCaP cells. Therefore it would be interesting to further investigate by which other pathway(s) HGF in combination with nRANKL exerted this pro-migratory response in LNCaP cells. It would also be interesting to investigate the pathway(s) in which BME and nRANKL appeared to result in a reduced migratory response.

Addition of nRANKL to LNCaP cells resulted in a notable decrease in cell invasion. Huang *et al* (2006) showed that β2-microglobulin promoted prostate cancer cell osteomimicry by inducing RANKL expression. Zhau *et al* (2008) subsequently demonstrated that this induction of RANKL expression promoted EMT in prostate cancer cells. These observations agree with the anticipated responses observed in this study, with the individual nRANKL treatment, through potential inhibition of EMT processes, resulting in significantly decreased LNCaP cell invasion. However, the most interesting observations were that the nRANKL response was negated under the influence of HGF, whilst BME treatment combined with nRANKL resulted in noticeable and almost significant increase in LNCaP cell invasion. Further investigation is required to isolate the predominant factors in the bone environment which might facilitate this pro-invasive phenotype.

Unfortunately given the time constraints of this study it was not possible to establish stable suppression of RANK in LNCaP cells. Establishment of this cell line in the future would allow investigation on how targeting RANK individually and in combination with the various treatments, would impact LNCaP cell tumourigenic potential.

Given the complex nature of the metastatic cascade the fight continues to identify those individual factors which are pivotal to prostate cancer disease progression and therefore provide novel specific therapeutic targets. This section of the study has potentially highlighted rhOPG may in the bone environment result in reduced

LNCaP cell migration and increased cell invasion, however further investigation into how this occurs, and other factors which facilitate this, is required. The role RANKL plays in prostate cancer is coming under greater and greater scrutiny, this study has provided several cellular traits, migration and invasion, which warrant further investigation into how several environmental factors (*e.g.* HGF and bone proteins) influence cellular responses to RANKL.

Chapter 6

Role of OPG, RANK and RANKL in breast cancer

6.1 Introduction

Despite the advancements in breast cancer care and treatments it still remains a major health burden in the Western world. Like prostate cancer it is also associated with latent disease states and high relapse rates which can re-present clinically as bone metastasis, as well as lung, liver and brain metastases. Breast cancer bone metastasis, unlikely prostate cancer, generally present phenotypically as osteolytic, which are detectable by x-ray. This has been shown to be accompanied by an increased number of osteoclasts, which further enhances tumour growth in bone.

The TNFRSF have previously been studied in breast cancer, especially circulating RANKL and OPG, due to their potential as biomarkers for predicting bone metastases (Ibrahim *et al* 2011, Mercatali *et al* 2011). Reinholz *et al* (2002) examined gene expression of TNF family members, including RANKL and OPG in normal, non-invasive, invasive and metastatic human breast cancer specimens. OPG expression was unchanged between normal and non-invasive breast tissues whilst tissue from liver metastases exhibited increased OPG expression, though no other forms of metastases exhibited similar patterns. Van Poznak *et al* (2006) detected OPG expression in 55% of the breast cancer cases studied also noticing a correlation with oestrogen status and OPG protein localisation. Several *in vitro* studies have been published demonstrating that OPG expression in breast cancer cell lines, MDA-MB-231, MDA-MB-436, MCF-7 and T47D enhance tumour cell survival by inhibiting TRAIL induced apoptosis (Neville-Webbe *et al* 2004, Park *et al* 2003, Holen *et al* 2005). It has also been demonstrated *in vitro* that the oestrogen receptor negative cell line, MDA-MB-231, produces enough OPG to bind TRAIL and in turn upregulate RANKL expression thus contributing to the 'vicious' bone cycle between tumour and bone cells (Nicolin and Narducci 2010). This taken into consideration with results from Neville-Webbe *et al* (2004) and Holen *et al* (2005) suggests that OPG may through this mechanism aid breast cancer cell survival.

However, Morony *et al* (2001) showed that, *in vivo,* the addition of recombinant OPG in a SCID mouse model inhibited tumour growth in bone. Therefore the role played by OPG may switch during the course of breast cancer progression.

Both RANK and RANKL have been implicated in mammary gland development and lactation accompanied by other growth factors and cytokines. Fata *et al* (2000) demonstrated that mice deficient in RANK or RANKL exhibited disturbed mammary gland morphogenesis due to decreased differentiation and proliferation as well as increased apoptosis in mammary epithelial cells during lactation. Subsequent evidence has also shown that RANK and RANKL are also implicated in mammary gland ductal side-branching, alveolar differentiation and lumen formation (Fernandez-Valdivia *et al* 2009, Gonzalez-Suarez *et al* 2007). Evidence has shown that both progesterone and prolactin stimulate RANKL expression in mouse mammary and human breast epithelial cells and therefore promote mammary gland morphogenesis by stimulating mammary epithelial cell proliferation and inhibiting apoptosis (Beleut *et al* 2010, Tanos *et al* 2013).

The TNFRSF have previously been studied in breast cancer especially, in recent years, under the influence of the progesterone axis (Joshi *et al* 2010, Seifert-Klauss *et al* 2012). A better understanding of the role osteoclasts, RANKL, and its association with PTHrP, in a variety of conditions, has led to the exploration of the potential to exploit these in therapies, this approach remains under intense investigation. This is pivotal given recent evidence that RANKL positively correlates with breast cancer cell proliferation and acts in a paracrine manner on RANK expressed in oestrogen negative/progesterone negative breast cancer cells (Dougall *et al* 2014). RANKL has also been shown to control the responsiveness of mammary gland stem cell and luminal progenitors (Dougall *et al* 2014). In preclinical breast cancer models targeted RANKL therapies have been shown to reduce tumour burden and prevent osteolysis. This has led to the licensing of the

neutralising RANKL antibody, Denosuamab for the treatment of breast cancer associated SREs. Besides this RANKL, both *in vitro* and *in vivo*, has been implicated in RANK-expressing breast cancer cell migration and upregulation of MMPs which can promote distant metastases (Dougall *et al* 2014). Taking this into consideration, with the knowledge that most clinical options for bone metastases still remain management only, a better understanding of the interplay between these family members in breast cancer may provide prophylactic opportunities in the future.

The interactions between bone stromal cells and tumour cells are critical in metastasis formation (Reddi *et al* 2003, Neville-Webbe *et al* 2004). Early work in co-culture models with breast cancer cells and bone stromal cells showed that primary breast cancer specimens and cultured breast tumour cells did not express RANKL, but this expression could be induced with stromal or osteoblast interactions, by several different tumour secreted factors, and result in enhanced osteoclast formation (Thomas *et al* 1999, Dougall *et al* 2012). There is also some evidence that interaction with bone marrow stromal cells inhibits OPG production, due to the presence of PTHrP, thus altering the RANKL:OPG ratio to favour osteoclastogenesis with the net result of aggressive osteolytic bone destruction. This can provoke osteoclast formation and metastatic growth (Kakonen and Grundy 2003, Park *et al* 2003, Thomas *et al* 1999).

In this section of the study, the transcript expression profiles of OPG, RANK and RANKL were screened in our clinical breast cancer cohort to assess the implications of these molecules in disease progression and prognosis using qPCR. This study aimed to establish if targeting OPG or RANK using hammerhead ribozyme transgenes influenced MDA-MB-231 breast cancer cell behaviour *in vitro*. Subsequently, this section also aimed to explore the potential effects treatment with

exogenous HGF or BME might further impose on the manipulated breast cancer cell behaviour in the establishment of osteolytic bone metastases.

6.2 Materials and Methods

6.2.1 Cell lines and breast cancer tissue

All data of breast cancer tissues was analysed anonymously and informed verbal consent given. As the tissues were collected before the introduction of the Human Tissue Act, UK 2004, no written consent was necessary and documentary measures not required. Primary breast cancer tissue and matching non-neoplastic mammary tissue were collected from the same mastectomy specimens' immediately after surgery and stored at -80^{o}C until use. All the specimens were verified and graded by a consultant pathologist, "Normal" is considered background tissue from matching mastectomy specimens' which showed no pathological signs of cancer. At time of use RNA concentrations were measured as previously stated in Section 2.7.3. Based on these concentrations all samples for this study were standardised to 50ng and reverse transcription carried out.

In this study ZR-75-1, MCF-7 and MDA-MB-231 breast cancer cells were used for screening. The MDA-MB-231 breast cancer cell line was also used to generate empty plasmid control cells (MDA-MB-231^{pEF6}) and transfectants for either OPG or RANK knockdown (MDA-MB-231^{OPGKD}, MDA-MB-231^{RANKKD}). Cells were maintained in DMEM medium supplemented with 10% FCS and ABS as described previously (Section 2.6.1). All transfectants were initially exposed to selection medium (DMEM complete medium supplemented with 5µg/ml Blasticidin S) for 10 days. All transfectants were subsequently maintained in DMEM complete medium supplemented with 0.5µg/ml Blasticidin S, to ensure the plasmid vector was retained.

All *in vitro* function assays were conducted in Blasticidin S free medium.

6.2.2 Treatment(s)

MCF-7 and MDA-MB-231 breast cancer cells, pre-starved in serum free medium for 12 hours, were treated with a variety of β-oestradiol concentrations (prepared in serum free medium). MDA-MB-231 transfectants were treated with 40ng/ml HGF and/or 50µg/ml BME. For experimental purposes all treatments were prepared at a 2x concentrate and added in 100µl volumes in each *in vitro* function assay carried out.

6.2.3 Generation of OPG and RANK ribozyme transgenes and cloning into pEF6 plasmid vectors, MDA-MB-231 cell transfection and generation of stable transfectants

Hammerhead ribozymes targeting OPG and RANK were designed and generated as previously described in Section 2.9.1 and Table 2.4. Following verification of the touchdown PCR, OPG and RANK transgenes were cloned into pEF6 plasmid vectors and subsequently transformed in *E.coli* (Section 2.9.3 and 2.9.4). Correctly oriented constructs were then amplified, purified and verified (Section 2.9.5) before being transfected into MDA-MB-231 cells using electroporation (Section 2.9.6).

6.2.4 RNA isolation, cDNA synthesis, RT-PCR and qPCR

RNA isolation was carried out using the TRI reagent kit as described in Section 2.7, after which reverse transcription was completed using a high capacity RT kit (full details Section 2.7.3). Following RT-PCR, products were separated

electrophoretically on an agarose gel and representative images, normalised against GAPDH, are shown. All qPCRs were performed and normalised against GAPDH as described in Section 2.7.7. Data presented represents results from at least 3 independent repeats.

6.2.5 Protein isolation, SDS-PAGE and Western blotting

Protein lysates were isolated and quantified as described previously (Section 2.8). After SDS-PAGE, protein was transferred onto PVDF membrane and subsequently probed with specific primary antibody (anti-GAPDH, anti-OPG, anti-RANK) and corresponding peroxidase conjugated secondary antibodies (1:1000). Protein bands were visualised using the chemiluminescent protein detection kit. At least 3 independent repeats were carried out of which a representative image is shown.

6.2.6 *In vitro* cell proliferation assay

MDA-MB-231 transfectant(s) were seeded at $3x10^3$ cells/well into triplicate 96 well plates and incubated for 1, 3 and 5 days with treatments as described in Section 2.10.1. Following incubation, cells were fixed in 4% formalin (v/v) and stained with 0.5% crystal violet (v/v). Subsequently, crystal violet stain was extracted from the cells using 10% acetic acid (v/v) and the absorbance at 540nm was determined using a spectrophotometer. Data presented is the mean percentage control of 4 independent repeats with SEM.

6.2.7 *In vitro* cell Matrigel adhesion assay

A 96 well plate was coated with 5ug/well of Matrigel and left to dry as described in Section 2.10.2. MDA-MB-231 transfectant(s) were seeded at $4.5x10^4$ cells/well and left to adhere for 45 minutes before being fixed in 4% formalin (v/v) and stained with 0.5% crystal violet (v/v). Four representative images were captured for each well and subsequently counted using Image J software. Data presented is the mean percentage control of 3 independent repeats with SEM.

6.2.8 *In vitro* cell migration assay

The cytodex bead motility assay was used to assess MDA-MB-231 cell motility (Section 2.10.3) where briefly, $1x10^6$ cells in 10ml of medium were left to incubate with cytodex beads (100µl) overnight. The following day, cells were washed twice with fresh medium before being re-suspended in 1.5ml of medium and added to a 96 well plate in triplicate (100µl/well) and the necessary treatments added. Cells were left in an incubator for 4 hours after which the plate was washed, fixed in 4% formalin (v/v) and stained with 0.5% crystal violet (v/v). Four representative images were captured for each well and subsequently counted. Data presented is the mean percentage control of 3 independent repeats with SEM.

6.2.9 *In vitro* Matrigel cell invasion assay

Transwell inserts were coated with 50µg/insert of Matrigel and dried before MDA-MB-231 cell transfectants were seeded ($2x10^4$/100µl) into each insert and incubated for 3 days with respective treatments (100µl), as described in Section 2.10.4. Following incubation, invaded cells were fixed in 4% formalin (v/v) and stained with 0.5% crystal violet (v/v). Five representative images were captured per transwell

insert and subsequently counted. Data presented is the mean percentage control of 3 independent repeats with SEM.

6.2.10 *In vivo* xenograft tumour growth and development model

The *in vivo* model was carried out under the strict guidelines of the UK Home Office to ensure that the 3R's were strictly adhered to. In brief, a 100µl suspension containing $1x10^6$ MDA-MB-231 transfectant cells and 0.5mg/ml Matrigel were subcutaneously injected into the left and right flanks of 4-6 week old athymic nude mice (CD-1) and allowed to develop. The mice were maintained in filter top units according to House Office regulations. The mice were weighed and the size of the developing tumour measured using vernier callipers under sterile conditions each week. At the conclusion of the experiment animals were humanely killed under Schedule One and tumours were dissected out if sufficiently sized.

6.3 Results

6.3 Clinical implications of OPG, RANK and RANKL in breast cancer

A breast cancer cohort of 133 primary breast cancer tissues specimens and 31 non-neoplastic matching mammary tissues with 120 months follow up data was available for use in this study. This provided the opportunity to explore the potential implications OPG, RANK and RANKL may have at a clinical level in breast cancer disease progression. Full details of the patient cohort are found in Table 6.1.

With regards those that were classified as "Died of breast cancer" these were identified as a group of patients who had died from the disease irrespective of the presence of metastases. For those that were classified as "Died with metastases",

though they had died of breast cancer, this group incorporated those patients in which metastases had been detected prior to their deaths.

6.3.1 Expression profiles of OPG, RANK and RANKL in breast cancer samples

In our cohort, the transcript expression levels of OPG, RANK and RANKL were quantified using qPCR. Using this method, transcript levels of OPG, RANK and RANKL were found to be reduced in the cancer samples compared to the transcript levels detected in the matching non-neoplastic specimens' (Figure 6.1). However none of these reductions in transcript expression were found to be statistically significant.

Table 6.1: Patients' clinicopathological information

Clinical information	Patient numbers
Grade	
Well differentiated	24
Moderately differentiated	43
Poorly differentiated	7
TNM stage	
TNM 1	2
TNM 2	40
TNM 3	7
TNM 4	4
NPI staging	
NPI <3.4	77
NPI 3.4 –5.4	38
NPI >5.4	16
ER status	
Negative (α)	75
Positive (α)	38
Negative (β)	91
Positive (β)	24
Clinical outcome	
Disease free	90
Metastasis	7
Local recurrence	5
Died of breast cancer	16
Bone metastasis	8
Died with metastasis	23

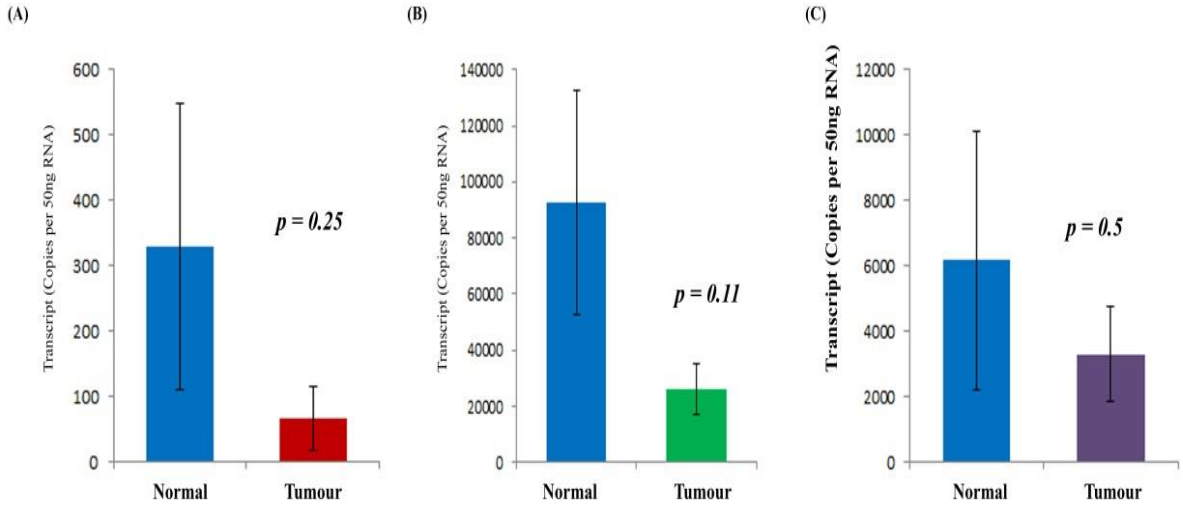

Figure 6.1: Expression profiles of OPG, RANK and RANKL in clinical breast cancer

OPG transcript levels were reduced in malignant breast specimens compared to matching non-neoplastic samples (A). Lower levels of RANK transcript were also detected in malignant breast specimens compared with matching non-neoplastic samples (B). RANKL transcripts were also reduced in malignant breast specimens compared to matching non-neoplastic samples (C). All are normalised against GAPDH. Data are mean ± SEM. N= Normal – 28, Tumour – 104. * - p=<0.05, ** - p=<0.01 and *** - p=<0.001.

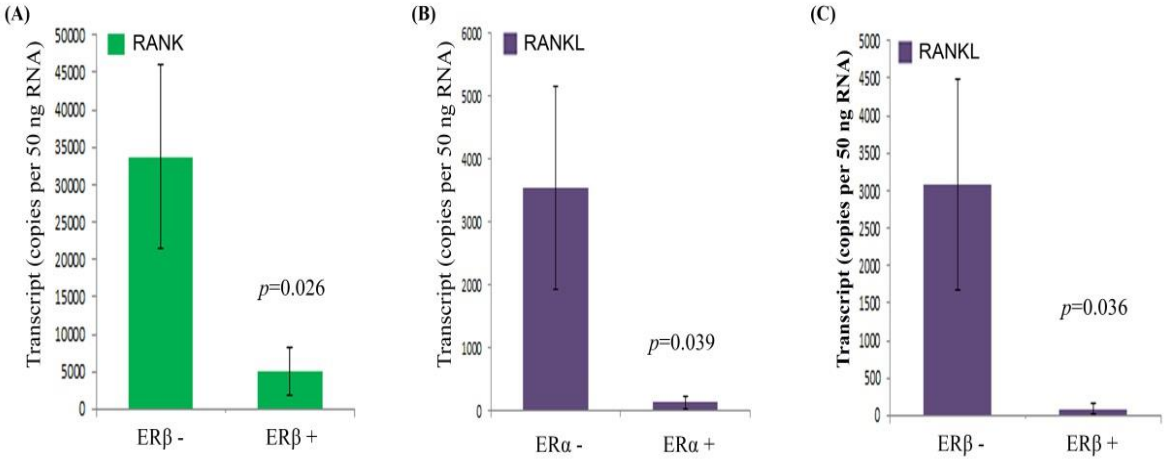

Figure 6.2: ER status correlation with RANK and RANKL transcript levels in clinical breast cancer

RANK transcript levels were significantly reduced in breast cancer patients who were ERβ positive compared with those who were ERβ negative (A). RANKL transcript levels were significantly reduced in breast cancer patients who were ERα positive (B) or ERβ positive (C) compared with those who were ERα negative or ERβ negative respectively. All are normalised against GAPDH. Data are mean ± SEM. N = ERα negative – 67, ERα positive – 34, ERβ negative – 80, ERβ positive – 24. * - p=<0.05, ** - p=<0.01 and *** - p=<0.001.

6.3.2 Oestrogen receptor (ER) status

The link between oestrogen status and breast cancer progression and prognosis is well established. In our cohort RANK transcript levels were found to be significantly reduced in ERβ positive samples compared with ERβ negative samples (Figure 6.2 A p=0.026). RANKL transcripts were shown to be significantly reduced in ERα positive samples compared with ERα negative samples (Figure 6.2 B, p=0.039). A similar trend was also seen with RANKL transcript levels in ERβ positive samples compared with ERβ negative samples (Figure 6.2 C, p=0.036). Similar trends for OPG transcript levels were seen in ERα positive and ERβ positive samples compared with the ER negative samples, however neither of these reached a statistically significant level (Data not shown).

6.3.3 Clinical outcomes of RANK and RANKL in breast cancer

Given the morbidity and mortality rates associated with osteolytic metastases in breast cancer, the potential prognostic implications of OPG, RANK and RANKL transcripts in our cohort were also assessed using their survival outcomes. After the 120 month follow-up of this patient cohort was complete (June 2004), patients were divided into four categories: disease free, with metastasis, with local recurrence or died due to breast cancer.

RANK transcript levels were found to be significantly lower in patients with metastases (p=0.039) or patients who had died from breast cancer (p=0.0052) compared with those who had remained disease free (Figure 6.3 A). In patients who had local recurrence however, RANK transcript levels appeared increased compared to those who had remained disease free, though this did not reach significance. Those who had metastases were further sub-divided into patients with or without bone metastases. Patients with bone metastases, displayed the same

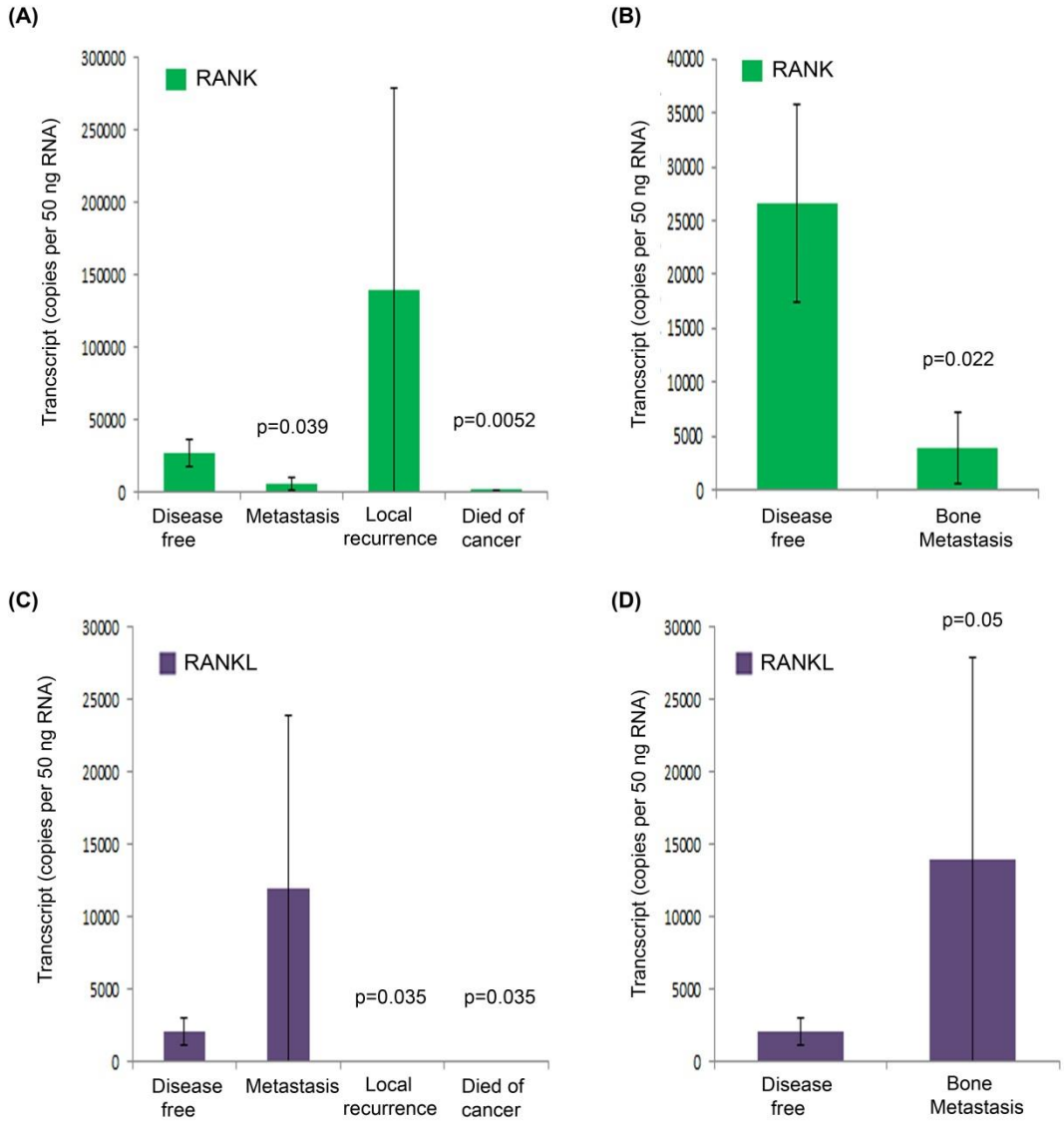

Figure 6.3: Clinical outcomes based on RANK and RANKL transcript expression in clinical breast cancer

RANK transcript levels were significantly reduced in patients who had metastases and those who had died from breast cancer compared with patients who had remained disease free (A). Isolating those patients that had bone metastases, RANK transcript levels were significantly reduced compared with patients who had remained disease free (B). RANKL transcript levels were significantly reduced in patients with local recurrence or who had died from breast cancer (C); however in those with metastases transcript levels were increased. Isolating those patients that had bone metastases, though the trend remained, RANKL transcript levels were significantly increased compared with patients who had remained disease free (D). All are normalised against GAPDH. Data are mean ± SEM.N= Disease free – 78, Metastases – 7, Local recurrence – 5, Died of breast cancer – 14, Bone metastases - 8. * - p=<0.05, ** - p=<0.01 and *** - p=<0.001.

trend as the general metastases group, showing significant reductions in RANK transcript level compared to those patients who remained disease free (Figure 6.3 B, p=0.022).

RANKL transcript levels were found to be significantly reduced in patients with local recurrence (p=0.035) and patients who had died of disease (p=0.035). In contrast, patients with metastases appeared to have increased RANKL transcript levels compared with those who had remained disease free, although this did not reach significant levels (Figure 6.3 C). However when patients with bone metastases were isolated from other metastases groups and compared with those who had remained disease free, RANKL transcript levels were significantly increased in the bone metastases samples compared with those with other metastases (Figure 6.3 D, p=0.05).

6.3.4 Kaplien Meier survival model for OPG, RANK and RANKL in breast cancer

Kaplan Meier survival analysis (Figure 6.4) showed that patients with higher RANK transcripts had significantly longer mean survival rates compared with patients with lower RANK transcripts (Figure 6.4 A; 140 months (95% CI 131-148 months) v 125 months (95% CI 110-139 months) p=0.031). Patients with high RANKL transcripts also had significantly longer mean survival rates compared with those with lower RANKL transcripts (Figure 6.4 B; 147 months (95% CI 138-156 months) v 117 months (95% CI 102 – 132months) p= 0.024). In contrast, high expression levels of OPG transcript were found to correlate with significantly poorer mean overall survival (108 months (95% CI 84-132 months) compared to patients with lower levels of OPG transcript (Figure 6.4 C; 142 months (95% CI 132-151 months) p=0.023). Taking these into account, low levels of OPG transcript combined with

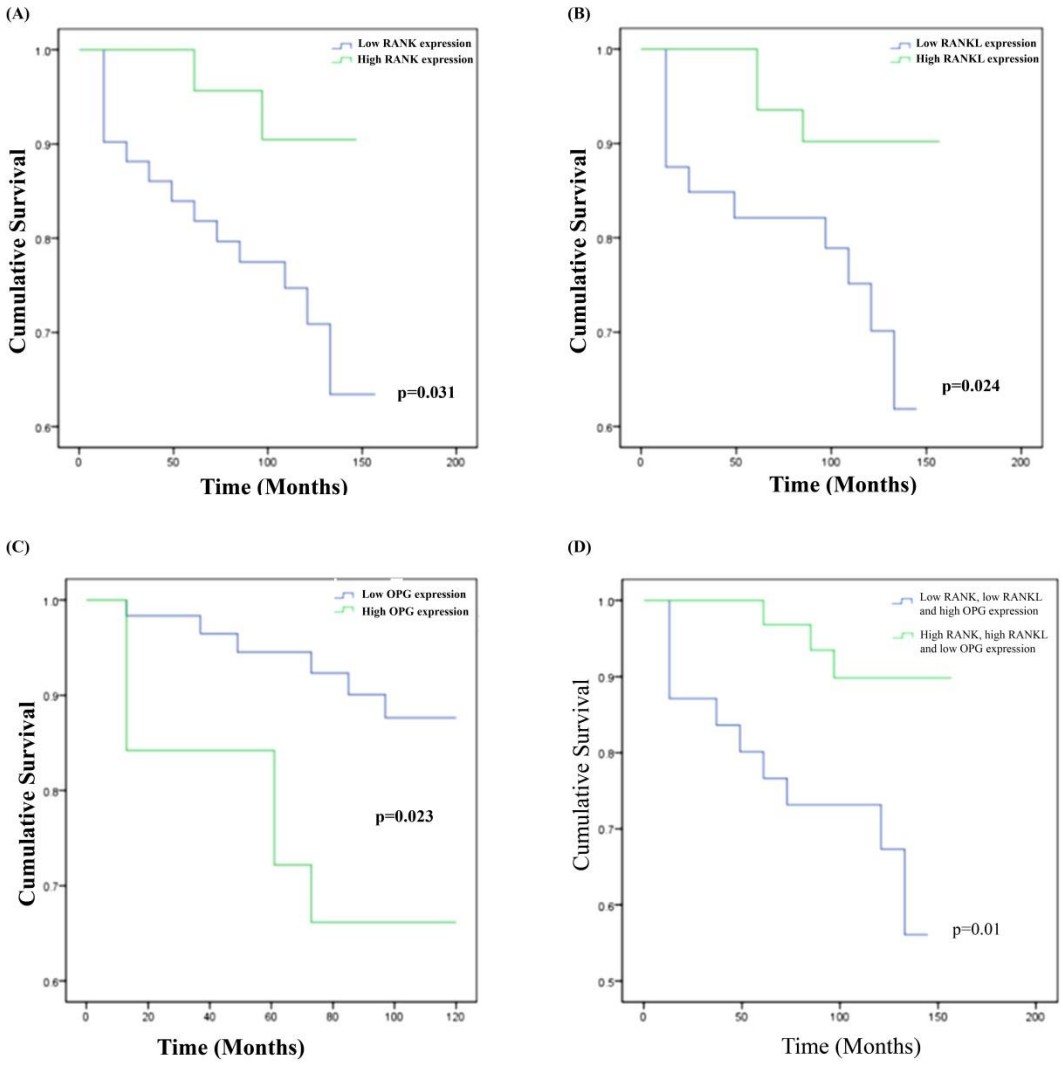

Figure 6.4: Kaplien Meier survival curves for RANK, RANKL and OPG in clinical breast cancer

Patients with low RANK transcript levels had significantly poorer overall survival compared with patients with high RANK transcript levels (A). Low RANKL transcript levels also resulted in significantly poorer long term survival compared with high RANKL transcript levels (B). Low OPG transcript levels correlated with significantly better long term survival compared with patients with high OPG transcript levels (C). As a combined power, low RANK and RANKL transcripts but high OPG transcripts resulted in poorer long term survival compared with patients who had high RANK and RANKL transcript levels but low OPG transcript expression (D). Individual N numbers unknown. * - p=<0.05, ** - p=<0.01 and *** - p=<0.001.

high levels of RANK and RANKL transcript expression were used to look at the potential combined power which OPG, RANK and RANKL transcripts might have on overall survival (Figure 6.4 D). When these factors were combined, patients with low OPG and high RANK and RANKL transcripts had significantly longer mean overall survival (148 months (95% CI 140-156 months p=0.01)) compared with those patients that had high OPG transcript levels and low RANK and RANKL transcript levels (112 months (95% CI 94-129 months) p=0.01).

6.4.1 Expression profiles of OPG, RANK and RANKL in β-oestradiol treated Breast Cancer cells

Based on some of the interesting trends which were seen in the breast cancer cohort, further investigation into the roles of OPG, RANK and RANKL in breast cancer disease progression were investigated *in vitro*.

6.4.1.1 Expression profiles of OPG, RANK and RANKL in breast cancer cells treated with a concentration gradient of β-oestradiol

Noting the observations of ER status and significant difference in RANK and RANKL transcript levels in the clinical cohort, MCF-7 (ER positive) and MDA-MB-231 (ER-negative) breast cancer cells were treated with several concentrations (10^{-7}, 10^{-8}, 10^{-9} and 10^{-10}M) of β-oestradiol for a 2 hour period after which RANK, RANKL and OPG transcript levels were assessed using qPCR (Figure 6.5).

MCF-7 breast cancer cells after treatment with each concentration, exhibited significant decreases in RANK transcript levels. The biggest decreases were seen in MCF-7 breast cancer cells treated with 10^{-7}M or 10^{-8}M β-oestradiol (Figure 6.5 A, p=<0.001 in both cases vs untreated control cells). At the lower treatment

concentrations (10^{-9}M and 10^{-10}M), the decreases in RANK transcript were not as dramatic, though these were still significant (p=0.01 and 0.04 respectively vs untreated control cells). In contrast, in the ER negative breast cancer cell line, MDA-MB-231 all treatments resulted in an increase in RANK transcript expression (Figure 6.7 B). RANK transcript expression appeared to increase significantly under treatment from 10^{-8}, 10^{-9} and 10^{-10}M β-oestradiol, though most notably so at 10^{-8}M (p=0.01, 0.03 and 0.008 respectively vs untreated control cells).

Treatment of MCF-7 breast cancer cells with each concentration of β-oestradiol also appeared to significantly reduce RANKL transcript levels (Figure 6.5 C). The biggest reduction in RANKL transcript expression was seen in MCF-7 cells treated with 10^{-8}M β-oestradiol (p=<0.001 vs untreated control cells). At all other concentrations tested (10^{-7}, 10^{-9} and 10^{-10}M) RANKL transcript expression also appeared to be significantly decreased compared to the control, though these were not as dramatic as that seen at the 10^{-8}M treatment (p=0.04, 0.04 and 0.01 respectively vs untreated control cells). As was observed with the RANK transcript levels, when MDA-MB-231 breast cancer cells were exposed to each of the β-oestradiol concentrations increases in RANKL transcript were observed. The most notable and significant increase in RANKL transcript occurred at β-oestradiol concentration 10^{-8}M (p=0.006 vs untreated control cells). RANKL transcript levels also appeared significantly increased at all the other concentrations tested (10^{-7}, 10^{-9} and 10^{-10}M) compared to the untreated MDA-MB-231 cells (p=0.009 and <0.001 respectively vs untreated control cells).

When MCF-7 breast cancer cells were treated with each concentration of β-oestradiol there appeared to be no significant overall trends observed on OPG transcript levels (Figure 6.5 E). At the lowest concentration tested (10^{-10}M), OPG transcript was significantly reduced compared to the untreated MCF-7 breast cancer treated with different β-oestradiol concentrations (10^{-7}, 10^{-9} and 10^{-10}M) a general

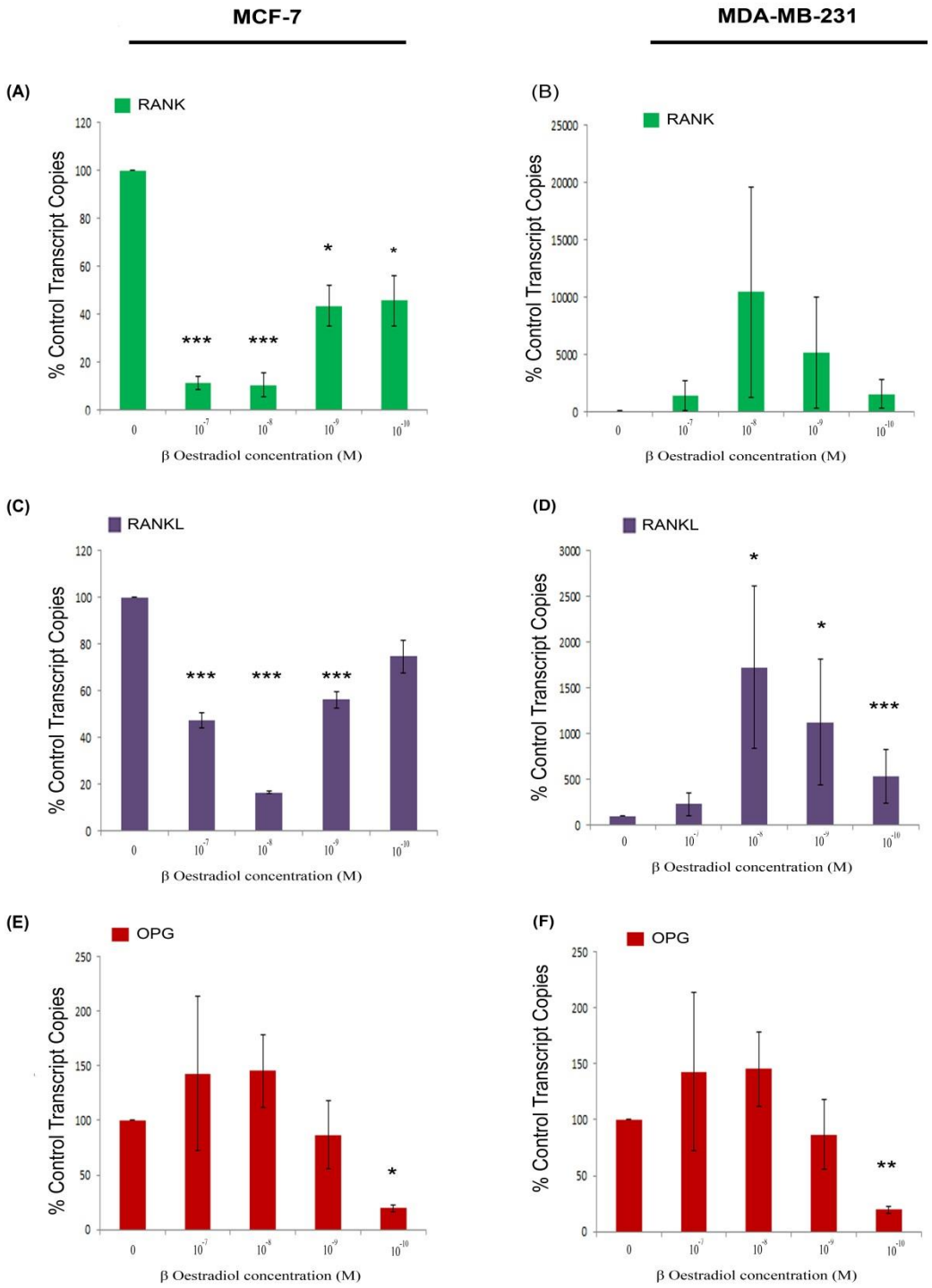

Figure 6.5: RANK, RANKL and OPG transcript levels in response to β-oestradiol treatment over a concentration gradient

RANK and RANKL transcript levels were significantly reduced in MCF-7 cells (A and C respectively) but significantly increased in MDA-MB-231 cells (B and D respectively) treated with different concentrations of β-oestradiol. OPG transcript levels fluctuated in β-oestradiol treated MCF-7 cells (E), but generally resulted in a significant increase in OPG transcript levels in MDA-MB-231 cells (F). Data shown is representative values from one independent repeat normalised against GAPDH with SD. *- p=<0.05, **- p=<0.01, *** - p=<0.001

cells (p=0.04 vs untreated control cells). In contrast, when MDA-MB-231 cells were significant increase in OPG expression was seen (Figure 6.5 F, p=0.02, <0.01 and 0.01 respectively vs untreated control cells).

6.4.1.2 Expression profiles of OPG, RANK and RANKL in β-oestradiol treated breast cancer cells in a time course

Using the results from the concentration gradients, a time course on MCF-7 and MDA-MB-231 breast cancer cells with β-oestradiol treatment (10^{-9}M) was also carried out, after which RANK, RANKL and OPG transcript levels were subsequently screened using qPCR (Figure 6.6).

MCF-7 breast cancer cells incubated with β-oestradiol, initially resulted (0.5 hour and 1 hour) in a slight, though insignificant, decrease in RANK transcript expression compared to the control cells. However, after 2 hours incubation a significant increase and peak in RANK transcript levels was observed (Figure 6.6 A, p=<0.001 vs untreated control cells). At the following two time points, 4 hours and 24 hours, RANK transcript levels still remained significantly elevated compared with the control MCF-7 breast cancer cells (p=0.005 and 0.02 respectively), however these levels were not as high as those that had been observed after 2 hours. In contrast, the MDA-MB-231 breast cancer cells, showed a reduction in RANK transcript expression which was evident after 0.5 hour, however this reduction in RANK transcript levels did not reach a significant level until 1 hour incubation (Figure 6.6 B, p=0.01). This significant reduction in RANK transcript was maintained for all the time points studied (p=0.03, 0.005 and 0.04), but lowest levels were observed after 4 hours incubation.

As seen with the RANK transcript levels, incubation of MCF-7 cells with β-oestradiol resulted in an initial decline in RANKL transcript levels (0.5 hour and 1 hour), before

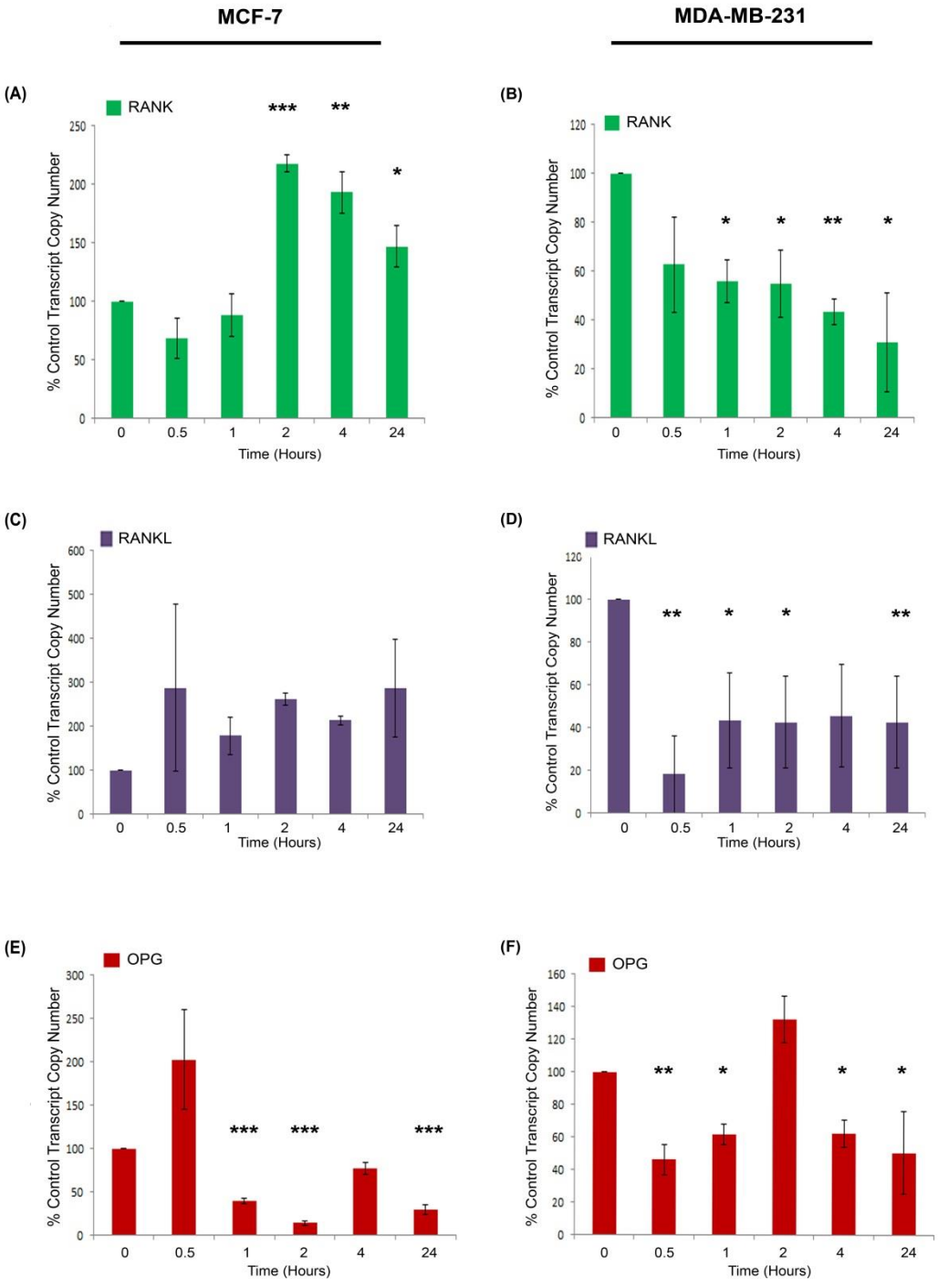

Figure 6.6: RANK, RANKL and OPG transcript levels in response to β-oestradiol treatment over time

RANK and RANKL transcript levels were significantly increased in MCF-7 cells after 2 hours, 4 hours and 24 hours after treatment (A and C respectively). In MDA-MB-231 cells RANK and RANKL transcript levels were significantly reduced at all the time points studied (B and D respectively).OPG transcript expression was significantly reduced in both MCF-7 (E) and MDA-MB-231 (F) treated cells. Data shown is representative values from one independent repeat normalised against GAPDH with SD. *- p=<0.05, **- p=<0.01, *** - p=<0.001

significantly increasing and peaking after 2 hours incubation (Figure 6.6 C, p=0.006). RANKL transcript levels subsequently appeared to reduce, though even after 4 hours incubation with β-oestradiol RANKL transcript levels remained significantly increased compared with control MCF-7 cells (p=0.02). MDA-MB-231 cells incubated with β-oestradiol resulted in a significant decrease in RANKL transcript expression, which was maintained through each of the time points studied (Figure 6.6 D). The biggest decrease in RANKL transcript was observed at the first time point (0.5 hour, p=0.002). In each of the subsequent time points studied, small recoveries were seen in RANKL transcript levels, however the level of RANKL transcript still remain significantly lower compared to the control cells (p=0.05, 0.01 and 0.002 respectively).

Interestingly, OPG transcript levels were significantly affected in both MCF-7 and MDA-MB-231 breast cancer cells when incubated with β-oestradiol over a 24 hour period (Figures 6.6 E and F respectively). Though an initial increase in OPG transcript levels was seen at 0.5 hour in the MCF-7 breast cancer cells, most subsequent time points studied show a significant decrease in OPG transcript levels compared to the control cells (Figure 6.6 E, all p=<0.001). The minor recovery in OPG transcript levels observed after 4 hours incubation was also close to being noted as a significant decrease compared to the control cells (p=0.07). The MDA-MB-231 cells incubated with β-oestradiol also resulted in significant decreases in OPG transcript levels (Figure 6.6 F). There appeared to be an initial significant decrease in OPG transcript levels after 0.5 and 1 hour incubations (p=0.003 and 0.01 respectively). Interestingly, after 2 hours incubation with β-oestradiol, OPG levels appear to recover to similar levels observed in the control cells. However, this recovery is not sustained, cells incubated with β-oestradiol for 4 hours or 24 hours, appeared to show significant reductions which were initially observed in the time course experiment (p=0.02).

6.4.2 Role of OPG in MDA-MB-231 cells *in vitro* and *in vivo*

6.4.2.1 Confirmation of ribozyme transgene knockdown of OPG expression in MDA-MB-231 breast cancer cells

Expression of OPG was successfully targeted in MDA-MB-231 breast cancer cells following transfection with an anti-OPG ribozyme transgene contained within a pEF6 plasmid (Figure 6.7). Following RNA isolation, RT-PCR and qPCR showed significantly reduced OPG transcript expression in MDA-MB-231^{OPGKD} cells to the MDA-MB-231^{pEF6} control cells (Figures 6.7 A and B respectively). Western blot analysis subsequently confirmed the knockdown of OPG at a protein level in comparison to the MDA-MB-231^{pEF6} control cells (Figure 6.7 C).

6.4.2.2 Effect of OPG suppression on MDA-MB-231 cell proliferation in vitro

Reduced OPG expression in MDA-MB-231 breast cancer cells resulted initially in an increase in cell proliferation compared to the MDA-MB-231^{pEF6} control cells (132% compared to control) (Figure 6.8 A); however, this trend did not reach significance. This trend was not continued over a 5 day incubation period (Figure 6.8 B). MDA-MB-231^{OPGKD} cells actually showed no difference in cell proliferation compared to the MDA-MB-231^{pEF6} control cells (98% compared to control).

When MDA-MB-231^{pEF6} control cells were treated with 40ng/ml HGF, 50µg/ml BME or a combination of 40ng/ml HGF and 50µg/ml BME, after 3 days incubation all treatments resulted in increased cell proliferation (113%, 131% and 129% of untreated control respectively) (Figure 6.8 C). However none of these reached significant levels. This trend of increased MDA-MB-231^{pEF6} control cell proliferation continued over the 5 day incubation period as well (116%, 117% and 113% of untreated control respectively) (Figure 6.8 D). After 5 days incubation with 40ng/ml

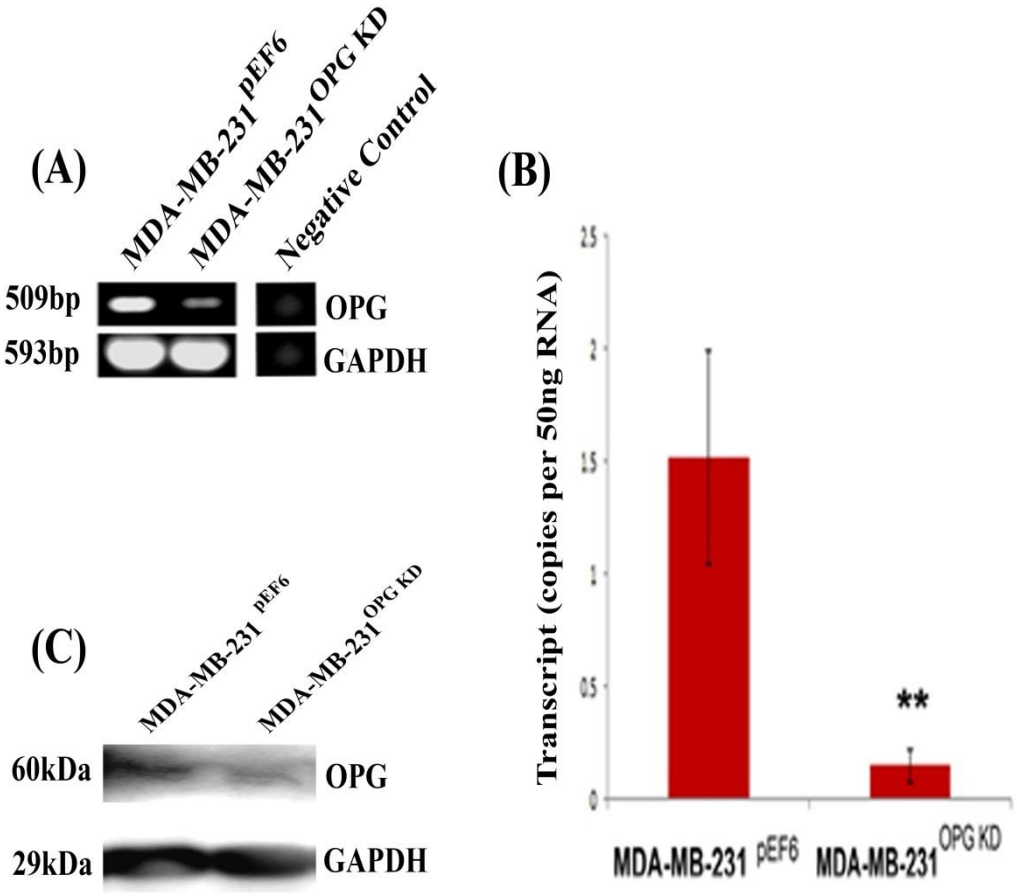

Figure 6.7: Verification of ribozyme transgene knockdown of OPG in MDA-MB-231 cells

Reduced expression of OPG was confirmed at a transcript level using RT-PCR (A) and qPCR (B) compared to the control cell line. Western blot (C) was used to confirm knockdown of OPG at a protein level. PCR and Western blot were normalised against GAPDH. Control = Nuclease free water and all gels were ran with a molecular weight marker used to identify band sizes. Representative images and data shown. * - p=<0.05, ** - p=<0.01 and *** - p=<0.001.

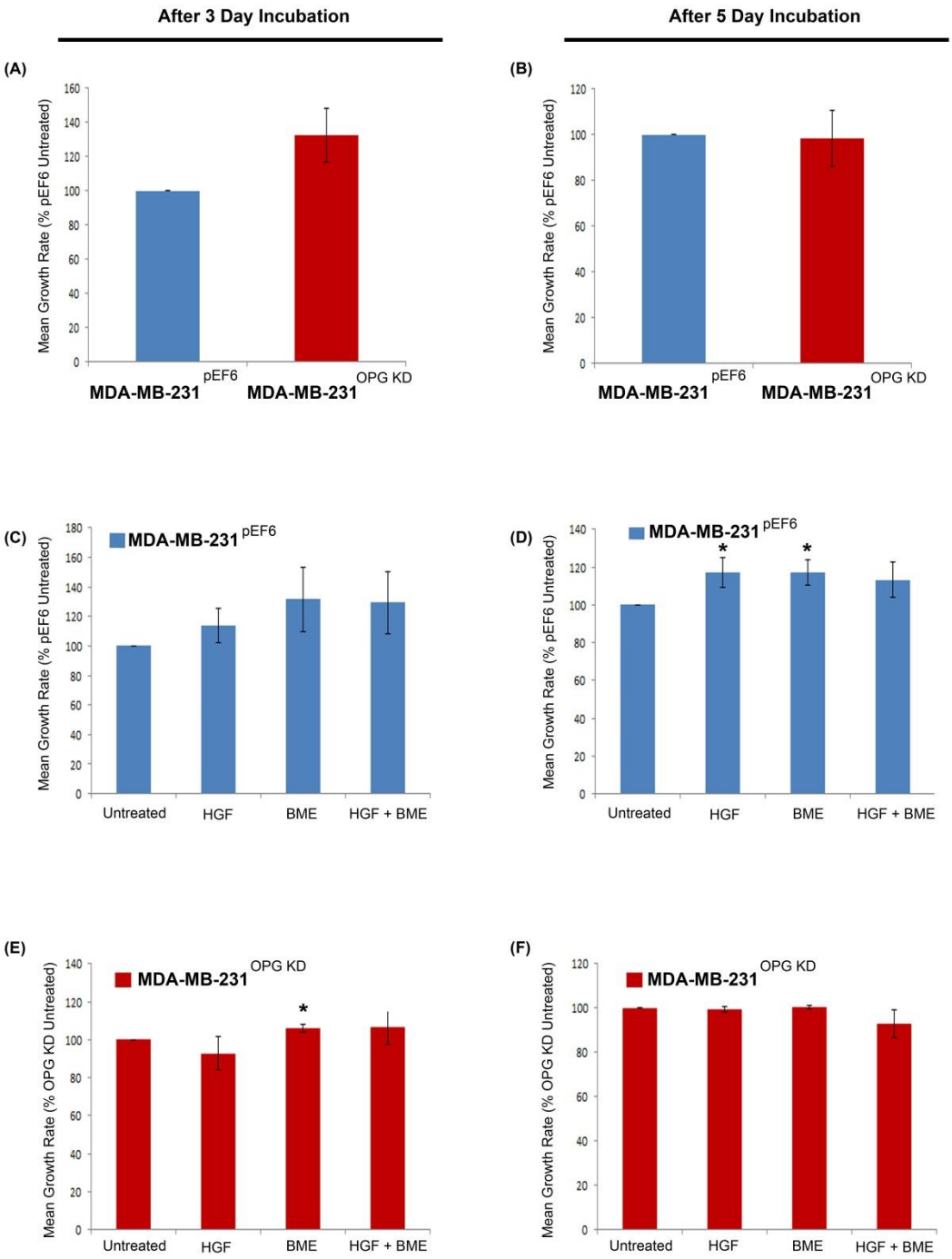

Figure 6.8: Impact of OPG knockdown on MDA-MB-231 cell proliferation *in vitro*

Reduced OPG expression resulted in increased MDA-MB-231 cell proliferation after 3 days incubation (A) compared to control cells, however this trend was not continued over 5 days incubation (B). Treatment of the MDA-MB-231^{pEF6} control cell line with 40ng/ml HGF, 50µg/ml BME or a combination of 40ng/ml HGF and 50µg/ml BME resulted in an increase in cell proliferation after 3 days incubation (C), which reached significant levels after 5 days incubation (D). Treatment of MDA-MB-231^{OPGKD} cells with 40ng/ml HGF, 50µg/ml BME or a combination of 40ng/ml HGF and 50µg/ml BME resulted in a minor increased in cell proliferation after 3 days (E) which was not seen after 5 days (F). Data represents mean of 4 independent repeats, error bars represent SEM. * - p=<0.05, ** - p=<0.01 and *** - p=<0.001.

HGF or 50µg/ml BME, MDA-MB-231^{pEF6} control cell proliferation was shown to be significantly increased (p=0.029). However, in the combined treatment of 40ng/ml HGF and 50µg/ml BME resulted in increased MDA-MB-231^{pEF6} control cell proliferation, this also did not reach significance.

When MDA-MB-231^{OPGKD} cells were incubated with 40ng/ml HGF for 3 days, there was a small but non-significant decrease in cell growth (92% of untreated control) (Figure 6.8 E). When MDA-MB-231^{OPGKD} cells were incubated with 50µg/ml BME, for 3 days, a very small increase in cell proliferation was observed, which was deemed significant (105% of untreated control, p=0.029). A similar observation was seen when MDA-MB-231^{OPGKD} cells were incubated with combined treatment of 40ng/ml HGF and 50µg/ml BME, however this did not reach significance (106% of untreated control). When MDA-MB-231^{OPGKD} cells were incubated with 40ng/ml HGF or 50µg/ml BME for 5 days, no apparent difference was seen between the treated and untreated MDA-MB-231^{OPGKD} cells (99% and 100% of untreated control respectively) (Figure 6.8 F). When MDA-MB-231^{OPGKD} cells were incubated with a combined treatment of 40ng/ml HGF and 50µg/ml BME for 5 days, a minor decrease in cell MDA-MB-231^{OPGKD} cell proliferation was observed however this again did not reach significance (92% of untreated control).

6.4.2.3 Suppression of OPG reduces MDA-MB-231 cell-matrix adhesion in vitro

MDA-MB-231^{OPGKD} cells showed reduced cell-matrix adhesion *in vitro* compared to MDA-MB-231^{pEF6} control cells (88% compared to control), however this change did not reach a significant level (Figure 6.9 A).

Treatment of MDA-MB-231^{pEF6} control cells with 40ng/ml HGF or 50µg/ml BME did not appear to have any significant impact on cell-matrix adhesion *in vitro* (105% and 102% of untreated control) (Figure 6.9 B representative images from one repeat in

Figure 6.9 D). Interestingly when MDA-MB-231^{pEF6} control cells were treated with both 40ng/ml HGF and 50µg/ml BME a very small decrease in cell-matrix adhesion was observed (95% of untreated control), though again this trend was not significant.

As seen with the MDA-MB-231^{pEF6} control cells, when MDA-MB-231^{OPGKD} cells were treated with 40ng/ml HGF a small non-significant increase in cell-matrix adhesion was observed (107% of untreated control) (Figure 6.9 C). Interestingly, when MDA-MB-231^{OPGKD} cells were treated with 50µg/ml BME a small decrease in cell-matrix adhesion was observed (92% of untreated control), however this did not reach significance. Of further interest was when MDA-MB-231^{OPGKD} cells were treated with a combination of 40ng/ml HGF and 50µg/ml BME cell-matrix adhesion was significantly decreased compared to untreated MDA-MB-231^{OPGKD} cells (83% of untreated control, p=0.024).

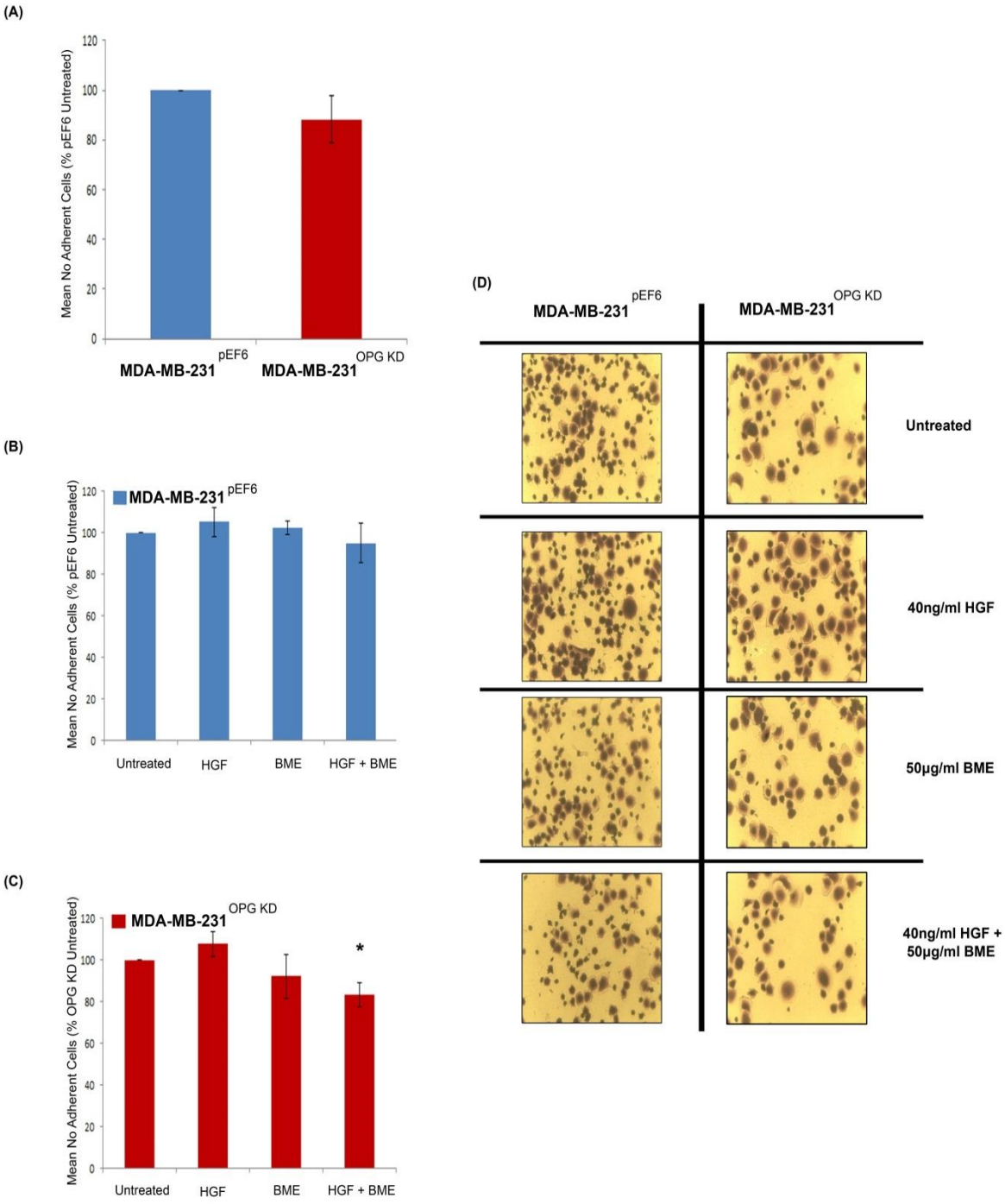

Figure 6.9: Impact of reduced OPG expression in MDA-MB-231 cells on cell-matrix adhesion *in vitro*

Reduced OPG expression resulted in a small but non-significant decrease in MDA-MB-231 cell-matrix adhesion compared with control cells (A). When MDA-MB-231^{pEF6} control cells were treated with 40ng/ml HGF or 50µg/ml BME, small increases in cell-matrix adhesion were seen (B), however combination of these treatments resulted in a decrease in cell-matrix adhesion. In the MDA-MB-231^{OPGKD} cells were treated with 40ng/ml HGF cell-matrix adhesion increased, however under 50µg/ml BME or combined HGF and BME treatment cell matrix adhesion decreased. Representative images from one repeat (D). Data represents mean of 4 independent repeats, error bars represent SEM. * - p=<0.05, ** - p=<0.01 and *** - p=<0.001.

6.4.2.4 OPG suppression significantly increases MDA-MB-231 cell motility in vitro

Knockdown of OPG in MDA-MB-231 cells resulted in significantly increased cell motility compared to the MDA-MB-231^{pEF6} control cells (314% compared to control) (Figure 6.10 A, p=0.029).

When the MDA-MB-231^{pEF6} control cells were treated with 40ng/ml HGF an increase in cell motility was observed (133% of untreated control), however this was not deemed significant (Figure 6.10 B). Interestingly when the MDA-MB-231^{pEF6} control cells were treated with 50µg/ml BME a small non-significant decrease in cell motility was observed (93% of untreated control). However, when 40ng/ml HGF and 50µg/ml BME were combined, MDA-MB-231^{pEF6} control cells showed a significant increase in MDA-MB-231 cell motility (117% of untreated control, p=0.029).

MDA-MB-231^{OPGKD} cells treated with 40ng/ml HGF or 50µg/ml BME showed a decrease in cell motility compared to the untreated MDA-MB-231^{OPGKD} cells (83% and 85% of untreated control respectively) (Figure 6.10 C). Interestingly, when MDA-MB-231^{OPGKD} cells were treated with both 40ng/ml HGF and 50µg/ml BME an increase in cell motility was observed (112% of untreated control); however this did not reach significance.

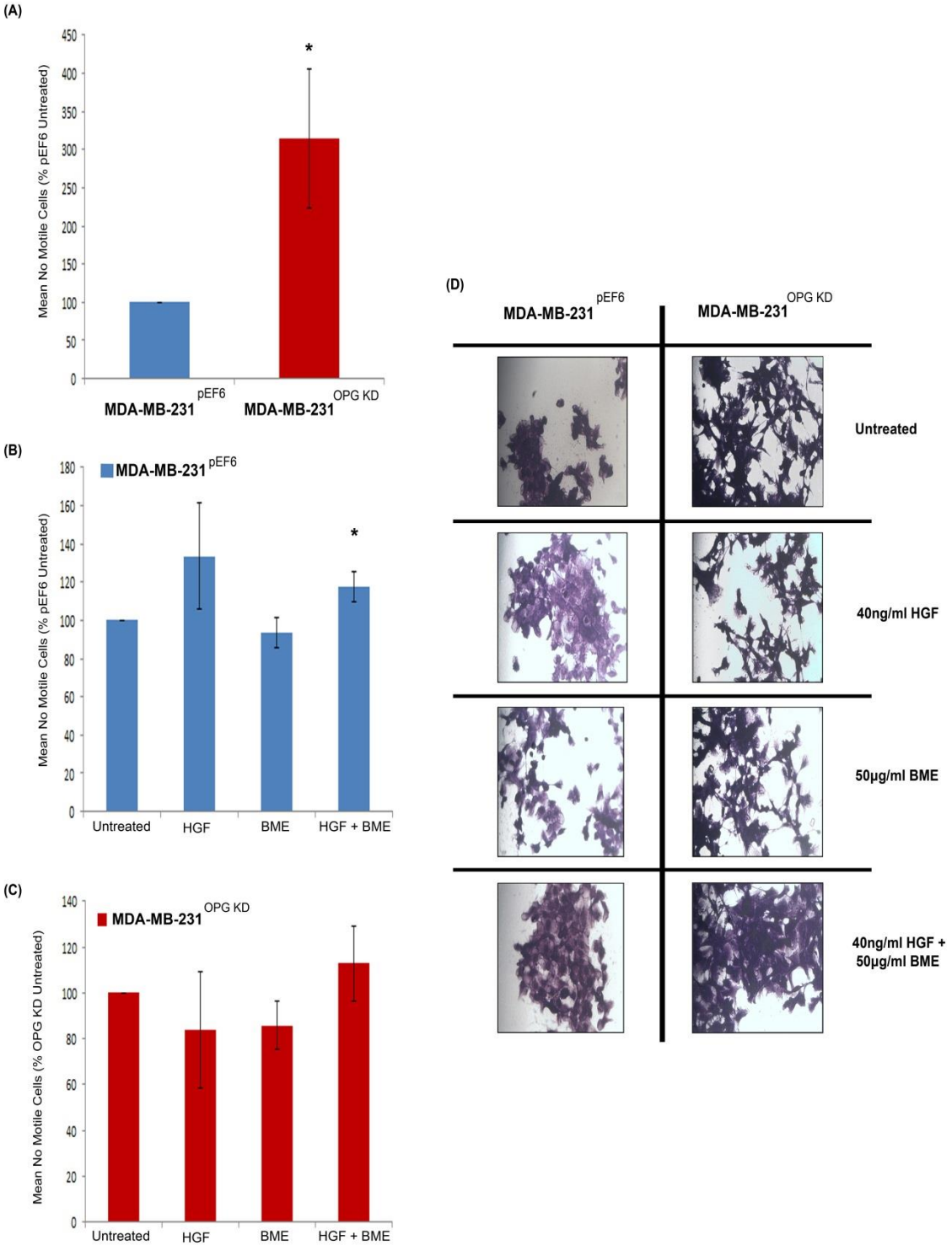

Figure 6.10: Effect of OPG knockdown on MDA-MB-231 cell motility
MDA-MB-231^{OPGKD} cells showed significantly increased motility compared with MDA-MB-231^{pEF6} control cells (A). Treatment of MDA-MB-231^{pEF6} control cells with 40ng/ml HGF or a combination of 40ng/ml HGF and 50µg/ml BME increased cell motility (B), though solo treatment of 50µg/ml BME appeared to have little effect. Treatment of MDA-MB-231^{OPGKD} cells with 40ng/ml HGF or 50µg/ml BME resulted in a decrease in cell motility (C), however the combined treatment of 40ng/ml HGF and 50µg/ml BME resulted in an increase in cell motility. Representative images from one repeat (D). Data represents mean of 4 independent repeats, error bars represent SEM. * - p=<0.05, ** - p=<0.01 and *** - p=<0.001.

6.4.2.5 OPG suppression significantly enhanced MDA-MB-231 cell invasion in vitro

When OPG expression was reduced in MDA-MB-231 cells, cell invasion *in vitro* was significantly increased compared to the MDA-MB-231^{pEF6} control cells (137% of control) (Figure 6.11 A, p=0.037).

When MDA-MB-231^{pEF6} control cells were treated with 40ng/ml HGF cell invasion was increased (118% of untreated control), however this result did not reach significance (Figure 6.11 B). A similar trend was seen when MDA-MB-231^{pEF6} control cells were treated with 50µg/ml BME (126% of untreated control), a result which just reached significance (p=0.05). However when 40ng/ml HGF and 50µg/ml BME were added together to MDA-MB-231^{pEF6} control cells, there was no difference in cell invasion compared to the untreated MDA-MB-231^{pEF6} control cells (104% of untreated control cells).

When the same treatments were added to MDA-MB-231^{OPGKD} cells no further increase in cell invasion was observed. The 40ng/ml HGF treatment resulted in a significant decrease in MDA-MB-231^{OPGKD} cell invasion (92% of untreated control) (Figure 6.11 C, p=0.002). This decrease observed in cell invasion after the HGF treatment resulted in levels returning to similar levels observed in untreated MDA-MB-231^{pEF6} control cells as seen in the representative images (Figure 6.11 D) (Data not shown). Treatment of MDA-MB-231^{OPGKD} cells with 50µg/ml BME resulted in a noticeable decrease in MDA-MB-231 cell invasion (83% of untreated control), as seen in the representative images (Figure 6.11 D); however this trend was not found to be significant. Treatment of MDA-MB-231^{OPGKD} cells with 40ng/ml HGF and 50µg/ml BME also resulted in a significant decrease in MDA-MB-231 cell invasion *in vitro* (90% of untreated control) (p=0.013).

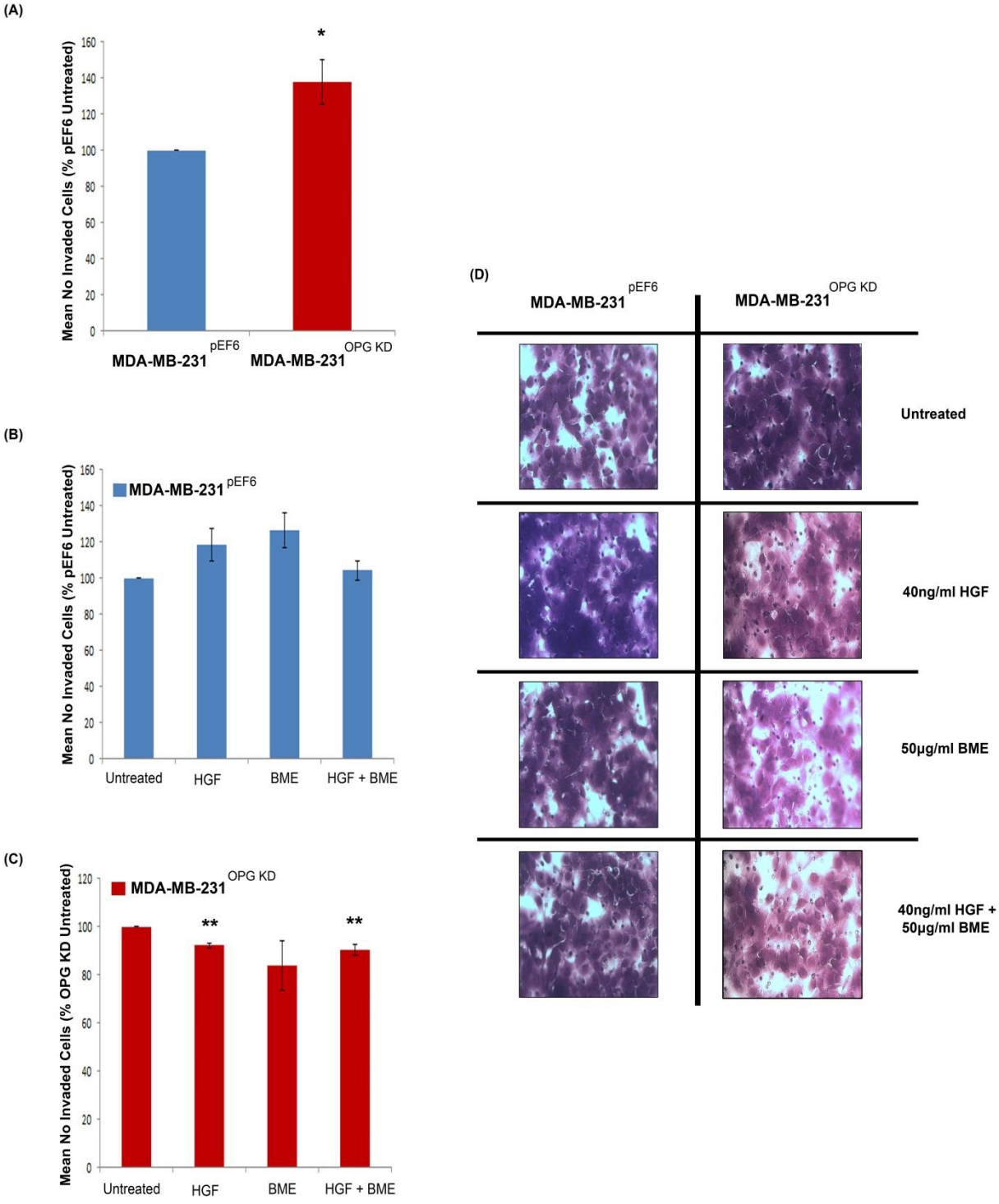

Figure 6.11: Impact of reduced OPG expression on MDA-MB-231 cell invasion *in vitro*

MDA-MB-231^{OPGKD} cells showed significantly increased cell invasion compared with MDA-MB-231^{pEF6} control cells (A). Treatment of MDA-MB-231^{pEF6} control cells with 40ng/ml HGF, 50µg/ml BME or a combination of 40ng/ml HGF and 50µg/ml BME increased cell invasion (B). Treatment of MDA-MB-231^{OPGKD} cells with 40ng/ml HGF, 50µg/ml BME or a combination of 40ng/ml HGF and 50µg/ml BME resulted in a decrease in cell invasion. Representative images from one repeat (D). Data represents mean of 3 independent repeats, error bars represent SEM. * - p=<0.05, ** - p=<0.01 and *** - p=<0.001.

6.4.2.6 OPG suppression significantly increased MDA-MB-231 cell growth in vivo

A preliminary *in vivo* study was conducted using a xenograft model in athymic mice (Figure 6.12). The MDA-MB-231^{OPGKD} cells, subcutaneously inoculated, showed a significant increase in growth and tumour development compared to the MDA-MB-231^{pEF6} control cells ($p=<0.001$). This reflected the increased MDA-MB-231 cell proliferation that was initially observed *in vitro* after 3 days incubation, though does not support the observations from the extended incubation period (5 days) (Figure 6.8 A).

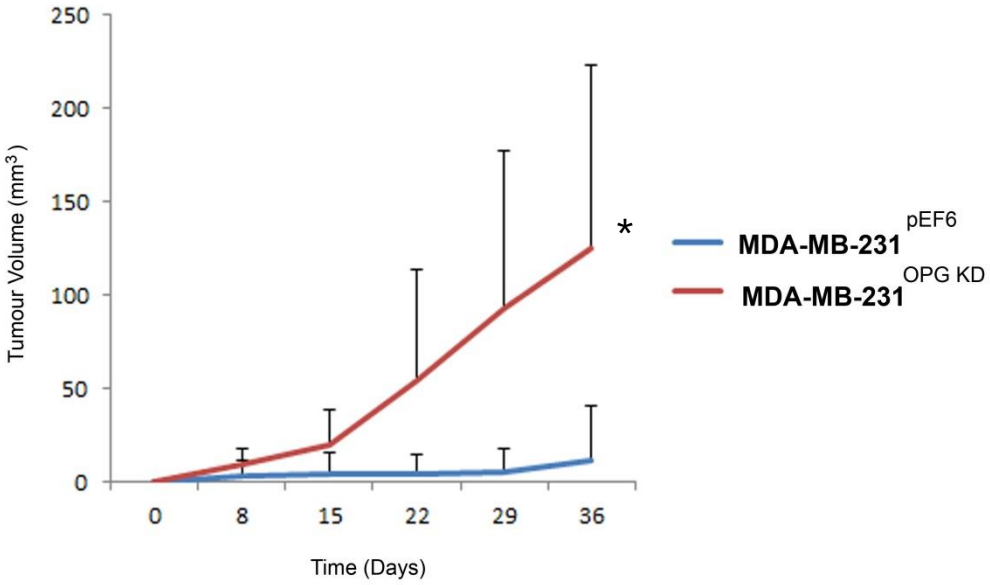

Figure 6.12: Effect of MDA-MB-231^{OPGKD} on cell growth *in vivo*
In the xenograft model, MDA-MB-231^{OPGKD} cells showed a significant increase in growth compared to the MDA-MB-231^{pEF6} control cells (p=<0.001). Tumour volume = 0.523xWidth^{2}xlength. N for each group = 6.

6.4.3 Role of RANK in MDA-MB-231 cells *in vitro*

6.4.3.1 Confirmation of ribozyme transgene knockdown of RANK expression in MDA-MB-231 breast cancer cells

Expression of RANK was successfully targeted in MDA-MB-231 breast cancer cells following transfection with an anti-RANK ribozyme transgene contained within a pEF6 plasmid (Figure 6.13). Following RNA isolation, RT-PCR and qPCR showed successful knockdown of RANK expression in MDA-MB-231 cells at a transcript level compared to the MDA-MB-231^{pEF6} control cell line (Figures 6.13 A and B respectively). Western blot analysis subsequently confirmed the knockdown of RANK at a protein level compared to the MDA-MB-231^{pEF6} control cells (Figure 6.13 C).

6.4.3.2 RANK suppression significantly reduces MDA-MB-231 breast cancer cell growth in vitro

Suppression of RANK expression in MDA-MB-231 cells resulted in a decrease in MDA-MB-231 cell proliferation after 3 day incubation compared with MDA-MB-231^{pEF6} control cells (91% compared to control) (Figure 6.14 A), a trend which reached significance after 5 days incubation (53% compared to control) (Figure 6.14 B, $p=0.029$).

When MDA-MB-231^{pEF6} control cells were treated with 40ng/ml HGF after 3 days incubation, MDA-MB-231 cell proliferation was increased (113% of untreated control) (Figure 6.14 C). This was a trend which continued after 5 days incubation at which point it reach significance (Figure 6.14 D, 116% of untreated control, $p=0.029$). A similar trend was observed in MDA-MB-231^{pEF6} control cells treated with 50µg/ml BME, which after 5 days incubation resulted in MDA-MB-231^{pEF6}

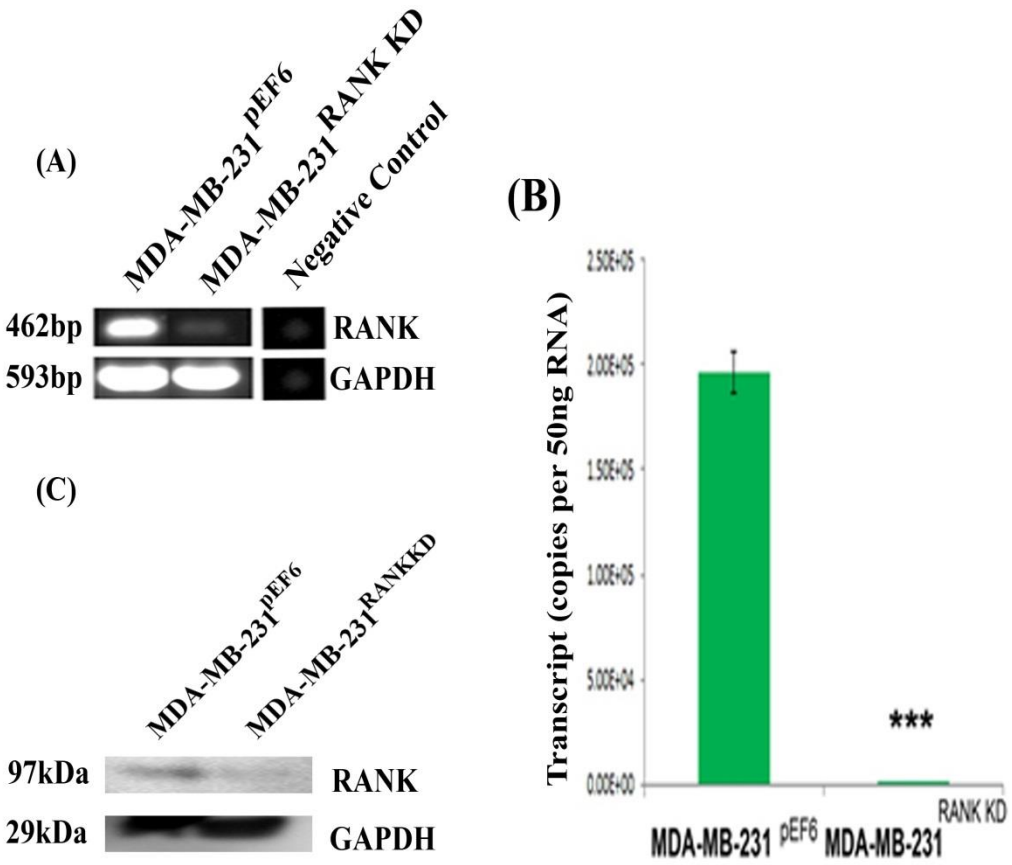

Figure 6.13: Verification of successful ribozyme transgene knockdown of RANK expression in MDA-MB-231 cells

Reduced expression of RANK was confirmed at a transcript level using RT-PCR (A) and qPCR (B) compared to the control cell line. Western blot (C) was used to confirm knockdown of RANK at a protein level. PCR and Western blot were normalised against GAPDH. Control = Nuclease free water and all gels were ran with a molecular weight marker used to identify band sizes. Representative images and data shown. * - p=<0.05, ** - p=<0.01 and *** - p=<0.001.

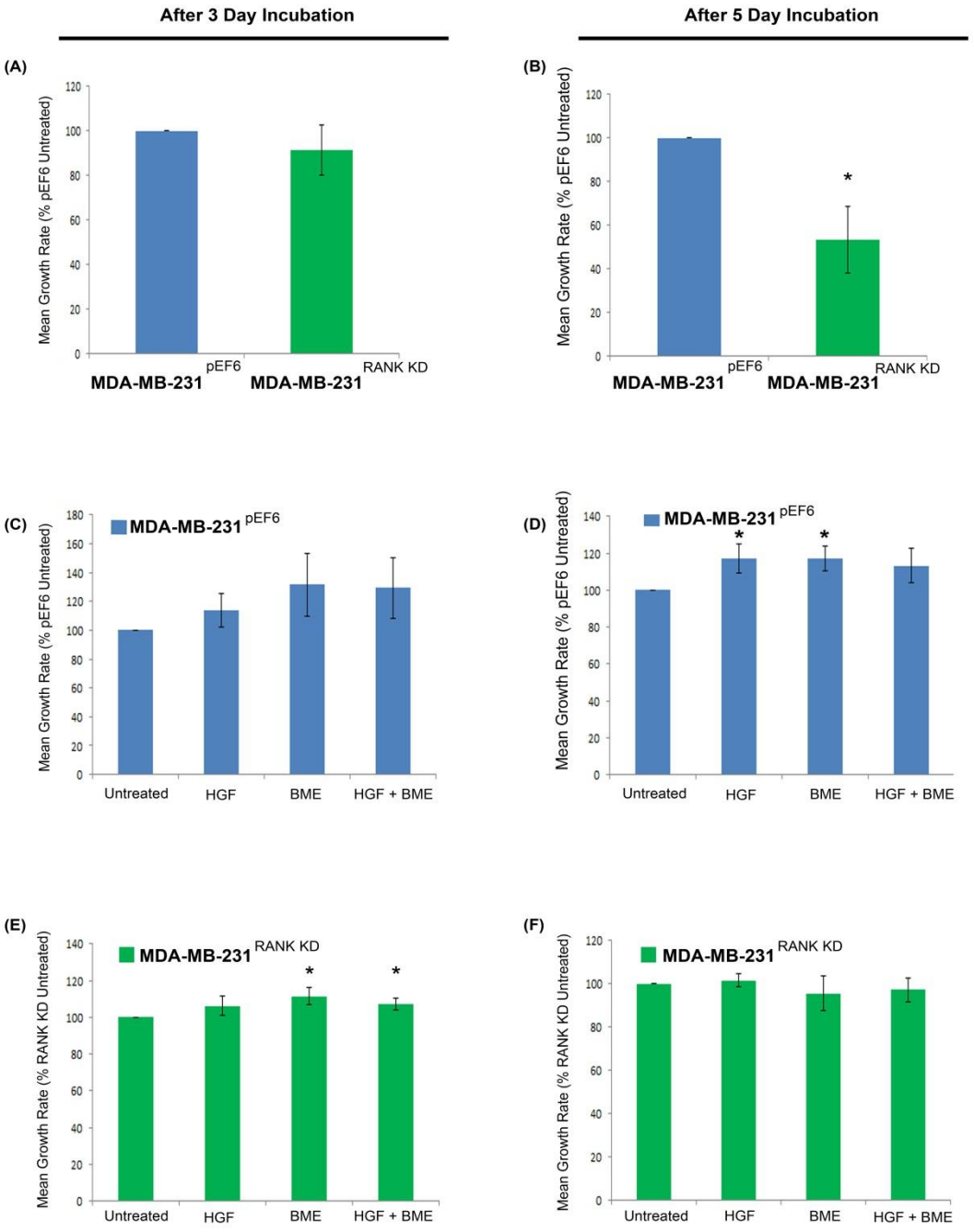

Figure 6.14: Effects of reduced RANK expression on MDA-MB-231 cell proliferation *in vitro*

Reduced RANK expression in MDA-MB-231 cells resulted in a decrease in cell proliferation after 3 days incubation (A) which became significant after 5 days incubation (B) compared with control cells. Treatment of the MDA-MB-231^{pEF6} control cell line with 40ng/ml HGF, 50µg/ml BME or a combination of 40ng/ml HGF and 50µg/ml BME resulted in an increase in cell proliferation after 3 days incubation (C), which reached significant levels after 5 days incubation (D). Treatment of MDA-MB-231^{RANKKD} cells with 40ng/ml HGF, 50µg/ml BME or a combination of 40ng/ml HGF and 50µg/ml BME resulted in an increase in cell proliferation after 3 days incubation (E), however this trend was not seen over a 5 day incubation period (F). Data represents mean of 4 independent repeats, error bars represent SEM. * - p=<0.05, ** - p=<0.01 and *** - p=<0.001.

treated cells showing a significant increase in cell proliferation (131% of untreated control after 3 days incubation, 117% of untreated control after 5 days incubation, p=0.029). The combination of 40ng/ml HGF and 50µg/ml BME, after 3 and 5 days incubation also resulted in increased cell proliferation (129% and 113% of untreated control respectively) (Figure 6.14 C and D respectively). However, neither of these increases reached significant levels.

When MDA-MB-231^{RANKKD} cells were treated with 40ng/ml HGF non-significant differences in cell proliferation were observed after 3 and 5 days incubation compared with untreated MDA-MB-231^{RANKKD} cells (106% and 101% of untreated control respectively) (Figure 6.14 E and F respectively). MDA-MB-231^{RANKKD} cells incubated with 50µg/ml BME for 3 days resulted in a significant increase in cell proliferation compared with untreated MDA-MB-231^{RANKKD} cells (111% of untreated control, p=0.029). However, this trend was not continued to the 5 day incubation period, in the 50µg/ml BME MDA-MB-231^{RANKKD} cell proliferation was actually slightly reduced compared with the untreated MDA-MB-231^{RANKKD} cells (95% of untreated control) (Figure 6.14 F). When MDA-MB-231^{RANKKD} cells were treated with 40ng/ml HGF and 50µg/ml BME after 3 days incubation, cell proliferation was significantly increased compared with untreated MDA-MB-231^{RANKKD} cells (Figure 6.14 E, 107% of untreated control, p=0.029). This trend was not continued over the 5 day incubation period, the combined treatment of 40ng/ml HGF and 50µg/ml BME resulted in a slight decrease in MDA-MB-231^{RANKKD} cell proliferation (97% of untreated control), though again like the individual 50µg/ml BME treatment this decrease did not reach significance (Figure 6.14 F).

6.4.3.3 RANK suppression significantly reduces MDA-MB-231 breast cancer cell-matrix adhesion

Reduced RANK expression in MDA-MB-231 cells resulted in a significant decrease in cell-matrix adhesion *in vitro* compared with MDA-MB-231^{pEF6} control cells (55% of control) (Figure 6.15 A, p=0.029, representative images Figure 6.15 D).

Treatment of MDA-MB-231^{pEF6} control cells with 40ng/ml HGF or 50µg/ml BME resulted in minor increases in cell-matrix adhesion *in vitro* (105% and 102% of untreated control respectively) (Figure 6.15 B). Both these trends were negligible and non-significant compared to the untreated MDA-MB-231^{pEF6} control cells. However, when MDA-MB-231^{pEF6} control cells were treated with both 40ng/ml HGF and 50µg/ml BME a decrease in cell-matrix adhesion was observed (95% of untreated control), though again this difference was not great enough to be significant.

MDA-MB-231^{RANKKD} cells under the influence of 40ng/ml HGF resulted in an increase in cell-matrix adhesion (130% of untreated control), however this increase was not significant (Figure 6.15 C). When MDA-MB-231^{RANKKD} cells were treated with 50µg/ml BME an increase in cell-matrix adhesion was observed (143% of untreated control), this was a greater increase than that seen after treatment with 40ng/ml HGF, though again this trend did not reach significance (p=0.343). A similar pattern was also seen when MDA-MB-231^{RANKKD} cells were treated with 40ng/ml HGF and 50µg/ml BME. An increase in cell-matrix adhesion was observed (124% of untreated control), though this trend was not as dramatic as that seen under the individual treatments, and therefore did not reach significance.

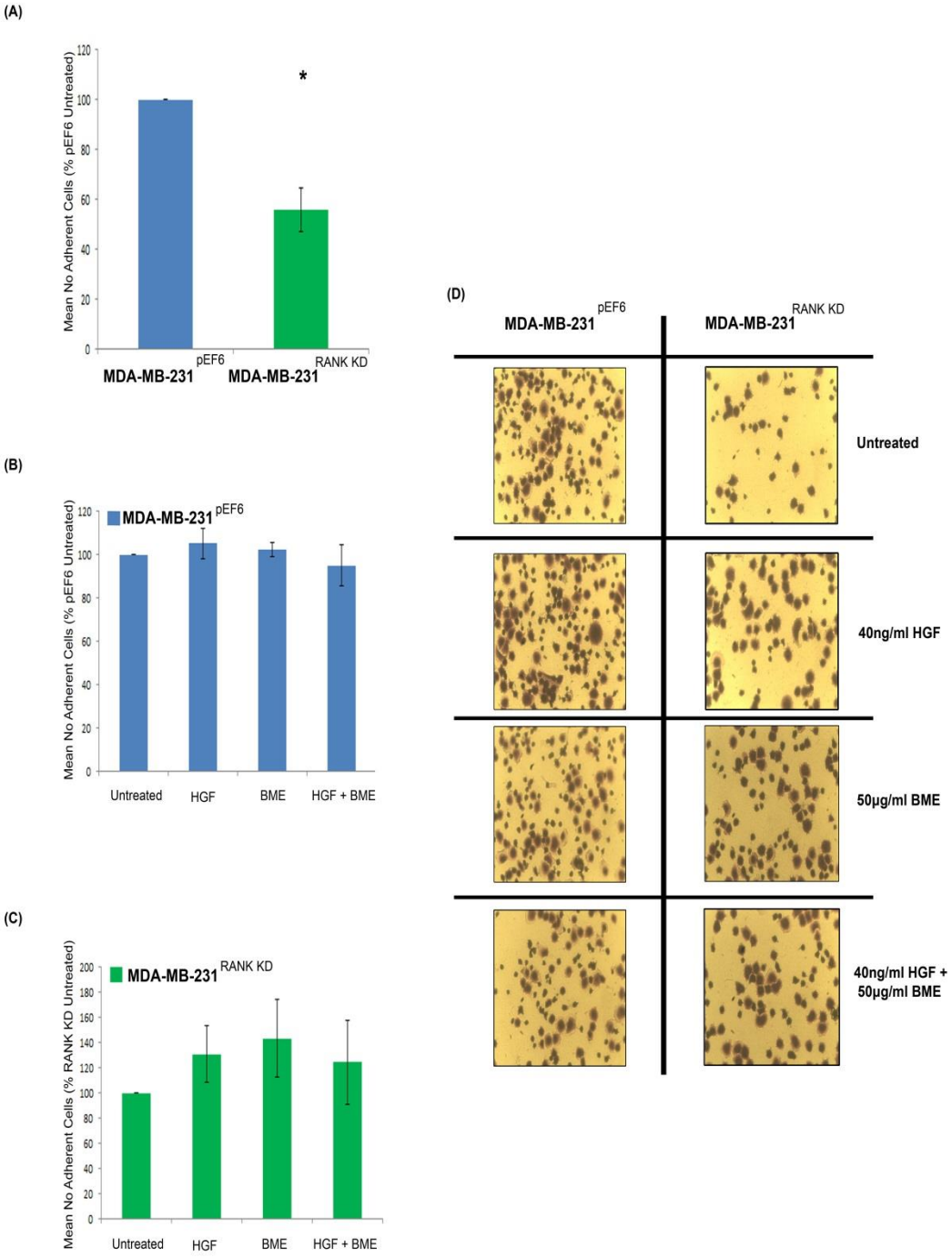

Figure 6.15: Effect of RANK knockdown on cell-matrix adhesion in MDA-MB-231 cells *in vitro*

Reduced RANK expression resulted in a significant decrease in MDA-MB-231 cell-matrix adhesion compared with control cells (A). When MDA-MB-231^{pEF6} control cells were treated with 40ng/ml HGF or 50µg/ml BME, small increases in cell-matrix adhesion were seen (B), however combination of these treatments resulted in a decrease in cell-matrix adhesion. MDA-MB-231^{RANKKD} cells treated with 40ng/ml HGF, 50µg/ml BME or combined HGF and BME increases in cell-matrix adhesion were seen compared with untreated MDA-MB-231^{RANKKD} cells. Representative images from one repeat (D). Data represents mean of 4 independent repeats, error bars represent SEM. * - p=<0.05, ** - p=<0.01 and *** - p=<0.001.

6.4.3.4 RANK suppression significantly reduced MDA-MB-231 breast cancer cell motility in vitro

MDA-MB-231^{RANKKD} cells exhibited significantly decreased cell motility compared to MDA-MB-231^{pEF6} control cells (53% of control) (Figure 6.16 A, p=<0.001, representative images in Figure 6.16 D). Though cell motility decreased, cell aggregation appeared similar in both the MDA-MB-231^{RANKKD} cells and the MDA-MB-231^{pEF6} control cells.

MDA-MB-231^{pEF6} control cells treated with 40ng/ml HGF, 50µg/ml BME or a combination of 40ng/ml HGF and 50µg/ml BME resulted in increased cell motility (113%, 104% and 105% of untreated control respectively), though none of these trends reached significance (Figure 6.16 B). Cell aggregation appeared to be a major trend in these treated cells (Representative images Figure 6.16 D).

Similar responses to each treatment were seen in the MDA-MB-231^{RANKKD} cells. MDA-MB-231^{RANKKD} cell treated with 40ng/ml HGF resulted in an increase in cell motility compared to the untreated MDA-MB-231^{RANKKD} cells (119% of untreated control); however this did not reach a significant level (Figure 6.16 C). Similar observations were also seen with MDA-MB-231^{RANKKD} cells that had been treated with 50µg/ml BME (113% of untreated control) or a combination of 40ng/ml HGF and 50µg/ml BME (111% of untreated control). Both these trends did not reach significance. In the individual 40ng/ml HGF or 50µg/ml BME treatments MDA-MB-231^{RANKKD} cells appeared to be less aggregated compared to the untreated cells and the combined 40ng/ml HGF and 50µg/ml BME treated cells.

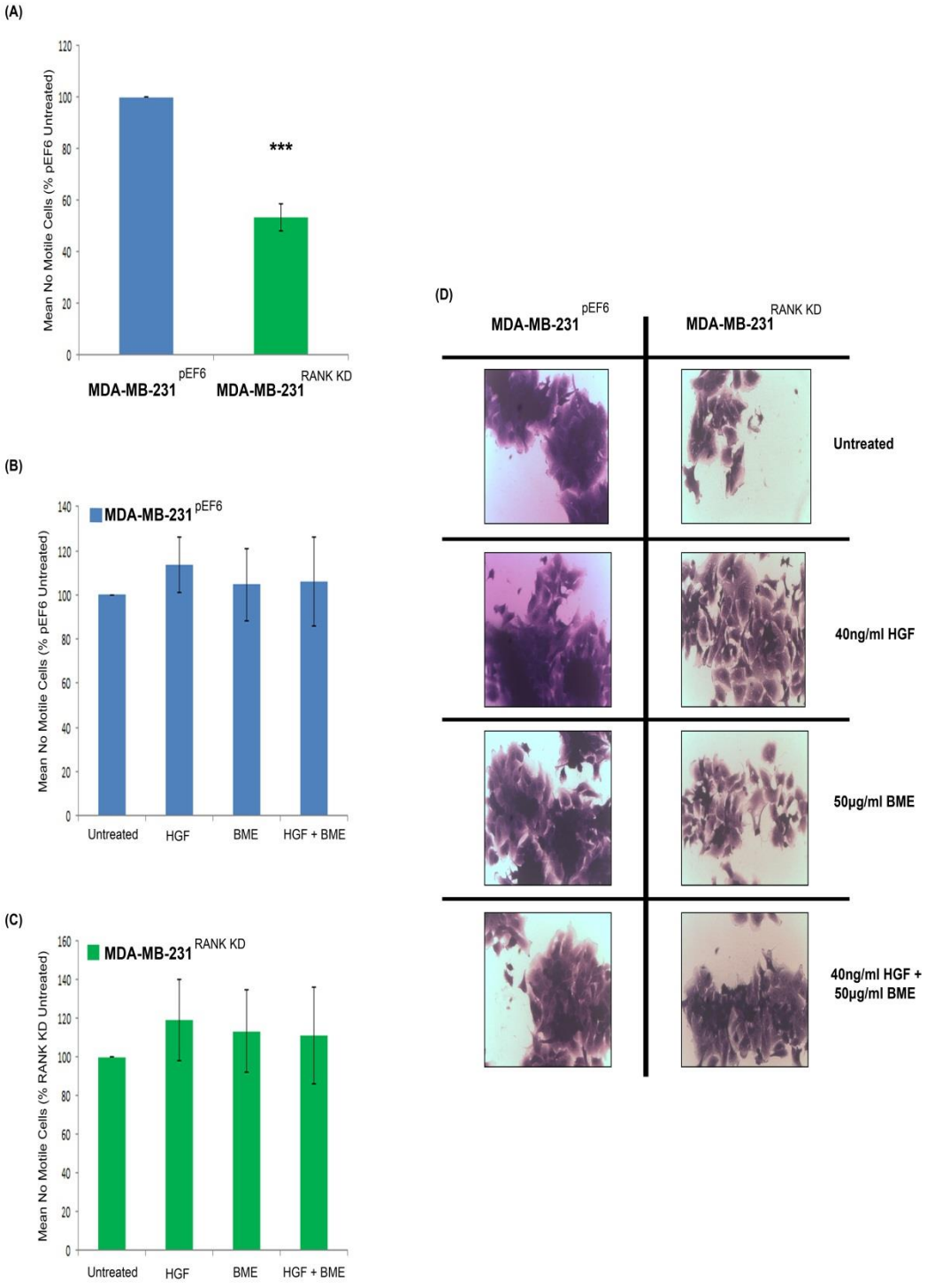

Figure 6.16: Effect of reduced RANK expression on MDA-MB-231 cell motility
Reduced RANK expression resulted in a significant decrease in MDA-MB-231 cell motility compared to MDA-MB-231^{pEF6} control cells (A). MDA-MB-231^{pEF6} control cells treated with 40ng/ml HGF, 50µg/ml BME or a combination of 40ng/ml HGF and 50µg/ml BME resulted in increased cell motility (B). A similar trend was observed when MDA-MB-231^{RANKKD} cells were treated with the same treatments (C). Representative images from one repeat (D). Data represents mean of 3 independent repeats, error bars represent SEM. * - p=<0.05, ** - p=<0.01 and *** - p=<0.001.

6.4.3.5 RANK suppression significantly reduces MDA-MB-231 breast cancer cell invasion in vitro

Reduced RANK expression in MDA-MB-231 cells resulted in significantly decreased cell invasion *in vitro* compared with MDA-MB-231^{pEF6} control cells (64% of control) (Figure 6.17 A, p=0.002).

When MDA-MB-231^{pEF6} control cells were treated with 40ng/ml HGF or 50µg/ml BME no effects on cell invasion was observed (101% and 102% compared to untreated control respectively) (Figure 6.17 B). However when 40ng/ml HGF and 50µg/ml BME were added together to MDA-MB-231^{pEF6} control cells, cell invasion was significantly decreased in relation to untreated MDA-MB-231^{pEF6} control cells (82% of untreated control, p=0.031) (Figure 6.17 D).

Interestingly, treatment of MDA-MB-231^{RANKKD} cells with 40ng/ml HGF resulted in an increase in cell invasion compared to the untreated MDA-MB-231^{RANKKD} cells (125% compared to untreated control), a similar pattern mirrored by MDA-MB-231^{RANKKD} cells treated with 50µg/ml BME (122% of untreated control), however both these trends did not reach significance (p=0.23 and 0.44 respectively) (Figure 6.17 C). A combined treatment of 40ng/ml HGF and 50µg/ml BME also resulted in a non-significant increase in MDA-MB-231^{RANKKD} cell invasion (106% of untreated control); however this increase was not as dramatic as that observed under the individual treatments.

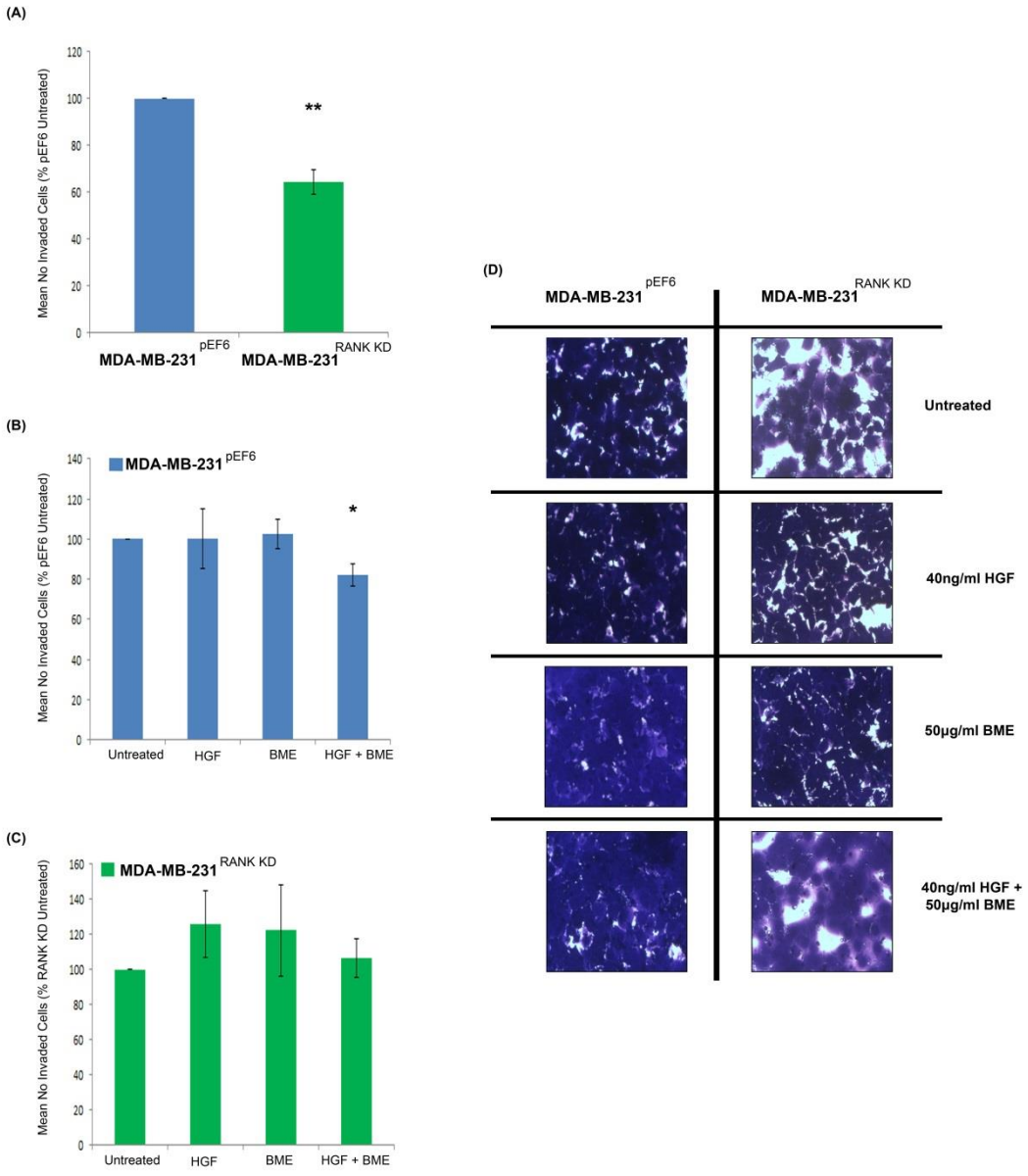

Figure 6.17: Effect of RANK knockdown on MDA-MB-231 cell invasion *in vitro*
MDA-MB-231^{RANKKD} cells showed reduced cell invasion compared with MDA-MB-231^{pEF6} control cells (A). When MDA-MB-231^{pEF6} control cells were treated with 40ng/ml HGF or 50µg/ml BME cell invasion increased, however the combined 40ng/ml HGF and 50µg/ml BME treatment decreased cell invasion (B). MDA-MB-231^{RANKKD} cells treated with 40ng/ml HGF, 50µg/ml BME or combined 40ng/ml HGF and 50µg/ml BME increases in cell invasion were seen (C). Representative images from one repeat (D). Data represents mean of 3 independent repeats, error bars represent SEM. * - p=<0.05, ** - p=<0.01 and *** - p=<0.001.

6.5 Discussion

With a combined effort from surgeons, oncologists and researchers primary treatments for breast cancer have improved, however one aspect of the disease which still remains poorly understood and controlled is its metastatic spread. Though some advances have been made in the treatment of SREs, such as the licensing of Denosumab, no preventative or screening tools are yet available to aid medics in the identification of those patients most at risk. In conducting this study the aim was to elucidate the potential impact targeting these molecules might have on breast cancer cell tumourigenesis.

6.5.1 Role of OPG, RANK and RANKL in clinical breast cancer

It is well known that breast carcinomas have the ability to metastasise to the bone; however, the mechanisms by which these are established remains unknown. The findings for OPG, RANK and RANKL expression in breast cancer tissues remain controversial. The clinical cohort data derived from this study indicated that RANK, RANKL and OPG transcripts were all reduced in tumour samples versus normal breast tissues. Thomas *et al* (1999) reported OPG mRNA expression, but no RANKL expression in 12 different primary breast cancer specimens. However, Reinholz *et al* (2002) reported detection of RANKL mRNA in a series of breast tumours. Holen *et al* (2005) found that there was a significant decrease in tumour OPG expression with increasing tumour grade. Though this study did not find an association between tumour grade and OPG expression a trend was identified in which OPG expression was decreased in tumour samples compared to normal breast tissue. Van Poznak *et al* (2006) showed IHC staining for OPG and RANKL in non-neoplastic breast tissue localised to different sub-cellular compartments. Whist Cross *et al* (2006a) demonstrated that, in their large study, RANKL expression was

apparently lost in the majority of breast cancer cases which supports the pattern of reduced RANKL transcript levels seen in the tumour samples in this study. Of further note from the Cross *et al* (2006a) study was the negative association between RANKL and ER status. This corroborates the connection between RANKL and ER status found in this study. ER levels are well known to affect the clinical outcome of breast cancer patients.

In our clinical cohort, reduced expression of *RANK* was found to be significantly associated with metastases and with patients who had died from the disease. In contrast RANKL expression appeared increased in patients with metastases but reduced in patients who had local recurrence or who had died from the disease. This was also supported by the Kaplien Meier curves in which both low RANK and low RANKL expression showed poor prognosis. This contradicts the microarray study by Santini *et al* (2011) which concludes that high RANK expression in their early stage breast cancer patients is predictive of worse prognosis. In contrast to the RANK and RANKL expression profiles, it was higher levels of *OPG* expression which correlated with a poorer overall survival in the current study, though again this contradicts the Santini *et al* (2011) and Van Poznak *et al* (2006) studies. Of interest from the Kaplein Meier survival curves was the statistically significant result that low RANK, low RANKL and high OPG expression resulted in poorer overall survival compared to those patients with high RANK, high RANKL and low OPG expression.

6.5.2 Impact of β-oestradiol treatment on RANK, RANKL and OPG expression in vitro

Based on the observations in the clinical data with regards to ER status and the correlations with RANK and RANKL, β-oestradiol treatments were carried out *in*

vitro on an oestrogen positive breast cancer cell line (MCF-7) and an oestrogen negative breast cancer cell line (MDA-MB-231).

6.5.2.1 Concentration gradient responses to β-oestradiol treatment

Both the ER positive and negative cell lines responded to the concentration gradient as expected. Both RANK and RANKL transcript levels decreased in response to the β-oestradiol gradient (10^{-7}M, 10^{-8}M, 10^{-9}M, and 10^{-10}M), with 10^{-8}M appearing to show the greatest reduction in transcript copies compared to the control. The ER negative cell line showed increases in RANK and RANKL transcript copy numbers under increasing concentrations of β-oestradiol, both peaking at 10^{-8}M. This corroborates our clinical cohort data which showed a negative correlation between ER positive status and RANK or RANKL transcript copies.

In contrast, and of interest, is the apparent reversal in trend which was observed in the OPG transcript levels. Though 10^{-7}M, 10^{-9}M and 10^{-10}M all showed decreased transcript copies, no apparent trend emerged in the ER positive cell line. In contrast, with the exception of the 10^{-8}M β-oestradiol treatment in the ER negative cell line all the other concentrations responded as would be expected from the clinical data. Rachner *et al* (2008) showed, using Northern blot, that β-oestradiol could inhibit the production of OPG in MCF-7 cells. The data from this study generally agrees with this conclusion, though it appears in our data that this was most effective in the lowest concentration tested (10^{-10}M). Rachner *et al* (2008) also, however, showed no effect on OPG transcripts in the MDA-MB-231 cell line, in contrast, it appears from our data that OPG transcript levels, for the majority of concentrations studied, appeared to be increased.

6.5.2.2 Time course responses to β-oestradiol treatment

The time course data for the transcript levels of RANK, RANKL and OPG over a 24 hour period after β-oestradiol stimulation is interesting. The ER positive cell line, MCF-7, appeared to initially respond as expected and RANK and RANKL transcript levels decreased, however the significant increase which was observed after 2 hours was unexpected, especially as normal levels had not been restored after 24 hours for the RANK expression. However, given the inhibitory effect on OPG which was observed after treatment with β-oestradiol by Rachner *et al* (2008), the significant decrease in OPG transcript copies after 1 hour incubation with β-oestradiol treatment was anticipated. The interesting observation from this study was that the impact on OPG transcript levels was maintained throughout the 24hour period studied.

The decrease in RANK and RANKL transcripts observed over the 24 hour period in the ER negative MDA-MB-231 cells was also unexpected, given the previous clinical data and concentration gradient data. These responses contradicted those from Rachner *et al* (2008) where they conclude after 6 hours treatment there was no change in RANKL transcript levels. qPCR may be considered a more sensitive technique than Northern blot, therefore the current study may have picked up the smaller fluctuations in the ER negative cell line. The decrease in OPG transcript levels over a 24hr period was also surprising in the ER negative cell line, especially given the increase observed previously, though at the 2 hour mark an increase was observed.

Therefore this poses an interesting question into how the roles of OPG, RANK and RANKL, as well as the natural fluctuations of oestrogen, may evolve and impact breast cancer disease progression, especially under the switch from oestrogen dependent to oestrogen independent disease states. Further work down this avenue

of study is required to completely understand the role played by these molecules and there responsiveness to oestrogen throughout the progression of breast cancer.

6.5.3 Effect of reduced OPG expression on MDA-MB-231 breast cancer cell behaviour

The impact of targeting OPG was assessed using several *in vitro* function assays after successful knockdown of OPG using ribozyme transgenes. Knockdown of OPG in MDA-MB-231 cells appeared initially to enhance cell proliferation; however this was not maintained over the 5 day incubation period compared to the control cells. Of interest was the lack of response the treatments with HGF, BME or HGF and BME appeared to have on MDA-MB-231^{OPGKD} cell proliferation. Though the BME treatment shows a statistically significant increase in MDA-MB-231^{OPGKD} cell proliferation, this increase is only ~5% of the control and therefore may not represent a true substantial change. This pattern is reflected in the 5 day incubation graph where the control and all the treatments appeared to be similar. Some interest is generated in the lack of response of the MDA-MB-231^{OPGKD} cells considering the control cells did respond to the treatment, though more investigation is required to see if this is a true trend. Similar observations were seen with MDA-MB-231^{OPGKD} cell-matrix adhesion, though a slight decrease in cell-matrix adhesion was observed compared to the control cell line it was not significant. The exogenous treatments added also appeared to have no noteworthy additional effects.

Many of the previous studies looking at breast cancer and the role OPG plays have focused on TRAIL-induced apoptosis. Holen *et al* (2005) showed that *in vitro* MDA-MB-231 and MDA-MB-436 cells had the ability to produce and secrete enough OPG (in 72hrs) to protect from TRAIL-induced apoptosis. They also noted that OPG is not

detected in normal breast tissue but it can be moderately detected in approximately 40% of primary breast cancer specimens.

Of interest was the significantly increased motility that was observed in the MDA-MB-231^{OPGKD} cells compared to the control cells. Interestingly this response was not sustained or enhanced by the pleiotropic growth factor HGF and no additional response was seen after treatment with BME. Also of interest was the observation that MDA-MB-231^{OPGKD} cell invasion was significantly increased compared to the control cells. Furthermore, the observation that all the treatments, HGF, BME and a combination of HGF and BME appeared to reduce MDA-MB-231^{OPGKD} cell invasion. The contrast in responses compared to those seen in the MDA-MB-231^{pEF6} control cell line provides an interesting direction for further investigation. Currently our *in vitro* data suggests a role for OPG in breast cancer cell motility and invasion, where it may act to supress these aggressive traits and furthermore, highlights that OPG may be involved in regulating the response of MDA-MB-231 breast cancer cells to various environmental signals, such as HGF and bone like conditions.

The preliminary xenograft model completed as part of this study, appears to contradict the proliferation assay that was conducted, showing the MDA-MB-231^{OPGKD} cells developed tumours and grow significantly faster than the controls (MDA-MB-231^{pEF6} cells). Though this may be a true trend, during the course of this experiment the control cells (MDA-MB-231^{pEF6}) did not react as tumourigenically as in previous *in vivo* studied. MDA-MB-231 cells are generally considered very tumourigenic and larger tumour development and growth was expected, thus these results need to be treated with caution and confirmed through repeat experimentation.

This study has tried to address the roles OPG may play in breast cancer cell behaviour traits involved in metastatic spread to the bone. As a result this study has

highlighted the potential roles OPG may have on breast cancer cell migration and invasion, though further investigation is required to understand by what mechanisms these traits are achieved. It would also be interesting to carry out a similar model in the oestrogen positive MCF-7 cell line to see what impact targeting cellular produced OPG has on ER positive tumourigenic breast cell behaviour.

6.5.4 Effect of reduced RANK expression on MDA-MB-231 breast cancer cell behaviour

After suppression of RANK expression was successfully achieved in MDA-MB-231 cells using ribozyme transgenes, the impact was assessed using several *in vitro* function assays. Knockdown of RANK expression in MDA-MB-231 cells resulted in significantly decreased cell proliferation, but only after 5 days incubation. Treatment with HGF appeared to have little impact on MDA-MB-231^{RANKKD} cell proliferation after both 3 days and 5 days incubation. Though the BME and combined HGF and BME treatments both gave significant results after 3 days incubation both changes are very slight and therefore the statistically significant values potentially do not represent a true substantial change.

Reduced RANK expression in MDA-MB-231 cells resulted in reduced cell-matrix adhesion, cell migration and invasion *in vitro*. Of further interest is the impact the treatments appear to have on the MDA-MB-231^{RANKKD} cell-matrix adhesion. Both individual HGF and BME treatments increased MDA-MB-231^{RANKKD} cell-matrix adhesion and invasion, though in this study these did not yield significant results these trends generate interest and need further investigation to identify possible changes in cell surface markers and pathway(s) which might be occurring.

The observation that targeting RANK *in vitro* reduces cancer cell behaviour traits is supported by a recent *in vivo* bone metastases study conducted by Blake *et al*

(2014). Blake *et al* (2014) showed that MDA-MB-231 cells overexpressing RANK resulted in greater metastatic bone colonisation and growth through RANKL signalling.

Though no other previous study has reduced RANK expression in MDA-MB-231 cells, others have studied how these cells interaction with RANKL and result in increased metastatic bone potential and increase migration and invasion *in vitro*. Casimiro *et al* (2013) showed that the bone-seeking sub-clones of MDA-MB-231 cells which were RANK positive increased cell migration and invasion through the RANKL JNK and ERK 1/2 signalling.

The interactions between OPG, RANK and RANKL are complex during breast cancer development and progression. Some contradictory results were seen between the clinical data and the *in vitro* single cell models. This is best highlighted by the role of OPG. In the clinical cohort, lower OPG levels were seen to correlate with good prognosis and survival, yet in the single cell model, suppression of OPG appeared to increase cell migration and invasion, two traits which are considered to reflect aggressive disease. The human body is an intricate combination of a variety of cell types and factors which could never be replicated in a 2-D model. Isolating this one molecule in a cell system has highlighted the role breast cancer cell produced OPG may play in breast cancer cell migration and invasiveness. It is unlikely that OPG produced intrinsically by breast cancer cells alone accounts for the diverse role that this molecule plays in breast cancer dissemination. Hence, this may account for the confliction between the clinical and i*n vitro* data. With more evidence implicating the role of RANK in breast cancer, research to elucidate all the pathways affected, and how these can be targeted therapeutically in a clinical setting must now be of greater emphasis.

Chapter 7

General Discussion

7.1 Bone metastases associated with breast and prostate cancer

The skeleton is the most common organ which is affected by cancer metastases, a site which still causes considerable morbidity and mortality (Coleman 2006). Due to the circulation flow through the bone and the venous blood through the vertebral-venous plexus of vessels from the breast and pelvis, this physical factor may play a role in the establishment of bone metastases particularly associated with breast and prostate cancer. However, as highlighted by the complexity of the metastatic cascade, mechanical factors cannot be the sole factor which drives the high incidence of bone metastases. Thus the understanding of molecular features which mark bone as a preferred metastatic site, has resulted in major therapeutic achievements, such as Denosuamab (Lacey *et al* 2012). However, much still remains unknown about the complex interplay between the cancer cells, the bone environment and the signalling transductions that are induced aiding cancer progression.

7.2 Thesis Aims

During the course of this thesis the aim was to look at the potential implications of targeting endogenously produced OPG, RANK and RANKL on cancer cell traits, including cell proliferation, migration and invasion, in breast and prostate cancer cell lines which generated differing osseous phenotypes.

Given the complex nature of the bone environment, this study also aimed to look at the influence the stromally produced growth factor, HGF and isolated bone proteins (BME) might have on manipulated osseous cancer cell lines.

7.3 Main conclusions from this study

7.3.1 Role of OPG in prostate cancer

Though OPG expression has been detected in normal prostate tissue, little is known about the potential roles it plays in normal prostate physiology. In this study all the cell lines screened expressed OPG, though the LNCaP cell line exhibited reduced expression in comparison to all the other prostate cancer cell lines, as has been noted elsewhere in the literature. Combining the observations from Brown *et al* (2001a), the hypothesis by Corey *et al* (2005) and the *in vitro* observations from this study, this evidence supports the idea that OPG influences prostate cancer development and progression rather than acts a causation factor.

This study suggests that the targeting of endogenous OPG in the PC-3 prostate cancer cells, can affect prostate cell proliferation, particularly over a long incubation period. After the targeting of endogenous OPG, the addition of external stimuli, despite giving some significant results after 3 days incubation, resulted in similar patterns seen in the control cells, therefore questioning if these are truly significant results. However, under long term (5 day) treatments with HGF and BME in this study, PC-3 cells appeared less responsive to these external stimuli than the control cells. Though this appears an interesting trend, these results require further investigation. This assay was conducted over a time period, in which PC-3 cells may reach confluence, given the observation that targeting endogenous OPG enhances cellular proliferation there needs to subsequent confirmation that apoptosis was not being induced due to over-confluence in these exogenously treated cells, thus affecting potential conclusions which can be drawn.

The addition of a recombinant form of OPG to LNCaP cells appeared to have no impact on cell proliferation over long term treatment both in its own right and when added with other external stimuli (HGF and BME). This highlights that potentially in

contrast to endogenously produced OPG, exogenous OPG may play a role in cancer progression but not through affecting prostate cancer cell proliferation. Further work is needed to investigate why such differences in response to endogenous and exogenous OPG are seen and highlights an avenue for further investigation into how OPG alters, through the course of the disease, and impacts both tumour cells and cells in the bone environment including osteoblasts, osteoclasts and bone marrow stromal cells.

OPG, either through being targeted or added, did not appear to impact either PC-3 or LNCaP prostate cancer cell-matrix adhesion or cell motility. However, after targeting endogenously produced OPG, both BME and BME and HGF treatments resulted in significant decreases in cell-matrix adhesion and promotion in cell motility, though these trends did not reach significance, the individual BME treatment was close ($p=0.084$). In contrast, addition of exogenous OPG with HGF or a combination of HGF and BME to LNCaP cells resulted in decreases in cell-matrix adhesion (the latter significantly so), which was not seen under the BME treatment. This was accompanied by the observation that rhOPG with HGF, or a combination of HGF and BME promoted LNCaP cell motility, whilst a combination of rhOPG and BME appeared to reduce LNCaP cell migration. This data strongly suggests that both endogenously produced OPG and exogenously produced OPG can influence prostate cancer cell adhesion and motility in response to factors present in a bone like environment, particularly as these trends were not noted in the respective controls.

Interestingly, the addition or removal of OPG appeared to impact cell invasion *in vitro*. Reducing expression levels of OPG in the aggressive androgen independent PC-3 cell line resulted in a more invasive phenotype, which was nullified by the addition of HGF. In contrast, the addition of rhOPG to the androgen dependent LNCaP cell line resulted in a decrease in cell invasion, which could be reversed

when added in combination with BME. Together this suggests that in prostate cancer cells, the expression of OPG can moderate invasive potential. The trends imply that under external stimuli, HGF and BME, or a component of the BME, may interfere with the anti-invasive properties of rhOPG. Of further interest are the changes in invasive potential between the cell lines themselves. LNCaP cells are androgen dependent, weakly metastatic prostate cancer cells, whilst PC-3 cells are androgen independent and highly metastatic. It would therefore be of interest to investigate what drives the potential for loss of endogenous OPG production to become pro-invasive, whether molecular or genetic?

7.3.2 Role of RANK and RANKL in prostate cancer

RANK expression was ubiquitous across all the prostate cancer cell lines studied, whilst in contrast RANKL expression seemed selective to those cell lines which have metastatic potential.

Targeting of RANK expression in PC-3 cells resulted in observations of significantly increased cell proliferation and cell-matrix adhesion. These trends also appeared to be affected by the influence of external stimuli. Suppression of RANK appeared to make PC-3 cell proliferation less responsive to all treatments, a trend which was seen across both incubation periods studied. This trend was also mirrored in the cell-matrix adhesion assay, though no significant trends were reported in either group, the relevance of these observations are debateable.

Interestingly, after targeting RANK expression in PC-3 cells, though motility did not appear to be affected, it allowed for an interesting observation. The PC-3^{RANKKD} cells appeared more aggregated in comparison to the control cells. This provides a bit of a conundrum. Is it possible that these cells have migrated as a colony, or is there potential that after initial cells have migrated induced secretion of

chemoattractant(s), encourages other cells to migrate to that location? Cell aggregation appeared particularly apparent under the influence of the growth factor, HGF. This is interesting since HGF is known as a scatter factor, possibly indicating that these cells are less responsive to HGF. Further investigation is now needed into potential cell-cell contact markers which might be influenced by the suppression of RANK in prostate cancer cells, and subsequently if this influences other factors which are secreted by the cells themselves.

Unfortunately, attempts to derive an LNCaP^{RANKKD} cell line were unsuccessful; to achieving this would allow further investigation into how targeting RANK might affect prostate cancer cell behaviour.

The literature suggests that immortalised prostate cancer cells which have metastatic osseous potential express RANKL (Corey *et al* 2002). The reason why our PC-3 prostate cancer cell line does not express any detectable levels of RANKL remains unknown, and attempts to generate an overexpression model were also unsuccessful. However, based on the observations in the literature that LNCaP cells are able to produce both membrane and soluble forms of RANKL, it provided a direction to investigate the role of targeting RANKL expression (Zhang *et al* 2001). Denosumab (neutralising RANKL monoclonal antibody, nRANKL) is not currently licensed by NICE for the treatment of SREs linked to prostate cancer, therefore a better understanding how RANKL influences prostate cancer progression, may in time allow for a similar, more effective therapy to become available.

nRANKL appeared to have similar effects on LNCaP cell proliferation and cell-matrix adhesion as those observed under the rhOPG treatment. This was to some extent expected due to the normal inhibitory role OPG plays physiologically on osteoblasts. The unexpected result came from the combination of nRANKL and HGF, this combination resulted in a significant decrease in LNCaP proliferation after

3 days incubation, an observation not noted elsewhere. This result was sustained over the 5 days analysed, but this result then becomes consensus with the other LNCaP cells treated with HGF. nRANKL and HGF in combination also appeared to enhance LNCaP cell motility. It would therefore be interesting to further investigate how the combination of nRANKL and HGF accelerate their anti-proliferative and pro-migratory effects *in vitro.*

7.3.3 Role of OPG in breast cancer

In breast cancer, the endogenous suppression of OPG in MDA-MB-321 cells, resulted in increased cell motility and invasive potential, however cell proliferation and cell-matrix adhesion appeared unaffected. Of further interest was the impact the external stimuli had on MDA-MB-231^{OPGKD} cell behaviour. As was previously noted in the PC-3 prostate cancer cell line, HGF appeared to reduce the invasive potential of these cells. Therefore further investigation into how HGF moderates the invasive potential of OPG in both cancer types is needed.

7.3.4 Role of RANK in breast cancer

Most of the literature regarding RANK in breast cancer focuses on generating over expression. Suppression of RANK expression in our MDA-MB-231 cells resulted in the observation of reduced breast cancer cell proliferation, cell-matrix adhesion, motility and invasive potential, none of which were further moderated by the addition of external stimuli. These results are therefore contradictory to the findings in the clinical data and warrant further investigation, potentially using a breast cancer cell line with differing metastatic potential, for example MCF-7.

7.3.5 Roles of OPG/RANK/ RANKL in clinical breast cancer

The clinical cohort data indicated that RANK, RANKL and OPG all demonstrate reduced expression in tumour samples versus normal breast tissues, however none of these reached significance. Transcript levels for *RANK* and *RANKL* were shown to be significantly lower in patients whose tumours were ERβ positive, suggesting a negative correlation with ER status.

Reduced expressions of *RANK* and *RANKL* transcript were found to be significantly correlated with poor overall survival. In contrast to this, higher levels of *OPG* expression correlated with a poorer overall survival.

7.3.6 Summary

Taken together, these results have strongly suggested a role for OPG in prostate cancer (in both osteolytic and mixed osteolytic and osteoblastic) cell migration and invasion especially under the influence of the isolated bone proteins and HGF. In addition targeting of OPG in the MDA-MB-231 breast cancer cell line also appeared to effect tumour cell migration and invasion, though the external stimuli appeared to be less of a driving force. This potentially highlights that some of the characteristic responses induced by OPG are similar across breast and prostate cancer types.

In contrast, the targeting of RANK in breast and prostate cancer cells resulted in differential effects. Suppression of prostate cell RANK in the osteolytic PC-3 model resulted in increased cell growth and matrix-adhesion, however, in the osteolytic MDA-MB-231 breast cancer model RANK suppression resulted in significant decreases in the cancer cell traits investigated.

7.4 Future perspectives

This study has demonstrated the potential involvement of OPG/RANK/RANKL in breast and prostate cancer and established a role for these molecules in translating signals in response to HGF and bone like conditions. Whilst substantial efforts have been made to characterise the impact of altering expression levels in these cancer types and their response to external stimuli, additional work is now required to take forward the observations of this study. Whilst this study has identified a number of interesting observations, it has also generated a number of questions which require further scientific evaluation. It is hoped that future work conducted following on from this thesis, will aid further elucidation into the importance of OPG/RANK/RANKL in osteotrophic prostate and breast cancer metastasis.

Specific areas of focus for future work are:

7.4.1 Establishment of mechanism

Focusing on the traits, proliferation, migration and invasion, which were affected either directly or indirectly by OPG, some preliminary work has been conducted to try and establish signalling pathways which may be involved in these observations. The primary focus has been to look at the MMPs as they have been implicated in metastases and the 'vicious' bone cycle (Lynch 2011). In the MDA-MB-231 cells, MMPs 3, 7 and 9 transcript expression was analysed. Though repeats are needed, it appears that suppression of OPG in the MDA-MB-231 cells resulted in increased levels of MMP-3. This is interesting since MMP-3 has been linked to the degradation of collagen (types II, III, IV, IX and X), proteoglycans, fibronectin, lamin and elastin in rheumatoid arthritis (Burrage *et al* 2006). If this is reproducible it could subsequently be confirmed by zymography and may highlight a mechanism linking OPG to breast cancer cell invasion.

Similar patterns were not observed in the PC-3 prostate cancer cell line, when screened for MMP-3 and -7. Further work into the screening of the remaining MMPs and TIMPs are needed together with analysis of their activity in response to endogenous OPG suppression. In breast cancer cells the intranuclear trafficking of the osteoblastic transcription factor RUNX2 has been shown to be impaired, therefore influencing metastatic potential and invasion through regulation of MMP-9 (Pratap *et al* 2009, Javed *et al* 2005). Whilst in prostate cancer RUNX2 has been shown to influence tumour cell osteomimicry (Leong *et al* 2010, Rucci *et al* 2010, Akech *et al* 2010, Brubaker *et al* 2003, Baniwal *et al* 2010). Therefore further efforts into elucidating the potential factors which mediate the observed responses are necessary, though complicated by the inter-linked network of cascades and transcription factors which could be influenced (Figure 7.1).

7.4.2 Additional cellular models

Due to the time constraints of this study, it was not possible to generate additional cell models. With more time this could be addressed. The most evident concern would be the lack of a reflective osteoblastic prostate cancer cell model, considering it is the predominant bone lesion phenotype associated with prostate cancer. Work into establishing the MDA-PCa-2b model was undertaken, however, the MDA-PCa-2b model was found to be unsuitable for this purpose. Recent efforts resulted in the purchasing of the VCaP cell line, which has been reported to generate osteoblastic lesions (Kirschenbaum *et al* 2011). Of great interest, is that from the initial PCR screen which has been conducted, this prostate cancer cell line showed positive transcript expression for both HGF and its receptor c-MET (Data not shown). If this can be replicated it will allow for further investigation into not only the paracrine influence HGF may have on cancer cells, but also the autocrine effects.

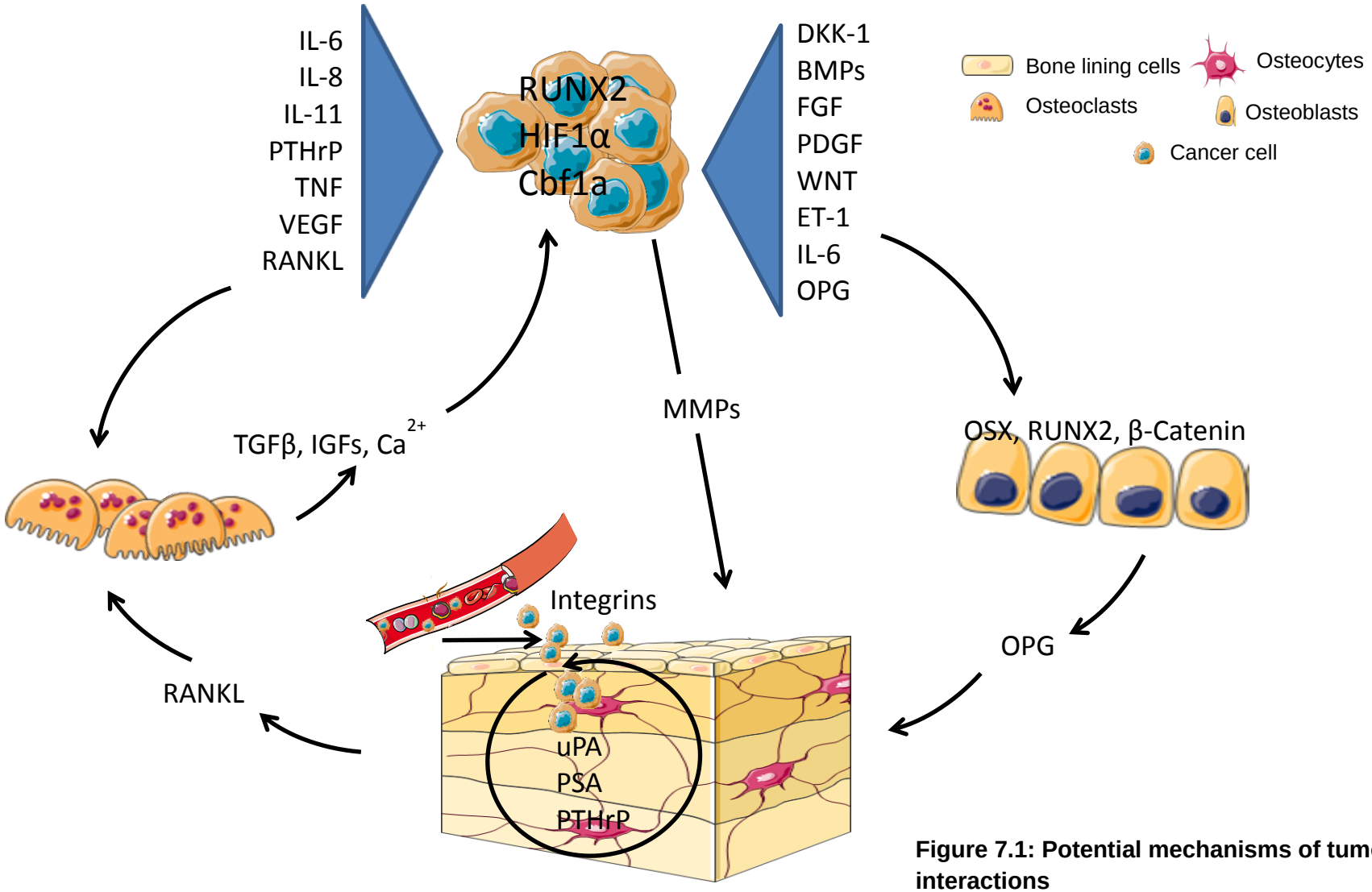

Figure 7.1: Potential mechanisms of tumour and bone cell interactions

These stimuli could potentially exert their effects through a variety of pathways by affecting signal transducers including SMADs, MAPK, FAK and the Rho GTPases (adapted from Weilbaecher et al 2011)

To fully understand *in vitro* the potential OPG may have on prostate cancer disease progression, both an immortalised normal prostate (PZHPV-7) and a primary prostate cancer (CAHPV-10) would also be of interest. Due to time constraints it was not possible to conduct this work as part of the current thesis, though these would represent interesting models for future study.

The MDA-MB-231 cell line is considered ER negative, given the close nature of both oestrogens and breast cancer progression, and oestrogens and bone it would therefore also be interesting to replicate similar cell models in the ER positive MCF-7 cell line. This is also of interest given the role androgens play in bone turnover and the increasing links which are being established with breast cancer progression.

7.4.3 Co-culture models

Looking at these cell models in isolation allows for intense study; however these do not replicate physiological models, either pre-clinical or clinical. Therefore, having looked at these models as part of this study, it would now be interesting to start establishing co-culture models with a variety of cell types from the bone environment. A human osteoblast cell line (hFOB1.19) is commercially available, however this does not appear to be the case for osteoclasts. In the literature two models have previously been described.

- In some co-culture models, mouse osteoclasts are used (RAW264.7) (Mouline *et al* 2010)
- Several research groups have reported to have isolated human pre-cursor osteoclasts (FLG29.1 and THP-1) and shown that it is possible to differentiate these in culture, though proliferation of mature osteoclasts does not appear to have been achieved (Gattei *et al* 1992, Aldinucci *et al* 1996, Jakob *et al* 1997, Shozu *et al* 1997).

Given that the cell models used in this study are human, it would be interesting to collaborate with these groups to potentially develop a co-culture model. Or to source these cells and experiment with the potential of co-culture looking at how these manipulated cancer cells effect osteoclast maturation and differentiation *in vitro*.

7.4.4 In-vivo xenograft and bone models

An initial xenograft model was conducted on the MDA-MB-231 cell line and though the results must be treated with caution they potentially highlighted something interesting (Figure 6.12). Unfortunately, shortly after this study had ended, the group project license expired. Upon renewal it would be interesting to repeat this model, and use the other manipulated cell lines. Efforts to establish an *in-vivo* bone model would also provide a new direction to explore the potential impact of tumour growth in bone and metastasis model.

Many challenges remain to try and better understand the complex interplay which occurs between tumour cells and bone. Through a process of discovery and elimination it is hoped that these efforts will ultimately result in improved therapeutic interventions or possibly even a preventative intervention.

References

Abate-Shen C, Shen MM. 2000. Molecular genetics of prostate cancer. Genes Dev 14(19):2410-2434.

Abate-Shen C, Shen MM, Gelmann E. 2008. Integrating differentiation and cancer: the Nkx3.1 homeobox gene in prostate organogenesis and carcinogenesis. Differentiation; research in biological diversity 76(6):717-727.

Aberle H, Bauer A, Stappert J, Kispert A, Kemler R. 1997. beta-catenin is a target for the ubiquitin-proteasome pathway. The EMBO journal 16(13):3797-3804.

Ablin R, Piana, R. 2014. The Great Prostate Hoax: How Big Medicine Hijacked the PSA Test and Caused a Public Health Disaster. New York: Palgragve MacMillan.

Adamopoulos IE, Xia Z, Lau YS, Athanasou NA. 2006. Hepatocyte growth factor can substitute for M-CSF to support osteoclastogenesis. Biochemical and biophysical research communications 350(2):478-483.

Adjei AA. 2001. Blocking oncogenic Ras signaling for cancer therapy. Journal of the National Cancer Institute 93(14):1062-1074.

Ahmad I, Patel R, Singh LB, Nixon C, Seywright M, Barnetson RJ, Brunton VG, Muller WJ, Edwards J, Sansom OJ, Leung HY. 2011. HER2 overcomes PTEN (loss)-induced senescence to cause aggressive prostate cancer. Proceedings of the National Academy of Sciences of the United States of America 108(39):16392-16397.

Ahman AK, Jonsson BA, Damber JE, Bergh A, Emanuelsson M, Gronberg H. 2000. Low frequency of allelic imbalance at the prostate cancer susceptibility loci HPC1 and 1p36 in Swedish men with hereditary prostate cancer. Genes, chromosomes & cancer 29(4):292-296.

Akech J, Wixted JJ, Bedard K, van der Deen M, Hussain S, Guise TA, van Wijnen AJ, Stein JL, Languino LR, Altieri DC, Pratap J, Keller E, Stein GS, Lian JB. 2010. Runx2 association with progression of prostate cancer in patients: mechanisms mediating bone osteolysis and osteoblastic metastatic lesions. Oncogene 29(6):811-821.

Alam N, Goel HL, Zarif MJ, Butterfield JE, Perkins HM, Sansoucy BG, Sawyer TK, Languino LR. 2007. The integrin-growth factor receptor duet. Journal of cellular physiology 213(3):649-653.

Albadine R, Latour M, Toubaji A, Haffner M, Isaacs WB, E AP, Meeker AK, Demarzo AM, Epstein JI, Netto GJ. 2009. TMPRSS2-ERG gene fusion status in minute (minimal) prostatic adenocarcinoma. Modern pathology : an

official journal of the United States and Canadian Academy of Pathology, Inc 22(11):1415-1422.

Albini A, Iwamoto Y, Kleinman HK, Martin GR, Aaronson SA, Kozlowski JM, McEwan RN. 1987. A rapid in vitro assay for quantitating the invasive potential of tumor cells. Cancer research 47(12):3239-3245.

Aldinucci D, Quinn JM, Degan M, Juzbasic S, Luliis AD, Improta S, Pinto A, Gattei V. 1996. In Vitro Cellular Systems for Studying OC Function and Differentiation : Primary OC Cultures and the FLG 29.1 Model. Methods in molecular medicine 2:277-306.

Allen MV, Smith GJ, Juliano R, Maygarden SJ, Mohler JL. 1998. Downregulation of the beta4 integrin subunit in prostatic carcinoma and prostatic intraepithelial neoplasia. Human pathology 29(4):311-318.

Anderson DM, Maraskovsky E, Billingsley WL, Dougall WC, Tometsko ME, Roux ER, Teepe MC, DuBose RF, Cosman D, Galibert L. 1997. A homologue of the TNF receptor and its ligand enhance T-cell growth and dendritic-cell function. Nature 390(6656):175-179.

Anderson HC. 2003. Matrix vesicles and calcification. Current rheumatology reports 5(3):222-226.

Andriole GL. 2009. The impact of prostate cancer and hormonal therapy on bone. Reviews in urology 11(4):185-189.

Andriole GL, Crawford ED, Grubb RL, 3rd, Buys SS, Chia D, Church TR, Fouad MN, Gelmann EP, Kvale PA, Reding DJ, Weissfeld JL, Yokochi LA, O'Brien B, Clapp JD, Rathmell JM, Riley TL, Hayes RB, Kramer BS, Izmirlian G, Miller AB, Pinsky PF, Prorok PC, Gohagan JK, Berg CD, Team PP. 2009. Mortality results from a randomized prostate-cancer screening trial. The New England journal of medicine 360(13):1310-1319.

Andriole GL, Jr. 2012. PSA screening and prostate cancer risk reduction. Urologic oncology 30(6):936-937.

Andriole GL, Levin DL, Crawford ED, Gelmann EP, Pinsky PF, Chia D, Kramer BS, Reding D, Church TR, Grubb RL, Izmirlian G, Ragard LR, Clapp JD, Prorok PC, Gohagan JK, Team PP. 2005. Prostate Cancer Screening in the Prostate, Lung, Colorectal and Ovarian (PLCO) Cancer Screening Trial: findings from the initial screening round of a randomized trial. Journal of the National Cancer Institute 97(6):433-438.

Armstrong AP, Miller RE, Jones JC, Zhang J, Keller ET, Dougall WC. 2008. RANKL acts directly on RANK-expressing prostate tumor cells and mediates

migration and expression of tumor metastasis genes. The Prostate 68(1):92-104.

Arya M, Bott SR, Shergill IS, Ahmed HU, Williamson M, Patel HR. 2006. The metastatic cascade in prostate cancer. Surgical oncology 15(3):117-128.

Ashcroft AJ, Cruickshank SM, Croucher PI, Perry MJ, Rollinson S, Lippitt JM, Child JA, Dunstan C, Felsburg PJ, Morgan GJ, Carding SR. 2003. Colonic dendritic cells, intestinal inflammation, and T cell-mediated bone destruction are modulated by recombinant osteoprotegerin. Immunity 19(6):849-861.

Attard G, Reid AH, Yap TA, Raynaud F, Dowsett M, Settatree S, Barrett M, Parker C, Martins V, Folkerd E, Clark J, Cooper CS, Kaye SB, Dearnaley D, Lee G, de Bono JS. 2008. Phase I clinical trial of a selective inhibitor of CYP17, abiraterone acetate, confirms that castration-resistant prostate cancer commonly remains hormone driven. J Clin Oncol 26(28):4563-4571.

Attard G, Swennenhuis JF, Olmos D, Reid AH, Vickers E, A'Hern R, Levink R, Coumans F, Moreira J, Riisnaes R, Oommen NB, Hawche G, Jameson C, Thompson E, Sipkema R, Carden CP, Parker C, Dearnaley D, Kaye SB, Cooper CS, Molina A, Cox ME, Terstappen LW, de Bono JS. 2009. Characterization of ERG, AR and PTEN gene status in circulating tumor cells from patients with castration-resistant prostate cancer. Cancer research 69(7):2912-2918.

Aubin JE. 2001. Regulation of osteoblast formation and function. Reviews in endocrine & metabolic disorders 2(1):81-94.

Autzen P, Robson CN, Bjartell A, Malcolm AJ, Johnson MI, Neal DE, Hamdy FC. 1998. Bone morphogenetic protein 6 in skeletal metastases from prostate cancer and other common human malignancies. British journal of cancer 78(9):1219-1223.

Baader E, Toloczko A, Fuchs U, Schmid I, Beltinger C, Ehrhardt H, Debatin KM, Jeremias I. 2005. Tumor necrosis factor-related apoptosis-inducing ligand-mediated proliferation of tumor cells with receptor-proximal apoptosis defects. Cancer research 65(17):7888-7895.

Bajaj GK, Zhang Z, Garrett-Mayer E, Drew R, Sinibaldi V, Pili R, Denmeade SR, Carducci MA, Eisenberger MA, DeWeese TL. 2007. Phase II study of imatinib mesylate in patients with prostate cancer with evidence of biochemical relapse after definitive radical retropubic prostatectomy or radiotherapy. Urology 69(3):526-531.

Baka S, Clamp AR, Jayson GC. 2006. A review of the latest clinical compounds to inhibit VEGF in pathological angiogenesis. Expert opinion on therapeutic targets 10(6):867-876.

Bakker AD, Kulkarni RN, Klein-Nulend J, Lems WF. 2014. IL-6 alters osteocyte signaling toward osteoblasts but not osteoclasts. Journal of dental research 93(4):394-399.

Balk SP, Knudsen KE. 2008. AR, the cell cycle, and prostate cancer. Nuclear receptor signaling 6:e001.

Banerjee C, McCabe LR, Choi JY, Hiebert SW, Stein JL, Stein GS, Lian JB. 1997. Runt homology domain proteins in osteoblast differentiation: AML3/CBFA1 is a major component of a bone-specific complex. Journal of cellular biochemistry 66(1):1-8.

Baniwal SK, Khalid O, Gabet Y, Shah RR, Purcell DJ, Mav D, Kohn-Gabet AE, Shi Y, Coetzee GA, Frenkel B. 2010. Runx2 transcriptome of prostate cancer cells: insights into invasiveness and bone metastasis. Mol Cancer 9:258.

Barbieri CE, Bangma CH, Bjartell A, Catto JW, Culig Z, Gronberg H, Luo J, Visakorpi T, Rubin MA. 2013. The mutational landscape of prostate cancer. European urology 64(4):567-576.

Baud'huin M, Duplomb L, Teletchea S, Lamoureux F, Ruiz-Velasco C, Maillasson M, Redini F, Heymann MF, Heymann D. 2013. Osteoprotegerin: multiple partners for multiple functions. Cytokine & growth factor reviews 24(5):401-409.

Bauer JJ, Sesterhenn IA, Mostofi KF, McLeod DG, Srivastava S, Moul JW. 1995. p53 nuclear protein expression is an independent prognostic marker in clinically localized prostate cancer patients undergoing radical prostatectomy. Clinical cancer research : an official journal of the American Association for Cancer Research 1(11):1295-1300.

Beer TM, Ryan CW, Venner PM, Petrylak DP, Chatta GS, Ruether JD, Redfern CH, Fehrenbacher L, Saleh MN, Waterhouse DM, Carducci MA, Vicario D, Dreicer R, Higano CS, Ahmann FR, Chi KN, Henner WD, Arroyo A, Clow FW, Investigators A. 2007. Double-blinded randomized study of high-dose calcitriol plus docetaxel compared with placebo plus docetaxel in androgen-independent prostate cancer: a report from the ASCENT Investigators. Journal of clinical oncology : official journal of the American Society of Clinical Oncology 25(6):669-674.

Beleut M, Rajaram RD, Caikovski M, Ayyanan A, Germano D, Choi Y, Schneider P, Brisken C. 2010. Two distinct mechanisms underlie progesterone-induced

proliferation in the mammary gland. Proceedings of the National Academy of Sciences of the United States of America 107(7):2989-2994.

Bellido T, Jilka RL, Boyce BF, Girasole G, Broxmeyer H, Dalrymple SA, Murray R, Manolagas SC. 1995. Regulation of interleukin-6, osteoclastogenesis, and bone mass by androgens. The role of the androgen receptor. The Journal of clinical investigation 95(6):2886-2895.

Berg A, Berner A, Lilleby W, Bruland OS, Fossa SD, Nesland JM, Kvalheim G. 2007. Impact of disseminated tumor cells in bone marrow at diagnosis in patients with nonmetastatic prostate cancer treated by definitive radiotherapy. International journal of cancer Journal international du cancer 120(8):1603-1609.

Bergthorsson JT, Johannesdottir G, Arason A, Benediktsdottir KR, Agnarsson BA, Bailey-Wilson JE, Gillanders E, Smith J, Trent J, Barkardottir RB. 2000. Analysis of HPC1, HPCX, and PCaP in Icelandic hereditary prostate cancer. Human genetics 107(4):372-375.

Berruti A, Tucci M, Mosca A, Tarabuzzi R, Gorzegno G, Terrone C, Vana F, Lamanna G, Tampellini M, Porpiglia F, Angeli A, Scarpa RM, Dogliotti L. 2005. Predictive factors for skeletal complications in hormone-refractory prostate cancer patients with metastatic bone disease. British journal of cancer 93(6):633-638.

Berry R, Schaid DJ, Smith JR, French AJ, Schroeder JJ, McDonnell SK, Peterson BJ, Wang ZY, Carpten JD, Roberts SG, Tester DJ, Blute ML, Trent JM, Thibodeau SN. 2000a. Linkage analyses at the chromosome 1 loci 1q24-25 (HPC1), 1q42.2-43 (PCAP), and 1p36 (CAPB) in families with hereditary prostate cancer. American journal of human genetics 66(2):539-546.

Berry R, Schroeder JJ, French AJ, McDonnell SK, Peterson BJ, Cunningham JM, Thibodeau SN, Schaid DJ. 2000b. Evidence for a prostate cancer-susceptibility locus on chromosome 20. American journal of human genetics 67(1):82-91.

Berry SJ, Coffey DS, Walsh PC, Ewing LL. 1984. The development of human benign prostatic hyperplasia with age. The Journal of urology 132(3):474-479.

Berthold DR, Pond GR, Soban F, de Wit R, Eisenberger M, Tannock IF. 2008. Docetaxel plus prednisone or mitoxantrone plus prednisone for advanced prostate cancer: updated survival in the TAX 327 study. Journal of clinical oncology : official journal of the American Society of Clinical Oncology 26(2):242-245.

Berthold DR, Sternberg CN, Tannock IF. 2005. Management of advanced prostate cancer after first-line chemotherapy. Journal of clinical oncology : official journal of the American Society of Clinical Oncology 23(32):8247-8252.

Berthon P, Valeri A, Cohen-Akenine A, Drelon E, Paiss T, Wohr G, Latil A, Millasseau P, Mellah I, Cohen N, Blanche H, Bellane-Chantelot C, Demenais F, Teillac P, Le Duc A, de Petriconi R, Hautmann R, Chumakov I, Bachner L, Maitland NJ, Lidereau R, Vogel W, Fournier G, Mangin P, Cussenot O, *et al*. 1998. Predisposing gene for early-onset prostate cancer, localized on chromosome 1q42.2-43. American journal of human genetics 62(6):1416-1424.

Bethel CR, Faith D, Li X, Guan B, Hicks JL, Lan F, Jenkins RB, Bieberich CJ, De Marzo AM. 2006. Decreased NKX3.1 protein expression in focal prostatic atrophy, prostatic intraepithelial neoplasia, and adenocarcinoma: association with gleason score and chromosome 8p deletion. Cancer research 66(22):10683-10690.

Bhatia-Gaur R, Donjacour AA, Sciavolino PJ, Kim M, Desai N, Young P, Norton CR, Gridley T, Cardiff RD, Cunha GR, Abate-Shen C, Shen MM. 1999. Roles for Nkx3.1 in prostate development and cancer. Genes Dev 13(8):966-977.

Blake ML, Tometsko M, Miller R, Jones JC, Dougall WC. 2014. RANK expression on breast cancer cells promotes skeletal metastasis. Clinical & experimental metastasis 31(2):233-245.

Blaszczyk N, Masri BA, Mawji NR, Ueda T, McAlinden G, Duncan CP, Bruchovsky N, Schweikert HU, Schnabel D, Jones EC, Sadar MD. 2004. Osteoblast-derived factors induce androgen-independent proliferation and expression of prostate-specific antigen in human prostate cancer cells. Clinical cancer research : an official journal of the American Association for Cancer Research 10(5):1860-1869.

Blyth K, Cameron ER, Neil JC. 2005. The RUNX genes: gain or loss of function in cancer. Nature reviews Cancer 5(5):376-387.

Boccaccio C, Ando M, Tamagnone L, Bardelli A, Michieli P, Battistini C, Comoglio PM. 1998. Induction of epithelial tubules by growth factor HGF depends on the STAT pathway. Nature 391(6664):285-288.

Bock CH, Cunningham JM, McDonnell SK, Schaid DJ, Peterson BJ, Pavlic RJ, Schroeder JJ, Klein J, French AJ, Marks A, Thibodeau SN, Lange EM, Cooney KA. 2001. Analysis of the prostate cancer-susceptibility locus HPC20 in 172 families affected by prostate cancer. American journal of human genetics 68(3):795-801.

Bodmer JL, Schneider P, Tschopp J. 2002. The molecular architecture of the TNF superfamily. Trends in biochemical sciences 27(1):19-26.

Bogenrieder T, Herlyn M. 2003. Axis of evil: molecular mechanisms of cancer metastasis. Oncogene 22(42):6524-6536.

Bonewald LF, Johnson ML. 2008. Osteocytes, mechanosensing and Wnt signaling. Bone 42(4):606-615.

Bonkhoff H, Stein U, Remberger K. 1993. Differential expression of alpha 6 and alpha 2 very late antigen integrins in the normal, hyperplastic, and neoplastic prostate: simultaneous demonstration of cell surface receptors and their extracellular ligands. Human pathology 24(3):243-248.

Bookstein R, MacGrogan D, Hilsenbeck SG, Sharkey F, Allred DC. 1993. p53 is mutated in a subset of advanced-stage prostate cancers. Cancer research 53(14):3369-3373.

Bostwick DG. 2000. Prostatic intraepithelial neoplasia. Current urology reports 1(1):65-70.

Bostwick DG, Amin MB, Dundore P, Marsh W, Schultz DS. 1993. Architectural patterns of high-grade prostatic intraepithelial neoplasia. Human pathology 24(3):298-310.

Bostwick DG, Brawer MK. 1987. Prostatic intra-epithelial neoplasia and early invasion in prostate cancer. Cancer 59(4):788-794.

Bostwick DG, Burke HB, Djakiew D, Euling S, Ho SM, Landolph J, Morrison H, Sonawane B, Shifflett T, Waters DJ, Timms B. 2004. Human prostate cancer risk factors. Cancer 101(10 Suppl):2371-2490.

Bostwick DG, Cheng L. 2012. Precursors of prostate cancer. Histopathology 60(1):4-27.

Bostwick DG, Norlen BJ, Denis L. 2000. Prostatic intraepithelial neoplasia: the preinvasive stage of prostate cancer. Overview of the prostate committee report. Scandinavian journal of urology and nephrology Supplementum(205):1-2.

Bottaro DP, Rubin JS, Faletto DL, Chan AM, Kmiecik TE, Vande Woude GF, Aaronson SA. 1991. Identification of the hepatocyte growth factor receptor as the c-met proto-oncogene product. Science 251(4995):802-804.

Bova GS, Carter BS, Bussemakers MJ, Emi M, Fujiwara Y, Kyprianou N, Jacobs SC, Robinson JC, Epstein JI, Walsh PC, *et al*. 1993. Homozygous deletion and frequent allelic loss of chromosome 8p22 loci in human prostate cancer. Cancer research 53(17):3869-3873.

Boyce BF. 2013. Advances in the regulation of osteoclasts and osteoclast functions. Journal of dental research 92(10):860-867.

Boyce BF, Xing L. 2008. Functions of RANKL/RANK/OPG in bone modeling and remodeling. Archives of biochemistry and biophysics 473(2):139-146.

Boyden LM, Mao J, Belsky J, Mitzner L, Farhi A, Mitnick MA, Wu D, Insogna K, Lifton RP. 2002. High bone density due to a mutation in LDL-receptor-related protein 5. The New England journal of medicine 346(20):1513-1521.

Boyle WJ, Simonet WS, Lacey DL. 2003. Osteoclast differentiation and activation. Nature 423(6937):337-342.

Bratt O. 2002. Hereditary prostate cancer: Clinical aspects. J Urology 168(3):906-913.

Bratt O, Damber JE, Emanuelsson M, Gronberg H. 2002. Hereditary prostate cancer: clinical characteristics and survival. The Journal of urology 167(6):2423-2426.

Bratt O, Kristoffersson U, Lundgren R, Olsson H. 1999. Familial and hereditary prostate cancer in southern Sweden. A population-based case-control study. European journal of cancer 35(2):272-277.

Brenner S, Whiting-Theobald N, Kawai T, Linton GF, Rudikoff AG, Choi U, Ryser MF, Murphy PM, Sechler JM, Malech HL. 2004. CXCR4-transgene expression significantly improves marrow engraftment of cultured hematopoietic stem cells. Stem cells 22(7):1128-1133.

Briganti A, Suardi N, Gallina A, Abdollah F, Novara G, Ficarra V, Montorsi F. 2014. Predicting the risk of bone metastasis in prostate cancer. Cancer treatment reviews 40(1):3-11.

Brown JM, Corey E, Lee ZD, True LD, Yun TJ, Tondravi M, Vessella RL. 2001a. Osteoprotegerin and rank ligand expression in prostate cancer. Urology 57(4):611-616.

Brown JM, Vessella RL, Kostenuik PJ, Dunstan CR, Lange PH, Corey E. 2001b. Serum osteoprotegerin levels are increased in patients with advanced prostate cancer. Clinical cancer research : an official journal of the American Association for Cancer Research 7(10):2977-2983.

Brown WM, Lange EM, Chen H, Zheng SL, Chang B, Wiley KE, Isaacs SD, Walsh PC, Isaacs WB, Xu J, Cooney KA. 2004. Hereditary prostate cancer in African American families: linkage analysis using markers that map to five candidate susceptibility loci. British journal of cancer 90(2):510-514.

Browner WS, Lui LY, Cummings SR. 2001. Associations of serum osteoprotegerin levels with diabetes, stroke, bone density, fractures, and mortality in elderly

women. The Journal of clinical endocrinology and metabolism 86(2):631-637.

Brubaker KD, Vessella RL, Brown LG, Corey E. 2003. Prostate cancer expression of runt-domain transcription factor Runx2, a key regulator of osteoblast differentiation and function. The Prostate 56(1):13-22.

Bryden AA, Freemont AJ, Clarke NW, George NJ. 1999. Paradoxical expression of E-cadherin in prostatic bone metastases. BJU international 84(9):1032-1034.

Bryden AA, Hoyland JA, Freemont AJ, Clarke NW, George NJ. 2002a. Parathyroid hormone related peptide and receptor expression in paired primary prostate cancer and bone metastases. British journal of cancer 86(3):322-325.

Bryden AA, Hoyland JA, Freemont AJ, Clarke NW, Schembri Wismayer D, George NJ. 2002b. E-cadherin and beta-catenin are down-regulated in prostatic bone metastases. BJU international 89(4):400-403.

Bubendorf L, Schopfer A, Wagner U, Sauter G, Moch H, Willi N, Gasser TC, Mihatsch MJ. 2000. Metastatic patterns of prostate cancer: an autopsy study of 1,589 patients. Human pathology 31(5):578-583.

Buckwalter JA, Glimcher MJ, Cooper RR, Recker R. 1996a. Bone biology. I: Structure, blood supply, cells, matrix, and mineralization. Instructional course lectures 45:371-386.

Buckwalter JA, Glimcher MJ, Cooper RR, Recker R. 1996b. Bone biology. II: Formation, form, modeling, remodeling, and regulation of cell function. Instructional course lectures 45:387-399.

Buijs JT, van der Pluijm G. 2009. Osteotropic cancers: from primary tumor to bone. Cancer letters 273(2):177-193.

Burgess TL, Qian Y, Kaufman S, Ring BD, Van G, Capparelli C, Kelley M, Hsu H, Boyle WJ, Dunstan CR, Hu S, Lacey DL. 1999. The ligand for osteoprotegerin (OPGL) directly activates mature osteoclasts. The Journal of cell biology 145(3):527-538.

Burrage PS, Mix KS, Brinckerhoff CE. 2006. Matrix metalloproteinases: role in arthritis. Frontiers in bioscience : a journal and virtual library 11:529-543.

Butt WP, Coral AP. 1998. Re: Imaging in transient regional osteoporosis. British journal of rheumatology 37(6):696-697; author reply 698-699.

Buttyan R, Sawczuk IS, Benson MC, Siegal JD, Olsson CA. 1987. Enhanced expression of the c-myc protooncogene in high-grade human prostate cancers. The Prostate 11(4):327-337.

Buxton EC, Yao W, Lane NE. 2004. Changes in serum receptor activator of nuclear factor-kappaB ligand, osteoprotegerin, and interleukin-6 levels in patients

with glucocorticoid-induced osteoporosis treated with human parathyroid hormone (1-34). The Journal of clinical endocrinology and metabolism 89(7):3332-3336.

Calabro F, Sternberg CN. 2007. Current indications for chemotherapy in prostate cancer patients. European urology 51(1):17-26.

Cancel-Tassin G, Latil A, Valeri A, Guillaume E, Mangin P, Fournier G, Berthon P, Cussenot O. 2001a. No evidence of linkage to HPC20 on chromosome 20q13 in hereditary prostate cancer. International journal of cancer Journal international du cancer 93(3):455-456.

Cancel-Tassin G, Latil A, Valeri A, Mangin P, Fournier G, Berthon P, Cussenot O. 2001b. PCAP is the major known prostate cancer predisposing locus in families from south and west Europe. European journal of human genetics : EJHG 9(2):135-142.

Caplan AI. 1991. Mesenchymal stem cells. Journal of orthopaedic research : official publication of the Orthopaedic Research Society 9(5):641-650.

Caplan AI, Correa D. 2011. The MSC: an injury drugstore. Cell stem cell 9(1):11-15.

Carducci MA, Saad F, Abrahamsson PA, Dearnaley DP, Schulman CC, North SA, Sleep DJ, Isaacson JD, Nelson JB, Atrasentan Phase IIISGI. 2007. A phase 3 randomized controlled trial of the efficacy and safety of atrasentan in men with metastatic hormone-refractory prostate cancer. Cancer 110(9):1959-1966.

Carlin BI, Andriole GL. 2000. The natural history, skeletal complications, and management of bone metastases in patients with prostate carcinoma. Cancer 88(12 Suppl):2989-2994.

Carter BS, Beaty TH, Steinberg GD, Childs B, Walsh PC. 1992a. Mendelian inheritance of familial prostate cancer. Proceedings of the National Academy of Sciences of the United States of America 89(8):3367-3371.

Carter BS, Bova GS, Beaty TH, Steinberg GD, Childs B, Isaacs WB, Walsh PC. 1993. Hereditary prostate cancer: epidemiologic and clinical features. The Journal of urology 150(3):797-802.

Carter HB, Pearson JD, Metter EJ, Brant LJ, Chan DW, Andres R, Fozard JL, Walsh PC. 1992b. Longitudinal evaluation of prostate-specific antigen levels in men with and without prostate disease. JAMA : the journal of the American Medical Association 267(16):2215-2220.

Casimiro S, Mohammad KS, Pires R, Tato-Costa J, Alho I, Teixeira R, Carvalho A, Ribeiro S, Lipton A, Guise TA, Costa L. 2013. RANKL/RANK/MMP-1

molecular triad contributes to the metastatic phenotype of breast and prostate cancer cells in vitro. PloS one 8(5):e63153.

Cerhan JR, Parker AS, Putnam SD, Chiu BC, Lynch CF, Cohen MB, Torner JC, Cantor KP. 1999. Family history and prostate cancer risk in a population-based cohort of Iowa men. Cancer epidemiology, biomarkers & prevention : a publication of the American Association for Cancer Research, cosponsored by the American Society of Preventive Oncology 8(1):53-60.

Cerveira N, Ribeiro FR, Peixoto A, Costa V, Henrique R, Jeronimo C, Teixeira MR. 2006. TMPRSS2-ERG gene fusion causing ERG overexpression precedes chromosome copy number changes in prostate carcinomas and paired HGPIN lesions. Neoplasia 8(10):826-832.

Chambers AF, Groom AC, MacDonald IC. 2002. Dissemination and growth of cancer cells in metastatic sites. Nature reviews Cancer 2(8):563-572.

Chan JM, Giovannucci EL. 2001. Dairy products, calcium, and vitamin D and risk of prostate cancer. Epidemiologic reviews 23(1):87-92.

Charhon SA, Chapuy MC, Delvin EE, Valentin-Opran A, Edouard CM, Meunier PJ. 1983. Histomorphometric analysis of sclerotic bone metastases from prostatic carcinoma special reference to osteomalacia. Cancer 51(5):918-924.

Che M, Grignon D. 2002. Pathology of prostate cancer. Cancer metastasis reviews 21(3-4):381-395.

Chen G, Shukeir N, Potti A, Sircar K, Aprikian A, Goltzman D, Rabbani SA. 2004. Up-regulation of Wnt-1 and beta-catenin production in patients with advanced metastatic prostate carcinoma: potential pathogenetic and prognostic implications. Cancer 101(6):1345-1356.

Chen G, Sircar K, Aprikian A, Potti A, Goltzman D, Rabbani SA. 2006. Expression of RANKL/RANK/OPG in primary and metastatic human prostate cancer as markers of disease stage and functional regulation. Cancer 107(2):289-298.

Cher ML, Bova GS, Moore DH, Small EJ, Carroll PR, Pin SS, Epstein JI, Isaacs WB, Jensen RH. 1996. Genetic alterations in untreated metastases and androgen-independent prostate cancer detected by comparative genomic hybridization and allelotyping. Cancer research 56(13):3091-3102.

Chinni SR, Sivalogan S, Dong Z, Filho JC, Deng X, Bonfil RD, Cher ML. 2006. CXCL12/CXCR4 signaling activates Akt-1 and MMP-9 expression in prostate cancer cells: the role of bone microenvironment-associated CXCL12. The Prostate 66(1):32-48.

Chino T, Draves KE, Clark EA. 2009. Regulation of dendritic cell survival and cytokine production by osteoprotegerin. Journal of leukocyte biology 86(4):933-940.

Chirgwin JM, Guise TA. 2007. Skeletal metastases: decreasing tumor burden by targeting the bone microenvironment. Journal of cellular biochemistry 102(6):1333-1342.

Chirgwin JMR, Roodman G.D. 2014. Pathophysiology of Bone Metastases. In: Vassiliou VC, E; Kardamakis, D, editor. Bone Metastases: A translational and Clinical Approach. 2nd ed: Springer. p 3-17.

Chodak G. 2006. Prostate cancer: epidemiology, screening, and biomarkers. Reviews in urology 8 Suppl 2:S3-8.

Chodak GW, Thisted RA, Gerber GS, Johansson JE, Adolfsson J, Jones GW, Chisholm GD, Moskovitz B, Livne PM, Warner J. 1994. Results of conservative management of clinically localized prostate cancer. The New England journal of medicine 330(4):242-248.

Choucair K, Ejdelman J, Brimo F, Aprikian A, Chevalier S, Lapointe J. 2012. PTEN genomic deletion predicts prostate cancer recurrence and is associated with low AR expression and transcriptional activity. BMC cancer 12:543.

Chu GC, Zhau HE, Wang R, Rogatko A, Feng X, Zayzafoon M, Liu Y, Farach-Carson MC, You S, Kim J, Freeman MR, Chung LW. 2014. RANK- and c-Met-mediated signal network promotes prostate cancer metastatic colonization. Endocrine-related cancer 21(2):311-326.

Clark JP, Munson KW, Gu JW, Lamparska-Kupsik K, Chan KG, Yoshida JS, Kawachi MH, Crocitto LE, Wilson TG, Feng Z, Smith SS. 2008. Performance of a single assay for both type III and type VI TMPRSS2:ERG fusions in noninvasive prediction of prostate biopsy outcome. Clinical chemistry 54(12):2007-2017.

Clarke B. 2008. Normal bone anatomy and physiology. Clinical journal of the American Society of Nephrology : CJASN 3 Suppl 3:S131-139.

Clarke NW, Hart CA, Brown MD. 2009. Molecular mechanisms of metastasis in prostate cancer. Asian journal of andrology 11(1):57-67.

Clarke NW, McClure J, George NJ. 1991. Morphometric evidence for bone resorption and replacement in prostate cancer. British journal of urology 68(1):74-80.

Clezardin P. 2009. Integrins in bone metastasis formation and potential therapeutic implications. Current cancer drug targets 9(7):801-806.

Clezardin P, Teti A. 2007. Bone metastasis: pathogenesis and therapeutic implications. Clinical & experimental metastasis 24(8):599-608.

Coffey RN, Watson RW, Fitzpatrick JM. 2001. Signaling for the caspases: their role in prostate cell apoptosis. The Journal of urology 165(1):5-14.

Cohen P, Graves HC, Peehl DM, Kamarei M, Giudice LC, Rosenfeld RG. 1992. Prostate-specific antigen (PSA) is an insulin-like growth factor binding protein-3 protease found in seminal plasma. The Journal of clinical endocrinology and metabolism 75(4):1046-1053.

Coleman RE. 2000. Management of bone metastases. The oncologist 5(6):463-470.

Coleman RE. 2001a. Metastatic bone disease and the role of biochemical markers of bone metabolism in benign and malignant diseases. Cancer treatment reviews 27(3):133-135.

Coleman RE. 2001b. Metastatic bone disease: clinical features, pathophysiology and treatment strategies. Cancer treatment reviews 27(3):165-176.

Coleman RE. 2001c. Should bisphosphonates be the treatment of choice for metastatic bone disease? Seminars in oncology 28(4 Suppl 11):35-41.

Coleman RE. 2006. Clinical features of metastatic bone disease and risk of skeletal morbidity. Clinical cancer research : an official journal of the American Association for Cancer Research 12(20 Pt 2):6243s-6249s.

Coleman RE, Major P, Lipton A, Brown JE, Lee KA, Smith M, Saad F, Zheng M, Hei YJ, Seaman J, Cook R. 2005. Predictive value of bone resorption and formation markers in cancer patients with bone metastases receiving the bisphosphonate zoledronic acid. Journal of clinical oncology : official journal of the American Society of Clinical Oncology 23(22):4925-4935.

Collin-Osdoby P. 2004. Regulation of vascular calcification by osteoclast regulatory factors RANKL and osteoprotegerin. Circulation research 95(11):1046-1057.

Compston JE. 2002. Bone marrow and bone: a functional unit. The Journal of endocrinology 173(3):387-394.

Corder EH, Guess HA, Hulka BS, Friedman GD, Sadler M, Vollmer RT, Lobaugh B, Drezner MK, Vogelman JH, Orentreich N. 1993. Vitamin D and prostate cancer: a prediagnostic study with stored sera. Cancer epidemiology, biomarkers & prevention : a publication of the American Association for Cancer Research, cosponsored by the American Society of Preventive Oncology 2(5):467-472.

Corey E, Brown LG, Kiefer JA, Quinn JE, Pitts TE, Blair JM, Vessella RL. 2005. Osteoprotegerin in prostate cancer bone metastasis. Cancer research 65(5):1710-1718.

Corey E, Quinn JE, Bladou F, Brown LG, Roudier MP, Brown JM, Buhler KR, Vessella RL. 2002. Establishment and characterization of osseous prostate cancer models: intra-tibial injection of human prostate cancer cells. The Prostate 52(1):20-33.

Costa L, Major PP. 2009. Effect of bisphosphonates on pain and quality of life in patients with bone metastases. Nature clinical practice Oncology 6(3):163-174.

Cotter MP, Gern RW, Ho GY, Chang RY, Burk RD. 2002. Role of family history and ethnicity on the mode and age of prostate cancer presentation. The Prostate 50(4):216-221.

Craft N, Shostak Y, Carey M, Sawyers CL. 1999. A mechanism for hormone-independent prostate cancer through modulation of androgen receptor signaling by the HER-2/neu tyrosine kinase. Nature medicine 5(3):280-285.

Cramer SD, Chen Z, Peehl DM. 1996. Prostate specific antigen cleaves parathyroid hormone-related protein in the PTH-like domain: inactivation of PTHrP-stimulated cAMP accumulation in mouse osteoblasts. The Journal of urology 156(2 Pt 1):526-531.

Crawford ED. 2009. Understanding the epidemiology, natural history, and key pathways involved in prostate cancer. Urology 73(5 Suppl):S4-10.

Crawford ED, Bennett CL, Andriole GL, Garnick MB, Petrylak DP. 2013. The utility of prostate-specific antigen in the management of advanced prostate cancer. BJU international 112(5):548-560.

Crawford ED, Stone NN, Yu EY, Koo PJ, Freedland SJ, Slovin SF, Gomella LG, Berger ER, Keane TE, Sieber P, Shore ND, Petrylak DP, Prostate Cancer Radiographic Assessments for Detection of Advanced Recurrence G. 2014. Challenges and recommendations for early identification of metastatic disease in prostate cancer. Urology 83(3):664-669.

Croft M, Duan W, Choi H, Eun SY, Madireddi S, Mehta A. 2012. TNF superfamily in inflammatory disease: translating basic insights. Trends in immunology 33(3):144-152.

Cross SS, Harrison RF, Balasubramanian SP, Lippitt JM, Evans CA, Reed MWR, Holen I. 2006a. Expression of receptor activator of nuclear factor kappa beta ligand (RANKL) and tumour necrosis factor related, apoptosis inducing ligand (TRAIL) in breast cancer, and their relations with osteoprotegerin, oestrogen receptor, and clinicopathological variables. Journal of clinical pathology 59(7):716-720.

Cross SS, Yang Z, Brown NJ, Balasubramanian SP, Evans CA, Woodward JK, Neville-Webbe HL, Lippitt JM, Reed MW, Coleman RE, Holen I. 2006b. Osteoprotegerin (OPG)--a potential new role in the regulation of endothelial cell phenotype and tumour angiogenesis? International journal of cancer Journal international of cancer 118(8):1901-1908.

Croucher PI, Shipman CM, Lippitt J, Perry M, Asosingh K, Hijzen A, Brabbs AC, van Beek EJ, Holen I, Skerry TM, Dunstan CR, Russell GR, Van Camp B, Vanderkerken K. 2001. Osteoprotegerin inhibits the development of osteolytic bone disease in multiple myeloma. Blood 98(13):3534-3540.

Dai J, Keller J, Zhang J, Lu Y, Yao Z, Keller ET. 2005. Bone morphogenetic protein-6 promotes osteoblastic prostate cancer bone metastases through a dual mechanism. Cancer research 65(18):8274-8285.

Dai J, Kitagawa Y, Zhang J, Yao Z, Mizokami A, Cheng S, Nor J, McCauley LK, Taichman RS, Keller ET. 2004. Vascular endothelial growth factor contributes to the prostate cancer-induced osteoblast differentiation mediated by bone morphogenetic protein. Cancer research 64(3):994-999.

Dallas SL, Rosser JL, Mundy GR, Bonewald LF. 2002. Proteolysis of latent transforming growth factor-beta (TGF-beta)-binding protein-1 by osteoclasts. A cellular mechanism for release of TGF-beta from bone matrix. The Journal of biological chemistry 277(24):21352-21360.

Davies G, Jiang WG, Mason MD. 2001. Matrilysin mediates extracellular cleavage of E-cadherin from prostate cancer cells: a key mechanism in hepatocyte growth factor/scatter factor-induced cell-cell dissociation and in vitro invasion. Clinical cancer research : an official journal of the American Association for Cancer Research 7(10):3289-3297.

Davis TL, Cress AE, Dalkin BL, Nagle RB. 2001. Unique expression pattern of the alpha6beta4 integrin and laminin-5 in human prostate carcinoma. The Prostate 46(3):240-248.

De La Taille A, Vacherot F, Salomon L, Druel C, Gil Diez De Medina S, Abbou C, Buttyan R, Chopin D. 2001. Hormone-refractory prostate cancer: a multi-step and multi-event process. Prostate cancer and prostatic diseases 4(4):204-212.

Dearnaley DP, Mason MD, Parmar MK, Sanders K, Sydes MR. 2009. Adjuvant therapy with oral sodium clodronate in locally advanced and metastatic prostate cancer: long-term overall survival results from the MRC PR04 and PR05 randomised controlled trials. The lancet oncology 10(9):872-876.

Demichelis F, Fall K, Perner S, Andren O, Schmidt F, Setlur SR, Hoshida Y, Mosquera JM, Pawitan Y, Lee C, Adami HO, Mucci LA, Kantoff PW, Andersson SO, Chinnaiyan AM, Johansson JE, Rubin MA. 2007. TMPRSS2:ERG gene fusion associated with lethal prostate cancer in a watchful waiting cohort. Oncogene 26(31):4596-4599.

Deng X, He G, Liu J, Luo F, Peng X, Tang S, Gao Z, Lin Q, Keller JM, Yang T, Keller ET. 2014. Recent advances in bone-targeted therapies of metastatic prostate cancer. Cancer treatment reviews 40(6):730-738.

Deras IL, Aubin SM, Blase A, Day JR, Koo S, Partin AW, Ellis WJ, Marks LS, Fradet Y, Rittenhouse H, Groskopf J. 2008. PCA3: a molecular urine assay for predicting prostate biopsy outcome. The Journal of urology 179(4):1587-1592.

Detchokul S, Frauman AG. 2011. Recent developments in prostate cancer biomarker research: therapeutic implications. British journal of clinical pharmacology 71(2):157-174.

Di Lorenzo G, Autorino R, De Laurentiis M, Cindolo L, D'Armiento M, Bianco AR, De Placido S. 2004. HER-2/neu receptor in prostate cancer development and progression to androgen independence. Tumori 90(2):163-170.

Di Lorenzo G, Tortora G, D'Armiento FP, De Rosa G, Staibano S, Autorino R, D'Armiento M, De Laurentiis M, De Placido S, Catalano G, Bianco AR, Ciardiello F. 2002. Expression of epidermal growth factor receptor correlates with disease relapse and progression to androgen-independence in human prostate cancer. Clinical cancer research : an official journal of the American Association for Cancer Research 8(11):3438-3444.

Diarra D, Stolina M, Polzer K, Zwerina J, Ominsky MS, Dwyer D, Korb A, Smolen J, Hoffmann M, Scheinecker C, van der Heide D, Landewe R, Lacey D, Richards WG, Schett G. 2007. Dickkopf-1 is a master regulator of joint remodeling. Nature medicine 13(2):156-163.

Dimakakos A, Armakolas A, Koutsilieris M. 2014. Novel tools for prostate cancer prognosis, diagnosis, and follow-up. BioMed research international 2014:890697.

Djavan B. 2011. Screening for prostate cancer: practical analysis of the ERSPC [corrected] and PLCO trials. European urology 59(3):365-369.

Doll JA, Reiher FK, Crawford SE, Pins MR, Campbell SC, Bouck NP. 2001. Thrombospondin-1, vascular endothelial growth factor and fibroblast growth factor-2 are key functional regulators of angiogenesis in the prostate. The Prostate 49(4):293-305.

Dougall WC. 2012. Molecular pathways: osteoclast-dependent and osteoclast-independent roles of the RANKL/RANK/OPG pathway in tumorigenesis and metastasis. Clinical cancer research : an official journal of the American Association for Cancer Research 18(2):326-335.

Dougall WC, Glaccum M, Charrier K, Rohrbach K, Brasel K, De Smedt T, Daro E, Smith J, Tometsko ME, Maliszewski CR, Armstrong A, Shen V, Bain S, Cosman D, Anderson D, Morrissey PJ, Peschon JJ, Schuh J. 1999. RANK is essential for osteoclast and lymph node development. Genes Dev 13(18):2412-2424.

Dougall WC, Holen I, Gonzalez Suarez E. 2014. Targeting RANKL in metastasis. BoneKEy reports 3:519.

Ducy P, Zhang R, Geoffroy V, Ridall AL, Karsenty G. 1997. Osf2/Cbfa1: a transcriptional activator of osteoblast differentiation. Cell 89(5):747-754.

Dunn JE. 1975. Cancer epidemiology in populations of the United States--with emphasis on Hawaii and California--and Japan. Cancer research 35(11 Pt. 2):3240-3245.

Dunn MW, Kazer MW. 2011. Prostate cancer overview. Seminars in oncology nursing 27(4):241-250.

Dunstan CR, Boyce R, Boyce BF, Garrett IR, Izbicka E, Burgess WH, Mundy GR. 1999. Systemic administration of acidic fibroblast growth factor (FGF-1) prevents bone loss and increases new bone formation in ovariectomized rats. Journal of bone and mineral research : the official journal of the American Society for Bone and Mineral Research 14(6):953-959.

Durand M, Gallant MA, de Brum-Fernandes AJ. 2008. Prostaglandin D2 receptors control osteoclastogenesis and the activity of human osteoclasts. Journal of bone and mineral research : the official journal of the American Society for Bone and Mineral Research 23(7):1097-1105.

Eaton CL, Wells JM, Holen I, Croucher PI, Hamdy FC. 2004. Serum osteoprotegerin (OPG) levels are associated with disease progression and response to androgen ablation in patients with prostate cancer. The Prostate 59(3):304-310.

Edwards JR, Mundy GR. 2011. Advances in osteoclast biology: old findings and new insights from mouse models. Nature reviews Rheumatology 7(4):235-243.

Ehrhardt H, Fulda S, Schmid I, Hiscott J, Debatin KM, Jeremias I. 2003. TRAIL induced survival and proliferation in cancer cells resistant towards TRAIL-induced apoptosis mediated by NF-kappaB. Oncogene 22(25):3842-3852.

Emery JG, McDonnell P, Burke MB, Deen KC, Lyn S, Silverman C, Dul E, Appelbaum ER, Eichman C, DiPrinzio R, Dodds RA, James IE, Rosenberg M, Lee JC, Young PR. 1998. Osteoprotegerin is a receptor for the cytotoxic ligand TRAIL. The Journal of biological chemistry 273(23):14363-14367.

Emmert-Buck MR, Vocke CD, Pozzatti RO, Duray PH, Jennings SB, Florence CD, Zhuang Z, Bostwick DG, Liotta LA, Linehan WM. 1995. Allelic loss on chromosome 8p12-21 in microdissected prostatic intraepithelial neoplasia. Cancer research 55(14):2959-2962.

Epker BN, Frost HM. 1965. Correlation of Bone Resorption and Formation with the Physical Behavior of Loaded Bone. Journal of dental research 44:33-41.

Epstein JI, Cho KR, Quinn BD. 1990. Relationship of severe dysplasia to stage A (incidental) adenocarcinoma of the prostate. Cancer 65(10):2321-2327.

Eskens FA, Dumez H, Hoekstra R, Perschl A, Brindley C, Bottcher S, Wynendaele W, Drevs J, Verweij J, van Oosterom AT. 2003. Phase I and pharmacokinetic study of continuous twice weekly intravenous administration of Cilengitide (EMD 121974), a novel inhibitor of the integrins alphavbeta3 and alphavbeta5 in patients with advanced solid tumours. European journal of cancer 39(7):917-926.

Ewing J. 1935. The General Pathological Conception of Cancer. Canadian Medical Association journal 33(2):125-135.

Fan S, Ma YX, Gao M, Yuan RQ, Meng Q, Goldberg ID, Rosen EM. 2001. The multisubstrate adapter Gab1 regulates hepatocyte growth factor (scatter factor)-c-Met signaling for cell survival and DNA repair. Molecular and cellular biology 21(15):4968-4984.

Farnham JM, Camp NJ, Swensen J, Tavtigian SV, Albright LA. 2005. Confirmation of the HPCX prostate cancer predisposition locus in large Utah prostate cancer pedigrees. Human genetics 116(3):179-185.

Fata JE, Kong YY, Li J, Sasaki T, Irie-Sasaki J, Moorehead RA, Elliott R, Scully S, Voura EB, Lacey DL, Boyle WJ, Khokha R, Penninger JM. 2000. The osteoclast differentiation factor osteoprotegerin-ligand is essential for mammary gland development. Cell 103(1):41-50.

Feldman BJ, Feldman D. 2001. The development of androgen-independent prostate cancer. Nature reviews Cancer 1(1):34-45.

Fernandez-Valdivia R, Mukherjee A, Ying Y, Li J, Paquet M, DeMayo FJ, Lydon JP. 2009. The RANKL signaling axis is sufficient to elicit ductal side-branching and alveologenesis in the mammary gland of the virgin mouse. Developmental biology 328(1):127-139.

Ferrer FA, Miller LJ, Andrawis RI, Kurtzman SH, Albertsen PC, Laudone VP, Kreutzer DL. 1997. Vascular endothelial growth factor (VEGF) expression in human prostate cancer: in situ and in vitro expression of VEGF by human prostate cancer cells. The Journal of urology 157(6):2329-2333.

Fesik SW. 2000. Insights into programmed cell death through structural biology. Cell 103(2):273-282.

Fiandalo MV, Kyprianou N. 2012. Caspase control: protagonists of cancer cell apoptosis. Experimental oncology 34(3):165-175.

Fidler IJ. 1970. Metastasis: guantitative analysis of distribution and fate of tumor embolilabeled with 125 I-5-iodo-2'-deoxyuridine. Journal of the National Cancer Institute 45(4):773-782.

Fidler IJ. 2003a. The pathogenesis of cancer metastasis: the 'seed and soil' hypothesis revisited. Nature reviews Cancer 3(6):453-458.

Fidler IJ. 2003b. Understanding bone metastases: the key to the effective treatment of prostate cancer. Clinical advances in hematology & oncology : H&O 1(5):278-279.

Fidler IJ, Gersten DM, Hart IR. 1978. The biology of cancer invasion and metastasis. Advances in cancer research 28:149-250.

Fidler IJ, Kripke ML. 1977. Metastasis results from preexisting variant cells within a malignant tumor. Science 197(4306):893-895.

Fisher JL, Thomas-Mudge RJ, Elliott J, Hards DK, Sims NA, Slavin J, Martin TJ, Gillespie MT. 2006. Osteoprotegerin overexpression by breast cancer cells enhances orthotopic and osseous tumor growth and contrasts with that delivered therapeutically. Cancer research 66(7):3620-3628.

Fizazi K, Carducci M, Smith M, Damiao R, Brown J, Karsh L, Milecki P, Shore N, Rader M, Wang H, Jiang Q, Tadros S, Dansey R, Goessl C. 2011. Denosumab versus zoledronic acid for treatment of bone metastases in men with castration-resistant prostate cancer: a randomised, double-blind study. Lancet 377(9768):813-822.

Flaherty KT. 2007. Sorafenib: delivering a targeted drug to the right targets. Expert review of anticancer therapy 7(5):617-626.

Fleming WH, Hamel A, MacDonald R, Ramsey E, Pettigrew NM, Johnston B, Dodd JG, Matusik RJ. 1986. Expression of the c-myc protooncogene in human prostatic carcinoma and benign prostatic hyperplasia. Cancer research 46(3):1535-1538.

Fleshner N, Fair WR, Huryk R, Heston WD. 1999. Vitamin E inhibits the high-fat diet promoted growth of established human prostate LNCaP tumors in nude mice. The Journal of urology 161(5):1651-1654.

Fornaro M, Manes T, Languino LR. 2001. Integrins and prostate cancer metastases. Cancer metastasis reviews 20(3-4):321-331.

Fornaro M, Manzotti M, Tallini G, Slear AE, Bosari S, Ruoslahti E, Languino LR. 1998. Beta1C integrin in epithelial cells correlates with a nonproliferative phenotype: forced expression of beta1C inhibits prostate epithelial cell proliferation. The American journal of pathology 153(4):1079-1087.

Fornaro M, Tallini G, Bofetiado CJ, Bosari S, Languino LR. 1996. Down-regulation of beta 1C integrin, an inhibitor of cell proliferation, in prostate carcinoma. The American journal of pathology 149(3):765-773.

Fornaro M, Tallini G, Zheng DQ, Flanagan WM, Manzotti M, Languino LR. 1999. p27(kip1) acts as a downstream effector of and is coexpressed with the beta1C integrin in prostatic adenocarcinoma. The Journal of clinical investigation 103(3):321-329.

Fowler JE, Jr., Lau JL, Ghosh L, Mills SE, Mounzer A. 1988. Epidermal growth factor and prostatic carcinoma: an immunohistochemical study. The Journal of urology 139(4):857-861.

Franz-Odendaal TA, Hall BK, Witten PE. 2006. Buried alive: how osteoblasts become osteocytes. Developmental dynamics : an official publication of the American Association of Anatomists 235(1):176-190.

Friedenstein AJ, Chailakhyan RK, Gerasimov UV. 1987. Bone marrow osteogenic stem cells: in vitro cultivation and transplantation in diffusion chambers. Cell and tissue kinetics 20(3):263-272.

Fudge K, Wang CY, Stearns ME. 1994. Immunohistochemistry analysis of platelet-derived growth factor A and B chains and platelet-derived growth factor alpha and beta receptor expression in benign prostatic hyperplasias and Gleason-graded human prostate adenocarcinomas. Modern pathology : an official journal of the United States and Canadian Academy of Pathology, Inc 7(5):549-554.

Fukuyama R, Ichijoh Y, Minoshima S, Kitamura N, Shimizu N. 1991. Regional localization of the hepatocyte growth factor (HGF) gene to human chromosome 7 band q21.1. Genomics 11(2):410-415.

Funa K, Nordgren H, Nilsson S. 1991. In situ expression of mRNA for proto-oncogenes in benign prostatic hyperplasia and in prostatic carcinoma. Scandinavian journal of urology and nephrology 25(2):95-100.

Galasko CS. 1975. The pathological basis for skeletal scintigraphy. The Journal of bone and joint surgery British volume 57(3):353-359.

Galindo M, Pratap J, Young DW, Hovhannisyan H, Im HJ, Choi JY, Lian JB, Stein JL, Stein GS, van Wijnen AJ. 2005. The bone-specific expression of Runx2 oscillates during the cell cycle to support a G1-related antiproliferative function in osteoblasts. The Journal of biological chemistry 280(21):20274-20285.

Gattei V, Bernabei PA, Pinto A, Bezzini R, Ringressi A, Formigli L, Tanini A, Attadia V, Brandi ML. 1992. Phorbol ester induced osteoclast-like differentiation of a novel human leukemic cell line (FLG 29.1). The Journal of cell biology 116(2):437-447.

Gaziano JM, Hennekens CH. 1995. Dietary fat and risk of prostate cancer. Journal of the National Cancer Institute 87(19):1427-1428.

Gazzerro E, Canalis E. 2006. Bone morphogenetic proteins and their antagonists. Reviews in endocrine & metabolic disorders 7(1-2):51-65.

Gburek BM, Kollmorgen TA, Qian J, D'Souza-Gburek SM, Lieber MM, Jenkins RB. 1997. Chromosomal anomalies in stage D1 prostate adenocarcinoma primary tumors and lymph node metastases detected by fluorescence in situ hybridization. The Journal of urology 157(1):223-227.

Gherardi E, Stoker M. 1990. Hepatocytes and scatter factor. Nature 346(6281):228.

Gibbs M, Stanford JL, McIndoe RA, Jarvik GP, Kolb S, Goode EL, Chakrabarti L, Schuster EF, Buckley VA, Miller EL, Brandzel S, Li S, Hood L, Ostrander EA. 1999. Evidence for a rare prostate cancer-susceptibility locus at chromosome 1p36. American journal of human genetics 64(3):776-787.

Giniger E. 2002. How do Rho family GTPases direct axon growth and guidance? A proposal relating signaling pathways to growth cone mechanics. Differentiation; research in biological diversity 70(8):385-396.

Gioeli D, Mandell JW, Petroni GR, Frierson HF, Jr., Weber MJ. 1999. Activation of mitogen-activated protein kinase associated with prostate cancer progression. Cancer research 59(2):279-284.

Giordano S, Zhen Z, Medico E, Gaudino G, Galimi F, Comoglio PM. 1993. Transfer of motogenic and invasive response to scatter factor/hepatocyte growth factor by transfection of human MET protooncogene. Proceedings of the National Academy of Sciences of the United States of America 90(2):649-653.

Giovannucci E. 1998. Dietary influences of 1,25(OH)2 vitamin D in relation to prostate cancer: a hypothesis. Cancer causes & control : CCC 9(6):567-582.

Giovannucci E, Stampfer MJ, Krithivas K, Brown M, Dahl D, Brufsky A, Talcott J, Hennekens CH, Kantoff PW. 1997. The CAG repeat within the androgen receptor gene and its relationship to prostate cancer. Proceedings of the National Academy of Sciences of the United States of America 94(7):3320-3323.

Giuliani N, Bataille R, Mancini C, Lazzaretti M, Barille S. 2001. Myeloma cells induce imbalance in the osteoprotegerin/osteoprotegerin ligand system in the human bone marrow environment. Blood 98(13):3527-3533.

Glass DA, 2nd, Bialek P, Ahn JD, Starbuck M, Patel MS, Clevers H, Taketo MM, Long F, McMahon AP, Lang RA, Karsenty G. 2005. Canonical Wnt signaling in differentiated osteoblasts controls osteoclast differentiation. Developmental cell 8(5):751-764.

Gleason DF. 1966. Classification of prostatic carcinomas. Cancer chemotherapy reports Part 1 50(3):125-128.

Gleave M, Hsieh JT, Gao CA, von Eschenbach AC, Chung LW. 1991. Acceleration of human prostate cancer growth in vivo by factors produced by prostate and bone fibroblasts. Cancer research 51(14):3753-3761.

Goel HL, Breen M, Zhang J, Das I, Aznavoorian-Cheshire S, Greenberg NM, Elgavish A, Languino LR. 2005. beta1A integrin expression is required for type 1 insulin-like growth factor receptor mitogenic and transforming activities and localization to focal contacts. Cancer research 65(15):6692-6700.

Goel HL, Li J, Kogan S, Languino LR. 2008. Integrins in prostate cancer progression. Endocrine-related cancer 15(3):657-664.

Goltzman D, Bolivar I, Rabbani SA. 1992. Studies on the pathogenesis of osteoblastic metastases by prostate cancer. Advances in experimental medicine and biology 324:165-171.

Gong Y, Slee RB, Fukai N, Rawadi G, Roman-Roman S, Reginato AM, Wang H, Cundy T, Glorieux FH, Lev D, Zacharin M, Oexle K, Marcelino J, Suwairi W, Heeger S, Sabatakos G, Apte S, Adkins WN, Allgrove J, Arslan-Kirchner M, Batch JA, Beighton P, Black GC, Boles RG, Boon LM, Borrone C, Brunner HG, Carle GF, Dallapiccola B, De Paepe A, Floege B, Halfhide ML, Hall B, Hennekam RC, Hirose T, Jans A, Juppner H, Kim CA, Keppler-Noreuil K, Kohlschuetter A, LaCombe D, Lambert M, Lemyre E, Letteboer T, Peltonen L, Ramesar RS, Romanengo M, Somer H, Steichen-Gersdorf E, Steinmann B, Sullivan B, Superti-Furga A, Swoboda W, van den Boogaard MJ, Van Hul W, Vikkula M, Votruba M, Zabel B, Garcia T, Baron R, Olsen BR, Warman

ML, Osteoporosis-Pseudoglioma Syndrome Collaborative G. 2001. LDL receptor-related protein 5 (LRP5) affects bone accrual and eye development. Cell 107(4):513-523.

Gonzalez-Suarez E, Branstetter D, Armstrong A, Dinh H, Blumberg H, Dougall WC. 2007. RANK overexpression in transgenic mice with mouse mammary tumor virus promoter-controlled RANK increases proliferation and impairs alveolar differentiation in the mammary epithelia and disrupts lumen formation in cultured epithelial acini. Molecular and cellular biology 27(4):1442-1454.

Gonzalez-Suarez E, Jacob AP, Jones J, Miller R, Roudier-Meyer MP, Erwert R, Pinkas J, Branstetter D, Dougall WC. 2010. RANK ligand mediates progestin-induced mammary epithelial proliferation and carcinogenesis. Nature 468(7320):103-107.

Graff JR, Herman JG, Lapidus RG, Chopra H, Xu R, Jarrard DF, Isaacs WB, Pitha PM, Davidson NE, Baylin SB. 1995. E-cadherin expression is silenced by DNA hypermethylation in human breast and prostate carcinomas. Cancer research 55(22):5195-5199.

Grano M, Galimi F, Zambonin G, Colucci S, Cottone E, Zallone AZ, Comoglio PM. 1996. Hepatocyte growth factor is a coupling factor for osteoclasts and osteoblasts in vitro. Proceedings of the National Academy of Sciences of the United States of America 93(15):7644-7648.

Gronberg H, Wiklund F, Damber JE. 1999. Age specific risks of familial prostate carcinoma: a basis for screening recommendations in high risk populations. Cancer 86(3):477-483.

Guileyardo JM, Johnson WD, Welsh RA, Akazaki K, Correa P. 1980. Prevalence of latent prostate carcinoma in two U.S. populations. Journal of the National Cancer Institute 65(2):311-316.

Guise TA, Mohammad KS, Clines G, Stebbins EG, Wong DH, Higgins LS, Vessella R, Corey E, Padalecki S, Suva L, Chirgwin JM. 2006. Basic mechanisms responsible for osteolytic and osteoblastic bone metastases. Clinical cancer research : an official journal of the American Association for Cancer Research 12(20 Pt 2):6213s-6216s.

Gupta A, Cao W, Chellaiah MA. 2012. Integrin alpha v beta 3 and CD44 pathways in metastatic prostate cancer cells support osteoclastogenesis via a Runx2/Smad 5/receptor activator of NF-kappa B ligand signaling axis. Mol Cancer 11.

Gurel B, Iwata T, Koh CM, Jenkins RB, Lan F, Van Dang C, Hicks JL, Morgan J, Cornish TC, Sutcliffe S, Isaacs WB, Luo J, De Marzo AM. 2008. Nuclear

MYC protein overexpression is an early alteration in human prostate carcinogenesis. Modern pathology : an official journal of the United States and Canadian Academy of Pathology, Inc 21(9):1156-1167.

Hall CL, Bafico A, Dai J, Aaronson SA, Keller ET. 2005. Prostate cancer cells promote osteoblastic bone metastases through Wnts. Cancer research 65(17):7554-7560.

Hall CL, Dai J, van Golen KL, Keller ET, Long MW. 2006. Type I collagen receptor (alpha 2 beta 1) signaling promotes the growth of human prostate cancer cells within the bone. Cancer research 66(17):8648-8654.

Hall CL, Dubyk CW, Riesenberger TA, Shein D, Keller ET, van Golen KL. 2008. Type I collagen receptor (alpha2beta1) signaling promotes prostate cancer invasion through RhoC GTPase. Neoplasia 10(8):797-803.

Hanahan D, Weinberg RA. 2000. The hallmarks of cancer. Cell 100(1):57-70.

Harris SE, Harris MA, Mahy P, Wozney J, Feng JQ, Mundy GR. 1994. Expression of bone morphogenetic protein messenger RNAs by normal rat and human prostate and prostate cancer cells. The Prostate 24(4):204-211.

Hart CA, Scott LJ, Bagley S, Bryden AA, Clarke NW, Lang SH. 2002. Role of proteolytic enzymes in human prostate bone metastasis formation: in vivo and in vitro studies. British journal of cancer 86(7):1136-1142.

Hart IR, Fidler IJ. 1980. Role of organ selectivity in the determination of metastatic patterns of B16 melanoma. Cancer research 40(7):2281-2287.

Hasegawa Y, Yamamoto M, Maeda S, Saitoh Y. 1995. Hepatocyte growth-factor and its receptor C-met regulate both cell-growth and invasion of human pancreatic-cancer. International journal of oncology 7(4):877-881.

Hayashida C, Ito J, Nakayachi M, Okayasu M, Ohyama Y, Hakeda Y, Sato T. 2014. Osteocytes produce interferon-beta as a negative regulator of osteoclastogenesis. The Journal of biological chemistry 289(16):11545-11555.

Heemers HV, Tindall DJ. 2007. Androgen receptor (AR) coregulators: a diversity of functions converging on and regulating the AR transcriptional complex. Endocrine reviews 28(7):778-808.

Heidenreich A, Bastian PJ, Bellmunt J, Bolla M, Joniau S, van der Kwast T, Mason M, Matveev V, Wiegel T, Zattoni F, Mottet N. 2014a. EAU guidelines on prostate cancer. Part II: Treatment of advanced, relapsing, and castration-resistant prostate cancer. European urology 65(2):467-479.

Heidenreich A, Bastian PJ, Bellmunt J, Bolla M, Joniau S, van der Kwast T, Mason M, Matveev V, Wiegel T, Zattoni F, Mottet N, European Association of U.

2014b. EAU guidelines on prostate cancer. part 1: screening, diagnosis, and local treatment with curative intent-update 2013. European urology 65(1):124-137.

Heidenreich A, Bellmunt J, Bolla M, Joniau S, Mason M, Matveev V, Mottet N, Schmid HP, van der Kwast T, Wiegel T, Zattoni F, European Association of U. 2011. EAU guidelines on prostate cancer. Part 1: screening, diagnosis, and treatment of clinically localised disease. European urology 59(1):61-71.

Heinonen OP, Albanes D, Virtamo J, Taylor PR, Huttunen JK, Hartman AM, Haapakoski J, Malila N, Rautalahti M, Ripatti S, Maenpaa H, Teerenhovi L, Koss L, Virolainen M, Edwards BK. 1998. Prostate cancer and supplementation with alpha-tocopherol and beta-carotene: incidence and mortality in a controlled trial. Journal of the National Cancer Institute 90(6):440-446.

Hernandez J, Thompson IM. 2004. Prostate-specific antigen: a review of the validation of the most commonly used cancer biomarker. Cancer 101(5):894-904.

Hess KR, Varadhachary GR, Taylor SH, Wei W, Raber MN, Lenzi R, Abbruzzese JL. 2006. Metastatic patterns in adenocarcinoma. Cancer 106(7):1624-1633.

Hessels D, Smit FP, Verhaegh GW, Witjes JA, Cornel EB, Schalken JA. 2007. Detection of TMPRSS2-ERG fusion transcripts and prostate cancer antigen 3 in urinary sediments may improve diagnosis of prostate cancer. Clinical cancer research : an official journal of the American Association for Cancer Research 13(17):5103-5108.

Hill TP, Spater D, Taketo MM, Birchmeier W, Hartmann C. 2005. Canonical Wnt/beta-catenin signaling prevents osteoblasts from differentiating into chondrocytes. Developmental cell 8(5):727-738.

Hiratsuka S, Nakamura K, Iwai S, Murakami M, Itoh T, Kijima H, Shipley JM, Senior RM, Shibuya M. 2002. MMP9 induction by vascular endothelial growth factor receptor-1 is involved in lung-specific metastasis. Cancer cell 2(4):289-300.

Hirbe AC, Uluckan O, Morgan EA, Eagleton MC, Prior JL, Piwnica-Worms D, Trinkaus K, Apicelli A, Weilbaecher K. 2007. Granulocyte colony-stimulating factor enhances bone tumor growth in mice in an osteoclast-dependent manner. Blood 109(8):3424-3431.

Hofbauer LC, Khosla S. 1999. Androgen effects on bone metabolism: recent progress and controversies. European journal of endocrinology / European Federation of Endocrine Societies 140(4):271-286.

Hofbauer LC, Kuhne CA, Viereck V. 2004. The OPG/RANKL/RANK system in metabolic bone diseases. Journal of musculoskeletal & neuronal interactions 4(3):268-275.

Hofbauer LC, Schoppet M. 2004. Clinical implications of the osteoprotegerin/RANKL/RANK system for bone and vascular diseases. JAMA : the journal of the American Medical Association 292(4):490-495.

Holen I, Cross SS, Neville-Webbe HL, Cross NA, Balasubramanian SP, Croucher PI, Evans CA, Lippitt JM, Coleman RE, Eaton CL. 2005. Osteoprotegerin (OPG) expression by breast cancer cells in vitro and breast tumours in vivo--a role in tumour cell survival? Breast cancer research and treatment 92(3):207-215.

Holen I, Croucher PI, Hamdy FC, Eaton CL. 2002. Osteoprotegerin (OPG) is a survival factor for human prostate cancer cells. Cancer research 62(6):1619-1623.

Holen I, Shipman CM. 2006. Role of osteoprotegerin (OPG) in cancer. Clin Sci 110(3):279-291.

Holman CD, Wisniewski ZS, Semmens JB, Rouse IL, Bass AJ. 1999. Mortality and prostate cancer risk in 19,598 men after surgery for benign prostatic hyperplasia. BJU international 84(1):37-42.

Hong H, Shi Z, Qiao P, Li H, McCoy EM, Mao P, Xu H, Feng X, Wang S. 2013. Interleukin-3 plays dual roles in osteoclastogenesis by promoting the development of osteoclast progenitors but inhibiting the osteoclastogenic process. Biochemical and biophysical research communications 440(4):545-550.

Horwood NJ, Elliott J, Martin TJ, Gillespie MT. 1998. Osteotropic agents regulate the expression of osteoclast differentiation factor and osteoprotegerin in osteoblastic stromal cells. Endocrinology 139(11):4743-4746.

Hoshi K, Komori T, Ozawa H. 1999. Morphological characterization of skeletal cells in Cbfa1-deficient mice. Bone 25(6):639-651.

Hsieh CL, Oakley-Girvan I, Balise RR, Halpern J, Gallagher RP, Wu AH, Kolonel LN, O'Brien LE, Lin IG, Van Den Berg DJ, Teh CZ, West DW, Whittemore AS. 2001. A genome screen of families with multiple cases of prostate cancer: evidence of genetic heterogeneity. American journal of human genetics 69(1):148-158.

Hu H, Hilton MJ, Tu X, Yu K, Ornitz DM, Long F. 2005. Sequential roles of Hedgehog and Wnt signaling in osteoblast development. Development 132(1):49-60.

Hu L, Shi Y, Hsu JH, Gera J, Van Ness B, Lichtenstein A. 2003. Downstream effectors of oncogenic ras in multiple myeloma cells. Blood 101(8):3126-3135.

Hu P, Chung LW, Berel D, Frierson HF, Yang H, Liu C, Wang R, Li Q, Rogatko A, Zhau HE. 2013. Convergent RANK- and c-Met-mediated signaling components predict survival of patients with prostate cancer: an interracial comparative study. PloS one 8(9):e73081.

Huang WC, Wu D, Xie Z, Zhau HE, Nomura T, Zayzafoon M, Pohl J, Hsieh CL, Weitzmann MN, Farach-Carson MC, Chung LW. 2006. beta2-microglobulin is a signaling and growth-promoting factor for human prostate cancer bone metastasis. Cancer research 66(18):9108-9116.

Humphrey PA. 2004. Gleason grading and prognostic factors in carcinoma of the prostate. Modern pathology : an official journal of the United States and Canadian Academy of Pathology, Inc 17(3):292-306.

Humphrey PA, Zhu X, Zarnegar R, Swanson PE, Ratliff TL, Vollmer RT, Day ML. 1995. Hepatocyte growth factor and its receptor (c-MET) in prostatic carcinoma. The American journal of pathology 147(2):386-396.

Hynes RO. 2002. Integrins: bidirectional, allosteric signaling machines. Cell 110(6):673-687.

Hynes RO, Lively JC, McCarty JH, Taverna D, Francis SE, Hodivala-Dilke K, Xiao Q. 2002. The diverse roles of integrins and their ligands in angiogenesis. Cold Spring Harbor symposia on quantitative biology 67:143-153.

Ibrahim T, Sacanna E, Gaudio M, Mercatali L, Scarpi E, Zoli W, Serra P, Ricci R, Serra L, Kang YB, Amadori D. 2011. Role of RANK, RANKL, OPG, and CXCR4 Tissue Markers in Predicting Bone Metastases in Breast Cancer Patients. Clinical breast cancer 11(6):369-375.

Idriss HT, Naismith JH. 2000. TNF alpha and the TNF receptor superfamily: structure-function relationship(s). Microscopy research and technique 50(3):184-195.

Ikeda F, Nishimura R, Matsubara T, Tanaka S, Inoue J, Reddy SV, Hata K, Yamashita K, Hiraga T, Watanabe T, Kukita T, Yoshioka K, Rao A, Yoneda T. 2004. Critical roles of c-Jun signaling in regulation of NFAT family and RANKL-regulated osteoclast differentiation. The Journal of clinical investigation 114(4):475-484.

Ikezoe T, Yang Y, Saito T, Koeffler HP, Taguchi H. 2004. Proteasome inhibitor PS-341 down-regulates prostate-specific antigen (PSA) and induces growth

arrest and apoptosis of androgen-dependent human prostate cancer LNCaP cells. Cancer science 95(3):271-275.

Imperato-McGinley J, Zhu YS. 2002. Androgens and male physiology the syndrome of 5alpha-reductase-2 deficiency. Molecular and cellular endocrinology 198(1-2):51-59.

Iwamura M, Hellman J, Cockett AT, Lilja H, Gershagen S. 1996. Alteration of the hormonal bioactivity of parathyroid hormone-related protein (PTHrP) as a result of limited proteolysis by prostate-specific antigen. Urology 48(2):317-325.

Jacobs SC, Lawson RK. 1980. Mitogenic factor in human prostate extracts. Urology 16(5):488-491.

Jacobsen K, Kravitz J, Kincade PW, Osmond DG. 1996. Adhesion receptors on bone marrow stromal cells: in vivo expression of vascular cell adhesion molecule-1 by reticular cells and sinusoidal endothelium in normal and gamma-irradiated mice. Blood 87(1):73-82.

Jakob F, Siggelkow H, Homann D, Kohrle J, Adamski J, Schutze N. 1997. Local estradiol metabolism in osteoblast- and osteoclast-like cells. The Journal of steroid biochemistry and molecular biology 61(3-6):167-174.

Javed A, Barnes GL, Pratap J, Antkowiak T, Gerstenfeld LC, van Wijnen AJ, Stein JL, Lian JB, Stein GS. 2005. Impaired intranuclear trafficking of Runx2 (AML3/CBFA1) transcription factors in breast cancer cells inhibits osteolysis in vivo. Proceedings of the National Academy of Sciences of the United States of America 102(5):1454-1459.

Jenkins RB, Qian J, Lieber MM, Bostwick DG. 1997. Detection of c-myc oncogene amplification and chromosomal anomalies in metastatic prostatic carcinoma by fluorescence in situ hybridization. Cancer research 57(3):524-531.

Jiang W, Hiscox S, Matsumoto K, Nakamura T. 1999. Hepatocyte growth factor/scatter factor, its molecular, cellular and clinical implications in cancer. Critical reviews in oncology/hematology 29(3):209-248.

Jiang W, Hiscox S, Nakamura T, Hallett M, Puntis M, Mansel R. 1996. Hepatocyte growth factor induces tyrosine phosphorylation of focal adhesion kinase (FAK) and paxillin and enhances cell-matrix interactions. Oncology reports 3(5):819-823.

Jiang WG, Davies G, Martin TA, Parr C, Watkins G, Mason MD, Mokbel K, Mansel RE. 2005a. Targeting matrilysin and its impact on tumor growth in vivo: the potential implications in breast cancer therapy. Clinical cancer research : an

official journal of the American Association for Cancer Research 11(16):6012-6019.

Jiang WG, Hiscox S, Hallett MB, Horrobin DF, Mansel RE, Puntis MC. 1995a. Regulation of the expression of E-cadherin on human cancer cells by gamma-linolenic acid (GLA). Cancer research 55(21):5043-5048.

Jiang WG, Hiscox S, Singhrao SK, Nakamura T, Puntis MC, Hallett MB. 1995b. Inhibition of HGF/SF-induced membrane ruffling and cell motility by transient elevation of cytosolic free Ca2+. Experimental cell research 220(2):424-433.

Jiang WG, Martin TA, Parr C, Davies G, Matsumoto K, Nakamura T. 2005b. Hepatocyte growth factor, its receptor, and their potential value in cancer therapies. Critical reviews in oncology/hematology 53(1):35-69.

Jin JK, Dayyani F, Gallick GE. 2011. Steps in prostate cancer progression that lead to bone metastasis. International journal of cancer Journal international du cancer 128(11):2545-2561.

Jin Z, El-Deiry WS. 2005. Overview of cell death signaling pathways. Cancer biology & therapy 4(2):139-163.

Johansson JE, Andren O, Andersson SO, Dickman PW, Holmberg L, Magnuson A, Adami HO. 2004. Natural history of early, localized prostate cancer. JAMA : the journal of the American Medical Association 291(22):2713-2719.

Johnstone RW, Ruefli AA, Lowe SW. 2002. Apoptosis: a link between cancer genetics and chemotherapy. Cell 108(2):153-164.

Jones DH, Nakashima T, Sanchez OH, Kozieradzki I, Komarova SV, Sarosi I, Morony S, Rubin E, Sarao R, Hojilla CV, Komnenovic V, Kong YY, Schreiber M, Dixon SJ, Sims SM, Khokha R, Wada T, Penninger JM. 2006. Regulation of cancer cell migration and bone metastasis by RANKL. Nature 440(7084):692-696.

Jono S, Ikari Y, Shioi A, Mori K, Miki T, Hara K, Nishizawa Y. 2002. Serum osteoprotegerin levels are associated with the presence and severity of coronary artery disease. Circulation 106(10):1192-1194.

Jorda M, Morales A, Ghorab Z, Fernandez G, Nadji M, Block N. 2002. Her2 expression in prostatic cancer: a comparison with mammary carcinoma. The Journal of urology 168(4 Pt 1):1412-1414.

Joshi PA, Jackson HW, Beristain AG, Di Grappa MA, Mote PA, Clarke CL, Stingl J, Waterhouse PD, Khokha R. 2010. Progesterone induces adult mammary stem cell expansion. Nature 465(7299):803-807.

Jung K, Lein M, Stephan C, Von Hosslin K, Semjonow A, Sinha P, Loening SA, Schnorr D. 2004. Comparison of 10 serum bone turnover markers in

prostate carcinoma patients with bone metastatic spread: diagnostic and prognostic implications. International journal of cancer Journal international du cancer 111(5):783-791.

Kakonen SM, Mundy GR. 2003. Mechanisms of osteolytic bone metastases in breast carcinoma. Cancer 97(3 Suppl):834-839.

Kallakury BV, Sheehan CE, Ambros RA, Fisher HA, Kaufman RP, Jr., Muraca PJ, Ross JS. 1998. Correlation of p34cdc2 cyclin-dependent kinase overexpression, CD44s downregulation, and HER-2/neu oncogene amplification with recurrence in prostatic adenocarcinomas. Journal of clinical oncology : official journal of the American Society of Clinical Oncology 16(4):1302-1309.

Kang Y, Siegel PM, Shu W, Drobnjak M, Kakonen SM, Cordon-Cardo C, Guise TA, Massague J. 2003. A multigenic program mediating breast cancer metastasis to bone. Cancer cell 3(6):537-549.

Kaplan RN, Psaila B, Lyden D. 2006. Bone marrow cells in the 'pre-metastatic niche': within bone and beyond. Cancer metastasis reviews 25(4):521-529.

Karadag A, Ogbureke KU, Fedarko NS, Fisher LW. 2004. Bone sialoprotein, matrix metalloproteinase 2, and alpha(v)beta3 integrin in osteotropic cancer cell invasion. Journal of the National Cancer Institute 96(12):956-965.

Karsenty G. 2003. The complexities of skeletal biology. Nature 423(6937):316-318.

Kasimir-Bauer S. 2009. Circulating tumor cells as markers for cancer risk assessment and treatment monitoring. Molecular diagnosis & therapy 13(4):209-215.

Katagiri T, Takahashi N. 2002. Regulatory mechanisms of osteoblast and osteoclast differentiation. Oral diseases 8(3):147-159.

Kelly T, Suva LJ, Huang Y, Macleod V, Miao HQ, Walker RC, Sanderson RD. 2005. Expression of heparanase by primary breast tumors promotes bone resorption in the absence of detectable bone metastases. Cancer research 65(13):5778-5784.

Kemler R. 1993. From cadherins to catenins: cytoplasmic protein interactions and regulation of cell adhesion. Trends in genetics : TIG 9(9):317-321.

Khosla S. 2001. Minireview: the OPG/RANKL/RANK system. Endocrinology 142(12):5050-5055.

Kiechl S, Schett G, Wenning G, Redlich K, Oberhollenzer M, Mayr A, Santer P, Smolen J, Poewe W, Willeit J. 2004. Osteoprotegerin is a risk factor for progressive atherosclerosis and cardiovascular disease. Circulation 109(18):2175-2180.

Kiefer JA, Vessella RL, Quinn JE, Odman AM, Zhang J, Keller ET, Kostenuik PJ, Dunstan CR, Corey E. 2004. The effect of osteoprotegerin administration on the intra-tibial growth of the osteoblastic LuCaP 23.1 prostate cancer xenograft. Clinical & experimental metastasis 21(5):381-387.

Kim JW, Lee MS, Lee CH, Kim HY, Chae SU, Kwak HB, Oh J. 2012. Effect of interferon-gamma on the fusion of mononuclear osteoclasts into bone-resorbing osteoclasts. BMB reports 45(5):281-286.

Kirby RS. 2003. An Atlas of Prostatic Diseases: Parthenon Publishing Group Inc.

Kirschenbaum A, Liu XH, Yao S, Leiter A, Levine AC. 2011. Prostatic acid phosphatase is expressed in human prostate cancer bone metastases and promotes osteoblast differentiation. Annals of the New York Academy of Sciences 1237:64-70.

Knekt P, Aromaa A, Maatela J, Aaran RK, Nikkari T, Hakama M, Hakulinen T, Peto R, Saxen E, Teppo L. 1988. Serum Vitamin-E and Risk of Cancer among Finnish Men during a 10-Year Follow-Up. American journal of epidemiology 127(1):28-41.

Knox JD, Cress AE, Clark V, Manriquez L, Affinito KS, Dalkin BL, Nagle RB. 1994. Differential expression of extracellular matrix molecules and the alpha 6-integrins in the normal and neoplastic prostate. The American journal of pathology 145(1):167-174.

Koch CA, Anderson D, Moran MF, Ellis C, Pawson T. 1991. SH2 and SH3 domains: elements that control interactions of cytoplasmic signaling proteins. Science 252(5006):668-674.

Koeneman KS, Yeung F, Chung LW. 1999. Osteomimetic properties of prostate cancer cells: a hypothesis supporting the predilection of prostate cancer metastasis and growth in the bone environment. The Prostate 39(4):246-261.

Komori T. 2010. Regulation of osteoblast differentiation by Runx2. Advances in experimental medicine and biology 658:43-49.

Komori T, Yagi H, Nomura S, Yamaguchi A, Sasaki K, Deguchi K, Shimizu Y, Bronson RT, Gao YH, Inada M, Sato M, Okamoto R, Kitamura Y, Yoshiki S, Kishimoto T. 1997. Targeted disruption of Cbfa1 results in a complete lack of bone formation owing to maturational arrest of osteoblasts. Cell 89(5):755-764.

Kong YY, Boyle WJ, Penninger JM. 1999. Osteoprotegerin ligand: a common link between osteoclastogenesis, lymph node formation and lymphocyte development. Immunology and cell biology 77(2):188-193.

Korah R, Boots M, Wieder R. 2004. Integrin alpha5beta1 promotes survival of growth-arrested breast cancer cells: an in vitro paradigm for breast cancer dormancy in bone marrow. Cancer research 64(13):4514-4522.

Kostenuik PJ. 2005. Osteoprotegerin and RANKL regulate bone resorption, density, geometry and strength. Current opinion in pharmacology 5(6):618-625.

Koutsilieris M. 1995. Skeletal metastases in advanced prostate cancer: cell biology and therapy. Critical reviews in oncology/hematology 18(1):51-64.

Koutsilieris M, Frenette G, Lazure C, Lehoux JG, Govindan MV, Polychronakos C. 1993. Urokinase-type plasminogen activator: a paracrine factor regulating the bioavailability of IGFs in PA-III cell-induced osteoblastic metastases. Anticancer research 13(2):481-486.

Koutsilieris M, Rabbani SA, Bennett HP, Goltzman D. 1987. Characteristics of prostate-derived growth factors for cells of the osteoblast phenotype. The Journal of clinical investigation 80(4):941-946.

Krumholtz JS, Carvalhal GF, Ramos CG, Smith DS, Thorson P, Yan Y, Humphrey PA, Roehl KA, Catalona WJ. 2002. Prostate-specific antigen cutoff of 2.6 ng/mL for prostate cancer screening is associated with favorable pathologic tumor features. Urology 60(3):469-473; discussion 473-464.

Kuba K, Matsumoto K, Date K, Shimura H, Tanaka M, Nakamura T. 2000. HGF/NK4, a four-kringle antagonist of hepatocyte growth factor, is an angiogenesis inhibitor that suppresses tumor growth and metastasis in mice. Cancer research 60(23):6737-6743.

Kubota T, Michigami T, Ozono K. 2009. Wnt signaling in bone metabolism. Journal of bone and mineral metabolism 27(3):265-271.

Kuhn EJ, Kurnot RA, Sesterhenn IA, Chang EH, Moul JW. 1993. Expression of the c-erbB-2 (HER-2/neu) oncoprotein in human prostatic carcinoma. The Journal of urology 150(5 Pt 1):1427-1433.

Kular J, Tickner J, Chim SM, Xu J. 2012. An overview of the regulation of bone remodelling at the cellular level. Clinical biochemistry 45(12):863-873.

Lacey DL, Boyle WJ, Simonet WS, Kostenuik PJ, Dougall WC, Sullivan JK, San Martin J, Dansey R. 2012. Bench to bedside: elucidation of the OPG-RANK-RANKL pathway and the development of denosumab. Nature reviews Drug discovery 11(5):401-419.

Lacey DL, Timms E, Tan HL, Kelley MJ, Dunstan CR, Burgess T, Elliott R, Colombero A, Elliott G, Scully S, Hsu H, Sullivan J, Hawkins N, Davy E, Capparelli C, Eli A, Qian YX, Kaufman S, Sarosi I, Shalhoub V, Senaldi G,

Guo J, Delaney J, Boyle WJ. 1998. Osteoprotegerin ligand is a cytokine that regulates osteoclast differentiation and activation. Cell 93(2):165-176.

Lane D, Matte I, Rancourt C, Piche A. 2012. Osteoprotegerin (OPG) protects ovarian cancer cells from TRAIL-induced apoptosis but does not contribute to malignant ascites-mediated attenuation of TRAIL-induced apoptosis. Journal of ovarian research 5(1):34.

Latil A, Cussenot O, Fournier G, Lidereau R. 1997. Infrequent allelic imbalance at the major susceptibility HPC1 locus in sporadic prostate tumours. International journal of cancer Journal international du cancer 71(6):1118.

Latil A, Lidereau R. 1998. Genetic aspects of prostate cancer. Virchows Archiv : an international journal of pathology 432(5):389-406.

Lee KS, Kim HJ, Li QL, Chi XZ, Ueta C, Komori T, Wozney JM, Kim EG, Choi JY, Ryoo HM, Bae SC. 2000. Runx2 is a common target of transforming growth factor beta1 and bone morphogenetic protein 2, and cooperation between Runx2 and Smad5 induces osteoblast-specific gene expression in the pluripotent mesenchymal precursor cell line C2C12. Molecular and cellular biology 20(23):8783-8792.

Lee MH, Javed A, Kim HJ, Shin HI, Gutierrez S, Choi JY, Rosen V, Stein JL, van Wijnen AJ, Stein GS, Lian JB, Ryoo HM. 1999. Transient upregulation of CBFA1 in response to bone morphogenetic protein-2 and transforming growth factor beta1 in C2C12 myogenic cells coincides with suppression of the myogenic phenotype but is not sufficient for osteoblast differentiation. Journal of cellular biochemistry 73(1):114-125.

Lee RJ, Saylor PJ, Smith MR. 2011. Treatment and prevention of bone complications from prostate cancer. Bone 48(1):88-95.

Lee SK, Lorenzo JA. 1999. Parathyroid hormone stimulates TRANCE and inhibits osteoprotegerin messenger ribonucleic acid expression in murine bone marrow cultures: correlation with osteoclast-like cell formation. Endocrinology 140(8):3552-3561.

Lehr JE, Pienta KJ. 1998. Preferential adhesion of prostate cancer cells to a human bone marrow endothelial cell line. Journal of the National Cancer Institute 90(2):118-123.

Leong DT, Lim J, Goh X, Pratap J, Pereira BP, Kwok HS, Nathan SS, Dobson JR, Lian JB, Ito Y, Voorhoeve PM, Stein GS, Salto-Tellez M, Cool SM, van Wijnen AJ. 2010. Cancer-related ectopic expression of the bone-related transcription factor RUNX2 in non-osseous metastatic tumor cells is linked to cell proliferation and motility. Breast cancer research : BCR 12(5):R89.

Lerch PG, Rickli EE, Lergier W, Gillessen D. 1980. Localization of individual lysine-binding regions in human plasminogen and investigations on their complex-forming properties. European journal of biochemistry / FEBS 107(1):7-13.

Lesko SM, Rosenberg L, Shapiro S. 1996. Family history and prostate cancer risk. American journal of epidemiology 144(11):1041-1047.

Li J, Sarosi I, Yan XQ, Morony S, Capparelli C, Tan HL, McCabe S, Elliott R, Scully S, Van G, Kaufman S, Juan SC, Sun Y, Tarpley J, Martin L, Christensen K, McCabe J, Kostenuik P, Hsu H, Fletcher F, Dunstan CR, Lacey DL, Boyle WJ. 2000. RANK is the intrinsic hematopoietic cell surface receptor that controls osteoclastogenesis and regulation of bone mass and calcium metabolism. Proceedings of the National Academy of Sciences of the United States of America 97(4):1566-1571.

Li J, Yen C, Liaw D, Podsypanina K, Bose S, Wang SI, Puc J, Miliaresis C, Rodgers L, McCombie R, Bigner SH, Giovanella BC, Ittmann M, Tycko B, Hibshoosh H, Wigler MH, Parsons R. 1997. PTEN, a putative protein tyrosine phosphatase gene mutated in human brain, breast, and prostate cancer. Science 275(5308):1943-1947.

Li L, Yu H, Schumacher F, Casey G, Witte JS. 2003. Relation of serum insulin-like growth factor-I (IGF-I) and IGF binding protein-3 to risk of prostate cancer (United States). Cancer causes & control : CCC 14(8):721-726.

Lian JB, Stein GS. 1995. Development of the osteoblast phenotype: molecular mechanisms mediating osteoblast growth and differentiation. The Iowa orthopaedic journal 15:118-140.

Liao J, Schneider A, Datta NS, McCauley LK. 2006. Extracellular calcium as a candidate mediator of prostate cancer skeletal metastasis. Cancer research 66(18):9065-9073.

Lichtinghagen R, Musholt PB, Lein M, Romer A, Rudolph B, Kristiansen G, Hauptmann S, Schnorr D, Loening SA, Jung K. 2002. Different mRNA and protein expression of matrix metalloproteinases 2 and 9 and tissue inhibitor of metalloproteinases 1 in benign and malignant prostate tissue. European urology 42(4):398-406.

Lilja H, Ulmert D, Vickers AJ. 2008. Prostate-specific antigen and prostate cancer: prediction, detection and monitoring. Nature reviews Cancer 8(4):268-278.

Lin JM, Callon KE, Lin CQ, Bava U, Zheng MH, Reid IR, Cornish J. 2007. Alteration of bone cell function by RANKL and OPG in different in vitro models. European journal of clinical investigation 37(5):407-415.

Linja MJ, Savinainen KJ, Saramaki OR, Tammela TL, Vessella RL, Visakorpi T. 2001. Amplification and overexpression of androgen receptor gene in hormone-refractory prostate cancer. Cancer research 61(9):3550-3555.

Lipton A, Ali SM, Leitzel K, Chinchilli V, Witters L, Engle L, Holloway D, Bekker P, Dunstan CR. 2002. Serum osteoprotegerin levels in healthy controls and cancer patients. Clinical cancer research : an official journal of the American Association for Cancer Research 8(7):2306-2310.

Liu XH, Kirschenbaum A, Yao S, Levine AC. 2005. Cross-talk between the interleukin-6 and prostaglandin E(2) signaling systems results in enhancement of osteoclastogenesis through effects on the osteoprotegerin/receptor activator of nuclear factor-{kappa}B (RANK) ligand/RANK system. Endocrinology 146(4):1991-1998.

Locke FB, King H. 1980. Cancer mortality risk among Japanese in the United States. Journal of the National Cancer Institute 65(5):1149-1156.

Locksley RM, Killeen N, Lenardo MJ. 2001. The TNF and TNF receptor superfamilies: integrating mammalian biology. Cell 104(4):487-501.

Logothetis CJ, Lin SH. 2005. Osteoblasts in prostate cancer metastasis to bone. Nature reviews Cancer 5(1):21-28.

Lokeshwar BL, Selzer MG, Block NL, Gunja-Smith Z. 1993. Secretion of matrix metalloproteinases and their inhibitors (tissue inhibitor of metalloproteinases) by human prostate in explant cultures: reduced tissue inhibitor of metalloproteinase secretion by malignant tissues. Cancer research 53(19):4493-4498.

Lorente D, De Bono JS. 2014. Molecular alterations and emerging targets in castration resistant prostate cancer. European journal of cancer 50(4):753-764.

Lozupone E, Palumbo C, Favia A, Ferretti M, Palazzini S, Cantatore FP. 1996. Intermittent compressive load stimulates osteogenesis and improves osteocyte viability in bones cultured "in vitro". Clinical rheumatology 15(6):563-572.

Lu X, Wang Q, Hu G, Van Poznak C, Fleisher M, Reiss M, Massague J, Kang Y. 2009. ADAMTS1 and MMP1 proteolytically engage EGF-like ligands in an osteolytic signaling cascade for bone metastasis. Genes Dev 23(16):1882-1894.

Luan X, Lu Q, Jiang Y, Zhang S, Wang Q, Yuan H, Zhao W, Wang J, Wang X. 2012. Crystal structure of human RANKL complexed with its decoy receptor osteoprotegerin. Journal of immunology 189(1):245-252.

Ludwig M, Weidner W. 2000. [Diagnosis and therapy of prostatitis syndrome]. Der Urologe Ausg A 39(4):371-382.

Lynch CC. 2011. Matrix metalloproteinases as master regulators of the vicious cycle of bone metastasis. Bone 48(1):44-53.

Lynch CC, Hikosaka A, Acuff HB, Martin MD, Kawai N, Singh RK, Vargo-Gogola TC, Begtrup JL, Peterson TE, Fingleton B, Shirai T, Matrisian LM, Futakuchi M. 2005. MMP-7 promotes prostate cancer-induced osteolysis via the solubilization of RANKL. Cancer cell 7(5):485-496.

Lynch CC, Vargo-Gogola T, Matrisian LM, Fingleton B. 2010. Cleavage of E-Cadherin by Matrix Metalloproteinase-7 Promotes Cellular Proliferation in Nontransformed Cell Lines via Activation of RhoA. Journal of oncology 2010:530745.

Lynch MP, Stein JL, Stein GS, Lian JB. 1995. The influence of type I collagen on the development and maintenance of the osteoblast phenotype in primary and passaged rat calvarial osteoblasts: modification of expression of genes supporting cell growth, adhesion, and extracellular matrix mineralization. Experimental cell research 216(1):35-45.

Macoska JA, Trybus TM, Benson PD, Sakr WA, Grignon DJ, Wojno KD, Pietruk T, Powell IJ. 1995. Evidence for three tumor suppressor gene loci on chromosome 8p in human prostate cancer. Cancer research 55(22):5390-5395.

Magi-Galluzzi C, Mishra R, Fiorentino M, Montironi R, Yao H, Capodieci P, Wishnow K, Kaplan I, Stork PJ, Loda M. 1997. Mitogen-activated protein kinase phosphatase 1 is overexpressed in prostate cancers and is inversely related to apoptosis. Laboratory investigation; a journal of technical methods and pathology 76(1):37-51.

Maier C, Herkommer K, Hoegel J, Vogel W, Paiss T. 2005. A genomewide linkage analysis for prostate cancer susceptibility genes in families from Germany. European journal of human genetics : EJHG 13(3):352-360.

Maier C, Vesovic Z, Bachmann N, Herkommer K, Braun AK, Surowy HM, Assum G, Paiss T, Vogel W. 2006. Germline mutations of the MSR1 gene in prostate cancer families from Germany. Human mutation 27(1):98-102.

Majeska RJ, Ryaby JT, Einhorn TA. 1994. Direct modulation of osteoblastic activity with estrogen. The Journal of bone and joint surgery American volume 76(5):713-721.

Majumder PK, Sellers WR. 2005. Akt-regulated pathways in prostate cancer. Oncogene 24(50):7465-7474.

Malyankar UM, Scatena M, Suchland KL, Yun TJ, Clark EA, Giachelli CM. 2000. Osteoprotegerin is an alpha vbeta 3-induced, NF-kappa B-dependent survival factor for endothelial cells. The Journal of biological chemistry 275(28):20959-20962.

Mansour SJ, Matten WT, Hermann AS, Candia JM, Rong S, Fukasawa K, Vande Woude GF, Ahn NG. 1994. Transformation of mammalian cells by constitutively active MAP kinase kinase. Science 265(5174):966-970.

Mark HF, Feldman D, Das S, Kye H, Mark S, Sun CL, Samy M. 1999. Fluorescence in situ hybridization study of HER-2/neu oncogene amplification in prostate cancer. Experimental and molecular pathology 66(2):170-178.

Marks LS. 2004. 5alpha-reductase: history and clinical importance. Reviews in urology 6 Suppl 9:S11-21.

Marks LS, Kojima M, Demarzo A, Heber D, Bostwick DG, Qian J, Dorey FJ, Veltri RW, Mohler JL, Partin AW. 2004. Prostate cancer in native Japanese and Japanese-American men: effects of dietary differences on prostatic tissue. Urology 64(4):765-771.

Marquardt H, Lioubin MN, Ikeda T. 1987. Complete amino acid sequence of human transforming growth factor type beta 2. The Journal of biological chemistry 262(25):12127-12131.

Marrocco DL, Tilley WD, Bianco-Miotto T, Evdokiou A, Scher HI, Rifkind RA, Marks PA, Richon VM, Butler LM. 2007. Suberoylanilide hydroxamic acid (vorinostat) represses androgen receptor expression and acts synergistically with an androgen receptor antagonist to inhibit prostate cancer cell proliferation. Molecular cancer therapeutics 6(1):51-60.

Mars WM, Zarnegar R, Michalopoulos GK. 1993. Activation of hepatocyte growth factor by the plasminogen activators uPA and tPA. The American journal of pathology 143(3):949-958.

Martin P, Liu YN, Pierce R, Abou-Kheir W, Casey O, Seng V, Camacho D, Simpson RM, Kelly K. 2011. Prostate epithelial Pten/TP53 loss leads to transformation of multipotential progenitors and epithelial to mesenchymal transition. The American journal of pathology 179(1):422-435.

Martin TA, Parr C, Davies G, Watkins G, Lane J, Matsumoto K, Nakamura T, Mansel RE, Jiang WG. 2003. Growth and angiogenesis of human breast cancer in a nude mouse tumour model is reduced by NK4, a HGF/SF antagonist. Carcinogenesis 24(8):1317-1323.

Martin TJ. 2013. Historically significant events in the discovery of RANK/RANKL/OPG. World journal of orthopedics 4(4):186-197.

Martini F, Nath, JL;. 2009. Fundamentals of Anatomy and Physiology. San Francisco: Pearson Benjamin Cummings.

Matsumoto K, Takehara T, Inoue H, Hagiya M, Shimizu S, Nakamura T. 1991. Deletion of kringle domains or the N-terminal hairpin structure in hepatocyte growth factor results in marked decreases in related biological activities. Biochemical and biophysical research communications 181(2):691-699.

Matuo Y, Nishi N, Wada F. 1987. Growth factors in the prostate. Archives of andrology 19(3):193-210.

McCabe NP, De S, Vasanji A, Brainard J, Byzova TV. 2007. Prostate cancer specific integrin alphavbeta3 modulates bone metastatic growth and tissue remodeling. Oncogene 26(42):6238-6243.

McDowell ME, Occhipinti S, Gardiner RA, Baade PD, Steginga SK. 2009. A review of prostate-specific antigen screening prevalence and risk perceptions for first-degree relatives of men with prostate cancer. European journal of cancer care 18(6):545-555.

McGonigle JS, Giachelli CM, Scatena M. 2009. Osteoprotegerin and RANKL differentially regulate angiogenesis and endothelial cell function. Angiogenesis 12(1):35-46.

McNeal JE. 1969. Origin and development of carcinoma in the prostate. Cancer 23(1):24-34.

McNeal JE. 1978. Origin and evolution of benign prostatic enlargement. Investigative urology 15(4):340-345.

McNeal JE. 1988a. Normal anatomy of the prostate and changes in benign prostatic hypertrophy and carcinoma. Seminars in ultrasound, CT, and MR 9(5):329-334.

McNeal JE. 1988b. Normal histology of the prostate. The American journal of surgical pathology 12(8):619-633.

McNeal JE, Bostwick DG. 1986. Intraductal dysplasia: a premalignant lesion of the prostate. Human pathology 17(1):64-71.

McNeal JE, Bostwick DG, Kindrachuk RA, Redwine EA, Freiha FS, Stamey TA. 1986. Patterns of progression in prostate cancer. Lancet 1(8472):60-63.

Mehlen P, Puisieux A. 2006. Metastasis: a question of life or death. Nature reviews Cancer 6(6):449-458.

Mehra R, Tomlins SA, Shen R, Nadeem O, Wang L, Wei JT, Pienta KJ, Ghosh D, Rubin MA, Chinnaiyan AM, Shah RB. 2007. Comprehensive assessment of TMPRSS2 and ETS family gene aberrations in clinically localized prostate

cancer. Modern pathology : an official journal of the United States and Canadian Academy of Pathology, Inc 20(5):538-544.

Mellon K, Thompson S, Charlton RG, Marsh C, Robinson M, Lane DP, Harris AL, Horne CH, Neal DE. 1992. p53, c-erbB-2 and the epidermal growth factor receptor in the benign and malignant prostate. The Journal of urology 147(2):496-499.

Mercatali L, Ibrahim T, Sacanna E, Flamini E, Scarpi E, Calistri D, Ricci M, Serra P, Ricci R, Zoli W, Kang Y, Amadori D. 2011. Bone metastases detection by circulating biomarkers: OPG and RANK-L. International journal of oncology 39(1):255-261.

Micalizzi DS, Farabaugh SM, Ford HL. 2010. Epithelial-mesenchymal transition in cancer: parallels between normal development and tumor progression. Journal of mammary gland biology and neoplasia 15(2):117-134.

Michalopoulos G, Houck KA, Dolan ML, Leutteke NC. 1984. Control of hepatocyte replication by two serum factors. Cancer research 44(10):4414-4419.

Michigami T, Shimizu N, Williams PJ, Niewolna M, Dallas SL, Mundy GR, Yoneda T. 2000. Cell-cell contact between marrow stromal cells and myeloma cells via VCAM-1 and alpha(4)beta(1)-integrin enhances production of osteoclast-stimulating activity. Blood 96(5):1953-1960.

Miller RE, Roudier M, Jones J, Armstrong A, Canon J, Dougall WC. 2008. RANK ligand inhibition plus docetaxel improves survival and reduces tumor burden in a murine model of prostate cancer bone metastasis. Molecular cancer therapeutics 7(7):2160-2169.

Miyake H, Hara I, Fujisawa M, Gleave ME. 2006. The potential of clusterin inhibiting antisense oligodeoxynucleotide therapy for prostate cancer. Expert opinion on investigational drugs 15(5):507-517.

Mizuno K, Tanoue Y, Okano I, Harano T, Takada K, Nakamura T. 1994. Purification and characterization of hepatocyte growth factor (HGF)-converting enzyme: activation of pro-HGF. Biochemical and biophysical research communications 198(3):1161-1169.

Montague R, Hart CA, George NJ, Ramani VA, Brown MD, Clarke NW. 2004. Differential inhibition of invasion and proliferation by bisphosphonates: anti-metastatic potential of Zoledronic acid in prostate cancer. European urology 46(3):389-401; discussion 401-382.

Montironi R, Galluzzi CM, Diamanti L, Giannulis I, Pisani E, Scarpelli M. 1993. Prostatic intra-epithelial neoplasia: expression and location of proliferating

cell nuclear antigen in epithelial, endothelial and stromal nuclei. Virchows Archiv A, Pathological anatomy and histopathology 422(3):185-192.

Morgan TM, Lange PH, Porter MP, Lin DW, Ellis WJ, Gallaher IS, Vessella RL. 2009. Disseminated tumor cells in prostate cancer patients after radical prostatectomy and without evidence of disease predicts biochemical recurrence. Clinical cancer research : an official journal of the American Association for Cancer Research 15(2):677-683.

Morgia G, Falsaperla M, Malaponte G, Madonia M, Indelicato M, Travali S, Mazzarino MC. 2005. Matrix metalloproteinases as diagnostic (MMP-13) and prognostic (MMP-2, MMP-9) markers of prostate cancer. Urological research 33(1):44-50.

Morony S, Capparelli C, Sarosi I, Lacey DL, Dunstan CR, Kostenuik PJ. 2001. Osteoprotegerin inhibits osteolysis and decreases skeletal tumor burden in syngeneic and nude mouse models of experimental bone metastasis. Cancer research 61(11):4432-4436.

Mosquera JM, Perner S, Demichelis F, Kim R, Hofer MD, Mertz KD, Paris PL, Simko J, Collins C, Bismar TA, Chinnaiyan AM, Rubin MA. 2007. Morphological features of TMPRSS2-ERG gene fusion prostate cancer. The Journal of pathology 212(1):91-101.

Mosquera JM, Perner S, Genega EM, Sanda M, Hofer MD, Mertz KD, Paris PL, Simko J, Bismar TA, Ayala G, Shah RB, Loda M, Rubin MA. 2008. Characterization of TMPRSS2-ERG fusion high-grade prostatic intraepithelial neoplasia and potential clinical implications. Clinical cancer research : an official journal of the American Association for Cancer Research 14(11):3380-3385.

Mouline CC, Quincey D, Laugier JP, Carle GF, Bouler JM, Rochet N, Scimeca JC. 2010. Osteoclastic differentiation of mouse and human monocytes in a plasma clot/biphasic calcium phosphate microparticles composite. European cells & materials 20:379-392.

Mountzios G, Dimopoulos MA, Bamias A, Papadopoulos G, Kastritis E, Syrigos K, Pavlakis G, Terpos E. 2007. Abnormal bone remodeling process is due to an imbalance in the receptor activator of nuclear factor-kappaB ligand (RANKL)/osteoprotegerin (OPG) axis in patients with solid tumors metastatic to the skeleton. Acta oncologica 46(2):221-229.

Mukherji D, Temraz S, Wehbe D, Shamseddine A. 2013. Angiogenesis and anti-angiogenic therapy in prostate cancer. Critical reviews in oncology/hematology 87(2):122-131.

Murant SJ, Handley J, Stower M, Reid N, Cussenot O, Maitland NJ. 1997. Co-ordinated changes in expression of cell adhesion molecules in prostate cancer. European journal of cancer 33(2):263-271.

Murthy RK, Morrow PK, Theriault RL. 2009. Bone biology and the role of the RANK ligand pathway. Oncology 23(14 Suppl 5):9-15.

Nagle RB, Brawer MK, Kittelson J, Clark V. 1991. Phenotypic relationships of prostatic intraepithelial neoplasia to invasive prostatic carcinoma. The American journal of pathology 138(1):119-128.

Nagle RB, Hao J, Knox JD, Dalkin BL, Clark V, Cress AE. 1995. Expression of hemidesmosomal and extracellular matrix proteins by normal and malignant human prostate tissue. The American journal of pathology 146(6):1498-1507.

Nagle RB, Knox JD, Wolf C, Bowden GT, Cress AE. 1994. Adhesion molecules, extracellular matrix, and proteases in prostate carcinoma. Journal of cellular biochemistry Supplement 19:232-237.

Nakagawa N, Kinosaki M, Yamaguchi K, Shima N, Yasuda H, Yano K, Morinaga T, Higashio K. 1998. RANK is the essential signaling receptor for osteoclast differentiation factor in osteoclastogenesis. Biochemical and biophysical research communications 253(2):395-400.

Nakamura T. 1989. [Molecular characterization of hepatocyte growth factor (HGF)]. Seikagaku The Journal of Japanese Biochemical Society 61(10):1243-1247.

Nakamura T. 2007. [Parathyroid and bone. Role of parathyroid hormone in the treatment of osteoporosis]. Clinical calcium 17(12):1823-1829.

Nakamura T, Nawa K, Ichihara A. 1984. Partial purification and characterization of hepatocyte growth factor from serum of hepatectomized rats. Biochemical and biophysical research communications 122(3):1450-1459.

Naldini L, Vigna E, Bardelli A, Follenzi A, Galimi F, Comoglio PM. 1995. Biological activation of pro-HGF (hepatocyte growth factor) by urokinase is controlled by a stoichiometric reaction. The Journal of biological chemistry 270(2):603-611.

Naldini L, Weidner KM, Vigna E, Gaudino G, Bardelli A, Ponzetto C, Narsimhan RP, Hartmann G, Zarnegar R, Michalopoulos GK, *et al*. 1991. Scatter factor and hepatocyte growth factor are indistinguishable ligands for the MET receptor. The EMBO journal 10(10):2867-2878.

Narod SA, Dupont A, Cusan L, Diamond P, Gomez JL, Suburu R, Labrie F. 1995. The impact of family history on early detection of prostate cancer. Nature medicine 1(2):99-101.

Navone NM, Labate ME, Troncoso P, Pisters LL, Conti CJ, von Eschenbach AC, Logothetis CJ. 1999. p53 mutations in prostate cancer bone metastases suggest that selected p53 mutants in the primary site define foci with metastatic potential. The Journal of urology 161(1):304-308.

Navone NM, Troncoso P, Pisters LL, Goodrow TL, Palmer JL, Nichols WW, von Eschenbach AC, Conti CJ. 1993. p53 protein accumulation and gene mutation in the progression of human prostate carcinoma. Journal of the National Cancer Institute 85(20):1657-1669.

Nelson JB, Fizazi K, Miller K, Higano C, Moul JW, Akaza H, Morris T, McIntosh S, Pemberton K, Gleave M. 2012. Phase 3, randomized, placebo-controlled study of zibotentan (ZD4054) in patients with castration-resistant prostate cancer metastatic to bone. Cancer 118(22):5709-5718.

Nelson JB, Hedican SP, George DJ, Reddi AH, Piantadosi S, Eisenberger MA, Simons JW. 1995. Identification of endothelin-1 in the pathophysiology of metastatic adenocarcinoma of the prostate. Nature medicine 1(9):944-949.

Nelson WG, De Marzo AM, Isaacs WB. 2003. Prostate cancer. The New England journal of medicine 349(4):366-381.

Neville-Webbe HL, Cross NA, Eaton CL, Nyambo R, Evans CA, Coleman RE, Holen I. 2004. Osteoprotegerin (OPG) produced by bone marrow stromal cells protects breast cancer cells from TRAIL-induced apoptosis. Breast cancer research and treatment 86(3):269-279.

Nicolin V, Narducci P. 2010. Soluble TRAIL could enhance bone destruction acting on Rank-ligand in estrogen-independent human breast cancer cell line MDA-MB-231. Acta histochemica 112(2):189-192.

Nupponen NN, Kakkola L, Koivisto P, Visakorpi T. 1998. Genetic alterations in hormone-refractory recurrent prostate carcinomas. The American journal of pathology 153(1):141-148.

Nyambo R, Cross N, Lippitt J, Holen I, Bryden G, Hamdy FC, Eaton CL. 2004. Human bone marrow stromal cells protect prostate cancer cells from TRAIL-induced apoptosis. Journal of bone and mineral research : the official journal of the American Society for Bone and Mineral Research 19(10):1712-1721.

O'Brien MF, Cronin AM, Fearn PA, Smith B, Stasi J, Guillonneau B, Scardino PT, Eastham JA, Vickers AJ, Lilja H. 2009. Pretreatment prostate-specific antigen (PSA) velocity and doubling time are associated with outcome but neither improves prediction of outcome beyond pretreatment PSA alone in patients treated with radical prostatectomy. Journal of clinical oncology :

official journal of the American Society of Clinical Oncology 27(22):3591-3597.

Oh WK, Tay MH, Huang J. 2007. Is there a role for platinum chemotherapy in the treatment of patients with hormone-refractory prostate cancer? Cancer 109(3):477-486.

Okano Y, Mizuno K, Osada S, Nakamura T, Nozawa Y. 1993. Tyrosine phosphorylation of phospholipase C gamma in c-met/HGF receptor-stimulated hepatocytes: comparison with HepG2 hepatocarcinoma cells. Biochemical and biophysical research communications 190(3):842-848.

Ooi LL, Zhou H, Kalak R, Zheng Y, Conigrave AD, Seibel MJ, Dunstan CR. 2010. Vitamin D deficiency promotes human breast cancer growth in a murine model of bone metastasis. Cancer research 70(5):1835-1844.

Orwoll ES, Klein RF. 1995. Osteoporosis in men. Endocrine reviews 16(1):87-116.

Osman I, Scher HI, Drobnjak M, Verbel D, Morris M, Agus D, Ross JS, Cordon-Cardo C. 2001. HER-2/neu (p185neu) protein expression in the natural or treated history of prostate cancer. Clinical cancer research : an official journal of the American Association for Cancer Research 7(9):2643-2647.

Otto F, Thornell AP, Crompton T, Denzel A, Gilmour KC, Rosewell IR, Stamp GW, Beddington RS, Mundlos S, Olsen BR, Selby PB, Owen MJ. 1997. Cbfa1, a candidate gene for cleidocranial dysplasia syndrome, is essential for osteoblast differentiation and bone development. Cell 89(5):765-771.

Overall CM, Lopez-Otin C. 2002. Strategies for MMP inhibition in cancer: innovations for the post-trial era. Nature reviews Cancer 2(9):657-672.

Owen M. 1988. Marrow stromal stem cells. Journal of cell science Supplement 10:63-76.

Paget S. 1989. The distribution of secondary growths in cancer of the breast. 1889. Cancer metastasis reviews 8(2):98-101.

Pantuck AJ, Zomorodian N, Belldegrun AS. 2007. Phase I, open-label, single-center, multiple-dose, dose-escalation clinical study of SUO11248 (sunitinib) in subjects with high-risk prostate cancer who have elected to undergo radical prostatectomy. Current urology reports 8(1):3-4.

Parish CR, Jakobsen KB, Coombe DR. 1992. A basement-membrane permeability assay which correlates with the metastatic potential of tumour cells. International journal of cancer Journal international du cancer 52(3):378-383.

Park BK, Zhang H, Zeng Q, Dai J, Keller ET, Giordano T, Gu K, Shah V, Pei L, Zarbo RJ, McCauley L, Shi S, Chen S, Wang CY. 2007a. NF-kappaB in

breast cancer cells promotes osteolytic bone metastasis by inducing osteoclastogenesis via GM-CSF. Nature medicine 13(1):62-69.

Park HR, Min SK, Cho HD, Kim DH, Shin HS, Park YE. 2003. Expression of osteoprotegerin and RANK ligand in breast cancer bone metastasis. Journal of Korean medical science 18(4):541-546.

Park JY, Park JM, Jang JS, Choi JE, Kim KM, Cha SI, Kim CH, Kang YM, Lee WK, Kam S, Park RW, Kim IS, Lee JT, Jung TH. 2006. Caspase 9 promoter polymorphisms and risk of primary lung cancer. Human molecular genetics 15(12):1963-1971.

Park K, Tomlins SA, Mudaliar KM, Chiu YL, Esgueva R, Mehra R, Suleman K, Varambally S, Brenner JC, MacDonald T, Srivastava A, Tewari AK, Sathyanarayana U, Nagy D, Pestano G, Kunju LP, Demichelis F, Chinnaiyan AM, Rubin MA. 2010. Antibody-based detection of ERG rearrangement-positive prostate cancer. Neoplasia 12(7):590-598.

Park M, Dean M, Kaul K, Braun MJ, Gonda MA, Vande Woude G. 1987. Sequence of MET protooncogene cDNA has features characteristic of the tyrosine kinase family of growth-factor receptors. Proceedings of the National Academy of Sciences of the United States of America 84(18):6379-6383.

Park SY, Murphy SP, Wilkens LR, Henderson BE, Kolonel LN. 2007b. Fat and meat intake and prostate cancer risk: the multiethnic cohort study. International journal of cancer Journal international du cancer 121(6):1339-1345.

Pawson T, Gish GD. 1992. SH2 and SH3 domains: from structure to function. Cell 71(3):359-362.

Pazolli E, Luo X, Brehm S, Carbery K, Chung JJ, Prior JL, Doherty J, Demehri S, Salavaggione L, Piwnica-Worms D, Stewart SA. 2009. Senescent stromal-derived osteopontin promotes preneoplastic cell growth. Cancer research 69(3):1230-1239.

Pearse RN, Sordillo EM, Yaccoby S, Wong BR, Liau DF, Colman N, Michaeli J, Epstein J, Choi Y. 2001. Multiple myeloma disrupts the TRANCE/ osteoprotegerin cytokine axis to trigger bone destruction and promote tumor progression. Proceedings of the National Academy of Sciences of the United States of America 98(20):11581-11586.

Pederson L, Kremer M, Judd J, Pascoe D, Spelsberg TC, Riggs BL, Oursler MJ. 1999. Androgens regulate bone resorption activity of isolated osteoclasts in vitro. Proceedings of the National Academy of Sciences of the United States of America 96(2):505-510.

Peehl DM, Wong ST, Bazinet M, Stamey TA. 1989. In vitro studies of human prostatic epithelial cells: attempts to identify distinguishing features of malignant cells. Growth factors 1(3):237-250.

Penno H, Silfversward CJ, Frost A, Brandstrom H, Nilsson O, Ljunggren O. 2002. Osteoprotegerin secretion from prostate cancer is stimulated by cytokines, in vitro. Biochemical and biophysical research communications 293(1):451-455.

Perlino E, Lovecchio M, Vacca RA, Fornaro M, Moro L, Ditonno P, Battaglia M, Selvaggi FP, Mastropasqua MG, Bufo P, Languino LR. 2000. Regulation of mRNA and protein levels of beta1 integrin variants in human prostate carcinoma. The American journal of pathology 157(5):1727-1734.

Pettersen I, Bakkelund W, Smedsrod B, Sveinbjornsson B. 2005. Osteoprotegerin is expressed in colon carcinoma cells. Anticancer research 25(6B):3809-3816.

Pisters LL, Troncoso P, Zhau HE, Li W, von Eschenbach AC, Chung LW. 1995. c-met proto-oncogene expression in benign and malignant human prostate tissues. The Journal of urology 154(1):293-298.

Pittenger MF, Mackay AM, Beck SC, Jaiswal RK, Douglas R, Mosca JD, Moorman MA, Simonetti DW, Craig S, Marshak DR. 1999. Multilineage potential of adult human mesenchymal stem cells. Science 284(5411):143-147.

Ploussard G, Mongiat-Artus P. 2013. Triptorelin in the management of prostate cancer. Future oncology 9(1):93-102.

Ponzetto C, Bardelli A, Maina F, Longati P, Panayotou G, Dhand R, Waterfield MD, Comoglio PM. 1993. A novel recognition motif for phosphatidylinositol 3-kinase binding mediates its association with the hepatocyte growth factor/scatter factor receptor. Molecular and cellular biology 13(8):4600-4608.

Ponzetto C, Bardelli A, Zhen Z, Maina F, dalla Zonca P, Giordano S, Graziani A, Panayotou G, Comoglio PM. 1994. A multifunctional docking site mediates signaling and transformation by the hepatocyte growth factor/scatter factor receptor family. Cell 77(2):261-271.

Porter AT, McEwan AJ, Powe JE, Reid R, McGowan DG, Lukka H, Sathyanarayana JR, Yakemchuk VN, Thomas GM, Erlich LE, *et al*. 1993. Results of a randomized phase-III trial to evaluate the efficacy of strontium-89 adjuvant to local field external beam irradiation in the management of endocrine resistant metastatic prostate cancer. International journal of radiation oncology, biology, physics 25(5):805-813.

Prakash G, Gautam G. 2013. Optimal bone health management strategies in patients with prostate cancer. Indian journal of urology : IJU : journal of the Urological Society of India 29(2):89-99.

Pratap J, Imbalzano KM, Underwood JM, Cohet N, Gokul K, Akech J, van Wijnen AJ, Stein JL, Imbalzano AN, Nickerson JA, Lian JB, Stein GS. 2009. Ectopic runx2 expression in mammary epithelial cells disrupts formation of normal acini structure: implications for breast cancer progression. Cancer research 69(17):6807-6814.

Pratap J, Javed A, Languino LR, van Wijnen AJ, Stein JL, Stein GS, Lian JB. 2005. The Runx2 osteogenic transcription factor regulates matrix metalloproteinase 9 in bone metastatic cancer cells and controls cell invasion. Molecular and cellular biology 25(19):8581-8591.

Price JE, Naito S, Fidler IJ. 1988. Growth in an organ microenvironment as a selective process in metastasis. Clinical & experimental metastasis 6(1):91-102.

Pritzker LB, Scatena M, Giachelli CM. 2004. The role of osteoprotegerin and tumor necrosis factor-related apoptosis-inducing ligand in human microvascular endothelial cell survival. Molecular biology of the cell 15(6):2834-2841.

Proff P, Romer P. 2009. The molecular mechanism behind bone remodelling: a review. Clinical oral investigations 13(4):355-362.

Qiu SD, Young CY, Bilhartz DL, Prescott JL, Farrow GM, He WW, Tindall DJ. 1990. In situ hybridization of prostate-specific antigen mRNA in human prostate. The Journal of urology 144(6):1550-1556.

Quinn BD, Cho KR, Epstein JI. 1990. Relationship of severe dysplasia to stage B adenocarcinoma of the prostate. Cancer 65(10):2328-2337.

Rabbani SA, Desjardins J, Bell AW, Banville D, Mazar A, Henkin J, Goltzman D. 1990. An amino-terminal fragment of urokinase isolated from a prostate cancer cell line (PC-3) is mitogenic for osteoblast-like cells. Biochemical and biophysical research communications 173(3):1058-1064.

Rabbani SA, Mazar AP, Bernier SM, Haq M, Bolivar I, Henkin J, Goltzman D. 1992. Structural requirements for the growth factor activity of the amino-terminal domain of urokinase. The Journal of biological chemistry 267(20):14151-14156.

Rabbani SA, Valentino ML, Arakelian A, Ali S, Boschelli F. 2010. SKI-606 (Bosutinib) blocks prostate cancer invasion, growth, and metastasis in vitro and in vivo through regulation of genes involved in cancer growth and skeletal metastasis. Molecular cancer therapeutics 9(5):1147-1157.

Rachner TD, Schoppet M, Niebergall U, Hofbauer LC. 2008. 17beta-Estradiol inhibits osteoprotegerin production by the estrogen receptor-alpha-positive human breast cancer cell line MCF-7. Biochemical and biophysical research communications 368(3):736-741.

Rauner MS, Stein N; Hofbauer, L. 2012. Basics of Bone Biology. In: Pietschmann P, editor. Principles of Osteoimmunology. Germany: Springer-Wein. p 1-17.

Reddi AH, Roodman D, Freeman C, Mohla S. 2003. Mechanisms of tumor metastasis to the bone: challenges and opportunities. Journal of bone and mineral research : the official journal of the American Society for Bone and Mineral Research 18(2):190-194.

Reid AH, Attard G, Danila DC, Oommen NB, Olmos D, Fong PC, Molife LR, Hunt J, Messiou C, Parker C, Dearnaley D, Swennenhuis JF, Terstappen LW, Lee G, Kheoh T, Molina A, Ryan CJ, Small E, Scher HI, de Bono JS. 2010. Significant and sustained antitumor activity in post-docetaxel, castration-resistant prostate cancer with the CYP17 inhibitor abiraterone acetate. J Clin Oncol 28(9):1489-1495.

Reid P, Holen I. 2009. Pathophysiological roles of osteoprotegerin (OPG). European journal of cell biology 88(1):1-17.

Reinholz MM, Iturria SJ, Ingle JN, Roche PC. 2002. Differential gene expression of TGF-beta family members and osteopontin in breast tumor tissue: analysis by real-time quantitative PCR. Breast cancer research and treatment 74(3):255-269.

Ren B, Yu YP, Tseng GC, Wu C, Chen K, Rao UN, Nelson J, Michalopoulos GK, Luo JH. 2007. Analysis of integrin alpha7 mutations in prostate cancer, liver cancer, glioblastoma multiforme, and leiomyosarcoma. Journal of the National Cancer Institute 99(11):868-880.

Rennebeck G, Martelli M, Kyprianou N. 2005. Anoikis and survival connections in the tumor microenvironment: is there a role in prostate cancer metastasis? Cancer research 65(24):11230-11235.

Roberts E, Cossigny DA, Quan GM. 2013. The role of vascular endothelial growth factor in metastatic prostate cancer to the skeleton. Prostate cancer 2013:418340.

Rodrigues P, Hering FO, Meller A. 2011. Adjuvant Effect of IV Clodronate on the Delay of Bone Metastasis in High-Risk Prostate Cancer Patients: A Prospective Study. Cancer research and treatment : official journal of Korean Cancer Association 43(4):231-235.

Rodriguez C, Calle EE, Tatham LM, Wingo PA, Miracle-McMahill HL, Thun MJ, Heath CW, Jr. 1998. Family history of breast cancer as a predictor for fatal prostate cancer. Epidemiology 9(5):525-529.

Rodriguez C, McCullough ML, Mondul AM, Jacobs EJ, Chao A, Patel AV, Thun MJ, Calle EE. 2006. Meat consumption among Black and White men and risk of prostate cancer in the Cancer Prevention Study II Nutrition Cohort. Cancer epidemiology, biomarkers & prevention : a publication of the American Association for Cancer Research, cosponsored by the American Society of Preventive Oncology 15(2):211-216.

Rodriguez C, McCullough ML, Mondul AM, Jacobs EJ, Fakhrabadi-Shokoohi D, Giovannucci EL, Thun MJ, Calle EE. 2003. Calcium, dairy products, and risk of prostate cancer in a prospective cohort of United States men. Cancer epidemiology, biomarkers & prevention : a publication of the American Association for Cancer Research, cosponsored by the American Society of Preventive Oncology 12(7):597-603.

Rogers A, Eastell R. 2005. Circulating osteoprotegerin and receptor activator for nuclear factor kappaB ligand: clinical utility in metabolic bone disease assessment. The Journal of clinical endocrinology and metabolism 90(11):6323-6331.

Rolli M, Fransvea E, Pilch J, Saven A, Felding-Habermann B. 2003. Activated integrin alphavbeta3 cooperates with metalloproteinase MMP-9 in regulating migration of metastatic breast cancer cells. Proceedings of the National Academy of Sciences of the United States of America 100(16):9482-9487.

Roodman GD. 2001. Biology of osteoclast activation in cancer. Journal of clinical oncology : official journal of the American Society of Clinical Oncology 19(15):3562-3571.

Roodman GD. 2004. Mechanisms of bone metastasis. The New England journal of medicine 350(16):1655-1664.

Rosen EM, Carley W, Goldberg ID. 1990. Scatter factor regulates vascular endothelial cell motility. Cancer investigation 8(6):647-650.

Ross JS, Sheehan CE, Hayner-Buchan AM, Ambros RA, Kallakury BV, Kaufman RP, Jr., Fisher HA, Rifkin MD, Muraca PJ. 1997. Prognostic significance of HER-2/neu gene amplification status by fluorescence in situ hybridization of prostate carcinoma. Cancer 79(11):2162-2170.

Roudier MP, Corey E, True LD, Hiagno CS, Ott SM, Vessell RL. 2004. Histological, immunophenotypic and histomorphometric characterization of prostate cancer bone metastases. Cancer treatment and research 118:311-339.

Rucci N, Teti A. 2010. Osteomimicry: how tumor cells try to deceive the bone. Frontiers in bioscience 2:907-915.

Russell WE, McGowan JA, Bucher NL. 1984. Partial characterization of a hepatocyte growth factor from rat platelets. Journal of cellular physiology 119(2):183-192.

Ryan CJ, Lin AM, Small EJ. 2006. Angiogenesis inhibition plus chemotherapy for metastatic hormone refractory prostate cancer: history and rationale. Urologic oncology 24(3):250-253.

Saad F, Chi K, Fleshner N. 2004. The role of bisphosphonates in the management of bone metastases in prostate cancer. The Canadian journal of urology 11(5):2376-2382.

Saad F, Clarke N, Colombel M. 2006. Natural history and treatment of bone complications in prostate cancer. European urology 49(3):429-440.

Sakr WA, Haas GP, Cassin BF, Pontes JE, Crissman JD. 1993. The frequency of carcinoma and intraepithelial neoplasia of the prostate in young male patients. The Journal of urology 150(2 Pt 1):379-385.

Salami SS, Schmidt F, Laxman B, Regan MM, Rickman DS, Scherr D, Bueti G, Siddiqui J, Tomlins SA, Wei JT, Chinnaiyan AM, Rubin MA, Sanda MG. 2013. Combining urinary detection of TMPRSS2:ERG and PCA3 with serum PSA to predict diagnosis of prostate cancer. Urologic oncology 31(5):566-571.

Santini D, Schiavon G, Vincenzi B, Gaeta L, Pantano F, Russo A, Ortega C, Porta C, Galluzzo S, Armento G, La Verde N, Caroti C, Treilleux I, Ruggiero A, Perrone G, Addeo R, Clezardin P, Muda AO, Tonini G. 2011. Receptor activator of NF-kB (RANK) expression in primary tumors associates with bone metastasis occurrence in breast cancer patients. PloS one 6(4):e19234.

Sato K, Qian J, Slezak JM, Lieber MM, Bostwick DG, Bergstralh EJ, Jenkins RB. 1999. Clinical significance of alterations of chromosome 8 in high-grade, advanced, nonmetastatic prostate carcinoma. Journal of the National Cancer Institute 91(18):1574-1580.

Scher HI. 2000. HER2 in prostate cancer--a viable target or innocent bystander? Journal of the National Cancer Institute 92(23):1866-1868.

Scher HI, Jia X, Chi K, de Wit R, Berry WR, Albers P, Henick B, Waterhouse D, Ruether DJ, Rosen PJ, Meluch AA, Nordquist LT, Venner PM, Heidenreich A, Chu L, Heller G. 2011. Randomized, open-label phase III trial of docetaxel plus high-dose calcitriol versus docetaxel plus prednisone for patients with

castration-resistant prostate cancer. Journal of clinical oncology : official journal of the American Society of Clinical Oncology 29(16):2191-2198.

Schneeweis LA, Willard D, Milla ME. 2005. Functional dissection of osteoprotegerin and its interaction with receptor activator of NF-kappaB ligand. The Journal of biological chemistry 280(50):41155-41164.

Schneider A, Kalikin LM, Mattos AC, Keller ET, Allen MJ, Pienta KJ, McCauley LK. 2005. Bone turnover mediates preferential localization of prostate cancer in the skeleton. Endocrinology 146(4):1727-1736.

Schneider JG, Amend SR, Weilbaecher KN. 2011. Integrins and bone metastasis: integrating tumor cell and stromal cell interactions. Bone 48(1):54-65.

Schoppet M, Henser S, Ruppert V, Stubig T, Al-Fakhri N, Maisch B, Hofbauer LC. 2007. Osteoprotegerin expression in dendritic cells increases with maturation and is NF-kappaB-dependent. Journal of cellular biochemistry 100(6):1430-1439.

Schoppet M, Preissner KT, Hofbauer LC. 2002. RANK ligand and osteoprotegerin: paracrine regulators of bone metabolism and vascular function. Arteriosclerosis, thrombosis, and vascular biology 22(4):549-553.

Schoppet M, Sattler AM, Schaefer JR, Herzum M, Maisch B, Hofbauer LC. 2003. Increased osteoprotegerin serum levels in men with coronary artery disease. The Journal of clinical endocrinology and metabolism 88(3):1024-1028.

Schramek D, Leibbrandt A, Sigl V, Kenner L, Pospisilik JA, Lee HJ, Hanada R, Joshi PA, Aliprantis A, Glimcher L, Pasparakis M, Khokha R, Ormandy CJ, Widschwendter M, Schett G, Penninger JM. 2010. Osteoclast differentiation factor RANKL controls development of progestin-driven mammary cancer. Nature 468(7320):98-102.

Schrecengost R, Knudsen KE. 2013. Molecular pathogenesis and progression of prostate cancer. Seminars in oncology 40(3):244-258.

Schroder FH. 2009. PSA screening--a review of recent studies. European journal of cancer 45 Suppl 1:402-404.

Scott LJ, Clarke NW, George NJ, Shanks JH, Testa NG, Lang SH. 2001. Interactions of human prostatic epithelial cells with bone marrow endothelium: binding and invasion. British journal of cancer 84(10):1417-1423.

Secchiero P, Corallini F, Rimondi E, Chiaruttini C, di Iasio MG, Rustighi A, Del Sal G, Zauli G. 2008. Activation of the p53 pathway down-regulates the osteoprotegerin expression and release by vascular endothelial cells. Blood 111(3):1287-1294.

Seifert-Klauss V, Schmidmayr M, Hobmaier E, Wimmer T. 2012. Progesterone and bone: a closer link than previously realized. Climacteric : the journal of the International Menopause Society 15 Suppl 1:26-31.

Seki T, Hagiya M, Shimonishi M, Nakamura T, Shimizu S. 1991. Organization of the human hepatocyte growth factor-encoding gene. Gene 102(2):213-219.

Semba S, Yamakawa M, Sasano H. 2001. The cadherin-catenin superfamily in endocrine tumors. Endocrine pathology 12(1):1-13.

Seshadri M, Spernyak JA, Maiery PG, Cheney RT, Mazurchuk R, Bellnier DA. 2007. Visualizing the acute effects of vascular-targeted therapy in vivo using intravital microscopy and magnetic resonance imaging: correlation with endothelial apoptosis, cytokine induction, and treatment outcome. Neoplasia 9(2):128-135.

Shariat SF, Shalev M, Menesses-Diaz A, Kim IY, Kattan MW, Wheeler TM, Slawin KM. 2001. Preoperative plasma levels of transforming growth factor beta(1) (TGF-beta(1)) strongly predict progression in patients undergoing radical prostatectomy. Journal of clinical oncology : official journal of the American Society of Clinical Oncology 19(11):2856-2864.

Shen MM, Abate-Shen C. 2010. Molecular genetics of prostate cancer: new prospects for old challenges. Gene Dev 24(18):1967-2000.

Shimizu H, Ross RK, Bernstein L, Yatani R, Henderson BE, Mack TM. 1991. Cancers of the prostate and breast among Japanese and white immigrants in Los Angeles County. British journal of cancer 63(6):963-966.

Shimomura T, Kondo J, Ochiai M, Naka D, Miyazawa K, Morimoto Y, Kitamura N. 1993. Activation of the zymogen of hepatocyte growth factor activator by thrombin. The Journal of biological chemistry 268(30):22927-22932.

Shin CS, Lecanda F, Sheikh S, Weitzmann L, Cheng SL, Civitelli R. 2000. Relative abundance of different cadherins defines differentiation of mesenchymal precursors into osteogenic, myogenic, or adipogenic pathways. Journal of cellular biochemistry 78(4):566-577.

Shiozawa Y, Pedersen EA, Havens AM, Jung Y, Mishra A, Joseph J, Kim JK, Patel LR, Ying C, Ziegler AM, Pienta MJ, Song J, Wang J, Loberg RD, Krebsbach PH, Pienta KJ, Taichman RS. 2011. Human prostate cancer metastases target the hematopoietic stem cell niche to establish footholds in mouse bone marrow. The Journal of clinical investigation 121(4):1298-1312.

Shiozawa Y, Pedersen EA, Patel LR, Ziegler AM, Havens AM, Jung Y, Wang J, Zalucha S, Loberg RD, Pienta KJ, Taichman RS. 2010. GAS6/AXL axis

regulates prostate cancer invasion, proliferation, and survival in the bone marrow niche. Neoplasia 12(2):116-127.

Shipman CM, Croucher PI. 2003. Osteoprotegerin is a soluble decoy receptor for tumor necrosis factor-related apoptosis-inducing ligand/Apo2 ligand and can function as a paracrine survival factor for human myeloma cells. Cancer research 63(5):912-916.

Shozu M, Zhao Y, Simpson ER. 1997. Estrogen biosynthesis in THP1 cells is regulated by promoter switching of the aromatase (CYP19) gene. Endocrinology 138(12):5125-5135.

Signoretti S, Montironi R, Manola J, Altimari A, Tam C, Bubley G, Balk S, Thomas G, Kaplan I, Hlatky L, Hahnfeldt P, Kantoff P, Loda M. 2000. Her-2-neu expression and progression toward androgen independence in human prostate cancer. Journal of the National Cancer Institute 92(23):1918-1925.

Sikes RA, Nicholson BE, Koeneman KS, Edlund NM, Bissonette EA, Bradley MJ, Thalmann GN, Cecchini MG, Pienta KJ, Chung LW. 2004. Cellular interactions in the tropism of prostate cancer to bone. International journal of cancer Journal international du cancer 110(4):497-503.

Simonet WS, Lacey DL, Dunstan CR, Kelley M, Chang MS, Luthy R, Nguyen HQ, Wooden S, Bennett L, Boone T, Shimamoto G, DeRose M, Elliott R, Colombero A, Tan HL, Trail G, Sullivan J, Davy E, Bucay N, Renshaw-Gegg L, Hughes TM, Hill D, Pattison W, Campbell P, Sander S, Van G, Tarpley J, Derby P, Lee R, Boyle WJ. 1997. Osteoprotegerin: a novel secreted protein involved in the regulation of bone density. Cell 89(2):309-319.

Sims NA, Gooi JH. 2008. Bone remodeling: Multiple cellular interactions required for coupling of bone formation and resorption. Seminars in cell & developmental biology 19(5):444-451.

Sloan EK, Pouliot N, Stanley KL, Chia J, Moseley JM, Hards DK, Anderson RL. 2006. Tumor-specific expression of alphavbeta3 integrin promotes spontaneous metastasis of breast cancer to bone. Breast cancer research : BCR 8(2):R20.

Smith CA, Farrah T, Goodwin RG. 1994. The TNF receptor superfamily of cellular and viral proteins: activation, costimulation, and death. Cell 76(6):959-962.

Smith JR, Freije D, Carpten JD, Gronberg H, Xu J, Isaacs SD, Brownstein MJ, Bova GS, Guo H, Bujnovszky P, Nusskern DR, Damber JE, Bergh A, Emanuelsson M, Kallioniemi OP, Walker-Daniels J, Bailey-Wilson JE, Beaty TH, Meyers DA, Walsh PC, Collins FS, Trent JM, Isaacs WB. 1996. Major

susceptibility locus for prostate cancer on chromosome 1 suggested by a genome-wide search. Science 274(5291):1371-1374.

Smith MR, Kabbinavar F, Saad F, Hussain A, Gittelman MC, Bilhartz DL, Wynne C, Murray R, Zinner NR, Schulman C, Linnartz R, Zheng M, Goessl C, Hei YJ, Small EJ, Cook R, Higano CS. 2005. Natural history of rising serum prostate-specific antigen in men with castrate nonmetastatic prostate cancer. Journal of clinical oncology : official journal of the American Society of Clinical Oncology 23(13):2918-2925.

Smith MR, Saad F, Coleman R, Shore N, Fizazi K, Tombal B, Miller K, Sieber P, Karsh L, Damiao R, Tammela TL, Egerdie B, Van Poppel H, Chin J, Morote J, Gomez-Veiga F, Borkowski T, Ye Z, Kupic A, Dansey R, Goessl C. 2012. Denosumab and bone-metastasis-free survival in men with castration-resistant prostate cancer: results of a phase 3, randomised, placebo-controlled trial. Lancet 379(9810):39-46.

Sommerfeldt DW, Rubin CT. 2001. Biology of bone and how it orchestrates the form and function of the skeleton. European spine journal : official publication of the European Spine Society, the European Spinal Deformity Society, and the European Section of the Cervical Spine Research Society 10 Suppl 2:S86-95.

Sottnik JL, Hall CL, Zhang J, Keller ET. 2012. Wnt and Wnt inhibitors in bone metastasis. BoneKEy reports 1:101.

Sporn MB. 1997. The war on cancer: a review. Annals of the New York Academy of Sciences 833:137-146.

Stamey TA, Yang N, Hay AR, McNeal JE, Freiha FS, Redwine E. 1987. Prostate-specific antigen as a serum marker for adenocarcinoma of the prostate. The New England journal of medicine 317(15):909-916.

Stanford JL, Just JJ, Gibbs M, Wicklund KG, Neal CL, Blumenstein BA, Ostrander EA. 1997. Polymorphic repeats in the androgen receptor gene: molecular markers of prostate cancer risk. Cancer research 57(6):1194-1198.

Stein GS, Lian JB. 1993. Molecular mechanisms mediating proliferation/differentiation interrelationships during progressive development of the osteoblast phenotype. Endocrine reviews 14(4):424-442.

Steinberg GD, Carter BS, Beaty TH, Childs B, Walsh PC. 1990. Family history and the risk of prostate cancer. The Prostate 17(4):337-347.

Stoker M, Perryman M. 1985. An epithelial scatter factor released by embryo fibroblasts. Journal of cell science 77:209-223.

Storey JA, Torti FM. 2007. Bone metastases in prostate cancer: a targeted approach. Current opinion in oncology 19(3):254-258.

Strohmeyer D, Rossing C, Bauerfeind A, Kaufmann O, Schlechte H, Bartsch G, Loening S. 2000. Vascular endothelial growth factor and its correlation with angiogenesis and p53 expression in prostate cancer. The Prostate 45(3):216-224.

Suarez BK, Lin J, Witte JS, Conti DV, Resnick MI, Klein EA, Burmester JK, Vaske DA, Banerjee TK, Catalona WJ. 2000. Replication linkage study for prostate cancer susceptibility genes. The Prostate 45(2):106-114.

Sun YX, Fang M, Wang J, Cooper CR, Pienta KJ, Taichman RS. 2007. Expression and activation of alpha v beta 3 integrins by SDF-1/CXC12 increases the aggressiveness of prostate cancer cells. The Prostate 67(1):61-73.

Sun YX, Schneider A, Jung Y, Wang J, Dai J, Wang J, Cook K, Osman NI, Koh-Paige AJ, Shim H, Pienta KJ, Keller ET, McCauley LK, Taichman RS. 2005. Skeletal localization and neutralization of the SDF-1(CXCL12)/CXCR4 axis blocks prostate cancer metastasis and growth in osseous sites in vivo. Journal of bone and mineral research : the official journal of the American Society for Bone and Mineral Research 20(2):318-329.

Suva LJ, Washam C, Nicholas RW, Griffin RJ. 2011. Bone metastasis: mechanisms and therapeutic opportunities. Nature reviews Endocrinology 7(4):208-218.

Swalwell JI, Vocke CD, Yang Y, Walker JR, Grouse L, Myers SH, Gillespie JW, Bostwick DG, Duray PH, Linehan WM, Emmert-Buck MR. 2002. Determination of a minimal deletion interval on chromosome band 8p21 in sporadic prostate cancer. Genes, chromosomes & cancer 33(2):201-205.

Swanton E, Savory P, Cosulich S, Clarke P, Woodman P. 1999. Bcl-2 regulates a caspase-3/caspase-2 apoptotic cascade in cytosolic extracts. Oncogene 18(10):1781-1787.

Taichman R, Reilly M, Verma R, Ehrenman K, Emerson S. 2001. Hepatocyte growth factor is secreted by osteoblasts and cooperatively permits the survival of haematopoietic progenitors. British journal of haematology 112(2):438-448.

Taichman RS, Loberg RD, Mehra R, Pienta KJ. 2007. The evolving biology and treatment of prostate cancer. Journal of Clinical Investigation 117(9):2351-2361.

Takayanagi H, Kim S, Matsuo K, Suzuki H, Suzuki T, Sato K, Yokochi T, Oda H, Nakamura K, Ida N, Wagner EF, Taniguchi T. 2002. RANKL maintains bone

homeostasis through c-Fos-dependent induction of interferon-beta. Nature 416(6882):744-749.

Takuwa Y, Ohse C, Wang EA, Wozney JM, Yamashita K. 1991. Bone morphogenetic protein-2 stimulates alkaline phosphatase activity and collagen synthesis in cultured osteoblastic cells, MC3T3-E1. Biochemical and biophysical research communications 174(1):96-101.

Talmadge JE, Fidler IJ. 2010. AACR centennial series: the biology of cancer metastasis: historical perspective. Cancer research 70(14):5649-5669.

Tan W, Zhang W, Strasner A, Grivennikov S, Cheng JQ, Hoffman RM, Karin M. 2011. Tumour-infiltrating regulatory T cells stimulate mammary cancer metastasis through RANKL-RANK signalling. Nature 470(7335):548-553.

Tan WW. 2006. Novel agents and targets in managing patients with metastatic prostate cancer. Cancer control : journal of the Moffitt Cancer Center 13(3):194-198.

Tang XH, Gudas LJ. 2011. Retinoids, retinoic acid receptors, and cancer. Annual review of pathology 6:345-364.

Tanos T, Sflomos G, Echeverria PC, Ayyanan A, Gutierrez M, Delaloye JF, Raffoul W, Fiche M, Dougall W, Schneider P, Yalcin-Ozuysal O, Brisken C. 2013. Progesterone/RANKL is a major regulatory axis in the human breast. Science translational medicine 5(182):182ra155.

Tansey MG, Szymkowski DE. 2009. The TNF superfamily in 2009: new pathways, new indications, and new drugs. Drug discovery today 14(23-24):1082-1088.

Tarin D, Price JE, Kettlewell MG, Souter RG, Vass AC, Crossley B. 1984. Clinicopathological observations on metastasis in man studied in patients treated with peritoneovenous shunts. British medical journal 288(6419):749-751.

Teitelbaum SL. 2011. The osteoclast and its unique cytoskeleton. Annals of the New York Academy of Sciences 1240:14-17.

Teitelbaum SL, Ross FP. 2003. Genetic regulation of osteoclast development and function. Nat Rev Genet 4(8):638-649.

Thalmann GN, Anezinis PE, Chang SM, Zhau HE, Kim EE, Hopwood VL, Pathak S, von Eschenbach AC, Chung LW. 1994. Androgen-independent cancer progression and bone metastasis in the LNCaP model of human prostate cancer. Cancer research 54(10):2577-2581.

Thalmann GN, Sikes RA, Wu TT, Degeorges A, Chang SM, Ozen M, Pathak S, Chung LW. 2000. LNCaP progression model of human prostate cancer:

androgen-independence and osseous metastasis. The Prostate 44(2):91-103 Jul 101;144(102).

Thiery JP. 2002. Epithelial-mesenchymal transitions in tumour progression. Nature reviews Cancer 2(6):442-454.

Thiessen EU. 1974. Concerning a familial association between breast cancer and both prostatic and uterine malignancies. Cancer 34(4):1102-1107.

Thirunavukkarasu K, Halladay DL, Miles RR, Yang X, Galvin RJ, Chandrasekhar S, Martin TJ, Onyia JE. 2000. The osteoblast-specific transcription factor Cbfa1 contributes to the expression of osteoprotegerin, a potent inhibitor of osteoclast differentiation and function. The Journal of biological chemistry 275(33):25163-25172.

Thobe MN, Clark RJ, Bainer RO, Prasad SM, Rinker-Schaeffer CW. 2011. From prostate to bone: key players in prostate cancer bone metastasis. Cancers 3(1):478-493.

Thomas RJ, Guise TA, Yin JJ, Elliott J, Horwood NJ, Martin TJ, Gillespie MT. 1999. Breast cancer cells interact with osteoblasts to support osteoclast formation. Endocrinology 140(10):4451-4458.

Thompson IM, Chi C, Ankerst DP, Goodman PJ, Tangen CM, Lippman SM, Lucia MS, Parnes HL, Coltman CA, Jr. 2006. Effect of finasteride on the sensitivity of PSA for detecting prostate cancer. Journal of the National Cancer Institute 98(16):1128-1133.

Tian QX, Huang GY, Zhou JL, Liu QH, Du XR. 2007. [Effects of calcitonin on osteoblast cell proliferation and OPG/RANKL expression: experiment with mouse osteoblasts]. Zhonghua yi xue za zhi 87(21):1501-1505.

Todenhofer T, Hennenlotter J, Schmiedel BJ, Hohneder A, Grimm S, Kuhs U, Salih HR, Buhring HJ, Fehm T, Gakis G, Blumenstock G, Aufderklamm S, Schilling D, Stenzl A, Schwentner C. 2013. Alterations of the RANKL pathway in blood and bone marrow samples of prostate cancer patients without bone metastases. The Prostate 73(2):162-168.

Tombal B, Lecouvet F. 2012. Modern Detection of Prostate Cancer's Bone Metastasis: Is the Bone Scan Era Over? Advances in urology 2012:893193.

Tomlins SA, Mehra R, Rhodes DR, Smith LR, Roulston D, Helgeson BE, Cao X, Wei JT, Rubin MA, Shah RB, Chinnaiyan AM. 2006a. TMPRSS2:ETV4 gene fusions define a third molecular subtype of prostate cancer. Cancer research 66(7):3396-3400.

Tomlins SA, Rubin MA, Chinnaiyan AM. 2006b. Integrative biology of prostate cancer progression. Annual review of pathology 1:243-271.

Trapman J. 2001. Molecular mechanisms of prostate cancer. European journal of cancer 37 Suppl 7:S119-125.

Travlos GS. 2006. Normal structure, function, and histology of the bone marrow. Toxicologic pathology 34(5):548-565.

Trudel D, Fradet Y, Meyer F, Harel F, Tetu B. 2003. Significance of MMP-2 expression in prostate cancer: an immunohistochemical study. Cancer research 63(23):8511-8515.

Tsuda E, Goto M, Mochizuki S, Yano K, Kobayashi F, Morinaga T, Higashio K. 1997. Isolation of a novel cytokine from human fibroblasts that specifically inhibits osteoclastogenesis. Biochemical and biophysical research communications 234(1):137-142.

Tu SM, Som A, Tu B, Logothetis CJ, Lee MH, Yeung SC. 2012. Effect of Paget's disease of bone (osteitis deformans) on the progression of prostate cancer bone metastasis. British journal of cancer 107(4):646-651.

Ulmert D, Cronin AM, Bjork T, O'Brien MF, Scardino PT, Eastham JA, Becker C, Berglund G, Vickers AJ, Lilja H. 2008. Prostate-specific antigen at or before age 50 as a predictor of advanced prostate cancer diagnosed up to 25 years later: a case-control study. BMC medicine 6:6.

Umbas R, Isaacs WB, Bringuier PP, Schaafsma HE, Karthaus HF, Oosterhof GO, Debruyne FM, Schalken JA. 1994. Decreased E-cadherin expression is associated with poor prognosis in patients with prostate cancer. Cancer research 54(14):3929-3933.

Umbas R, Schalken JA, Aalders TW, Carter BS, Karthaus HF, Schaafsma HE, Debruyne FM, Isaacs WB. 1992. Expression of the cellular adhesion molecule E-cadherin is reduced or absent in high-grade prostate cancer. Cancer research 52(18):5104-5109.

Vakar-Lopez F, Cheng CJ, Kim J, Shi GG, Troncoso P, Tu SM, Yu-Lee LY, Lin SH. 2004. Up-regulation of MDA-BF-1, a secreted isoform of ErbB3, in metastatic prostate cancer cells and activated osteoblasts in bone marrow. The Journal of pathology 203(2):688-695.

Valero C, Olmos JM, Rivera F, Hernandez JL, Vega ME, Macias JG. 2006. Osteoprotegerin and bone mass in squamous cell head and neck cancer patients. Calcified tissue international 78(6):343-347.

van Leenders GJ, Boormans JL, Vissers CJ, Hoogland AM, Bressers AA, Furusato B, Trapman J. 2011. Antibody EPR3864 is specific for ERG genomic fusions in prostate cancer: implications for pathological practice. Modern pathology :

an official journal of the United States and Canadian Academy of Pathology, Inc 24(8):1128-1138.

Van Poznak C, Cross SS, Saggese M, Hudis C, Panageas KS, Norton L, Coleman RE, Holen I. 2006. Expression of osteoprotegerin (OPG), TNF related apoptosis inducing ligand (TRAIL), and receptor activator of nuclear factor kappaB ligand (RANKL) in human breast tumours. Journal of clinical pathology 59(1):56-63.

van Zonneveld AJ, Veerman H, Pannekoek H. 1986. On the interaction of the finger and the kringle-2 domain of tissue-type plasminogen activator with fibrin. Inhibition of kringle-2 binding to fibrin by epsilon-amino caproic acid. The Journal of biological chemistry 261(30):14214-14218.

Vandyke K, Jackson P, Rowe A, Russell PJ, Blair JM. 2007. Androgen decreases osteoprotegerin expression in prostate cancer cells. Prostate cancer and prostatic diseases 10(2):160-166.

Varambally S, Yu J, Laxman B, Rhodes DR, Mehra R, Tomlins SA, Shah RB, Chandran U, Monzon FA, Becich MJ, Wei JT, Pienta KJ, Ghosh D, Rubin MA, Chinnaiyan AM. 2005. Integrative genomic and proteomic analysis of prostate cancer reveals signatures of metastatic progression. Cancer cell 8(5):393-406.

Vickers AJ, Wolters T, Savage CJ, Cronin AM, O'Brien MF, Pettersson K, Roobol MJ, Aus G, Scardino PT, Hugosson J, Schroder FH, Lilja H. 2009. Prostate-specific antigen velocity for early detection of prostate cancer: result from a large, representative, population-based cohort. European urology 56(5):753-760.

Virchow R. 1989. Cellular pathology. As based upon physiological and pathological histology. Lecture XVI--Atheromatous affection of arteries. 1858. Nutrition reviews 47(1):23-25.

Virk MS, Alaee F, Petrigliano FA, Sugiyama O, Chatziioannou AF, Stout D, Dougall WC, Lieberman JR. 2011. Combined inhibition of the BMP pathway and the RANK-RANKL axis in a mixed lytic/blastic prostate cancer lesion. Bone 48(3):578-587.

Vis AN, Schroder FH. 2009a. Key targets of hormonal treatment of prostate cancer. Part 1: the androgen receptor and steroidogenic pathways. BJU international 104(4):438-448.

Vis AN, Schroder FH. 2009b. Key targets of hormonal treatment of prostate cancer. Part 2: the androgen receptor and 5alpha-reductase. BJU international 104(9):1191-1197.

Visakorpi T, Kallioniemi OP, Heikkinen A, Koivula T, Isola J. 1992. Small subgroup of aggressive, highly proliferative prostatic carcinomas defined by p53 accumulation. Journal of the National Cancer Institute 84(11):883-887.

Vlietstra RJ, van Alewijk DC, Hermans KG, van Steenbrugge GJ, Trapman J. 1998. Frequent inactivation of PTEN in prostate cancer cell lines and xenografts. Cancer research 58(13):2720-2723.

Vocke CD, Pozzatti RO, Bostwick DG, Florence CD, Jennings SB, Strup SE, Duray PH, Liotta LA, Emmert-Buck MR, Linehan WM. 1996. Analysis of 99 microdissected prostate carcinomas reveals a high frequency of allelic loss on chromosome 8p12-21. Cancer research 56(10):2411-2416.

Voeller HJ, Truica CI, Gelmann EP. 1998. Beta-catenin mutations in human prostate cancer. Cancer research 58(12):2520-2523.

Wallner L, Dai J, Escara-Wilke J, Zhang J, Yao Z, Lu Y, Trikha M, Nemeth JA, Zaki MH, Keller ET. 2006. Inhibition of interleukin-6 with CNTO328, an anti-interleukin-6 monoclonal antibody, inhibits conversion of androgen-dependent prostate cancer to an androgen-independent phenotype in orchiectomized mice. Cancer research 66(6):3087-3095.

Wang G, Nikolovska-Coleska Z, Yang CY, Wang R, Tang G, Guo J, Shangary S, Qiu S, Gao W, Yang D, Meagher J, Stuckey J, Krajewski K, Jiang S, Roller PP, Abaan HO, Tomita Y, Wang S. 2006. Structure-based design of potent small-molecule inhibitors of anti-apoptotic Bcl-2 proteins. Journal of medicinal chemistry 49(21):6139-6142.

Wang L, McDonnell SK, Cunningham JM, Hebbring S, Jacobsen SJ, Cerhan JR, Slager SL, Blute ML, Schaid DJ, Thibodeau SN. 2003. No association of germline alteration of MSR1 with prostate cancer risk. Nature genetics 35(2):128-129.

Wei ZF, Tong B, Xia YF, Lu Q, Chou GX, Wang ZT, Dai Y. 2013. Norisoboldine suppresses osteoclast differentiation through preventing the accumulation of TRAF6-TAK1 complexes and activation of MAPKs/NF-kappaB/c-Fos/NFATc1 Pathways. PloS one 8(3):e59171.

Weidner KM, Arakaki N, Hartmann G, Vandekerckhove J, Weingart S, Rieder H, Fonatsch C, Tsubouchi H, Hishida T, Daikuhara Y, *et al*. 1991. Evidence for the identity of human scatter factor and human hepatocyte growth factor. Proceedings of the National Academy of Sciences of the United States of America 88(16):7001-7005.

Weigelt B, Peterse JL, van 't Veer LJ. 2005. Breast cancer metastasis: markers and models. Nature reviews Cancer 5(8):591-602.

Weilbaecher KN, Guise TA, McCauley LK. 2011. Cancer to bone: a fatal attraction. Nature reviews Cancer 11(6):411-425.

Weis SM, Cheresh DA. 2011. Tumor angiogenesis: molecular pathways and therapeutic targets. Nature medicine 17(11):1359-1370.

Weiss L. 1992. Comments on hematogenous metastatic patterns in humans as revealed by autopsy. Clinical & experimental metastasis 10(3):191-199.

Weitzmann MN. 2013. The Role of Inflammatory Cytokines, the RANKL/OPG Axis, and the Immunoskeletal Interface in Physiological Bone Turnover and Osteoporosis. Scientifica 2013:125705.

Wen S, Niu Y, Lee SO, Chang C. 2014. Androgen receptor (AR) positive vs negative roles in prostate cancer cell deaths including apoptosis, anoikis, entosis, necrosis and autophagic cell death. Cancer treatment reviews 40(1):31-40.

Whang PG, Schwarz EM, Gamradt SC, Dougall WC, Lieberman JR. 2005. The effects of RANK blockade and osteoclast depletion in a model of pure osteoblastic prostate cancer metastasis in bone. Journal of orthopaedic research : official publication of the Orthopaedic Research Society 23(6):1475-1483.

Whang YE, Wu X, Suzuki H, Reiter RE, Tran C, Vessella RL, Said JW, Isaacs WB, Sawyers CL. 1998. Inactivation of the tumor suppressor PTEN/MMAC1 in advanced human prostate cancer through loss of expression. Proceedings of the National Academy of Sciences of the United States of America 95(9):5246-5250.

Whittemore AS, Kolonel LN, Wu AH, John EM, Gallagher RP, Howe GR, Burch JD, Hankin J, Dreon DM, West DW, *et al*. 1995. Prostate cancer in relation to diet, physical activity, and body size in blacks, whites, and Asians in the United States and Canada. Journal of the National Cancer Institute 87(9):652-661.

Wiley SR, Schooley K, Smolak PJ, Din WS, Huang CP, Nicholl JK, Sutherland GR, Smith TD, Rauch C, Smith CA, *et al*. 1995. Identification and characterization of a new member of the TNF family that induces apoptosis. Immunity 3(6):673-682.

Wojta J, Kaun C, Breuss JM, Koshelnick Y, Beckmann R, Hattey E, Mildner M, Weninger W, Nakamura T, Tschachler E, Binder BR. 1999. Hepatocyte growth factor increases expression of vascular endothelial growth factor and plasminogen activator inhibitor-1 in human keratinocytes and the vascular endothelial growth factor receptor flk-1 in human endothelial cells.

Laboratory investigation; a journal of technical methods and pathology 79(4):427-438.

Wolff JM, Zimny M, Borchers H, Wildberger J, Buell U, Jakse G. 1998. Is prostate-specific antigen a reliable marker of bone metastasis in patients with newly diagnosed cancer of the prostate? European urology 33(4):376-381.

Wong BR, Besser D, Kim N, Arron JR, Vologodskaia M, Hanafusa H, Choi Y. 1999. TRANCE, a TNF family member, activates Akt/PKB through a signaling complex involving TRAF6 and c-Src. Molecular cell 4(6):1041-1049.

Wong BR, Josien R, Lee SY, Sauter B, Li HL, Steinman RM, Choi Y. 1997. TRANCE (tumor necrosis factor [TNF]-related activation-induced cytokine), a new TNF family member predominantly expressed in T cells, is a dendritic cell-specific survival factor. The Journal of experimental medicine 186(12):2075-2080.

Wood M, Fudge K, Mohler JL, Frost AR, Garcia F, Wang M, Stearns ME. 1997. In situ hybridization studies of metalloproteinases 2 and 9 and TIMP-1 and TIMP-2 expression in human prostate cancer. Clinical & experimental metastasis 15(3):246-258.

Wu GS. 2009. TRAIL as a target in anti-cancer therapy. Cancer letters 285(1):1-5.

Wu HC, Hsieh JT, Gleave ME, Brown NM, Pathak S, Chung LW. 1994. Derivation of androgen-independent human LNCaP prostatic cancer cell sublines: role of bone stromal cells. International journal of cancer Journal international du cancer 57(3):406-412.

Wu JD, Haugk K, Coleman I, Woodke L, Vessella R, Nelson P, Montgomery RB, Ludwig DL, Plymate SR. 2006. Combined in vivo effect of A12, a type 1 insulin-like growth factor receptor antibody, and docetaxel against prostate cancer tumors. Clinical cancer research : an official journal of the American Association for Cancer Research 12(20 Pt 1):6153-6160.

Xu J, Meyers D, Freije D, Isaacs S, Wiley K, Nusskern D, Ewing C, Wilkens E, Bujnovszky P, Bova GS, Walsh P, Isaacs W, Schleutker J, Matikainen M, Tammela T, Visakorpi T, Kallioniemi OP, Berry R, Schaid D, French A, McDonnell S, Schroeder J, Blute M, Thibodeau S, Gronberg H, Emanuelsson M, Damber JE, Bergh A, Jonsson BA, Smith J, Bailey-Wilson J, Carpten J, Stephan D, Gillanders E, Amundson I, Kainu T, Freas-Lutz D, Baffoe-Bonnie A, Van Aucken A, Sood R, Collins F, Brownstein M, Trent J. 1998. Evidence for a prostate cancer susceptibility locus on the X chromosome. Nature genetics 20(2):175-179.

Xu J, Zheng SL, Hawkins GA, Faith DA, Kelly B, Isaacs SD, Wiley KE, Chang B, Ewing CM, Bujnovszky P, Carpten JD, Bleecker ER, Walsh PC, Trent JM, Meyers DA, Isaacs WB. 2001. Linkage and association studies of prostate cancer susceptibility: evidence for linkage at 8p22-23. American journal of human genetics 69(2):341-350.

Xu J, Zheng SL, Komiya A, Mychaleckyj JC, Isaacs SD, Hu JJ, Sterling D, Lange EM, Hawkins GA, Turner A, Ewing CM, Faith DA, Johnson JR, Suzuki H, Bujnovszky P, Wiley KE, DeMarzo AM, Bova GS, Chang B, Hall MC, McCullough DL, Partin AW, Kassabian VS, Carpten JD, Bailey-Wilson JE, Trent JM, Ohar J, Bleecker ER, Walsh PC, Isaacs WB, Meyers DA. 2002. Germline mutations and sequence variants of the macrophage scavenger receptor 1 gene are associated with prostate cancer risk. Nature genetics 32(2):321-325.

Yamaguchi A, Katagiri T, Ikeda T, Wozney JM, Rosen V, Wang EA, Kahn AJ, Suda T, Yoshiki S. 1991. Recombinant human bone morphogenetic protein-2 stimulates osteoblastic maturation and inhibits myogenic differentiation in vitro. The Journal of cell biology 113(3):681-687.

Yamaguchi A, Komori T, Suda T. 2000. Regulation of osteoblast differentiation mediated by bone morphogenetic proteins, hedgehogs, and Cbfa1. Endocrine reviews 21(4):393-411.

Yamaguchi K, Kinosaki M, Goto M, Kobayashi F, Tsuda E, Morinaga T, Higashio K. 1998. Characterization of structural domains of human osteoclastogenesis inhibitory factor. The Journal of biological chemistry 273(9):5117-5123.

Yasuda H, Shima N, Nakagawa N, Mochizuki SI, Yano K, Fujise N, Sato Y, Goto M, Yamaguchi K, Kuriyama M, Kanno T, Murakami A, Tsuda E, Morinaga T, Higashio K. 1998a. Identity of osteoclastogenesis inhibitory factor (OCIF) and osteoprotegerin (OPG): a mechanism by which OPG/OCIF inhibits osteoclastogenesis in vitro. Endocrinology 139(3):1329-1337.

Yasuda H, Shima N, Nakagawa N, Yamaguchi K, Kinosaki M, Mochizuki S, Tomoyasu A, Yano K, Goto M, Murakami A, Tsuda E, Morinaga T, Higashio K, Udagawa N, Takahashi N, Suda T. 1998b. Osteoclast differentiation factor is a ligand for osteoprotegerin/osteoclastogenesis-inhibitory factor and is identical to TRANCE/RANKL. Proceedings of the National Academy of Sciences of the United States of America 95(7):3597-3602.

Yatani R, Shiraishi T, Nakakuki K, Kusano I, Takanari H, Hayashi T, Stemmermann GN. 1988. Trends in frequency of latent prostate carcinoma in Japan from

1965-1979 to 1982-1986. Journal of the National Cancer Institute 80(9):683-687.

Yavropoulou MP, van Lierop AH, Hamdy NA, Rizzoli R, Papapoulos SE. 2012. Serum sclerostin levels in Paget's disease and prostate cancer with bone metastases with a wide range of bone turnover. Bone 51(1):153-157.

Ye XC, Choueiri M, Tu SM, Lin SH. 2007. Biology and clinical management of prostate cancer bone metastasis. Frontiers in bioscience : a journal and virtual library 12:3273-3286.

Yen ML, Hsu PN, Liao HJ, Lee BH, Tsai HF. 2012. TRAF-6 dependent signaling pathway is essential for TNF-related apoptosis-inducing ligand (TRAIL) induces osteoclast differentiation. PloS one 7(6):e38048.

Yoneda T, Tanaka S, Hata K. 2013. Role of RANKL/RANK in primary and secondary breast cancer. World journal of orthopedics 4(4):178-185.

Yu EY, Wilding G, Posadas E, Gross M, Culine S, Massard C, Morris MJ, Hudes G, Calabro F, Cheng S, Trudel GC, Paliwal P, Sternberg CN. 2009. Phase II study of dasatinib in patients with metastatic castration-resistant prostate cancer. Clinical cancer research : an official journal of the American Association for Cancer Research 15(23):7421-7428.

Yue L, Haroun S, Parent JL, de Brum-Fernandes AJ. 2014. Prostaglandin D(2) induces apoptosis of human osteoclasts through ERK1/2 and Akt signaling pathways. Bone 60:112-121.

Yun TJ, Chaudhary PM, Shu GL, Frazer JK, Ewings MK, Schwartz SM, Pascual V, Hood LE, Clark EA. 1998. OPG/FDCR-1, a TNF receptor family member, is expressed in lymphoid cells and is up-regulated by ligating CD40. Journal of immunology 161(11):6113-6121.

Zauli G, Melloni E, Capitani S, Secchiero P. 2009. Role of full-length osteoprotegerin in tumor cell biology. Cellular and molecular life sciences : CMLS 66(5):841-851.

Zhang J, Dai J, Qi Y, Lin DL, Smith P, Strayhorn C, Mizokami A, Fu Z, Westman J, Keller ET. 2001. Osteoprotegerin inhibits prostate cancer-induced osteoclastogenesis and prevents prostate tumor growth in the bone. The Journal of clinical investigation 107(10):1235-1244.

Zhao Y, Bachelier R, Treilleux I, Pujuguet P, Peyruchaud O, Baron R, Clement-Lacroix P, Clezardin P. 2007. Tumor alphavbeta3 integrin is a therapeutic target for breast cancer bone metastases. Cancer research 67(12):5821-5830.

Zhau HE, Li CL, Chung LW. 2000. Establishment of human prostate carcinoma skeletal metastasis models. Cancer 88(12 Suppl):2995-3001.

Zhau HE, Odero-Marah V, Lue HW, Nomura T, Wang R, Chu G, Liu ZR, Zhou BP, Huang WC, Chung LW. 2008. Epithelial to mesenchymal transition (EMT) in human prostate cancer: lessons learned from ARCaP model. Clinical & experimental metastasis 25(6):601-610.

Zheng DQ, Woodard AS, Fornaro M, Tallini G, Languino LR. 1999. Prostatic carcinoma cell migration via alpha(v)beta3 integrin is modulated by a focal adhesion kinase pathway. Cancer research 59(7):1655-1664.

Zheng SL, Xu J, Isaacs SD, Wiley K, Chang B, Bleecker ER, Walsh PC, Trent JM, Meyers DA, Isaacs WB. 2001. Evidence for a prostate cancer linkage to chromosome 20 in 159 hereditary prostate cancer families. Human genetics 108(5):430-435.

Zielie PJ, Mobley JA, Ebb RG, Jiang Z, Blute RD, Ho SM. 2004. A novel diagnostic test for prostate cancer emerges from the determination of alpha-methylacyl-coenzyme a racemase in prostatic secretions. The Journal of urology 172(3):1130-1133.

Zuker M. 2003. Mfold web server for nucleic acid folding and hybridization prediction. Nucleic acids research 31(13):3406-3415.